Echolocation-based foraging by harbor porpoises and sperm whales, including effects of noise and acoustic propagation

By

Stacy Lynn DeRuiter
B.A., St. Olaf College, 2000

Submitted in partial fulfillment of the requirements for the degree of
Doctor of Philosophy
at the
MASSACHUSETTS INSTITUTE OF TECHNOLOGY
and the
WOODS HOLE OCEANOGRAPHIC INSTITUTION
September 2008

Signature of Author

_____

Joint Program in Oceanography/Applied Ocean Science and Engineering
Massachusetts Institute of Technology
and Woods Hole Oceanographic Institution
August 4, 2008

Certified by

_____

Peter Tyack
Thesis Supervisor

Accepted by

_____

Ed DeLong
Chair, Joint Committee for Biology
Woods Hole Oceanographic Institution

Echolocation-based foraging by harbor porpoises and sperm whales, including effects of noise and acoustic propagation

By
Stacy Lynn DeRuiter

Submitted to the Department of Biology
on August 4, 2008
in partial fulfillment of the requirements for the Degree of
Doctor of Philosophy in Biological Oceanography

Abstract

In this thesis, I provide quantitative descriptions of toothed whale echolocation and foraging behavior, including assessment of the effects of noise on foraging behavior and the potential influence of ocean acoustic propagation conditions on biosonar detection ranges and whale noise exposure. In addition to presenting some novel basic science findings, the case studies presented in this thesis have implications for future work and for management.

In Chapter 2, I describe the application of a modified version of the Dtag to studies of harbor porpoise echolocation behavior. The study results indicate how porpoises vary the rate and level of their echolocation clicks during prey capture events; detail the differences in echolocation behavior between different animals and in response to differences in prey fish; and show that, unlike bats, porpoises continue their echolocation buzz after the moment of prey capture.

Chapters 3-4 provide case studies that emphasize the importance of applying realistic models of ocean acoustic propagation in marine mammal studies. These chapters illustrate that, although using geometric spreading approximations to predict communication/target detection ranges or noise exposure levels is appropriate in some cases, it can result in large errors in other cases, particularly in situations where refraction in the water column or multi-path acoustic propagation are significant.

Finally, in Chapter 5, I describe two methods for statistical analysis of whale behavior data, the rotation test and a semi-Markov chain model. I apply those methods to test for changes in sperm whale foraging behavior in response to airgun noise exposure. Test results indicate that, despite the low-level exposures experienced by the whales in the study, some (but not all) of them reduced their buzz production rates and altered other foraging behavior parameters in response to the airgun exposure.

Thesis Supervisor: Peter L. Tyack
Title: Senior Scientist, Woods Hole Oceanographic Institution Biology Department

Acknowledgements

Many, many thanks to my advisor, Peter Tyack, and the members of my thesis committee: James Lynch, Dale Morgan, Peter Madsen, and Heather Koopman. Their support and advice have been invaluable.

Sincere thanks also to the many other people who have helped with data collection and analysis over the course of my graduate work, and also to everyone who offered comments on drafts of this thesis. More detailed acknowledgments can be found at the end of each chapter, but here I would especially like to thank the following. For help with field work and data collection: Kristian Beedholm, Marie-Anne Blanchet, Michael Hansen, Sabina Hansen, Heather Koopman, Jakob Kristensen, Peter Madsen, Lee Miller, Magnus Wahlberg, Andrew Westgate, and everyone else at the Fjord & Baelt Center and the Grand Manan Whale and Seabird Research Station; for help with porpoise tag design and construction: Alexander Bahr, Alex Bocconcelli, Tom Hurst, and Mark Johnson; for data analysis advice: my thesis committee, Hal Caswell, Mike Neubert, Arthur Newhall, Andrew Solow, and Ying-Tsong Lin; and finally, for comments on thesis drafts: my thesis committee, Regina Campbell-Malone, Michael Hansen, Patrick Miller, and Andrew Solow.

I am also very grateful for the support and friendship of all my labmates in the Tyack lab, past and present: Anne Allen, Amanda Hansen, Wu-Jung Lee, Peter Madsen, Susan Parks, Amanda Searby, Stephanie Watwood, Jeremy Winn, Becky Woodward, and especially Ari Shapiro, who went through every stage of the Joint Program with me.

Work presented in this thesis was supported by a National Science Foundation Graduate Research Fellowship, the WHOI Ocean Life Institute (Grant Numbers 32031300 and 25051351), the Office of Naval Research, the U.S. Department of the Interior Minerals Management Service (Cooperative Agreement Numbers 1435-01-02-CA-85186 and NA87RJ0445; WHOI Grant Number 15205601), the Industry Research Funding Coalition, and the WHOI/MIT Joint Program in Oceanography/Applied Ocean Science & Engineering (including a Fye Teaching Fellowship).

Table of Contents

Chapter 1. Introduction

1.1 Thesis Objectives and Chapter 1 Overview

The goal of my thesis research has been to provide quantitative descriptions of toothed whale echolocation and foraging behavior (Chapters 2 and 5), including assessment of the effects of noise on foraging behavior (Chapter 5) and the potential influence of ocean acoustic propagation conditions on biosonar detection ranges (Chapter 3) and whale noise exposure (Chapter 4). I have focused on two study species, the harbor porpoise (*Phocoena phocoena*, Chapters 2-3) and the sperm whale (*Physeter macrocephalus*, Chapters 4-5).

The following sections present background information relevant to the research presented in the rest of the thesis, beginning with a review of previous research on the use of echolocation by foraging animals. This review is followed by brief discussions of several issues that deserve consideration in studies of whale foraging behavior: effects of human-generated noise on behavior, implications of ocean sound propagation conditions for behavior, and quantitative analysis techniques appropriate for behavior data. Finally, this introductory chapter concludes with a brief outline of the thesis.

1.2 Echolocation by Animals

1.2.1 General Overview of Animal Echolocation

Animal echolocation involves the production of acoustic signals and use of the returning echoes to obtain information about the environment. Echolocation, or biosonar, has been described in various taxa including bats, whales, and birds (Griffin, 1958; Thomas *et al.*, 2002). As early as the 18th century, Italian scientists Spallanzani and Jurine observed that while blinded bats could fly and navigate normally, deafened bats or bats whose ears had been plugged were apparently disoriented and often collided with obstacles (Griffin, 2001). Around the mid-20th century, researchers demonstrated that bats emit ultrasonic vocalizations and use the resulting echoes to sense their environment via

echolocation (Griffin, 1958; Griffin, 2001). They carried out experiments that demonstrated use of echolocation for navigation and obstacle avoidance by showing that echolocation was required for captive bats to navigate successfully through a maze of wires (reviewed in Novick, 1973). Subsequently, field observations of a correlation between echolocation click emission rates and prey capture events suggested a role for echolocation in prey detection and localization during foraging, a hypothesis later confirmed and elaborated by laboratory and field experiments (for example, Griffin, 1958; Griffin *et al.*, 1960; Novick, 1973; Simmons *et al.*, 1979; Griffin, 2001).

Echolocation has also been described in several cave-dwelling bird taxa, which use echolocation mainly for navigation in dark caves: oilbirds *Steatornis caripensis* (Konishi and Knudsen, 1979) and cave swiftlets of genera *Aerodramus*, *Collocalia* and *Hydrochous* (reviewed in Price *et al.*, 2005). The birds all echolocate at low frequencies (within the range of human hearing, ~2-10 kHz) presumed to be unsuitable for detection of their small insect prey (Griffin, 1954; Konishi and Knudsen, 1979; Price *et al.*, 2005). Unlike most bats, the birds seem to use echolocation only for navigation and obstacle avoidance. There is no evidence that they use echolocation to find or capture prey, but captive oilbirds with plugged ears collided with walls during flight in a dark room (Griffin, 1954).

A few species of odontocetes (toothed whales) have been shown experimentally to use echolocation for navigation or for prey detection and capture, and most other odontocetes produce sounds potentially useful for echolocation (Evans, 1973; Au, 1993; Reynolds and Rommel, 1999). Early demonstrations of echolocation ability in cetaceans included the abilities of Amazon River dolphins (*Inia geoffrensis*) and bottlenose dolphins (*Tursiops truncatus*) to detect and discriminate between pairs of targets while blindfolded or in the dark; the animals produced broadband clicks as they performed the tasks

(Norris, 1969; Evans, 1973). Those experiments suggested a possible role for echolocation in prey detection and selection. The target detection and discrimination abilities of captive dolphins and harbor porpoises (*Phocoena phocoena*) were later described in much greater detail (Au, 1993; Au *et al.*, 1999; Kastelein *et al.*, 1999). In addition, porpoises, like bats, have been shown to be able to navigate through mazes of thin wires with no or few collisions, again suggesting a role for echolocation in navigation and obstacle avoidance (Evans, 1973). More recently, Verfuss and colleagues (2005) further described captive porpoise click emission rates during navigation; their data indicate that porpoises use specific landmarks for orientation, and provide more evidence that porpoises use echolocation for navigation as well as foraging.

Until recently, the difficulties of observing wild whales underwater or keeping large whales in captivity for controlled experimentation have limited detailed studies of whale echolocation to a few species of dolphin and porpoise that have been trained and studied in captivity (mainly the bottlenose dolphin, *Tursiops truncatus*, but also to a lesser extent the harbor porpoise (*Phocoena phocoena*) and other species (Au, 1993)). Current research using digital archival tags (Burgess *et al.*, 1998; Madsen *et al.*, 2002; Johnson and Tyack, 2003) to record marine mammal movements concurrent with audio recordings have provided insight into the echolocation and foraging behavior of larger whales like sperm whales *Physeter macrocephalus* (Miller *et al.*, 2004a) and beaked whales *Mesoplodon densirostris* and *Ziphius cavirostris* (Madsen *et al.*, 2005b; Zimmer *et al.*, 2005a). Such work provides data and motivation for comparative studies of echolocation, including intraspecific comparisons of wild and captive animals and interspecific comparisons of whales and other echolocating species.

1.2.2 Prey Responses to Echolocation Signals

The co-evolution of predator echolocation signals and prey hearing and avoidance strategies has been well described for bats and their prey (Miller and

Surlykke, 2001; Denzinger *et al.*, 2004; Rydell, 2004; Tougaard *et al.*, 2004). There is evidence that some fishes on which toothed whales prey can detect ultrasound (cod *Gadus morhua*, when conditioned: Astrup and Møhl, 1993; American shad *Alosa sapidissima*: Mann *et al.*, 1998; gulf menhaden *Brevoortia patronus*: Mann *et al.*, 2001). In addition, herring (*Clupea harengus*) and shad (*Alosa* sp.) show behavioral responses to broadband clicks that are acoustically similar to some odontocete echolocation signals (herring: Wilson and Dill, 2002; shad: Wilson *et al.*, 2008). However, similar responses have not been observed in the squid *Loligo pealeii* or in unconditioned cod (squid: Wilson *et al.*, 2007; cod: Schack *et al.*, 2008). The fact that some fishes do show behavioral responses to ultrasonic clicks, combined with the observation that bottlenose dolphins regularly use passive listening rather than echolocation in prey detection (Gannon *et al.*, 2005), suggest that predator-prey co-evolution similar to that observed in bats and insects may be occurring between toothed whales and their prey.

1.2.3 Bat Biosonar: Echolocation Phases & Niche Adaptation

Of all taxa that employ echolocation, bats are perhaps the best studied, since they can be maintained in captivity, trained to perform behavioral experiments, and subjected to neurophysiological testing. Free-ranging bats have also been studied in the wild in some cases.

Echolocation by most foraging bats consists of several distinct phases: first, a search phase consisting of regularly-spaced echolocation signals; next, an approach phase, in which the bat focuses its attention on one prey target and begins to approach it; then, a terminal phase, during which echolocation signals (whose acoustic characteristics often differ from the search signals) are emitted at a faster, increasing repetition rate, ending sometimes with prey capture (Schnitzler and Kalko, 2001). During the terminal phase, acoustic characteristics of the echolocation signals are specialized for precise target localization and

range determination, and the more closely-spaced cries provide more frequent updates of prey location.

Comparative studies of echolocating bat species have revealed that bats employ several echolocation signal types and strategies, corresponding to the environments in which they typically forage. Bats foraging for flying insects in open space typically use relatively long, narrowband, lower-frequency echolocation signals, which researchers hypothesize are optimized to detect targets at maximum ranges and to distinguish insects' fluttering wings from other airborne targets (Schnitzler and Kalko, 2001). In contrast, bats foraging in background-cluttered habitats such as forest edge environments often use a combination of shallowly-modulated narrowband signals (constant-frequency or CF signals) and frequency-modulated (FM) signals that cover a broader bandwidth (Schnitzler and Kalko, 2001). The CF signals are often considered optimal for prey detection, while FM signals are thought to be optimal for target localization and characterization (Simmons, 1974; Schnitzler and Kalko, 2001). Bats foraging for flying insects close to vegetation or in other highly cluttered environments use a third class of echolocation strategies. They tend to use longer duration, higher-frequency narrowband (CF) signals, and they employ Doppler-shift compensation of the transmitted signal to maintain constant-frequency echoes from moving prey. The Doppler shift for moving prey also means prey echoes and clutter echoes generally have different frequencies that are perceptually distinguishable by the bats, allowing bats to distinguish targets from clutter (Schnitzler and Kalko, 2001). The echolocation signals of many bats that forage in highly cluttered environments also include an FM component, which creates echoes useful for precise target localization but potentially masked by clutter echoes (Simmons, 1974; Schnitzler and Kalko, 2001). Finally, bats foraging for stationary prey in highly cluttered environments tend to use shorter signals, FM over a relatively broad bandwidth, often emitted at low sound pressure levels to minimize echoes from clutter. They use their echolocation to

navigate and may also use it to detect insect targets, if the prey have echo characteristics unique enough to distinguish them from background objects (Schnitzler and Kalko, 2001).

1.2.4 Toothed Whale Biosonar: Echolocation Phases & Signal Diversity

A sequence of events analogous to that described for bats has been recorded from echolocating narwhals *Monodon monoceros* (Miller *et al.*, 1995), sperm whales (Miller *et al.*, 2004a), and beaked whales (Johnson *et al.*, 2004; Madsen *et al.*, 2005b; Johnson *et al.*, 2008), although it has not been characterized as thoroughly in relation to prey approach and capture. All toothed whale species studied do emit regularly spaced clicks, thought to function in echolocation as does the search phase of bat echolocation, and they also produce terminal buzzes, as bats do (Miller *et al.*, 1995; Madsen *et al.*, 2002; Johnson *et al.*, 2004; Miller *et al.*, 2004a; Madsen *et al.*, 2005b).

Various types of echolocation signals have been recorded from toothed whales. Examples include the lower-frequency, broadband, multi-pulsed clicks of sperm whales (Zimmer *et al.*, 2005b), the high-frequency, broadband, impulsive clicks of bottlenose dolphins (Au *et al.*, 1974), the high-frequency, frequency-modulated clicks of Cuvier's beaked whales *Ziphius cavirostris* (Zimmer *et al.*, 2005a), and the very high-frequency, narrowband clicks of porpoises (Au *et al.*, 1999). Researchers have noted some connections between the ecological niches of cetaceans and their echolocation signals; for example, small near-shore and riverine species that hunt small prey in acoustically cluttered habitats tend to use higher-frequency (>100kHz), more narrow-band echolocation signals, while larger offshore species hunt larger prey in less cluttered habitats and use lower-frequency, broadband signals (Ketten, 2000). However, exceptions to this pattern exist; for example, pygmy sperm whales *Kogia breviceps*, which forage in deeper waters for squid, also produce narrowband echolocation signals centered at about 130 kHz (Madsen *et al.*, 2005a).

Rather than attempting to describe and explain the differences between echolocation signal characteristics between odontocete species, many studies to date have assumed a very simple model of whale sonar source/receiver characteristics. According to that model, an animal emits an impulse-like click and then processes returning echoes as an energy detector with an integration time of a few hundred microseconds (Au, 1993). The variation in click characteristics for different species, along with the variation in their habitats, suggests that this model may not fully describe echolocation of all toothed whales. As more data on the echolocation signals and the detailed foraging strategies of various whale species emerge, they can be integrated with information on preferred prey types and the acoustic environment in which animals forage. Such synthesis should provide insight into how selective pressures may have mediated the evolution of different echolocation signals and strategies in toothed whales, allowing comparative analysis with bats, whose echolocation evolved in parallel with that of odontocetes (Thomas *et al.*, 2002).

1.2.5 Overview of Harbor Porpoise and Sperm Whale Echolocation

Two toothed whale species, the harbor porpoise and the sperm whale, are considered specifically in this thesis. They contrast strongly in terms of size, habitat, prey species consumed, echolocation signals produced, and also the state of current research on their echolocation and foraging behavior. The following sections offer a brief overview of the biology and biosonar of each species.

1.2.5.1 Sperm Whales

Sperm whales are the largest toothed whales, reaching lengths of up to 13 meters (females) or 18 meters (males) (Reynolds and Rommel, 1999; Whitehead, 2003). Females and immature animals live in stable matrilineal social groups that contain about 10.5 individuals on average, and are generally found in waters greater than 1 km deep at latitudes of less than 50 degrees

(Whitehead, 2003). Males, on the other hand, are much more solitary as adults, and have more extensive ranges including polar latitudes and shallower areas (Whitehead, 2003).

Unlike many dolphins, pilot whales, belugas and killer whales, which use tonal sounds for social communication, sperm whales use clicks for both echolocation and communication (Whitehead, 2003). They do produce at least one type of tonal sound, the trumpet (Teloni *et al.*, 2005), but codas are their most common social sound (Watkins and Schevill, 1977; Whitehead, 2003; Rendell and Whitehead, 2005). Codas are short, stereotyped rhythmic series of clicks (Watkins and Schevill, 1977; Whitehead, 2003); sperm whales from different regions seem to have distinct coda repertoires (Rendell and Whitehead, 2005). The individual coda clicks are distinguishable from regular echolocation clicks based on their lower frequency (centroid ~5 kHz), longer duration, and lower decay rate of multipulses (Madsen *et al.*, 2002; Whitehead, 2003).

Sperm whales produce echolocation clicks that are high-amplitude (240 dB re 1 µPa peak-to-peak) and relatively low-frequency (centroid frequency ~15 kHz) (Møhl *et al.*, 2000; Møhl *et al.*, 2003). Sperm whales use echolation to locate prey (Møhl *et al.*, 2000; Miller *et al.*, 2004a). They produce regular echolocation clicks almost continuously while foraging at depth, interrupted only by short pauses and buzzes (short series of rapid echolocation clicks indicative of attempted prey capture (Whitehead 2003, Miller et al. 2004a)). Whales begin producing echolocation clicks during the descent phase of foraging dives, and stop clicking during or just prior to ascent (Watwood *et al.*, 2006). With the exception of mature males foraging at high latitudes (Teloni *et al.*, 2008), they do not generally produce series of regular echolocation clicks while at the surface or during shallow dives (Watwood et al. 2006).

Historically, sperm whale populations were decimated by whaling; Whitehead (2002) estimated that global sperm whale populations in 1999 were

68% smaller than pre-whaling populations. Currently, concern has arisen that exposure to human generated noise (for example, shipping noise, naval sonars, and airguns) may have adverse effects on their behavior and population dynamics (Richardson *et al.*, 1995; Ocean Studies Board, 2003; Anonymous, 2004; Barlow and Gentry, 2004; Tyack, 2008).

1.2.5.2 Harbor Porpoises

Harbor porpoises are very small toothed whales which inhabit temperate and subarctic waters. Other than mother-calf pairs, they do not usually form stable social groups. Like sperm whales, they use clicks for both echolocation and communication, and are not known to produce any tonal sounds (Amundin, 1991; Au, 1993).

Porpoises use echolocation for foraging and navigation (Au, 1993; Verfuss *et al.*, 2005). Their echolocation signals are much more narrowband than those of most larger toothed whales; porpoise echolocation clicks are about 150 µsec long, with peak frequency between 120 - 140 kHz and a -3 dB bandwidth of about 10 - 15 kHz (Au, 1993). They tend to forage in shallow, coastal waters (less than a few hundred meters deep) (Westgate *et al.*, 1995; Read and Westgate, 1997; Reynolds and Rommel, 1999), and they consume species of fish that tend to be found at or near the sea floor (Fontaine *et al.*, 1994; Santos *et al.*, 2004; Akamatsu *et al.*, 2007). Consequently, they may forage in a highly cluttered acoustic environment. This fact, combined with the observed differences between porpoise echolocation signals and those of other whales, suggests that porpoises may deploy their biosonar differently from better-studied oceanic species.

The porpoise auditory system is specialized for ultrasonic hearing. The range of best hearing for harbor porpoises is 16-140 kHz, and for frequencies above 32 kHz, porpoises have the most acute hearing of any odontocete species that has been tested (Kastelein *et al.*, 2002).

Harbor porpoises also seem to be especially sensitive to anthropogenic noise, showing strong avoidance reactions in response to pingers and other ultrasonic sounds (Kraus *et al.*, 1997; Kastelein *et al.*, 2000; Johnston, 2002). Porpoises live in coastal areas where fisheries are active, vessel traffic is intense, and marine construction (e.g., for offshore wind farms) may occur, so they face mortality from entanglement in bottom-set gillnets or other fishing gear, entrapment in herring weirs, and behavioral disruption or habitat exclusion due to anthropogenic noise.

Bycatch in fishing gear has well-documented effects on harbor porpoise populations, and controlled experiments have shown that pingers (devices attached to fishing gear that emit high-frequency sounds designed to deter porpoises coming near gear) effectively reduce porpoise approaches to gear, at least over short deployment periods of less than a day (Kraus *et al.*, 1997; Kastelein *et al.*, 2000; Culik *et al.*, 2001; Carlstrom *et al.*, 2002). In the U.S., Canada, and the E.U., management agencies are working to reduce porpoise bycatch by closing areas to certain types of fishing gear and mandating use of pingers (Bowen *et al.*, 2001; ASCOBANS, 2002; Joint Nature Conservation Committee U.K., 2006). Field studies have indicated that, although porpoises are displaced from the vicinity of pingers upon initial deployment, the effect disappears after about 10 days of pinger operation (Cox *et al.*, 2001). Recent research with captive animals also suggests that porpoises may become habituated to pinger-like sounds after repeated exposures over several days, failing to avoid the sound source in later exposures (Teilmann *et al.*, 2006). However, research to date includes very few field observations of individual porpoise movements and vocalizations near fishing gear or in response to noise stimuli (for example, pingers, vessels, or construction noise). Unless researchers can measure how porpoises normally deploy their echolocation to forage and navigate in the presence and absence of fishing gear or other obstacles, it will be nearly impossible for them to quantify the effects of pingers or other disturbance

on foraging behavior. Field observations of porpoise acoustic behavior could aid in the design and testing of gear to reduce bycatch, and could inform more effective management strategies.

Finally, because the porpoise's longer, high-frequency, narrowband signal closely resembles some signals used in human-made sonar, a better understanding of how porpoises navigate and forage in acoustically cluttered environments could provide insight for engineers designing automated acoustic navigation systems.

1.3 Need for New Technology to Study Porpoise Echolocation

Current technology, which includes hydrophones and several tagging techniques, is poorly suited for gathering concurrent audio and behavior data on individual harbor porpoises.

Porpoise acoustic behavior can be studied in the field with hydrophones, but in most cases such studies will not record any individual porpoise for more than a few minutes (Villadsgaard *et al.*, 2007). Because porpoise clicks are so high-frequency (centered at about 130 kHz (Au *et al.*, 1999)), they are quickly attenuated as they travel through the ocean, limiting the detection range of hydrophones. Clicks are highly directional, so they may remain undetected even at ranges of tens of meters if the animal does not direct clicks toward the recording apparatus.

Satellite tags have been deployed on harbor porpoises for weeks or months to track surfacing locations (Westgate *et al.*, 1995), but they do not provide detailed short-timescale data or information about underwater behavior or vocalizations.

Akamatsu and collaborators have developed a small-whale tag that logs up to 72 hours of data, including time and level of porpoise clicks along with movement data (Akamatsu *et al.*, 2005); however, the tag employs a click

detector that may miss clicks or detect false positives, and it does not store a broadband audio recording. Broadband audio is critical for some studies of porpoise foraging ecology (especially analysis of outgoing signal and returning echo characteristics, and studies relating variability in acoustic characteristics of outgoing signals to environmental conditions, target properties, and foraging phase).

The Dtag, developed by Mark Johnson and others, is an archival whale tag that records broadband audio along with movement data (Johnson and Tyack, 2003). The Dtag is designed for deployment on large whales, and its housing and attachment system are too large and bulky for porpoises. Also, the Dtag records audio at up to 192 kHz; harbor porpoise clicks are centered at about 130 kHz, requiring a higher sampling rate (Au, 1993). To facilitate studies of echolocation, foraging, and navigation of individual harbor porpoises, researchers need a new device with the appropriate audio recording capability and movement sensors, packaged to allow minimally invasive, low-drag attachment to a porpoise.

However, recent tagging research highlights the power of acoustic recording tags to study echolocation strategies. For example, beaked whale tagging experiments have resulted in recordings of both outgoing whale echolocation clicks and returning echoes (Johnson *et al.*, 2004; Madsen *et al.*, 2005b). Records of echolocation behavior that include echoes can provide insight into the acoustic features used by whales to select prey items, as well as the type of information they glean from their biosonar (Madsen *et al.*, 2005b; Johnson *et al.*, 2008; Jones *et al.*, 2008). Because of porpoises' small size and sloping head shape, a dorsally mounted acoustic tag may be able to record similar echoes, allowing comparison between oceanic, deep-diving beaked whales and coastal porpoises.

Given the considerations outlined above, a major objective of my thesis has been to develop a tag to better characterize the echolocation and foraging behavior of harbor porpoises. In the field of basic and comparative studies of animal echolocation, some of the most important outstanding research questions relate to the details of porpoise movements during foraging events, including the ranges at which they can detect echoes from targets and select them as potential prey; possible variations in the acoustic properties of their biosonar signals depending on their acoustic environment and the phase of foraging; and the acoustic features of echoes returning from prey or surroundings that porpoises could use for prey selection, prey capture, or navigation. Recent work to develop behavior and audio-recording tags for whales has allowed researchers to collect data on the underwater behavior of the animals in unprecedented detail.

1.4 Need for Analytical Tools for Marine Mammal Behavior Data

Because of the cost and logistical difficulties involved with field work, most studies of marine mammal behavior involve relatively few individual animals. This 'small sample size' problem often means that studies have little power to detect changes in behavior. Even when anecdotal evidence of behavioral reactions to a certain stimulus exists, careful experimentation and rigorous statistical analysis of the data seldom happen, and even more rarely provide results definitive enough to allow scientists to generalize from the behavior of a few individuals to predict behavior or response of a population.

Analysis of ethological data, and whale behavior data in particular, is complicated by several factors. First, rather than collecting a limited dataset suited for application of a specific analytical method to test a particular hypothesis, experiments often produce enormous datasets containing acoustic data, animal movement data, or other ethological data. Researchers are then faced with the difficulty of summarizing all that data and testing for "differences in behavior" under varying experimental conditions. Rather than seeking out or

designing statistical methods suited to the characteristics of each dataset and each hypothesis to be tested, may researchers prefer to choose from among a small set of familiar statistical tests, regardless of the application. This approach can produce misleading results if the selected tests are not appropriate to the dataset.

For example, many studies result in data on the occurrence of particular behaviors over time. In such datasets, behavioral events in the time series are seldom statistically independent; instead the identity, duration, or timing of an event usually depends on the features of previous events (for examples, see Chapter 5 and Appendix A of this thesis; Haccou and Meelis, 1992; Miller *et al.*, 2004a; Miller *et al.*, 2004b). Most familiar parametric statistical tools are inappropriate for such serially dependent time series (see Appendix A for a more detailed discussion of this topic). In addition, such tests generally have low power when the dataset comprises observations of a small number of individuals; since small sample size is a perpetual problem in marine mammal studies especially, small behavior changes could often go undetected.

A wide variety of parametric and nonparametric statistical methods and computational approaches for analysis of time-series data have been developed (for example, Cox and Lewis, 1978; Haccou and Meelis, 1992; Huzurbazar, 2004), but ethologists have not always worked closely with statisticians and mathematical modelers to customize them for application to animal behavior data. In Chapter 5 of this thesis, I present an attempt at such development of customized analytical techniques to test for changes in sperm whale behavior in response to airgun sounds.

In this thesis, I do not specifically address the many difficulties involved in designing studies to gauge responses of individual marine mammals to sound. However, I do describe the development and application of several analytical

tools specifically designed to extract data efficiently from behavioral time-series and to compare behavior under various conditions.

1.4 Implications of Ocean Sound Propagation for Marine Mammals

Investigations of marine mammal bioacoustics often face an obstacle analogous to the inapplicability of standard statistical methods to whale behavior data: standard, simplified descriptions of ocean acoustics often prove inadequate to accurately characterize sound propagation in marine mammal habitats. However, accurate characterization of sound transmission is critical for estimating the ranges at which whales can communicate, detect echolocation targets, or be affected by anthropogenic noise. Therefore, realistic modeling of acoustic propagation is critical in marine mammal science, both for basic science and for management.

Ocean acousticians have developed many tools to allow such modeling (Jensen *et al.*, 1994; Medwin and Clay, 1998); these tools are increasingly applied in marine mammal studies (for example, Erbe and Farmer, 2000a; b; Croll *et al.*, 2001; Širović *et al.*, 2007; Tiemann *et al.*, 2007). Even so, many research papers (e.g., Møhl *et al.*, 2003; Au *et al.*, 2004; Madsen *et al.*, 2004; Mooney *et al.*, 2004) and management protocols (e.g., National Marine Fisheries Service, 2003; Barlow and Gentry, 2004; Gordon *et al.*, 2004) continue to use highly simplified descriptions of acoustic propagation without verifying their validity (either to simplify calculations, because they wish to present results relevant to a generic rather than a particular location, or because data on the environmental characteristics (required for more detailed models) was unavailable). In some cases, as detailed in Chapters 3-4 of this thesis, failing to model acoustic propagation realistically can lead to large errors in estimates of animal detection ranges or noise exposure levels.

1.5 Thesis Overview and Chapter Summaries

In my thesis research, I address several of the key research questions discussed in previous sections:

1. How do porpoises deploy their echolocation during prey capture in captivity? Are their strategies similar to those of bats or of larger, deep-diving oceanic toothed whales?
2. Is it possible to develop analytical models of whale foraging behavior, and to use them to compare behavior during exposure to noise or other environmental factors?
3. How can the environmental characteristics of marine mammal habitats affect acoustic propagation and thus the ranges at which whales can communicate, detect echolocation targets, or be affected by anthropogenic noise?

The following sections present brief summaries of each chapter my thesis.

1.5.1 Chapter 1 – Introduction

In this chapter, I describe the motivation and objectives of my thesis, including a review of previous work on animal echolocation and background information on applications of acoustic propagation models and quantitative modeling techniques to marine mammal behavior and bioacoustics. The chapter concludes with a thesis outline, which comprises brief summaries of each thesis chapter.

1.5.2 Chapter 2 – Acoustic Behavior of Echolocating Porpoises During Prey Capture

Porpoise echolocation has been studied previously in target detection experiments using stationed animals and steel spheres as targets, but little is known about the acoustic behavior of free swimming porpoises echolocating for prey. This chapter describes the application of a newly developed tag, which records audio and animal movement data; the tag was deployed on trained

captive porpoises during prey capture experiments in which the porpoises used echolocation to catch (dead) fish. Results include detailed analysis of the porpoises' echolocation behavior leading up to and following prey capture events, including variability in that behavior in response to vision restriction, fish species captured, and individual porpoise tested.

1.5.3 Chapter 3 – Transmission Loss in Porpoise Habitats

This chapter presents a comparison of measured and modeled transmission loss in porpoise habitats near Grand Manan Island, New Brunswick, Canada and Aarhus, Denmark. Two models, one based on a simple spherical spreading law and one on output from the Bellhop ray-trace acoustic propagation model, were tested. Output from both models matched field observations quite well in most cases. However, when refraction in the water column or surface/bottom interactions played an important role in determining transmission loss, the spreading law model failed. The results of the study indicate that variable sound propagation conditions in porpoise habitats can cause significant variability in transmission loss. Variations in transmission loss will change the ranges at which porpoises can communicate acoustically, detect echolocation targets, and be detected via passive acoustic monitoring.

1.5.4 Chapter 4 -- Modeling acoustic propagation of airgun array pulses recorded on tagged sperm whales

Airgun arrays, which are used for oil industry and geophysical exploration of the sea floor, produce high-amplitude, low-frequency sound that could potentially have adverse effects on whale behavior. Chapter 4 describes the application of several acoustic propagation models to explain observed patterns in sperm whale exposure to airgun sounds. The data, which comprise airgun pulses recorded on free-ranging tagged sperm whales, include observations of unexpectedly high-amplitude exposure levels at long ranges and unexpectedly high-frequency airgun pulses recorded on animals near the surface. The

propagation model output allows explanation of those observations in terms of sound refraction in the water column, interaction of sound with the sea floor and surface, and airgun array directivity. The results of this study emphasize the importance of realistic characterization of sound sources and acoustic propagation in marine mammal noise exposure management.

1.5.5 Chapter 5 – Modeling Sperm Whale Response to Airgun Sounds

This chapter describes the development and application of statistical and modeling approaches to quantify changes in sperm whale behavior in response to airgun sound exposure. One approach involves the rotation test, a nonparametric statistical test for changes in behavioral rates. The other method is a continuous-time semi-Markov chain model of sperm whale foraging behavior, which allows for detection of behavioral changes in response to noise exposure or changes in other experimental conditions. Strengths of the two methods include their applicability to either individual-whale or multi-individual datasets, and their relatively high power to detect changes in behavior even when the number of animals tested is small. Application of the methods indicated that, even at the low exposure levels observed in the study, some individual sperm whales significantly altered their foraging behavior in response to airgun noise.

1.5.6 Chapter 6 – Conclusions

This concluding chapter briefly assesses the implications of the thesis as a whole, and discusses several directions in which future research on the thesis topics could proceed.

1.5.7 Appendices

Appendix A is a manuscript entitled “A rotation test for behavioural point process data” by Stacy DeRuiter and Andrew Solow, which describes in detail the rotation test used in Chapter 5. Appendix B contains selected annotated Matlab computer code used for various analyses.

References

Akamatsu, T., Teilmann, J., Miller, L. A., Tougaard, J., Dietz, R., Wang, D., Wang, K. X., Siebert, U., and Naito, Y. (**2007**). "Comparison of echolocation behaviour between coastal and riverine porpoises," Deep-Sea Research Part II -Topical Studies in Oceanography **54**, 290-297.

Akamatsu, T., Wang, D., Wang, K. X., and Naito, Y. (**2005**). "Biosonar behaviour of free-ranging porpoises," Proceedings of the Royal Society B-Biological Sciences **272**, 797-801.

Amundin, M. (**1991)**. "Sound production in Odontocetes with emphasis on the harbour porpoise *Phocoena phocoena*," PhD Thesis, Department of Zoology, Division of Functional Morphology, University of Stockholm.

Anonymous (**2004**). "Seismic surveys & marine mammals: Joint OGP/IAGC position paper," (OGP and IAGC, London, UK and Houston, TX, USA).

ASCOBANS (**2002**). "Recovery Plan for Baltic Harbor Porpoises (Jastarnia Plan)," (Bonn, Germany).

Astrup, J., and Møhl, B. (**1993**). "Detection of intense ultrasound by the cod *Gadus morhua*," Journal of Experimental Biology **182**, 71-80.

Au, Floyd, R. W., Penner, R. H., and Murchison, A. E. (**1974**). "Measurement of echolocation signals of the Atlantic bottlenose dolphin, *Tursiops truncatus* Montagu, in open waters," Journal of the Acoustical Society of America **56**, 1280-1290.

Au, W. W. L. (**1993**). *The sonar of dolphins* (Springer-Verlag, New York, NY).

Au, W. W. L., Ford, J. K. B., Horne, J. K., and Allman, K. A. N. (**2004**). "Echolocation signals of free-ranging killer whales (*Orcinus orca*) and modeling of foraging for chinook salmon (*Oncorhynchus tshawytscha*)," Journal of the Acoustical Society of America **115**, 901-909.

Au, W. W. L., Kastelein, R. A., Rippe, T., and Schooneman, N. M. (**1999**). "Transmission beam pattern and echolocation signals of a harbor porpoise (*Phocoena phocoena*)," Journal of the Acoustical Society of America **106**, 3699-3705.

Barlow, J., and Gentry, R. (**2004**). "Report of the NOAA Workshop on Anthropogenic Sound and Marine Mammals, 19-20 February 2004," in *NOAA Technical Memorandum NMFS* (U.S. Department of Commerce, National Oceanic and Atmospheric Administration, National Marine Fisheries Service, Southwest Fisheries Science Center).

Bowen, D., Brodie, P., Conway, J., Gearin, P., Hammill, M., Hood, C. C., Kingsley, M. C., Lesage, V., Lien, J., Metuzals, K., Palka, D., Potter, D., Read, A. J., Rosel, P., Simon, P., and Stenson, G. (**2001**). "Proceedings of the International Harbour Porpoise Workshop," in *International Harbour Porpoise Workshop*, edited by G. Stenson (Canadian Science Advisory Secretariat, Bedford Institute of Oceanography, Dartmouth, Nova Scotia, Canada).

Burgess, W. C., Tyack, P. L., Le Boeuf, B. J., and Costa, D. P. (**1998**). "A programmable acoustic recording tag and first results from free-ranging northern elephant seals," Deep-Sea Research Part II -Topical Studies in Oceanography **45**, 1327-1351.

Carlstrom, J., Berggren, P., Dinnetz, F., and Borjesson, P. (**2002**). "A field experiment using acoustic alarms (pingers) to reduce harbour porpoise by-catch in bottom-set gillnets," ICES Journal of Marine Science **59**, 816-824.

Cox, D. R., and Lewis, P. A. W. (**1978**). *The statistical analysis of series of events* (Chapman & Hall, London).

Cox, T. M., Read, A. J., Solow, A., and Tregenza, N. (**2001**). "Will harbour porpoises (*Phocoena phocoena*) habituate to pingers?," Journal of Cetacean Research and Management **3**, 81-86.

Croll, D. A., Clark, C. W., Calambokidis, J., Ellison, W. T., and Tershy, B. R. (**2001**). "Effect of anthropogenic low-frequency noise on the foraging ecology of Balaenoptera whales," Animal Conservation **4**, 13-27.

Culik, B. M., Koschinski, S., Tregenza, N., and Ellis, G. M. (**2001**). "Reactions of harbor porpoises *Phocoena phocoena* and herring *Clupea harengus* to acoustic alarms," Marine Ecology Progress Series **211**, 255-260.

Denzinger, A., Kalko, E. K. V., and Jones, G. (**2004**). "Chapter 42: Introduction: Ecological and evolutionary aspects of echolocation in bats," in *Echolocation in bats and dolphins*, edited by J. A. Thomas, C. F. Moss, and M. Vater (University of Chicago Press, Chicago, IL), pp. 311-326.

Erbe, C., and Farmer, D. M. (**2000a**). "A software model to estimate zones of impact on marine mammals around anthropogenic noise," Journal of the Acoustical Society of America **108**, 1327-1331.

Erbe, C., and Farmer, D. M. (**2000b**). "Zones of impact around icebreakers affecting beluga whales in the Beaufort Sea," Journal of the Acoustical Society of America **108**, 1332-1340.

Evans, W. E. (**1973**). "Echolocation by Marine Delphinids and One Species of Freshwater Dolphin," Journal of the Acoustical Society of America **54**, 191-199.

Fontaine, P. M., Hammill, M. O., Barrette, C., and Kingsley, M. C. (**1994**). "Summer diet of the harbor porpoise (*Phocoena phocoena*) in the estuary and the northern Gulf-of-St-Lawrence," Canadian Journal of Fisheries and Aquatic Sciences **51**, 172-178.

Gannon, D. P., Barros, N. B., Nowacek, D. P., Read, A. J., Waples, D. M., and Wells, R. S. (**2005**). "Prey detection by bottlenose dolphins, *Tursiops truncatus*: an experimental test of the passive listening hypothesis," Animal Behavior **69**, 709-720.

Gordon, J., Gillespie, D., Potter, J., Frantzis, A., Simmonds, M. P., Swift, R., and Thompson, D. (**2004**). "A review of the effects of seismic surveys on marine mammals," Marine Technology Society Journal **37**, 16-34.

Griffin, D. R. (**1954**). "Acoustic orientation in the oil bird, *Steatornis*," Proceedings of the National Academy of Sciences **39**, 884-893.

Griffin, D. R. (**1958**). *Listening in the Dark* (Yale University Press, New Haven, CT).

Griffin, D. R. (**2001**). "Return to the magic well: Echolocation behavior of bats and responses of insect prey," Bioscience **51**, 555-556.

Griffin, D. R., Webster, F. A., and Michael, C. R. (**1960**). "The echolocation of flying insects by bats," Animal Behaviour **8**, 141-154.

Haccou, P., and Meelis, E. (**1992**). *Statistical Analysis of Behavioural Data* (Oxford University Press, Oxford, U.K.).

Huzurbazar, A. V. (**2004**). *Flowgraph Models for Multistate Time-to-Event Data* (John Wiley & Sons, Inc., New York, NY).

Jensen, F. B., Kuperman, W. A., Porter, M. B., and Schmidt, H. (**1994**). *Computational Ocean Acoustics* (AIP Press, Woodbury, NY).

Johnson, M., Hickmott, L. S., Soto, N. A., and Madsen, P. T. (**2008**). "Echolocation behaviour adapted to prey in foraging Blainville's beaked whale (*Mesoplodon densirostris*)," Proceedings of the Royal Society B-Biological Sciences **275**, 133-139.

Johnson, M. P., Madsen, P. T., Zimmer, W. M. X., de Soto, N. A., and Tyack, P. L. (**2004**). "Beaked whales echolocate on prey," Biology Letters **271**, S383-S386.

Johnson, M. P., and Tyack, P. L. (**2003**). "A digital acoustic recording tag for measuring the response of wild marine mammals to sound," IEEE Journal of Oceanic Engineering **28**, 3-12.

Johnston, D. W. (**2002**). "The effect of acoustic harassment devices on harbour porpoises (*Phocoena phocoena*) in the Bay of Fundy, Canada," Biological Conservation **108**, 113-118.

Joint Nature Conservation Committee U.K. (**2006**). *Marine Mammal Bycatch,* http://www.jncc.gov.uk/default.aspx?page=1564, accessed March 6, 2006.

Jones, B. A., Stanton, T. K., Lavery, A. C., Johnson, M. P., Madsen, P. T., and Tyack, P. L. (**2008**). "Classification of broadband echoes from prey of a foraging Blainville's beaked whale," Journal of the Acoustical Society of America **123**, 1753-1762.

Kastelein, R. A., Au, W. W. L., Rippe, H. T., and Schooneman, N. M. (**1999**). "Target detection by an echolocating harbor porpoise (*Phocoena phocoena*)," Journal of the Acoustical Society of America **105**, 2493-2498.

Kastelein, R. A., Bunskoek, P., Hagedoorn, M., Au, W. W., and de Haan, D. (**2002**). "Audiogram of a harbor porpoise (*Phocoena phocoena*) measured with narrow-band frequency-modulated signals," Journal of the Acoustical Society of America **112**, 334-344.

Kastelein, R. A., Rippe, H. T., Vaughan, N., Schooneman, N. M., Verboom, W. C., and De Haan, D. (**2000**). "The effects of acoustic alarms on the behavior of harbour porpoises (*Phocoena phocoena*) in a floating pen," Marine Mammal Science **16**, 46-64.

Ketten, D. R. (**2000**). "Cetacean Ears," in *Hearing by Whales and Dolphins*, edited by W. W. L. Au, A. N. Popper, and R. R. Fay (Springer, New York, NY), pp. 43-108.

Konishi, M., and Knudsen, E. I. (**1979**). "Oilbird - Hearing and Echolocation," Science **204**, 425-427.

Kraus, S. D., Read, A. J., Solow, A., Baldwin, K., Spradlin, T., Anderson, E., and Williamson, J. (**1997**). "Acoustic alarms reduce porpoise mortality," Nature **388**, 525-525.

Madsen, P. T., Carder, D. A., Bedholm, K., and Ridgway, S. H. (**2005a**). "Porpoise clicks from a sperm whale nose - Convergent evolution of 130 kHz pulses in toothed whale sonars?," Bioacoustics **15**, 195-206.

Madsen, P. T., Johnson, M., de Soto, N. A., Zimmer, W. M. X., and Tyack, P. (**2005b**). "Biosonar performance of foraging beaked whales (*Mesoplodon densirostris*)," Journal of Experimental Biology **208**, 181-194.

Madsen, P. T., Kerr, I., and Payne, R. (**2004**). "Echolocation clicks of two free-ranging, oceanic delphinids with different food preferences: false killer whales *Pseudorca crassidens* and Risso's dolphins *Grampus griseus*," Journal of Experimental Biology **207**, 1811-1823.

Madsen, P. T., Payne, R., Kristiansen, N. U., Wahlberg, M., Kerr, I., and Møhl, B. (**2002**). "Sperm whale sound production studied with ultrasound time/depth recording tags," Journal of Experimental Biology **205**, 1899-1906.

Mann, D. A., Higgs, D. M., Tavolga, W. N., Souza, M. J., and Popper, A. N. (**2001**). "Ultrasound detection by clupeiform fishes," Journal of the Acoustical Society of America **109**, 3048-3054.

Mann, D. A., Lu, Z., Hastings, M. C., and Popper, A. N. (**1998**). "Detection of ultrasonic tones and simulated dolphin echolocation clicks by a teleost fish, the American shad (*Alosa sapidissima*)," Journal of the Acoustical Society of America **104**, 562-568.

Medwin, H., and Clay, C. S. (**1998**). *Fundamentals of Acoustical Oceanography* (Academic Press, Boston, MA).

Miller, L. A., Pristed, J., Møhl, B., and Surlykke, A. (**1995**). "The Click-Sounds of Narwhals (*Monodon monoceros*) in Inglefield Bay, Northwest Greenland," Marine Mammal Science **11**, 491-502.

Miller, L. A., and Surlykke, A. (**2001**). "How some insects detect and avoid being eaten by bats: Tactics and countertactics of prey and predator," Bioscience **51**, 570-581.

Miller, P. J., Johnson, M. P., and Tyack, P. L. (**2004a**). "Sperm whale behavior indicates the use of echolocation click buzzes 'creaks' in prey capture," Proceedings of the Royal Society of London B **271**, 2239-2247.

Miller, P. J. O., Shapiro, A. D., Tyack, P. L., and Solow, A. R. (**2004b**). "Call-type matching in vocal exchanges of free-ranging resident killer whales, *Orcinus orca*," Animal Behaviour **67**, 1099-1107.

Møhl, B., Wahlberg, M., Madsen, P. T., Heerfordt, A., and Lund, A. (**2003**). "The monopulsed nature of sperm whale clicks," Journal of the Acoustical Society of America **114**, 1143-1154.

Møhl, B., Wahlberg, M., Madsen, P. T., Miller, L. A., and Surlykke, A. (**2000**). "Sperm whale clicks: Directionality and source level revisited," Journal of the Acoustical Society of America **107**, 638-648.

Mooney, T. A., Natchigall, P. E., and Au, W. W. L. (**2004**). "Target strength of a nylon monofilament and an acoustically enhanced gillnet: Predictions of biosonar detection ranges," Aquatic Mammals **30**, 220-226.

National Marine Fisheries Service (**2003**). "Taking and importing marine mammals; Taking marine mammals incidental to conducting oil and gas exploration activities in the Gulf of Mexico," Federal Register **68**, 9991–9996.

Norris, K. S. (**1969**). "Chapter 10: The echolocation of marine mammals," in *The Biology of Marine Mammals*, edited by H. T. Andersen (Academic Press, New York, NY), pp. 391-423.

Novick, A. (**1973**). "Echolocation in Bats - A Zoologist's View," Journal of the Acoustical Society of America **54**, 139-146.

Ocean Studies Board (**2003**). *Ocean noise and marine mammals: committee on Potential impacts of ambient noise in the ocean on marine mammals* (National Academic Press, Washington, D.C.).

Price, J. J., Johnson, K. P., Bush, S. E., and Clayton, D. H. (**2005**). "Phylogenetic relationships of the Papuan Swiftlet *Aerodramus papuensis* and implications for the evolution of avian echolocation," Ibis **147**, 790-796.

Read, A. J., and Westgate, A. J. (**1997**). "Monitoring the movements of harbor porpoises (*Phocoena phocoena*) with satellite telemetry," Marine Biology **130**, 315-322.

Rendell, L., and Whitehead, H. (**2005**). "Spatial and temporal variation in sperm whale coda vocalizations: stable usage and local dialects," Animal Behaviour **70**, 191-198.

Reynolds, J. E. I., and Rommel, S. A. (eds). (**1999**). *Biology of Marine Mammals* (Smithsonian Institution Press, Washington, D.C.).

Richardson, W. J., Greene, C. R., Jr., Malme, C. I., and Thompson, D. H. (**1995**). *Marine Mammals and Noise* (Academic Press, San Diego, CA).

Rydell, J. (**2004**). "Chapter 43: Evolution of bat defense in Lepidoptera: Alternatives and complements to ultrasonic hearing," in *Echolocation in Bats and Dolphins*, edited by J. A. Thomas, C. F. Moss, and M. Vater (University of Chicago Press, Chicago, IL), pp. 327-330.

Santos, M. B., Pierce, G. J., Learmonth, J. A., Reid, R. J., Ross, H. M., Patterson, I. A. P., Reid, D. G., and Beare, D. (**2004**). "Variability in the diet of harbor porpoises (*Phocoena phocoena*) in Scottish waters 1992-2003," Marine Mammal Science **20**, 1-27.

Schack, H. B., Malte, H., and Madsen, P. T. (**2008**). "The responses of Atlantic cod (*Gadus morhua* L.) to ultrasound-emitting predators: stress, behavioural changes or debilitation?," Journal of Expermental Biology **211**, 2079-2086.

Schnitzler, H. U., and Kalko, E. K. V. (**2001**). "Echolocation by insect-eating bats," Bioscience **51**, 557-569.

Simmons, J. A. (**1974**). "Response of Doppler Echolocation System in Bat, *Rhinolophus ferrumequinum*," Journal of the Acoustical Society of America **56**, 672-682.

Simmons, J. A., Fenton, M. B., and Ofarrell, M. J. (**1979**). "Echolocation and Pursuit of Prey by Bats," Science **203**, 16-21.

Širović, A., Hildebrand, J. A., and Wiggins, S. M. (**2007**). "Blue and fin whale call source levels and propagation range in the Southern Ocean," Journal of the Acoustical Society of America **122**, 1208-1215.

Teilmann, J., Tougaard, J., Miller, L. A., Kirketerp, T., Hansen, K., and Brando, S. (**2006**). "Reactions of captive harbor porpoises (*Phocoena phocoena*) to pinger-like sounds," Marine Mammal Science **22**, 240-260.

Teloni, V., Johnson, M. P., Miller, P. J. O., and Madsen, P. T. (**2008**). "Shallow food for deep divers: Dynamic foraging behavior of male sperm whales in a high latitude habitat," Journal of Experimental Marine Biology and Ecology **354**, 119-131.

Teloni, V., Zimmer, W. M. X., and Tyack, P. L. (**2005**). "Sperm whale trumpet sounds," Bioacoustics **15**, 163-174.

Thomas, J. A., Moss, C. F., and Vater, M. (eds). (**2002**). *Echolocation in bats and dolphins* (University of Chicago Press, Chicago, IL).

Tiemann, C. O., Martin, S. W., and Mobley, J. R. (**2007**). "Aerial and Acoustic Marine Mammal Detection and Localization on Navy Ranges," IEEE Journal of Oceanic Engineering **31**, 107-119.

Tougaard, J., Miller, L. A., and Simmons, J. A. (**2004**). "Chapter 50: The role of Arctiid moth clicks in defense against echolocating bats: Interference with temporal processing," in *Echolocation in Bats and Dolphins*, edited by J. A. Thomas, C. F. Moss, and M. Vater (University of Chicago Press, Chicago, IL), pp. 365-371.

Tyack, P. L. (**2008**). "Implications for marine mammals of large-scale changes in the marine acoustic environment," Journal of Mammalogy **89**, 549–558.

Verfuss, U. K., Miller, L. A., and Schnitzler, H. U. (**2005**). "Spatial orientation in echolocating harbour porpoises (*Phocoena phocoena*)," Journal of Experimental Biology **208**, 3385-3394.

Villadsgaard, A., Wahlberg, M., and Tougaard, J. (**2007**). "Echolocation signals of wild harbour porpoises, *Phocoena phocoena*," Journal of Experimental Biology **210**, 56-64.

Watkins, W. A., and Schevill, W. E. (**1977**). "Sperm whale codas," Journal of the Acoustical Society of America **62**, 1485-1490.

Watwood, S. L., Miller, P. J. O., Johnson, M., Madsen, P. T., and Tyack, P. L. (**2006**). "Deep-diving foraging behaviour of sperm whales (*Physeter macrocephalus*)," Journal of Animal Ecology **75**, 814-825.

Westgate, A. J., Read, A. J., Berggren, P., Koopman, H. N., and Gaskin, D. E. (**1995**). "Diving Behavior of Harbor Porpoises, *Phocoena phocoena*," Canadian Journal of Fisheries and Aquatic Sciences **52**, 1064-1073.

Whitehead, H. (**2002**). "Estimates of the current global population size and historical trajectory for sperm whales," Marine Ecology Progress Series **242**, 295-304.

Whitehead, H. (**2003**). *Sperm Whales: Social Evolution in the Ocean* (University of Chicago Press, Chicago, IL).

Wilson, B., and Dill, L. M. (**2002**). "Pacific herring respond to simulated odontocete echolocation sounds," Canadian Journal of Fisheries and Aquatic Sciences **59**, 542-553.

Wilson, M., Acolas, M.-L., Bégout, M.-L., Madsen, P. T., and Wahlberg, M. (**2008**). "Ultrasound detection and intensity-graded anti-predator response in Allis shad (*Alosa alosa*)," JASA Express Letters, (in press).

Wilson, M., Hanlon, R. T., Tyack, P. L., and Madsen, P. T. (**2007**). "Intense ultrasonic clicks from echolocating toothed whales do not elicit anti-predator responses or debilitate the squid *Loligo pealeii*," Biology Letters **3**, 225-227.

Zimmer, W. M., Johnson, M. P., Madsen, P. T., and Tyack, P. L. (**2005a**). "Echolocation clicks of free-ranging Cuvier's beaked whales (*Ziphius cavirostris*)," Journal of the Acoustical Society of America **117**, 3919-3927.

Zimmer, W. M. X., Tyack, P. L., Johnson, M. P., and Madsen, P. T. (**2005b**). "Three-dimensional beam pattern of regular sperm whale clicks confirms bent-horn hypothesis " Journal of the Acoustical Society of America **117**, 1473-1485.

Chapter 2. Acoustic behavior of echolocating porpoises during prey capture

2.1 Introduction

Echolocation by most foraging bats consists of several distinct phases: first, a search phase consisting of regularly-spaced echolocation signals; next, an approach phase, in which the bat focuses its attention on one prey target and begins to approach it; then, a terminal phase, during which echolocation signals are emitted at a faster, increasing repetition rate (Schnitzler and Kalko, 2001). Often, each phase of echolocation is characterized by specific signal waveforms and patterns of signal repetition rate (Schnitzler and Kalko, 2001). The terminal phase is often termed a buzz (Schnitzler and Kalko, 2001). During the terminal phase or buzz, acoustic characteristics of the echolocation clicks are specialized for precise target localization and range determination, and the more closely-spaced clicks provide more frequent updates of prey location. Bat buzz production generally stops at the time of prey capture or slightly before (Griffin *et al.*, 1960; Kalko and Schnitzler, 1989; Hartley, 1992b; Kalko, 1995; Moss and Surlykke, 2001; Hiryu *et al.*, 2007). After a buzz, bats generally pause echolocation click production for a period of several hundred milliseconds to several seconds (Griffin *et al.*, 1960; Kalko and Schnitzler, 1989; Hartley, 1992b; Kalko, 1995; Moss and Surlykke, 2001; Hiryu *et al.*, 2007). The mean duration of the post-buzz pause is often longer after successful captures than after unsuccessful ones (Acharya and Fenton, 1992; Britton and Jones, 1999; Surlykke *et al.*, 2003). This increase in pause duration may be related to time required for prey handling; however, Britton and Jones (1999) found that pause duration did not increase as prey size (and thus inferred handling time required) increased. Some studies have also demonstrated that clicks emitted after successful captures have larger inter-pulse intervals and distinctive frequency characteristics (Britton and Jones, 1999; Surlykke *et al.*, 2003). Combined, these

features may allow researchers to distinguish successful prey capture attempts from unsuccessful ones on the basis of acoustic data alone, without requiring high-resolution visual observations of each prey capture attempt. Accurate estimates of bat foraging success could thus be derived from acoustic recordings.

A few species of toothed whales have been shown experimentally to use echolocation for navigation or for prey detection and capture, and most other odontocetes produce sounds potentially useful for echolocation (Evans, 1973; Au, 1993; Reynolds and Rommel, 1999). A sequence of events analogous to that described for bats has been recorded from echolocating narwhals *Monodon monoceros* (Miller *et al.*, 1995), sperm whales *Physeter macrocephalus* (Miller *et al.*, 2004), and beaked whales *Mesoplodon densirostris* and *Ziphius cavirostris* (Johnson *et al.*, 2004; Madsen *et al.*, 2005; Johnson *et al.*, 2008). All toothed whale species studied do emit regularly spaced clicks, thought to function in echolocation as does the search phase of bat echolocation, and they also produce terminal buzzes, as bats do (Au, 1993; Miller *et al.*, 1995; Møhl *et al.*, 2000; Johnson *et al.*, 2004; Miller *et al.*, 2004; Thomas *et al.*, 2004).

Buzz production rate has been proposed as a proxy for toothed whale foraging success rate (Miller *et al.*, 2004; Watwood *et al.*, 2006). Since direct observation of prey capture events by foraging toothed whales is difficult or impossible, classifying echolocation buzzes as successful or failed prey capture attempts has also proved elusive; therefore studies of toothed whales to date have not reported any reliable acoustic indicators of prey capture success. Without such indicators, it is difficult to estimate the actual mass of prey consumed based on the buzz rate proxy.

The majority of buzzes produced by sperm whales are followed by pauses of about 5 seconds (Miller *et al.*, 2004), while beaked whales often pause for much less than a second after buzzes (Johnson *et al.*, 2004). Sperm whales

also pause regular clicking at intervals during the search phase of echolocation; these pauses are thought to be related to redistribution of air within the sound generating apparatus (Wahlberg, 2002). Pauses following buzzes might serve the same function, or might be related to prey handling time as is thought to be the case in bats.

Beaked whales initiate buzzes when they are about one body length (~4 m) from their selected prey item (Madsen *et al.*, 2005). In comparison, bats initiate buzzes at distances of about 2-10 body lengths (Daubenton's bat *Myotis daubentonii*, 10-22 cm (Kalko and Schnitzler, 1989); European pipistrelles *Pippistrellus* sp., about 50 cm (Kalko, 1995)). Published data on toothed whales do not indicate whether prey capture occurs during or after the buzz, but for beaked whales and sperm whales, capture has been assumed to occur at or near the end of the buzz based on two lines of evidence: the timing of impact sounds in tag audio recordings (Johnson *et al.*, 2004) and the observed increase in angular acceleration near the end of the buzz (Johnson *et al.*, 2004; Miller *et al.*, 2004).

In summary, toothed whales, like bats, use echolocation for orientation and prey capture. Although the echolocation signal characteristics and target detection abilities of various toothed whale species have been investigated, there have been relatively few experiments that recorded the acoustic behavior of free swimming animals as they use echolocation to find prey. Tagging studies have provided data on sound production and animal movements during foraging behavior for a variety of species, including sperm whales (*Physeter macrocephalus*: Madsen *et al.*, 2002a; Miller *et al.*, 2004; Teloni *et al.*, 2008a), beaked whales (*Mesoplodon densirostris* and *Ziphius cavirostris*: Madsen *et al.*, 2005; Johnson *et al.*, 2006; Tyack *et al.*, 2006), pilot whales (*Globicephala macrorhynchus*; Aguilar Soto *et al.*, 2008), finless porpoises (*Neophocaena phocaenoides*; Akamatsu *et al.*, 2005), and harbor porpoises (*Phocoena*

phocoena; Akamatsu *et al.*, 2007). While these studies have provided a wealth of information on echolocation click production rates and characteristics in relation to animal depth and movements, none of them were able to collect data on timing of capture or prey capture success rates. Several papers also describe and discuss intriguing evidence of variability in the echolocation strategies of beaked whales (Madsen *et al.*, 2005; Johnson *et al.*, 2008) and sperm whales (Teloni *et al.*, 2008a). The studies linked different prey capture strategies to variation in prey type pursued, as evidenced by variation in prey echo characteristics (Johnson *et al.*, 2008) or capture depth (Teloni *et al.*, 2008b); however, none of the researchers had the means to collect field data on prey species captured. Without such data, it is more difficult to interpret variability in echolocation strategies in response to different prey types, and it is not possible to assess how the timing of echolocation phases relates to the actual capture time.

In the current study, I applied archival tags to captive harbor porpoises as they captured fish. The tags logged acoustic and movement data during the prey captures, allowing me to analyze and describe the animals' detailed echolocation behavior leading up to and following prey capture events. Specifically, I was able to test the hypotheses that the porpoises would:

- initiate echolocation buzzes just before the time of prey capture, when they were about one body length away from the prey fish;
- terminate those buzzes at or just before the time of prey capture;
- reduce their click amplitude significantly during buzzes; and
- respond to differences in experimental conditions (primarily, availability of visual cues and prey type) by varying the timing of their approach to prey and the level and timing of their echolocation clicks.

2.2 Methods

2.2.1 Tag development and tag specifications

To carry out the prey capture experiments, a modified version of the Dtag (Johnson and Tyack, 2003) was developed for use with captive harbor porpoises. The current version of the Dtag has a maximum sampling frequency of 192 kHz, which is insufficient to record high-frequency porpoise vocalizations. Since porpoise clicks are centered at about 130 kHz and have a -3dB bandwidth of about 16 kHz (Au *et al.*, 1999), audio recordings of porpoise clicks must be sampled at 300 kHz or more to avoid aliasing. To add this high-frequency sampling capacity to the Dtag, I worked with Alexander Bahr, who developed a new audio recording circuit for the tag. The resulting porpoise tag records audio data in stereo, digitizing the data at sampling frequencies of up to 500 kHz per channel at 16-bit resolution and storing it in onboard memory. The peak clip level of the tag audio recordings was 191 dB re 1 µPa. The tag synchronously records data from movement sensors (sampled 50 times per second), including 3-axis accelerometers and magnetometers and a pressure sensor, which allow calculation of the animal's acceleration, pitch, roll, heading and depth. With lossless data compression, the tag can record about an hour of audio and sensor data in its 3 GB memory. The tag attaches to porpoises noninvasively, with custom-made suction cups, as shown in Figure 2.1.

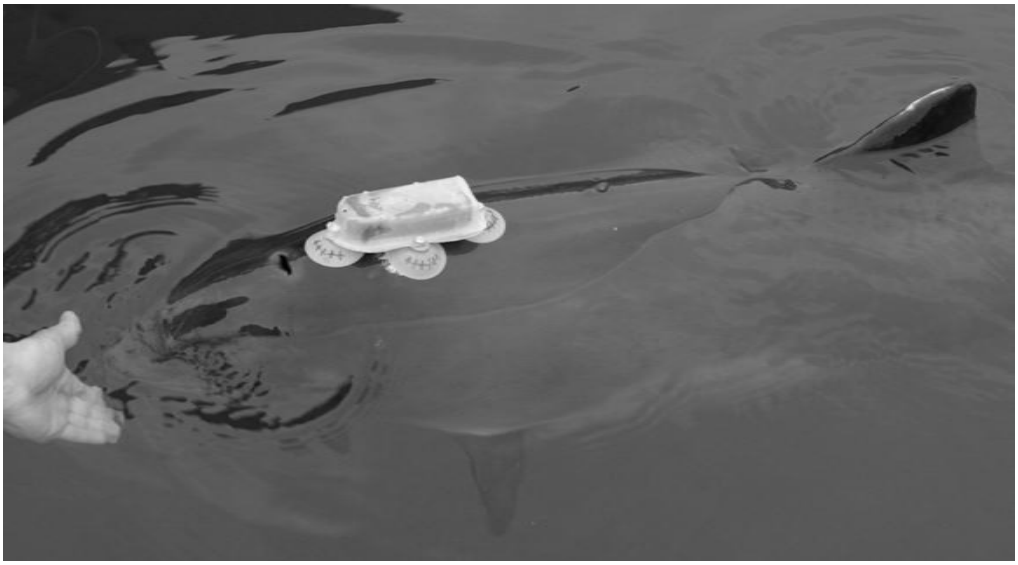

Figure 2.1. The porpoise tag attached to a captive porpoise at the Fjord & Baelt Center, Kerteminde, Denmark. Photo by Alexander Bahr.

2.2.2 Prey capture experiments

Prey capture experiments took place at the Fjord & Baelt Center in Kerteminde, Denmark, which houses 4 captive harbor porpoises. Two porpoises, Eigil (male; at Fjord & Baelt since April 1997) and Sif (female; at Fjord & Baelt since July 2004) participated in the experiments. The porpoises were trained to carry the tag, which was attached dorsally just behind the blowhole as shown in Figure 2.1. At the start of each prey capture trial, a trainer called the tagged porpoise to a station at one end of the experimental pool. On a cue from the trainer, the tagged porpoise was sent across the pool; at the same cue, an assistant at the other end of the pool slapped the water surface with a stick (as an initial orientation cue for the porpoise) and then dropped a fish into the water at the same location. The porpoises' task was to find and eat the fish, then return to station with the trainer at the other end of the pool. During each trial, in addition to tag data, I made underwater video recordings of the prey captures, and I collected stopwatch data on the times of key events (trainer cues, fish release, and prey capture (defined as first physical contact between the

porpoise's mouth and the fish)). The tag, video and stopwatch data were all time-synchronized.

Trials were conducted with and without eyecups (suction cups that covered the porpoises' eyes like blindfolds and forced them to locate the fish without the aid of vision). I ran 71 prey capture trials between January 9 and January 13, 2008. Trials were carried out in 12 sessions of 4-8 trials per session; all sessions contained trials with and without eyecups and trials with different fish types. Fish used in the trials were dead, frozen fish from the same stock that comprised the porpoises' normal diet at Fjord & Baelt. They included herring (*Clupea harengus*, 28 fish total, mean fork length 21.0 cm), capelin (*Mallotus villosus*, 37 total, mean fork length 15.1 cm), and sprat (*Sprattus sprattus*, 6 fish total, mean fork length 12.6 cm). Table 2.1 presents detailed information on the characteristics of each trial.

Date	Session	Trial #	Porpoise	Eye Cups Y/N	Fish	Success Y/N
1/9/2008	pp08_009a	1	Eigil	N	C	Y
1/9/2008	pp08_009a	2	Eigil	N	H	Y
1/9/2008	pp08_009a	3	Eigil	Y	S	Y
1/9/2008	pp08_009a	4	Eigil	Y	H	Y
1/9/2008	pp08_009a	5	Eigil	Y	H	Y
1/9/2008	pp08_009a	6	Eigil	N	S	Y
1/9/2008	pp08_009b	1	Eigil	N	S	Y
1/9/2008	pp08_009b	2	Eigil	N	H	Y
1/9/2008	pp08_009b	3	Eigil	Y	H	Y
1/9/2008	pp08_009b	4	Eigil	Y	C	Y
1/9/2008	pp08_009b	5	Eigil	Y	C	Y
1/9/2008	pp08_009b	6	Eigil	Y	H	Y
1/9/2008	pp08_009b	7	Eigil	N	H	Y
1/9/2008	pp08_009c	1	Eigil	Y	C	Y
1/9/2008	pp08_009c	2	Eigil	Y	H	Y
1/9/2008	pp08_009c	3	Eigil	N	C	Y
1/9/2008	pp08_009c	4	Eigil	N	H	Y
1/10/2008	pp08_010a	1	Eigil	N	C	Y
1/10/2008	pp08_010a	2	Eigil	N	H	Y
1/10/2008	pp08_010a	3	Eigil	Y	C	Y
1/10/2008	pp08_010a	4	Eigil	Y	H	Y
1/10/2008	pp08_010a	5	Eigil	Y	H	Y
1/10/2008	pp08_010a	6	Eigil	N	C	Y
1/10/2008	pp08_010c	1	Eigil	Y	C	Y
1/10/2008	pp08_010c	2	Eigil	Y	H	Y
1/10/2008	pp08_010c	3	Eigil	Y	H	Y
1/10/2008	pp08_010c	4	Eigil	N	C	Y

1/10/2008	pp08_010c	5	Eigil	N	S	Y
1/10/2008	pp08_010c	6	Eigil	N	H	Y
1/11/2008	pp08_011a	1	Eigil	N	C	Y
1/11/2008	pp08_011a	2	Eigil	N	C	Y
1/11/2008	pp08_011a	3	Eigil	Y	C	Y
1/11/2008	pp08_011a	4	Eigil	Y	C	Y
1/11/2008	pp08_011a	5	Sif	N	C	Y
1/11/2008	pp08_011a	6	Sif	N	C	Y
1/11/2008	pp08_011a	7	Sif	N	C	Y
1/11/2008	pp08_011a	8	Sif	N	C	Y
1/12/2008	pp08_012a	1	Sif	N	C	Y
1/12/2008	pp08_012a	2	Sif	N	C	Y
1/12/2008	pp08_012a	3	Sif	Y	H	Y
1/12/2008	pp08_012a	4	Sif	Y	C	Y
1/12/2008	pp08_012a	5	Sif	Y	S	N
1/12/2008	pp08_012a	6	Sif	N	C	Y
1/12/2008	pp08_012a	7	Sif	f	C	Y
1/12/2008	pp08_012b	1	Sif	Y	C	N*
1/12/2008	pp08_012b	2	Sif	Y	C	Y
1/12/2008	pp08_012b	3	Sif	Y	H	Y
1/12/2008	pp08_012b	4	Sif	N	C	Y
1/12/2008	pp08_012c	1	Sif	N	H	Y
1/12/2008	pp08_012c	2	Sif	N	H	Y
1/12/2008	pp08_012c	3	Sif	Y	C	Y
1/12/2008	pp08_012c	4	Sif	Y	C	Y
1/12/2008	pp08_012c	5	Sif	f	C	Y
1/12/2008	pp08_012c	6	Sif	Y	C	N
1/12/2008	pp08_012c	7	Sif	Y	C	Y
1/13/2008	pp08_013a	1	Sif	Y	H	N

1/13/2008	pp08_013a	2	Sif	Y	C	Y
1/13/2008	pp08_013a	3	Sif	Y	C	Y
1/13/2008	pp08_013a	4	Sif	Y	H	Y
1/13/2008	pp08_013a	5	Sif	f	H	Y
1/13/2008	pp08_013a	6	Sif	Y	H	Y
1/13/2008	pp08_013c	1	Sif	N	H	Y
1/13/2008	pp08_013c	2	Sif	N	H	Y
1/13/2008	pp08_013c	3	Sif	N	C	Y
1/13/2008	pp08_013c	4	Sif	Y	H	Y
1/13/2008	pp08_013c	5	Sif	Y	C	Y
1/13/2008	pp08_013c	6	Sif	Y	C	Y
1/13/2008	pp08_013e	1	Sif	Y	H	Y
1/13/2008	pp08_013e	2	Sif	Y	H	Y
1/13/2008	pp08_013e	3	Sif	N	S	Y
1/13/2008	pp08_013e	4	Sif	N	C	Y

Table 2.1. Detailed information on prey capture trials. Abbreviations of fish type are as follows: C, capelin; H, herring; S, sprat. An "f" in the eyecups column means that eyecups fell off before the prey capture attempt; these trials were analyzed as no-eyecups trials. *Indicates a trial in which the porpoise did not catch the fish, not because of failure to find it, but because it was stolen by another porpoise before he arrived.

2.2.4 Data analysis

Timing of prey capture

For each trial, I used the stopwatch data to calculate the time it took the porpoises to catch each fish, defined as the time from trainer cue until the fish (or part of the fish) was in the porpoise's mouth. (In these experiments, porpoises were never observed to lose or drop fish after having them in their mouths,

although they did sometimes manipulate or carry the fish briefly before swallowing them.) I applied a two-sample t-test to check whether the mean capture duration was different for trials with and without eyecups.

Porpoise acoustic behavior during prey capture

For each trial, a 30-second segment of the tag audio recording was analyzed: 15 seconds before and 15 seconds after the stopwatch time of prey capture. Tag audio data were filtered in Matlab (The Mathworks, Natick, MA) with a 4-pole Butterworth bandpass filter between 100 and 200 kHz. (The filter was applied in both forward and reverse directions, using the filtfilt Matlab command, to avoid time-shifting of the output signal.) Porpoise clicks were detected in the filtered audio recordings using a custom-written envelope-based click detector in Matlab. Selected Matlab code used in the analysis is included in Appendix B. The click detection algorithm was designed to detect clicks despite high variability in data click levels and inter-click intervals. Briefly, it proceeded as follows:

1. Calculate the envelope of the audio signal; detect candidate clicks at any time point where the envelope of the signal exceeds the detection threshold.
2. After a candidate click is detected, do not detect any additional clicks within 1.3 msec following the initial detection. (This blanking time was selected after manual inspection of prey capture buzzes in the dataset; none of the examined buzzes contained inter-click intervals of less than 1.3 msec.)
3. Compare the maximum envelope level of the detected click to L, the mean of the maximum envelope levels of the preceding three clicks. Compare the inter-click interval (ICI) preceding the detected click to I, the mean ICI of the preceding three clicks. If the detected click level is at least $0.5L$ and the detected click ICI is at least $0.2I$, accept it; otherwise reject. This

criterion serves to eliminate many surface and bottom reflections from the set of detected clicks.

4. If the detected click does not meet the ICI acceptance criterion in (3), but its level is at least *3L*, accept it anyway.
5. If the detected click does not meet the level acceptance criterion in (3), but its ICI is at least *3I*, accept it anyway, and reset *I* to 100 msec. This rule allows detection of trains of quiet clicks even after sudden drops in click level, without promoting detection of quiet reflections/echoes between higher amplitude clicks.

Click detector performance was checked visually by examining plots of the data waveforms overlaid with click detections. The time (in seconds until prey capture) and peak-to-peak (pp) level of each detected click was recorded. For plotting and further analysis, the click time-series data were binned into 0.2 second time periods, and the mean level and click rate were calculated for each bin.

To allow calculation of echolocation buzz start times, end times and durations, I arbitrarily defined the buzz as the time period during which click rate exceeded 125 clicks per second (about 3-4 times the mean pre-buzz click rate, and slightly higher than the upper values observed in transient variations about that mean (Fig. 2.3)). For the purposes of my calculations, a buzz started when the threshold click rate of 125 clicks per second was first exceeded, and ended when the click rate fell below threshold for the last time. Using the above criteria, I calculated the start time, end time and duration of each prey capture buzz, as well as the mean start time, end time and buzz duration for the set of all 67 successful captures. I did not include buzzes that ended more than 5 seconds before prey capture or began more than 5 seconds after prey capture in our analysis. Those time limits are somewhat arbitrary, but as Figure 2.3 shows, buzzes outside those time limits did not seem to be associated with prey capture.

Rather, the rare buzzes that occurred more than 5 seconds before capture were probably related to non-prey objects (including landmarks or other porpoises) in the pool, and the buzzes that occurred more than 5 seconds after capture were likely related to the porpoises' returning to station with the trainers.

Bats and toothed whales often fall silent for a short period following an echolocation buzz; the duration of this pause was calculated for each of the 67 successful prey captures by determining the longest inter-click interval in the 5 seconds following prey capture.

2.3 Results

Timing of prey capture

It took the porpoises an average of 19.6 seconds to find and collect a fish while wearing eyecups, significantly longer than the 15.9 second average time without eyecups (t-test, df = 32, p = 0.000027).

Porpoise acoustic behavior during prey capture

The porpoises produced echolocation buzzes in 66 of the 67 successful prey capture trials. Figure 2.2 shows the data on click rate as a function of time for all 67 prey capture trials; it clearly indicates that, on average, the porpoises began buzzing before they captured the fish, and continued to buzz after the capture event. On average, maximum buzz rates exceeded 300 clicks per seconds, and coincided with the time of prey capture.

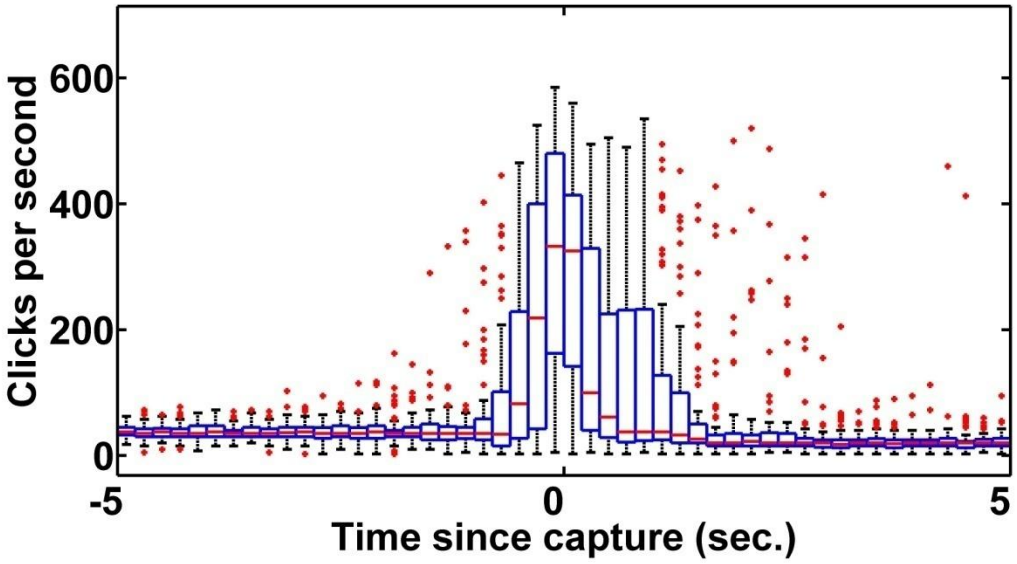

Figure 2.2. Box-and-whiskers plot of click rate as a function of time for 67 prey captures by harbor porpoises (data in 0.2 sec bins). The red horizontal lines indicate the median value in each time bin; the top and bottom of the blue rectangle indicate the upper and lower quartiles within the bin. The dotted black lines extend to the largest and smallest observed values in the time bin, up to 1.5 times the interquartile range beyond the blue box. Larger and smaller observed values are outliers, plotted as red dots.

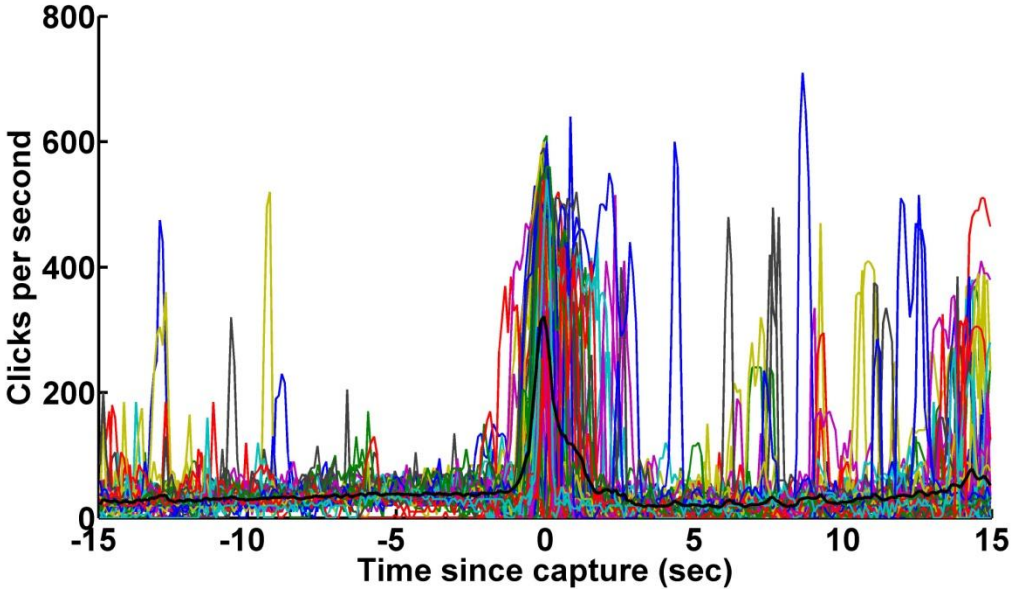

Figure 2.3. Click rate as a function of time since prey capture. Each trace presents data from one prey capture trial; the thick black line presents the mean click rate over all 67 trials.

For the 66 captures in which buzzes were detected, the mean buzz start time was 0.53 seconds before prey capture, end time was 0.83 seconds after prey capture, and mean buzz duration was 1.37 seconds. Figure 2.4 shows a stack plot of the start times, end times, and durations of all detected buzzes. After buzzes, porpoises paused their echolocation clicks for brief periods ranging from 65 msec to 2.1 sec; average pause duration over 67 successful captures was about 481 msec. This mean duration was about 10 times the average pre-capture inter-click interval (Figure 2.2). The minimum observed pause durations, however, were only slightly longer than the mean observed inter-click interval, and thus probably do not represent readily discernable pauses in click emission. Only 9 of the 67 pauses had durations of 1 second or greater.

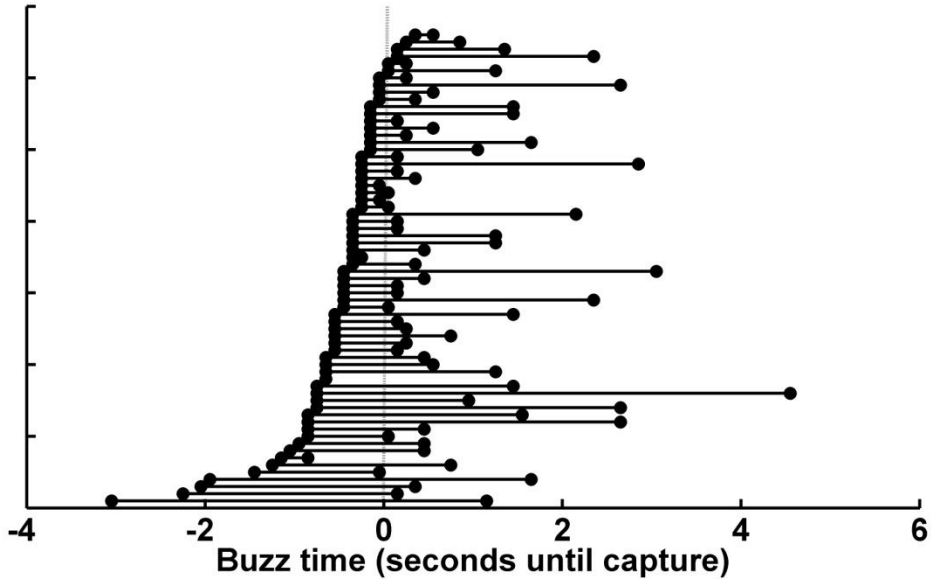

Figure 2.4. Start times, end times, and durations of buzzes detected during 66 prey captures. Y axis indicates buzz number (in this figure, buzzes are ordered according to start time). Some buzzes apparently begin after prey capture, probably because low-amplitude clicks earlier in the buzz were not detectable on the tag recordings (see Discussion section for further explanation).

During buzzes, porpoises not only increased their click rate but also apparently decreased the level of their emitted clicks by about 12 dB. Figure 2.5 shows the data on tag-recorded click level as a function of time for all 67 successful prey captures. Because the tag was attached physically to the animal and positioned off-axis, behind the sound generator, these level measurements do not indicate source levels. They are probably at least 40 dB lower than on-axis source levels (Hansen, 2007). However, they may still provide some information about the relative amplitudes of emitted clicks.

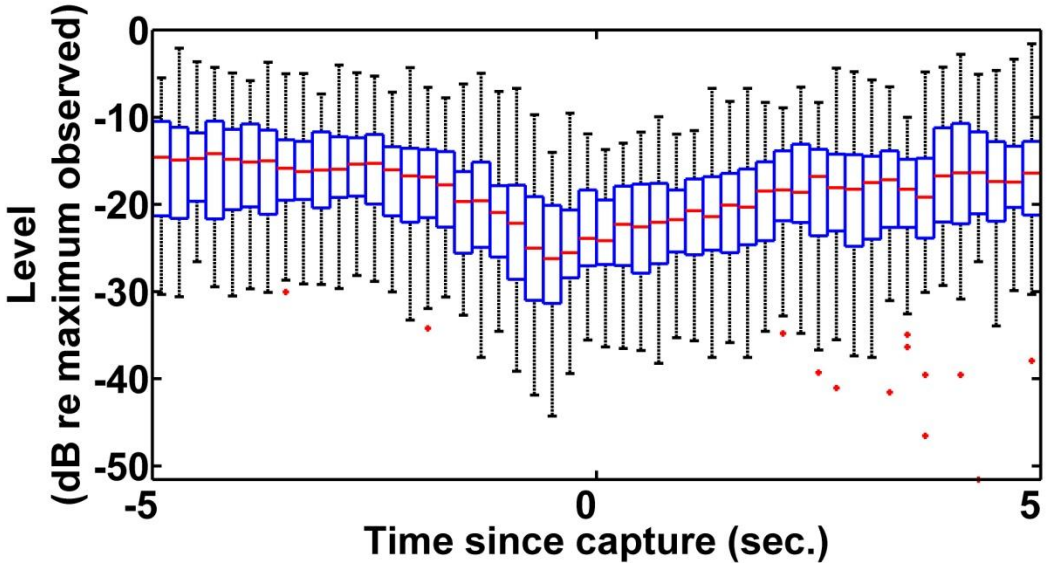

Figure 2.5. Box-and-whiskers plot of click level as a function of time for 67 prey captures by harbor porpoises (data in 0.2 sec bins). Levels are the off-axis, on-animal levels from the tag recordings, not click source levels. The red horizontal lines indicate the median value in each time bin; the top and bottom of the blue rectangle indicate the upper and lower quartiles within the bin. The dotted black lines extend to the largest and smallest observed values in the time bin, up to 1.5 times the interquartile range beyond the blue box. Larger and smaller observed values are outliers, plotted as red dots.

As a summary of the information presented in Figures 2.2 and 2.5, Figure 2.6 shows mean click rates and levels as a function of time for the 67 capture trials. This format does not give an accurate indication of the amount of scatter in the observations, but is convenient for comparing click rate and level under various conditions, so I have used it for subsequent figures.

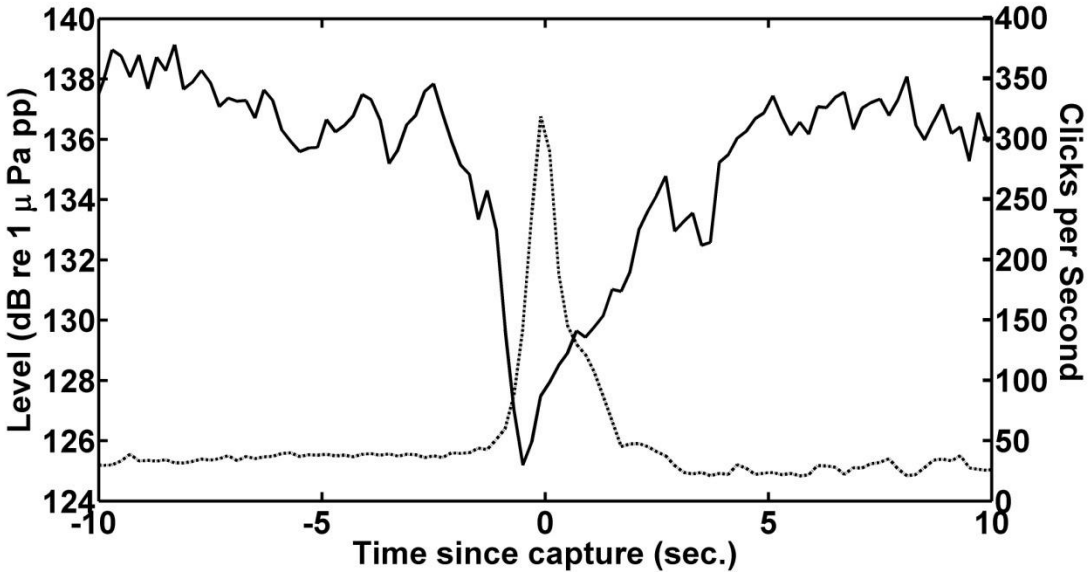

Figure 2.6. Mean click rate and level as a function of time for 67 prey captures. The solid line indicates click level, while the dotted line indicates click rate.

Figures 2.9 – 2.10 compare click rates and levels between varying sets of conditions: with and without eyecups (Fig. 2.7); Eigil versus Sif (Fig. 2.8); herring versus capelin (Fig. 2.9); and herring vs. capelin, for Eigil and Sif individually (Fig. 2.10). As shown in Figure 2.7, the presence or absence of eyecups had no obvious effect on maximum buzz click rate; buzzes appeared to begin slightly earlier in trials with eyecups, and they were slightly longer (or included a second peak in click rate after capture) in trials with eyecups. Compared to trials without eyecups, click levels during trials with eyecups tended to be a bit lower before capture and a bit higher after. Figure 2.8 shows that Sif tended to use click levels about 5-10 dB higher than Eigil at all times; in addition, her buzz click rate was much faster than his. Figure 2.9 compares click rates and levels for herring and capelin captures. While click rates were very similar for these conditions, mean click levels were about 3 dB higher for capelin captures, except immediately preceding prey capture, when they were equal. Sif tended to produce higher-amplitude clicks than Eigil, and she also participated in more

trials with capelin than he did – a combination of conditions that might account for part or all of the observed herring/capelin level difference. To investigate that possibility, I plotted click rate and level for herring versus capelin for Eigil and Sif individually (Fig. 2.10). Like the pooled data in Figure 2.9, the individual-animal data showed that click levels were about 3 dB higher during capelin captures than during herring captures.

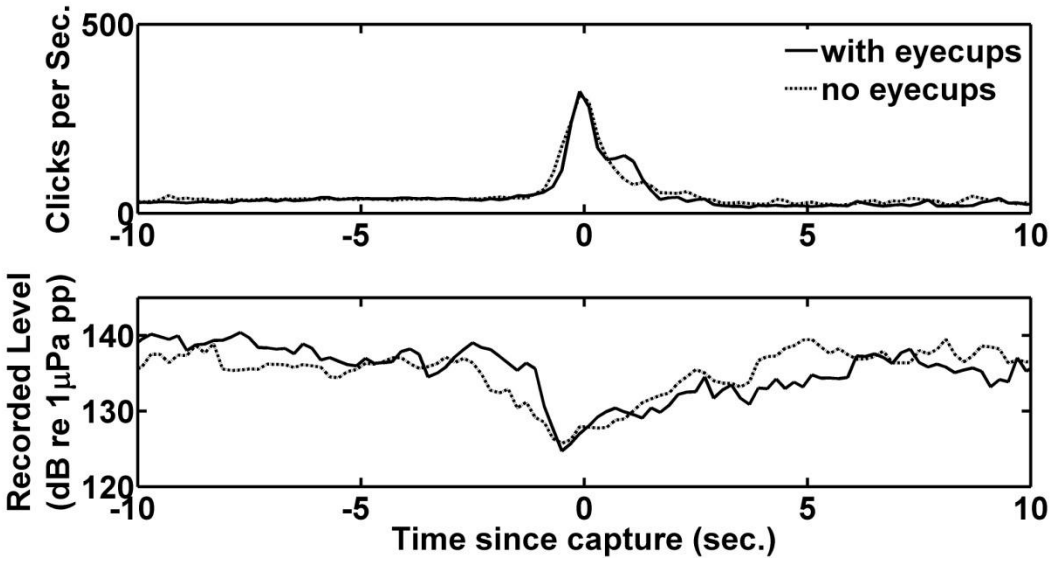

Figure 2.7. Porpoise click rates (top panel) and levels (bottom panel) as a function of time. Solid traces show data from trials without eyecups (n = 34); dotted traces show data from trials with eyecups (n = 33).

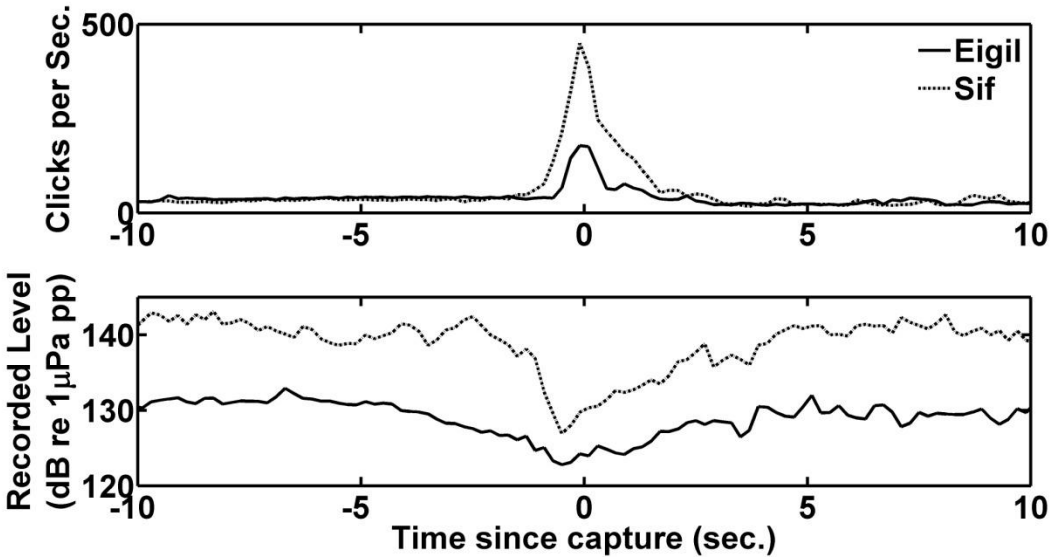

Figure 2.8. Porpoise click rates (top panel) and levels (bottom panel) as a function of time. Solid traces show data from trials with Eigil (n = 33); dotted traces show data from trials with Sif (n = 34).

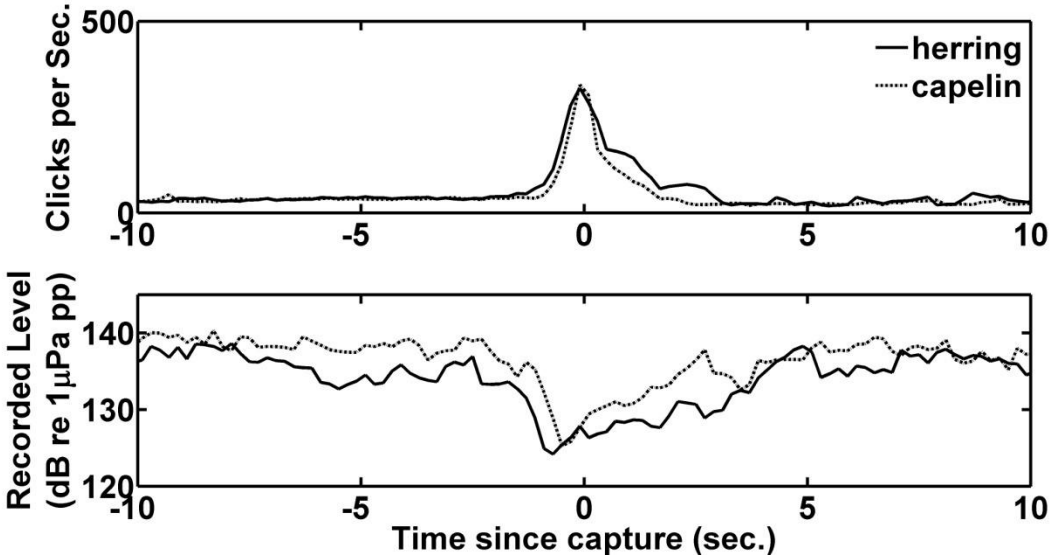

Figure 2.9. Porpoise click rates (top panel) and levels (bottom panel) as a function of time. Solid traces show data from trials with herring (n = 27); dotted traces show data from trials with capelin (n = 35).

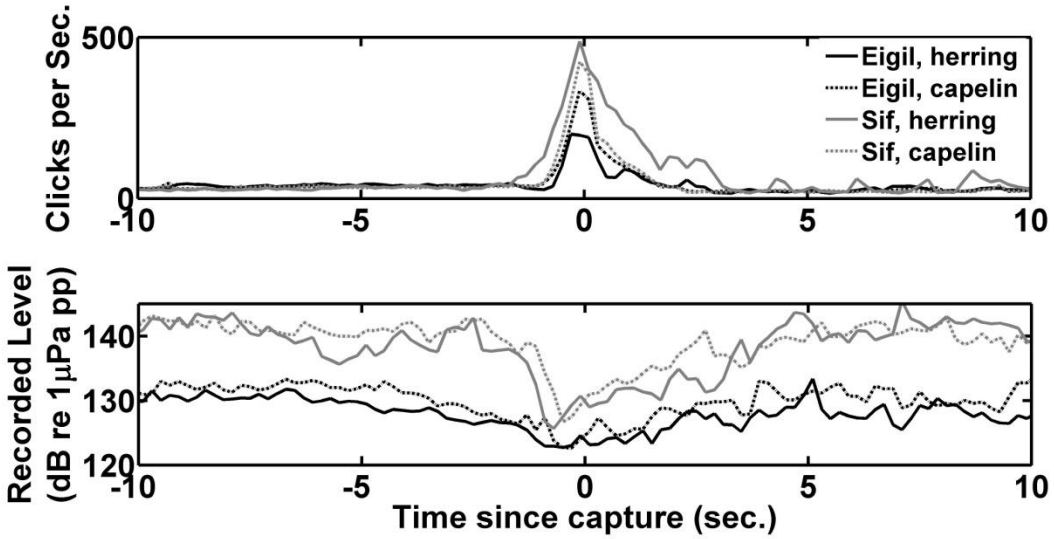

Figure 2.10. Porpoise click rates (top panel) and levels (bottom panel) as a function of time. Solid black traces show data from trials with Eigil catching herring (n = 15); dotted black traces show data from trials with Eigil catching capelin (n = 14); solid grey traces show data from trials with Sif catching herring (n = 12); dotted grey traces show data from trials with Sif catching capelin (n = 21).

In addition to considering variations in click rate and level as functions of time since prey capture, I also investigated click level as a function of inter-click interval, or ICI (Figure 2.11). Click levels were relatively constant for ICIs greater than about 40 msec, but they decreased with decreasing ICI for ICIs less than about 40 msec. As shown in Figure 2.11, for ICIs of about 10-50 msec (corresponding to click rates of 20-100 clicks/second), the increase in median and maximum observed click levels as a function of ICI seemed to fit a $20\log_{10}(\text{ICI})$ curve relatively well. Figure 2.12 shows the click level versus ICI data as a scatter plot. The figure does not provide evidence for a clear distinction between buzz clicks and regular clicks on the basis of either ICI or click level. It is important to note that, although I tried to optimize the click detector to detect only clicks produced by the tagged porpoise, I cannot be

certain that none of the detected clicks were produced by other animals; some of the clicks in Figure 2.12 (perhaps especially the highest-amplitude clicks) may have been produced by animals other than the tagged porpoise.

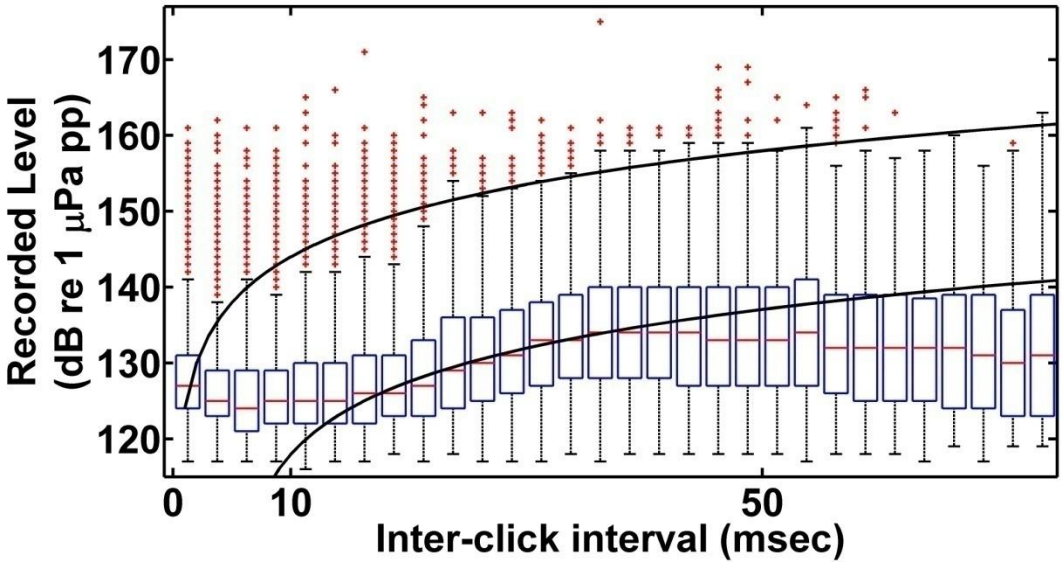

Figure 2.11. Box-and-whiskers plot of click level as a function of inter-click interval (or ICI; data in 2.5 msec bins). The red horizontal lines indicate the median value in each ICI bin; the top and bottom of the blue rectangle indicate the upper and lower quartiles within the bin. The dotted black lines extend to the largest and smallest observed values in the ICI bin, up to 1.5 times the interquartile range beyond the blue box. Larger and smaller observed values are outliers, plotted as red dots. The solid black lines show expected click levels, if levels varied as a function of ICI according to $level = 20\log_{10}(ICI) + constant.$ The lines have the same rate of increase, but are roughly scaled to fit mean and maximum observed click levels.

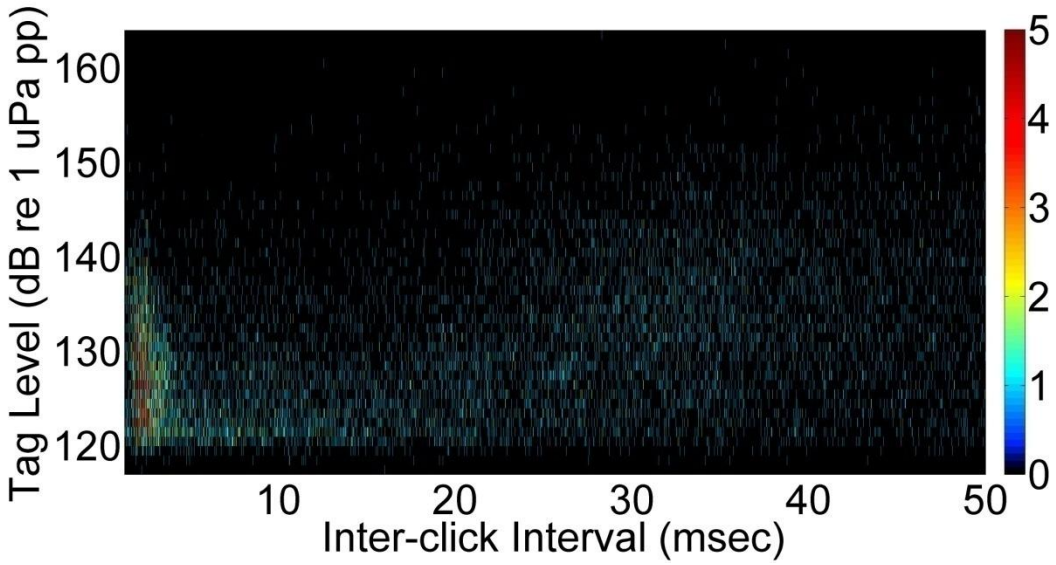

Figure 2.12. Click level as a function of inter-click interval for all 171138 detected clicks in 67 prey capture trials. Color scale indicates the number of times a particular level/inter-click interval combination was observed.

2.4 Discussion

2.4.1 Use of Echolocation and Buzz Timing

In all 67 of the successful prey capture trials, porpoises produced echolocation clicks throughout the prey capture trial regardless of whether or not they were wearing eyecups; in only one of the 67 trials did the porpoise capture the fish without producing an echolocation buzz. In certain conditions, some bats and dolphins have been shown to use passive listening rather than echolocation to find and capture prey (Fiedler, 1979; Wood and Evans, 1980; Gannon *et al.*, 2005). In these experiments, however, it seems that the porpoises always relied on active biosonar rather than passive listening to locate and capture prey fish. That finding is relatively unsurprising given my experimental set-up; passive listening for splashes could have provided the porpoises with information about the location where the prey fish was thrown into the water, but the dead fish would not have produced much further noise as they sunk and drifted in the

water. Passive listening may be favored when active echolocation has high ecological costs. However, given the extremely high frequency of porpoise clicks, the probability of their detection by either prey fish or predators is very low, so the ecological cost of porpoise echolocation is limited. Another reason to choose passive listening over biosonar might be energetic costs associated with sound production (Gannon *et al.*, 2005), which have not been quantified for toothed whales. In bats, the cost of producing echolocation calls is high for stationary animals (Speakman *et al.*, 1989), but the added cost of calling once flying is extremely low, because the muscular exertions required for sound production also occur during flight (Speakman and Racey, 1991). In any case, my experiments probably do not provide reliable data to test the hypothesis that energetic costs favor adoption of a passive listening strategy, since the captive porpoises I studied were consistently well fed.

To my knowledge, no previously published study has been able to determine the timing and duration of toothed whale echolocation buzzes in relation to the time of prey capture. Unlike bats, for which the end of the echolocation buzz occurs before or coincides with prey capture (Griffin *et al.*, 1960; Kalko and Schnitzler, 1989; Hartley, 1992b; Kalko, 1995; Moss and Surlykke, 2001; Hiryu *et al.*, 2007; Melcón *et al.*, 2007), the harbor porpoises in this study continued their buzzes after the capture event occurred. This extension of the buzz phase may not be physically possible for bats once they have actually begun to consume prey, since chewing and swallowing prey could prevent them from vocalizing. However, it has been suggested that certain bats' pre-capture buzzes continue beyond the last moment at which they would actually have time to receive and process returning-echo information (Melcón *et al.*, 2007). In porpoises, the continuation of the buzz post-capture may also stem from a physiological limitation related to their pneumatic click production mechanism; they may not be able to terminate buzz production abruptly at a precise time. Alternately, continuing to buzz after capture may be adaptive,

allowing immediate re-localization of prey items that escape after nearly-successful capture attempts or facilitating post-capture pursuit of new, nearby prey items (for schooling prey like herring).

Almost all of the porpoises' prey capture attempts were successful during our experimental trials, probably because of the lack of escape reactions in the prey. Consequently, my dataset is not suitable for comparing the post-buzz pause durations and click characteristics of successful and unsuccessful capture attempts. I did not analyze the frequency characteristics of the post-buzz clicks in detail, and it is possible that distortion and reverberation caused by recording clicks off-axis with a recorder in contact with the animal would obscure potential frequency spectrum-related indicators of capture success (Surlykke *et al.*, 2003). Nevertheless, my future plans for continued analysis of our dataset include attempts to identify possible acoustic cues indicating prey capture success.

2.4.2 Click Rates

In this study, I observed click rates of up to 640 clicks per second during echolocation buzzes, corresponding to an inter-click interval (ICI) of about 1.6 msec. The average peak click rate during a buzz was 321 clicks per second (3.1 msec ICI). These rates are consistent with previous observations of harbor porpoise buzzes (Verboom and Kastelein, 2004; Akamatsu *et al.*, 2007). However, I consider them to be minimum estimates of the actual observed click rates, since many buzz clicks had levels near the lower detection limits of the tag; I therefore suspect that a significant number of additional, even quieter clicks went undetected during buzzes.

During pre-buzz periods, the average click rate of the porpoises in this study was about 35 clicks per second, corresponding to an ICI of about 29 msec (Figs. 2.2-2.3). The mean ICI was relatively constant over time, decreasing slightly from about 39 msec 15 seconds before capture to about 26 msec just prior to initiation of the echolocation buzz (Fig. 2.3). Assuming that porpoises

wait for echoes from one click to arrive before producing the next click, the maximum distance inspected by clicks with 26-39 msec ICIs would be about 19-29 m (calculated by assuming that ICI = two-way travel time from source to target, with a sound speed of 1500 m/s; this method estimates a maximum inspected distance because it makes no time allowance for auditory processing between receipt of the returning echo and emission of the next click). This 19-29 m maximum inspected range estimate makes sense given that the net pen in which the animals were enclosed during the experiments is about 20 m long. The average ICI observed in this study (29 msec) was very similar to the minimum ICI of 30 msec observed in Villadsgaard and colleagues' (2007) study of free-ranging harbor porpoises in Danish waters. ICIs of up to 200 msec were also observed in the Danish study. Thus, free-ranging animals may use longer ICIs to inspect somewhat more distant targets than the porpoises in my study; an ICI of 58 msec (the median observed by Villadsgaard *et al.*, 2007) would correspond to a maximum inspected distance of 43.5 m, and an ICI of 200 msec (the maximum observed by Villadsgaard *et al.*, 2007) would correspond to a maximum inspected distance of 150 m (calculated as above). If the assumption that inter-click interval is related to inspected range is correct, and assuming that porpoises do need some time to process echoes from one click before emitting the next, it seems likely that porpoises generally focus their echolocation on targets at ranges of less than 40m.

For captive bottlenose dolphins echolocating on synthetic targets, inter-click interval increases as a function of dolphin-target range; it is equal to the two-way travel time between dolphin and target, plus a fixed lag time thought to be related to auditory processing (Au, 1993). I do not currently have data on porpoise-prey ranges for our prey capture experiments, so I cannot analyze the relationship between ICI and target range in detail. However, I note that the distance from the porpoises' start position to the prey capture location was approximately 18 m. If porpoises vary their ICI as a function of target range like

dolphins do, one would expect ICI to decrease by about 24 msec over the 15-20 seconds between trainer cue and prey capture (2 × 18 m ÷ 1500 m/sec = 0.024 sec). This estimated decrease of 24 msec is almost double the 13 msec decrease observed in the mean data ICI (Fig. 2.3); in addition, the median data ICI shows a much smaller change of about 7 msec (Fig. 2.2).

The above calculations, though very approximate, do not provide convincing evidence that porpoise inter-click intervals leading up to prey capture are timed to match the two-way travel time to target plus a fixed lag time. Previous studies with porpoises provide conflicting findings on this topic; while Verfuss and colleagues (2005) found that captive porpoises did reduce their ICIs as they neared an echolocation target during a navigation task, Teilmann and others (2002) found that they did not make similar adjustments during a target detection task.

Given the large amount of scatter in my data and the small range differences considered in this study, it is very possible that the observed relationship between ICI and inferred prey range is not significant. In other words, porpoise inter-click intervals may remain relatively constant as porpoise-prey range declines, then increase rapidly following buzz initiation. This pattern would match more closely with observations from free-ranging echolocating beaked whales and sperm whales. Those species have been found to produce regular clicks at a relatively constant ICI (which far exceeds the expected or measured two-way travel time to their prey) during the search and approach phases, then abruptly switch to a buzz phase during which lower-amplitude clicks are produced much more rapidly (Madsen *et al.*, 2005). However, unlike Madsen and colleagues' (2005) data for Blainville's beaked whales (*Mesoplodon densirostris*), our porpoise data do not indicate a clear distinction between buzz clicks and regular clicks in terms of either level or ICI (Figure 2.12).

On average, the porpoises initiated echolocation buzzes about half a second before prey capture, when they were within a body length or so of the prey fish. The click rate within the buzz generally increased rapidly and peaked around the time of prey capture. Given the small porpoise-target range variation over the course of the buzz, this rapid reduction in ICI (greater than 20 msec) cannot be explained solely as an adjustment to changes in the two-way travel time between porpoise and prey (less than 4 msec). The minimum ICI during buzzes (on average 3.1 msec) was much smaller than the estimated lag time for bottlenose dolphins (about 30 msec; Au, 1993). A rough estimate of porpoise lag time from our data, assuming an ICI of about 30-40 msec at a porpoise-prey range of about 10 m, would be slightly lower, about 15-20 msec – still much longer than the observed buzz ICIs. Assuming that the dolphin lag-time estimate is accurate and the lag time for porpoises is similar, our data suggest the possibility that porpoises may adjust their ICI to allow processing of one echo at a time during the search and approach phases, but process multiple echoes simultaneously during the terminal buzz phase.

2.4.3 Click Levels

My data indicate that porpoises reduce the amplitude of their clicks by about 12 dB during buzzes. While this observation matches the general trend observed in other free-ranging foraging toothed whales, other species display even greater reductions in click levels during buzzes; Blainville's beaked whale buzz clicks are 15-20 dB lower in amplitude than regular clicks (Madsen *et al.*, 2005), and sperm whale buzz clicks about 20 dB lower (Madsen *et al.*, 2002b).

The level of the lowest-amplitude clicks I was able to detect in the tag recordings was 117 dB re 1 µPa peak-to-peak (pp). Because the tag was attached to the animal and positioned directly behind the sound-generating apparatus, this level is of course not an on-axis source level; in fact, on-tag click levels are probably at least 40 dB less than the on-axis source levels of the same

clicks (Hansen, 2007). At 117 dB re 1 µPa pp, the tag detection threshold was too high to detect all porpoise clicks; even so, that threshold was much lower than the detection threshold (136 dB re 1 µPa pp) of tags previously deployed on porpoises in a similar position (Akamatsu *et al.*, 2007). It is likely that many low-level clicks, especially buzz clicks, have gone undetected in tagging studies of porpoises to date (including the present study as well as those of Akamatsu and colleagues (2005; 2007)). In fact, I suspect that my data underestimate porpoise click level reductions during buzzes, and that many buzz clicks had amplitudes too low to be recorded on the tag and detected by the click detector. Since lower-level clicks tended to occur near the start and end of buzzes, failure to detect those lower-level clicks could also have led to error in my estimates of buzz start times, end times and durations.

To address these shortcomings, I have increased the gain on the tag and repeated the prey capture experiments. Analysis of the resulting data should allow more accurate determination of buzz click rates and levels, as well as buzz start times, end times and durations. I also hope that the increased signal-to-noise ratio in the new dataset may render echoes from prey fish detectable in the tag recordings. Echo data would allow me to calculate porpoise-prey ranges, estimate prey detection distances, and investigate whether or not the porpoises can tolerate temporal overlap between outgoing clicks and echoes. Such investigations would greatly facilitate interspecific comparisons of echolocation by porpoises, other toothed whale species, and bats.

My data also indicate that apparent click levels decrease as click rates increase (Figure 2.11). This result may simply reflect the fact that faster clicks during buzzes tend to be quieter than other clicks. It is also possible that the porpoise click generator can output a fixed amount of acoustic energy per unit time, resulting in lower click levels at higher click rates. Acoustic power is proportional to the square of click amplitude. Therefore, if the hypothesis of

limited power output per unit time were correct, one would expect click level to increase with the square of ICI (up to a certain point, at which the inter-click time was sufficient for full recovery or "resetting" of the click production mechanism and all clicks could attain maximum level). Despite the large amount of scatter in my data, they do not contradict the hypothesis (Fig. 2.11).

As discussed earlier, the porpoises in this study did not seem to vary their ICI as a function of range to target. If they did, though, ICI would be directly proportional to range. In that case, it might be possible to explain reductions in click level with ICI as transmit-side automatic gain control (AGC) to correct for transmission loss and stabilize returning echo levels. For echolocation on a single target, one would expect such AGC to result in click levels that increase according to $40\log_{10}(\text{ICI})$ or 12 dB per doubling of ICI, a relationship that does not fit my data.

An increase of 6 dB per doubling of ICI ($20 \log_{10}(\text{ICI})$) is a better, but still relatively unconvincing, fit to the data (Fig. 2.11). A similar pattern, in which click source level increased by 6 dB per doubling of range, has been reported for three species of free-ranging toothed whales: Atlantic spotted dolphins *Stenella frontalis*, white-beaked dolphins *Lagenorhynchus albirostris*, and killer whales *Orcinus orca* (Au and Benoit-Bird, 2003).

For bat species that do use transmit-side AGC, increases in outgoing signal level are also in the range of 6 dB per doubling of range (Hartley, 1992b; Hiryu *et al.*, 2007), resulting in relatively constant intensity incident on the echolocation target. In conjunction with this transmit-side AGC, some bats employ receiver-side AGC, reducing their middle-ear sensitivity by about 4-7 dB per halving of target range (Kick and Simmons, 1984; Hartley, 1992a; Boonman and Jones, 2002). Together, transmit- and receiver-side AGC can maintain constant echo intensity at the level of the cochlea despite changes in bat-target range, which may simplify the bats' echo-processing task.

However, returning to the case of the harbor porpoise, experiments with a captive porpoise provided no evidence of receiver-side AGC (Beedholm *et al.*, 2006). Without receiver-side AGC, increasing outgoing signal intensity by 6 dB per doubling of range would not be enough to maintain constant echo levels as porpoise-prey range varies. It remains unclear whether, or why, most echolocating animals prefer to maintain constant echo levels as they approach prey items; continued and comparative studies of AGC in bats and toothed whales may help clarify the matter. To explore this question further using my dataset, supplementing ICI data with estimates of porpoise-target ranges during the prey capture experiments will be critical.

2.4.4 Comparison of Various Conditions

There were no major differences in echolocation behavior between trials with and without eyecups; this finding suggests that visual information does not strongly influence echolocation click rates and levels. However, porpoises took longer to capture prey when wearing eyecups, so visual input must play some role in prey capture behavior. In trials without eyecups, porpoises seemed to produce slightly longer echolocation buzzes, while in trials with eyecups, they reduced their click levels sooner and more gradually leading up to the buzz (Fig. 2.7).

I observed a striking difference in click levels between the two animals that participated in the study; Sif's clicks had about 5-10 dB higher amplitude than Eigil's, and she also appeared to click faster than Eigil during buzzes. It is possible that the increased buzz click rate observed during Sif's trials is due to the fact that her clicks were louder, and thus more of her buzz clicks were detectable above threshold levels. The large differences observed between Eigil and Sif highlight the potential for intraspecific variation in biosonar click rates and levels, and the need to include multiple animals in studies of echolocation behavior whenever possible. However, Sif is thought to have sustained hearing

damage in the past that caused her to increase her outgoing echolocation click levels (M. Wahlberg, pers. comm.). Consequently, the differences between her and Eigil may exceed the normal range of intraspecific variation; even if so, they provide a useful benchmark for the click level variations that may result from permanent or temporary differences in hearing sensitivity.

Interestingly, I also observed differences in echolocation click levels between trials with herring and capelin; both porpoises' click amplitudes were about 3 dB higher for capelin than for herring (Figs. 2.9-2.10). In my experiments, the acoustic target strength of capelin was measured to be -55dB, about 18dB less than that of herring (-37 dB; S. DeRuiter, data not shown). It is possible that the porpoises were increasing their click amplitude when echolocating for weaker targets to ensure that the echoes were detectable to them; however, a 3dB increase in outgoing click level would probably result in very modest gains in target detectability. For example, consider a wild porpoise producing echolocation clicks with source levels of 191 dB re 1 µPa peak-to-peak at 1 m (Villadsgaard *et al.*, 2007), equivalent to an energy flux density of 140 dB re 1 μPa^2s (Kastelein *et al.*, 1999). Assume that the porpoise listens for returning echoes with a detection threshold of about 27 dB re 1 μPa^2s (Kastelein *et al.*, 1999). In a habitat where transmission loss can be approximated as spherical spreading plus absorption of 0.04 dB/m, the porpoise would be able to detect a herring with a target strength of -37 dB (Ona, 2003) at a range of up to 60 m; for a fish with target strength of -55 dB (18 dB less), that range would be reduced to only 25 m. Increasing the source level of the outgoing click by 3 dB would render the lower-target-strength fish detectable at 29 m rather than 25 m, a very modest increase. (All above calculations were made by equating detection threshold with the sum of source level, two-way transmission loss, and target strength, then solving for range.)

While previous studies have indicated that many bats vary their signal amplitude to compensate for range-dependent transmission loss and maintain prey echoes at relatively constant levels (Hartley, 1992a; Surlykke and Kalko, 2008), similar transmit-side automatic gain control to compensate for variations in prey target strength has not previously been observed (but see Au, 1993 for a brief discussion of the topic for dolphins). In fact, Boonman and Jones (2002) found that while Daubenton's bats (*Myotis daubentonii*) varied their click intensity with target range, their signal amplitude increased by only about 4 dB when target strength was reduced by about 17-18 dB. The corresponding increase in signal amplitude for porpoises echolocating on herring was only about 3 dB. My results are thus consistent with those of Boonman and Jones (2002), who concluded that their bats did not adjust outgoing click amplitude to stabilize received echo levels. Since the difference in herring and capelin target strength is so much larger than the observed increase in click amplitude, it is unlikely that the porpoises were using transmit-side automatic gain control alone to keep echo levels from all prey constant. If possible, quantifying echo levels in increased-gain tag data from recently completed prey capture experiments may shed further light on this issue.

Acknowledgements

Many thanks to Alex Bahr, who designed and built the porpoise tag electronics and suction cups; he also helped with field work. Tom Hurst, Mark Johnson, Alex Bocconcelli and Jeremy Winn provided help with tag design and construction. Carrick Detweiler and Iuliu Vasilescu assisted with suction cup fabrication. I am very grateful to Magnus Wahlberg, Peter Madsen, Marie-Anne Blanchet, Sabina Hansen, Jakob Kristensen, Ida Eskessen, Sanja Heikillä, Laura Delgado, Michael Hansen, Anne Villadsgaard, Kristian Beedholm, Lee Miller, and everyone else at the Fjord & Baelt center for help with data collection, and helpful advice. Peter Tyack provided important comments and advice throughout the project. This project was funded by grant 32031300 from the WHOI Ocean Life Institute. All

experiments with porpoises were approved by the WHOI Institutional Animal Care and Use Committee.

References

Acharya, L., and Fenton, M. B. (**1992**). "Echolocation behavior of Vespertilionid bats (*Lasiurus cinereus* and *Lasiurus borealis*) attacking airborne targets including Arctiid moths," Canadian Journal of Zoology **70**, 1292-1298.

Aguilar Soto, N., Johnson, M. P., Madsen, P. T., Díaz, F., Domínguez, I., Brito, A., and Tyack, P. L. (**2008**). "Cheetahs of the deep sea: deep foraging sprints in short-finned pilot whales off Tenerife (Canary Islands)," Journal of Animal Ecology **OnlineEarly Article**, doi:10.1111/j.1365-2656.2008.01393.x

Akamatsu, T., Teilmann, J., Miller, L. A., Tougaard, J., Dietz, R., Wang, D., Wang, K. X., Siebert, U., and Naito, Y. (**2007**). "Comparison of echolocation behaviour between coastal and riverine porpoises," Deep-Sea Research Part II -Topical Studies in Oceanography **54**, 290-297.

Akamatsu, T., Wang, D., Wang, K. X., and Naito, Y. (**2005**). "Biosonar behaviour of free-ranging porpoises," Proceedings of the Royal Society B-Biological Sciences **272**, 797-801.

Au, W. W. L. (**1993**). *The sonar of dolphins* (Springer-Verlag, New York, NY).

Au, W. W. L., and Benoit-Bird, K. J. (**2003**). "Automatic gain control in the echolocation system of dolphins," Nature **423**, 861-863.

Au, W. W. L., Kastelein, R. A., Rippe, T., and Schooneman, N. M. (**1999**). "Transmission beam pattern and echolocation signals of a harbor porpoise (*Phocoena phocoena*)," Journal of the Acoustical Society of America **106**, 3699-3705.

Beedholm, K., Miller, L. A., and Blanchet, M. A. (**2006**). "Auditory brainstem response in a harbor porpoise show lack of automatic gain control for simulated echoes," Journal of the Acoustical Society of America **119**, EL41-46.

Boonman, A., and Jones, G. (**2002**). "Intensity control during target approach in echolocating bats; stereotypical sensori-motor behaviour in Daubenton's bats, *Myotis daubentonii*," Journal of Experimental Biology **205**, 2865-2874.

Britton, A. R. C., and Jones, G. (**1999**). "Echolocation behaviour and prey-capture success in foraging bats: Laboratory and field experiments on *Myotis Daubentonii*," Journal of Experimental Biology **202**, 1793-1801.

Evans, W. E. (**1973**). "Echolocation by marine delphinids and one species of freshwater dolphin," Journal of the Acoustical Society of America **54**, 191-199.

Fiedler, J. (**1979**). "Prey catching with and without echolocation in the Indian false vampire (*Megaderma lyra*)," Behavioural Ecology and Sociobiology **6**, 155-160.

Gannon, D. P., Barros, N. B., Nowacek, D. P., Read, A. J., Waples, D. M., and Wells, R. S. (**2005**). "Prey detection by bottlenose dolphins, *Tursiops truncatus*: an experimental test of the passive listening hypothesis," Animal Behaviour **69**, 709-720.

Griffin, D. R., Webster, F. A., and Michael, C. R. (**1960**). "The echolocation of flying insects by bats," Animal Behaviour **8**, 141-154.

Hansen, M. (**2007)**. "High and low frequency components in harbour porpoise (*Phocoena phocoena*) clicks for echolocation and communication - facts or artefacts?," M.Sc. Thesis, Zoophysiology Department, Faculty of Science, University of Aarhus.

Hartley, D. J. (**1992a**). "Stabilization of perceived echo amplitudes in echolocating bats 1. Echo detection and automatic gain-control in the big brown bat, *Eptesicus fuscus*, and the fishing bat, *Noctilio leporinus*," Journal of the Acoustical Society of America **91**, 1120-1132.

Hartley, D. J. (**1992b**). "Stabilization of perceived echo amplitudes in echolocating bats 2. The acoustic behavior of the big brown bat, *Eptesicus fuscus*, when tracking moving prey," Journal of the Acoustical Society of America **91**, 1133-1149.

Hiryu, S., Hagino, T., Riquimaroux, H., and Watanabe, Y. (**2007**). "Echo-intensity compensation in echolocating bats (*Pipistrellus abramus*) during flight measured by a telemetry microphone," Journal of the Acoustical Society of America **121**, 1749-1757.

Johnson, M., Hickmott, L. S., Soto, N. A., and Madsen, P. T. (**2008**). "Echolocation behaviour adapted to prey in foraging Blainville's beaked whale (*Mesoplodon densirostris*)," Proceedings of the Royal Society B-Biological Sciences **275**, 133-139.

Johnson, M., Madsen, P. T., Zimmer, W. M. X., de Soto, N. A., and Tyack, P. L. (**2006**). "Foraging Blainville's beaked whales (*Mesoplodon densirostris*) produce distinct click types matched to different phases of echolocation," Journal of Experimental Biology **209**, 5038-5050.

Johnson, M. P., Madsen, P. T., Zimmer, W. M. X., de Soto, N. A., and Tyack, P. L. (**2004**). "Beaked whales echolocate on prey," Biology Letters **271**, S383-S386.

Johnson, M. P., and Tyack, P. L. (**2003**). "A digital acoustic recording tag for measuring the response of wild marine animals to sound," IEEE Journal of Oceanic Engineering **28**, 3-12.

Kalko, E. K. V. (**1995**). "Insect pursuit, prey capture and echolocation in pipistrelle bats (Microchiroptera)," Animal Behaviour **50**, 861-880.

Kalko, E. K. V., and Schnitzler, H. U. (**1989**). "The Echolocation and Hunting Behavior of Daubenton Bat, *Myotis daubentoni*," Behavioral Ecology and Sociobiology **24**, 225-238.

Kastelein, R. A., Au, W. W. L., Rippe, H. T., and Schooneman, N. M. (**1999**). "Target detection by an echolocating harbor porpoise (*Phocoena phocoena*)," Journal of the Acoustical Society of America **105**, 2493-2498.

Kick, S. A., and Simmons, J. A. (**1984**). "Automatic gain control in the bat's sonar receiver and the neuroethology of echolocation," Journal of Neuroscience **4**, 2725-2737.

Madsen, P. T., Johnson, M., de Soto, N. A., Zimmer, W. M. X., and Tyack, P. (**2005**). "Biosonar performance of foraging beaked whales (*Mesoplodon densirostris*)," Journal of Experimental Biology **208**, 181-194.

Madsen, P. T., Payne, R., Kristiansen, N. U., Wahlberg, M., Kerr, I., and Møhl, B. (**2002a**). "Sperm whale sound production studied with ultrasound time/depth recording tags," Journal of Experimental Biology **205**, 1899-1906.

Madsen, P. T., Wahlberg, M., and Møhl, B. (**2002b**). "Male sperm whale (*Physeter macrocephalus*) acoustics in a high-latitude habitat: implications for echolocation and communication," Behavioral Ecology and Sociobiology **53**, 31-41.

Melcón, M. L., Denzinger, A., and Schnitzler, H. U. (**2007**). "Aerial hawking and landing: approach behaviour in Natterer's bats, *Myotis nattereri* (Kuhl 1818)," Journal of Experimental Biology **210**, 4457-4464.

Miller, L. A., Pristed, J., Møhl, B., and Surlykke, A. (**1995**). "The Click-Sounds of Narwhals (*Monodon monoceros*) in Inglefield Bay, Northwest Greenland," Marine Mammal Science **11**, 491-502.

Miller, P. J., Johnson, M. P., and Tyack, P. L. (**2004**). "Sperm whale behavior indicates the use of echolocation click buzzes 'creaks' in prey capture," Proceedings of the Royal Society B - Biological Sciences **271**, 2239-2247.

Møhl, B., Wahlberg, M., Madsen, P. T., Miller, L. A., and Surlykke, A. (**2000**). "Sperm whale clicks: Directionality and source level revisited," Journal of the Acoustical Society of America **107**, 638-648.

Moss, C. F., and Surlykke, A. (**2001**). "Auditory scene analysis by echolocation in bats," Journal of the Acoustical Society of America **110**, 2207-2226.

Ona, E. (**2003**). "An expanded target-strength relationship for herring," ICES Journal of Marine Science **60**, 493-499.

Reynolds, J. E., and Rommel, S. A. (eds). (**1999**). *Biology of Marine Mammals* (Smithsonian Institution, Washington, D.C.).

Schnitzler, H. U., and Kalko, E. K. V. (**2001**). "Echolocation by insect-eating bats," Bioscience **51**, 557-569.

Speakman, J. R., Anderson, M. E., and Racey, P. A. (**1989**). "The energy-cost of echolocation in pipistrelle bats (*Pipistrellus pipistrellus*) " Journal of Comparative Physiology A - Sensory Neural and Behavioral Physiology **165**, 679-685.

Speakman, J. R., and Racey, P. A. (**1991**). "No cost of echolocation for bats in flight," Nature **350**, 421-423.

Surlykke, A., Futtrup, V., and Tougaard, J. (**2003**). "Prey-capture success revealed by echolocation signals in pipistrelle bats (*Pipistrellus pygmaeus*)," Journal of Experimental Biology **206**, 93-104.

Surlykke, A., and Kalko, E. K. (**2008**). "Echolocating bats cry out loud to detect their prey," PLoS ONE **3**, e2036.

Teilmann, J., Miller, L. A., Kirketerp, T., Kastelein, R. A., Madsen, P. T., Neilsen, B. K., and Au, W. W. L. (**2002**). "Characteristics of echolocation signals used by a harbour porpoise (*Phocoena phocoena*) in a target detection experiment," Aquatic Mammals **28**, 275-284.

Teloni, V., Johnson, M. P., Miller, P. J. O., and Madsen, P. T. (**2008a**). "Shallow food for deep divers: Dynamic foraging behavior of male sperm whales in a high latitude habitat," Journal of Experimental Marine Biology and Ecology **354**, 119-131.

Teloni, V., Johnson, M. P., Miller, P. J. O., and Madsen, P. T. (**2008b**). "Shallow food for deep divers: Dynamic foraging behvior of male sperm whales in a high latitude habitat," Journal of Experimental Marine Biology and Ecology **354**, 119-131.

Thomas, J. A., Moss, C. F., and Vater, M. (eds). (**2004**). *Echolocation in bats and dolphins* (University of Chicago Press, Chicago, IL).

Tyack, P. L., Johnson, M., Soto, N. A., Sturlese, A., and Madsen, P. T. (**2006**). "Extreme diving of beaked whales," Journal of Experimental Biology **209**, 4238-4253.

Verboom, W. C., and Kastelein, R. A. (**2004**). "Structure of harbor porpoise (*Phocoena phocoena*) acoustic signals with high repetition rates," in *Echolocation in Bats and Dolphins*, edited by J. A. Thomas, C. F. Moss, and M. Vater (University of Chicago Press, Chicago, IL), pp. 40-43.

Verfuss, U. K., Miller, L. A., and Schnitzler, H. U. (**2005**). "Spatial orientation in echolocating harbour porpoises (*Phocoena phocoena*)," Journal of Experimental Biology **208**, 3385-3394.

Villadsgaard, A., Wahlberg, M., and Tougaard, J. (**2007**). "Echolocation signals of wild harbour porpoises, *Phocoena phocoena*," Journal of Experimental Biology **210**, 56-64.

Wahlberg, M. (**2002**). "The acoustic behaviour of diving sperm whales observed with a hydrophone array," Journal of Experimental Marine Biology and Ecology **281**, 53-62.

Watwood, S. L., Miller, P. J. O., Johnson, M., Madsen, P. T., and Tyack, P. L. (**2006**). "Deep-diving foraging behaviour of sperm whales (*Physeter macrocephalus*)," Journal of Animal Ecology **75**, 814-825.

Wood, F. G., and Evans, W. E. (**1980**). "Adaptiveness and ecology of echolocation in toothed whales," in *Animal Sonar Systems*, edited by R.-G. Busnel, and J. F. Fish (Plenum Press, New York, NY), pp. 381-425.

Chapter 3. Transmission Loss in Porpoise Habitats

3.1 Introduction

Harbor porpoises (*Phocoena phocoena*) are small toothed whales that inhabit temperate and subarctic waters; like all toothed whale species investigated, they use echolocation for foraging and navigation. The click signals of porpoises are more narrow-band and higher in frequency than those of most larger odontocetes, and little is known about the behavior and echolocation strategies of porpoises in the wild (Au, 1993; Akamatsu *et al.*, 2005; Akamatsu *et al.*, 2007). Porpoises live in coastal areas where fisheries are active, vessel traffic is intense, and marine construction (e.g., for offshore wind farms) may occur. Consequently, they face mortality from entanglement in bottom-set gillnets or other fishing gear (Read *et al.*, 1993; Dawson *et al.*, 1998; Bowen *et al.*, 2001; Kaschner, 2003). Behavioral disruption or habitat exclusion due to anthropogenic noise may also threaten porpoise populations (Koschinski *et al.*, 2003; Kastelein *et al.*, 2005b; Carstensen *et al.*, 2006).

There is very little information on how porpoises deploy their echolocation in the wild to forage and navigate, either in the presence or absence of fishing gear or disturbance. However, estimating the range at which porpoises can detect prey items and other environmental objects (including obstacles such as fishing gear that they must avoid, or other features that might be used as navigational landmarks) is an integral part of studies of harbor porpoise biosonar; it is also a key to understanding obstacle detection and avoidance behavior relevant to bycatch reduction strategies (Au and Jones, 1991; Kastelein *et al.*, 2000; Mooney *et al.*, 2004; Mooney *et al.*, 2007). To predict the range at which a porpoise (or other echolocating whale) can detect an object using echolocation, one must measure or estimate 1) the source level of the outgoing click signal; 2) the minimum received echo level which is detectable by the echolocating animal (limited either by ambient noise levels or by the animal's auditory threshold); 3)

the acoustic target strength of the prey item or target of interest; and 4) the transmission loss of the signal as it travels from the source to the target and back again.

Echolocation click source levels have been characterized for captive and wild harbor porpoises (Au *et al.*, 1999; Villadsgaard *et al.*, 2007), and for other free-ranging odontocete species including the bottlenose dolphin *Tursiops truncatus* (Au *et al.*, 1974; Au, 1993; Au and Benoit-Bird, 2003b); the false killer whale *Pseudorca crassidens* and Risso's dolphin *Grampus griseus* (Madsen *et al.*, 2004a); the pygmy killer whale *Feresa attenuata* (Madsen *et al.*, 2004b); the white-beaked dolphin *Lagenorhynchus albirostris* (Rasmussen *et al.*, 2002); the orca *Orcinus orca* (Au *et al*., 2004), and the sperm whale *Physeter macrocephalus* (Møhl *et al.*, 2000; Møhl *et al.*, 2003). Where comparison has been possible, click source levels of free-ranging animals have been 30-40 dB higher than those of captive animals in tanks (Au *et al.*, 1974; Au and Benoit-Bird, 2003b; Madsen *et al.*, 2004a; Villadsgaard *et al.*, 2007).

Hearing capabilities of harbor porpoises (Popov *et al.*, 1986; Kastelein *et al.*, 2002; Kastelein *et al.*, 2005a) and several other species have also been tested experimentally (false killer whale (Thomas *et al.*, 1988); finless porpoise *Neophocaena phocaenoides asiaeorientalis* (Popov *et al.*, 2005); striped dolphin *Stenella coeruleoalba* (Kastelein *et al.*, 2003); orca (Szymanski *et al.*, 1999); tucuxi *Sotalia fluviatilis guianensis* (Sauerland and Dehnhardt, 1998); false killer whale (Yuen *et al.*, 2005); Risso's dolphin *Grampus griseus* (Nachtigall *et al.*, 2005)) or predicted by anatomical or computational models (e.g., Ketten, 1997; Hemilä *et al.*, 2001). Whale hearing capabilities remain an area of ongoing research.

Ocean noise levels have also been well-studied over broad frequency ranges and in a variety of environments and conditions (*e.g.*, Wenz, 1962; Urick, 1975; Medwin and Clay, 1998), so it may be possible to estimate a realistic range

of potential noise conditions in odontocete habitats based on the literature; alternatively, noise levels at a specific site can be measured readily.

The target strength of fish (reviewed in Medwin and Clay, 1998) and the acoustic reflectivity of other objects such as fishing gear (Au and Jones, 1991; Kastelein *et al.*, 2000; Trippel *et al.*, 2003) have also been studied, and both theoretical and empirical predictive models for target strength have been developed for many types of fish (e.g., Rose, 1998; Ona, 2003; Reeder *et al.*, 2004). Although most of the target strength studies mentioned above describe the acoustic reflectivity of an object ensonified by narrow band sound pulses, target strength measurements of some fish species (Au and Benoit-Bird, 2003a; Benoit-Bird *et al.*, 2003; Au *et al.*, 2007) and acoustic reflectivity measurement for some fishing gear (Au and Jones, 1991; Kastelein *et al.*, 2000; Mooney *et al.*, 2004; Mooney *et al.*, 2007) have been made with short, click-like signals similar to toothed whale echolocation clicks.

Finally, transmission loss of acoustic signals in the marine environment has been the subject of a great deal of theoretical and empirical study (Urick, 1975; Jensen *et al.*, 1994). In certain conditions, transmission loss can be simply described by spherical spreading law. Spherical spreading describes the reduction in acoustic intensity with range from a sound source in a lossless, homogeneous medium with no boundaries. In that case, total acoustic power must remain constant over time. Power is the product of intensity and area. Since the area over which the sound is distributed (the surface of a sphere) increases with the square of source-receiver range, sound intensity must decrease with the square of range; mathematically, in decibel notation, $TL = 10\log_{10}(r^2) = 20\log_{10}(r)$ (Urick, 1975). A similar argument leads to the derivation of the cylindrical spreading law, $TL = 10\log_{10}(r)$, for a lossless, homogeneous medium with parallel, perfectly reflective boundaries (Urick, 1975). In more complex environments, transmission loss can generally be modeled successfully

using theoretically-derived computational acoustic propagation models as long as the environmental features (sound speed profile, bathymetry, bottom properties, etc.) and acoustic source characteristics (source level, frequency, and beam pattern) are well known (Jensen *et al.*, 1994; Medwin and Clay, 1998). At high frequencies, including the frequencies of most whale echolocation clicks, attenuation due to sound absorption in the medium contributes significantly to the transmission loss. Absorption losses can be predicted according to well-established theoretical and empirical models (Schulkin and Marsh, 1962; Thorp, 1965; 1967; Francois and Garrison, 1982a; b), and can generally be included in the computational propagation models mentioned earlier.

As described in detail above, relatively accurate estimates or predictions of all necessary quantities are available for estimating the maximum echolocation detection ranges of harbor porpoises and many other odontocete species. Such estimates have been published for several species, including harbor porpoises (Au *et al.*, 2007; Mooney *et al.*, 2007; Villadsgaard *et al.*, 2007), bottlenose dolphins (Au *et al.*, 2007), orcas (Au *et al.*, 2004), false killer whales and Risso's dolphins (Madsen *et al.*, 2004a). These studies have used the best available estimates for outgoing click source levels, ambient noise, and hearing thresholds for click detection (in the rare cases where signal detection is not noise-limited). Most also use established, published estimates of target strength (although Au and colleagues (2007) point out that target strength measurements made using whale-like clicks are most appropriate for such studies, and were the first to apply them). However, all of the studies use a spherical spreading law with an attenuation term to describe transmission loss. The assumption that this type of transmission loss estimate can accurately describe transmission loss of echolocation clicks in toothed whale habitats has not been validated comprehensively, although Villadsgaard and colleagues (2007) did verify experimentally that, at their study site, spherical spreading with attenuation

estimated TL within 4 dB of observed data values at source-receiver ranges of 50 m or less.

Passive acoustic monitoring (PAM) with automatic click detection devices such as T-PODs porpoise detectors (Thomsen *et al.*, 2005) has become an increasingly common method for monitoring the presence and abundance of whales, especially harbor porpoises; T-PODs have been used both to study abundance patterns (Philpott *et al.*, 2007; Verfuss *et al.*, 2007) and to quantify changes in abundance in response to anthropogenic noise (Cox *et al.*, 2001; Culik *et al.*, 2001; Koschinski *et al.*, 2003; Carstensen *et al.*, 2006; Leeney *et al.*, 2007). Passive acoustic monitoring with devices like T-PODs provides data on the time and intensity of detected clicks, not spatial abundance data. Understanding transmission loss in porpoise habitats can play an important role in the interpretation of this data, since an estimate of TL is required to estimate the maximum distance at which a device can detect animals or to convert PAM data to a more conventional abundance measure such as spatial density of animals. Although such conversions are generally not attempted yet because data relating the number of porpoises present to the number of click trains detected are not currently available (Carstensen *et al.*, 2006), they are likely to become more widespread in the future. A test of the assumption that spherical spreading with attenuation accurately describes transmission loss in porpoise habitats is thus critical for accurate interpretation of passive acoustic monitoring data.

The purpose of this paper is to test the hypothesis that a spherical spreading law with attenuation can accurately predict the transmission loss of harbor porpoise-like clicks in porpoise habitats, and to compare the performance of the spreading law/attenuation model with that of a more sophisticated acoustic propagation model. To accomplish that goal, I measured the transmission loss of

porpoise-like clicks in porpoise habitats in Canada and Denmark, and I compared the measured values to those predicted by both models.

3.2 Methods

3.2.1 Field Sites

Field measurements of transmission loss of porpoise-like clicks we made in two areas: near Grand Manan Island in New Brunswick, Canada; and in Aarhus Bay near Aarhus, Denmark. Figures 3.1-3.3 show maps show maps of the sites near Grand Manan, and Figures 3.4-3.5 show maps of the Danish experiment site. All of the sites are within known porpoise habitat; that is, porpoises are commonly sighted at all the experimental locations.

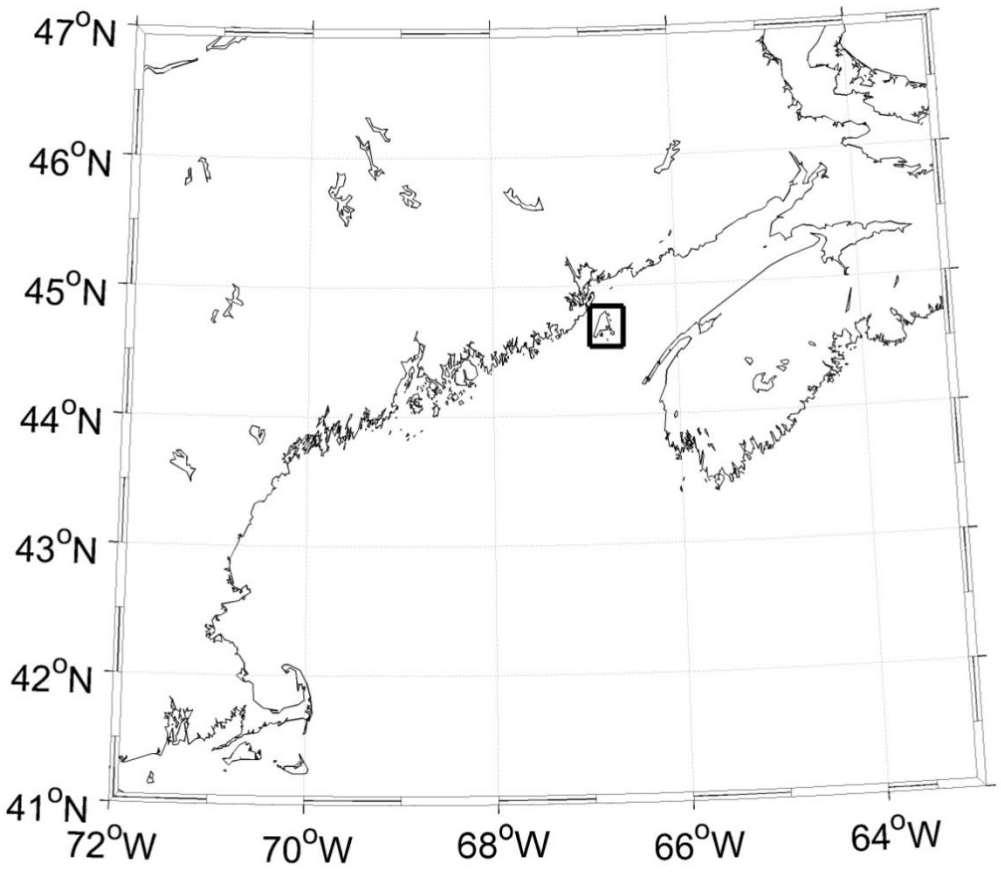

Figure 3.1. Large-scale map of the experiment location near Grand Manan Island, NB, Canada. Black rectangle shows area mapped in Figure 3.2.

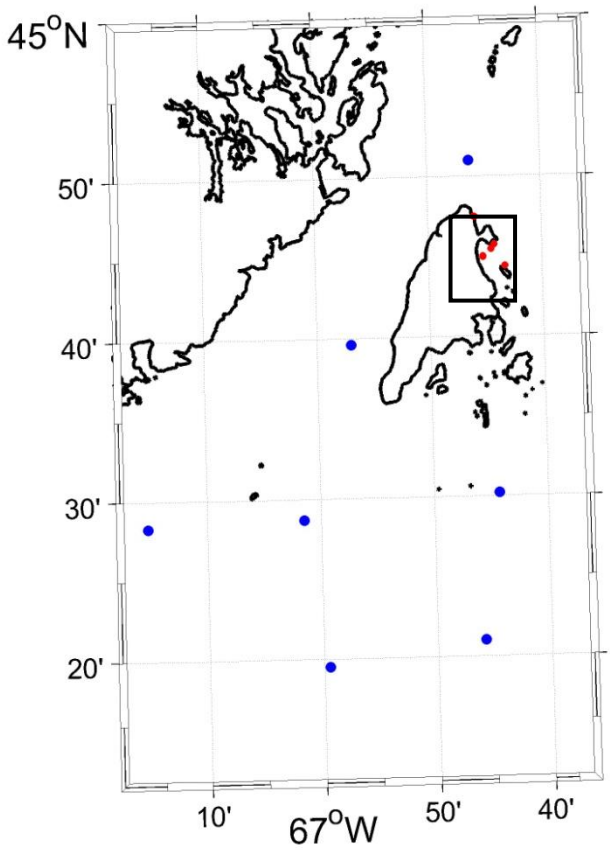

Figure 3.2. Map of Grand Manan Island. Red dots indicate sites of transmission loss experiments. Blue dots indicate the collection locations of sediment samples (Paskevich et al. 2001, Poppe et al. 2001) used to help establish the bottom properties at the experiment sites for acoustic propagation modeling. Black rectangle indicates the area mapped in Figure 3.3.

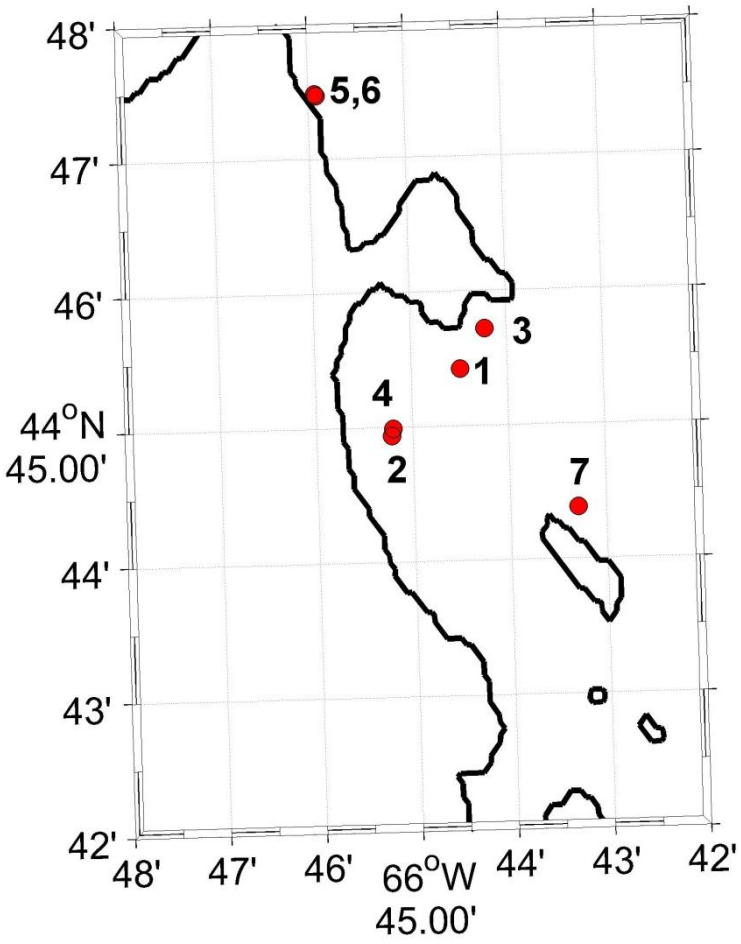

Figure 3.3. Detailed map of the sites of transmission loss experiments (indicated by red dots) near Grand Manan Island.

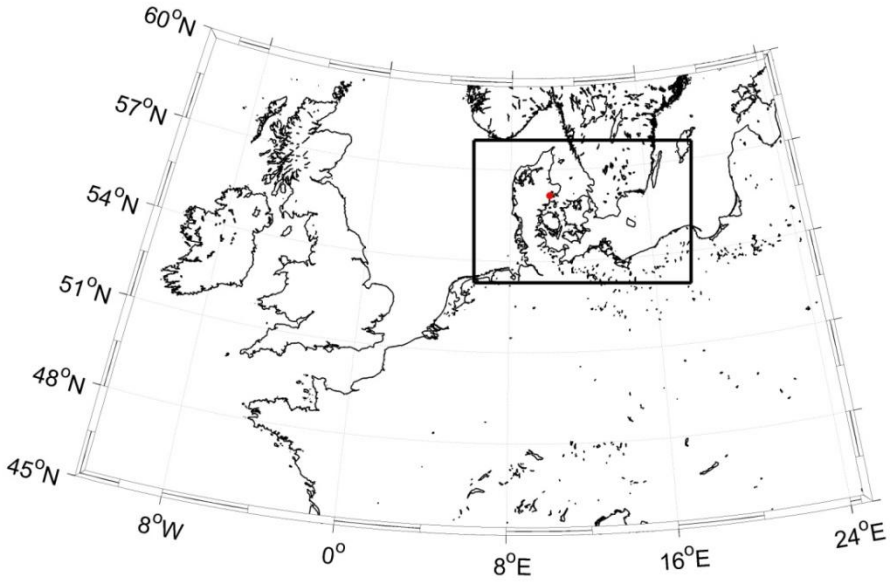

Figure 3.4. Map of the experiment location (red dot) in Aarhus Bay, Denmark. Black rectangle indicated the area mapped in Figure 3.5.

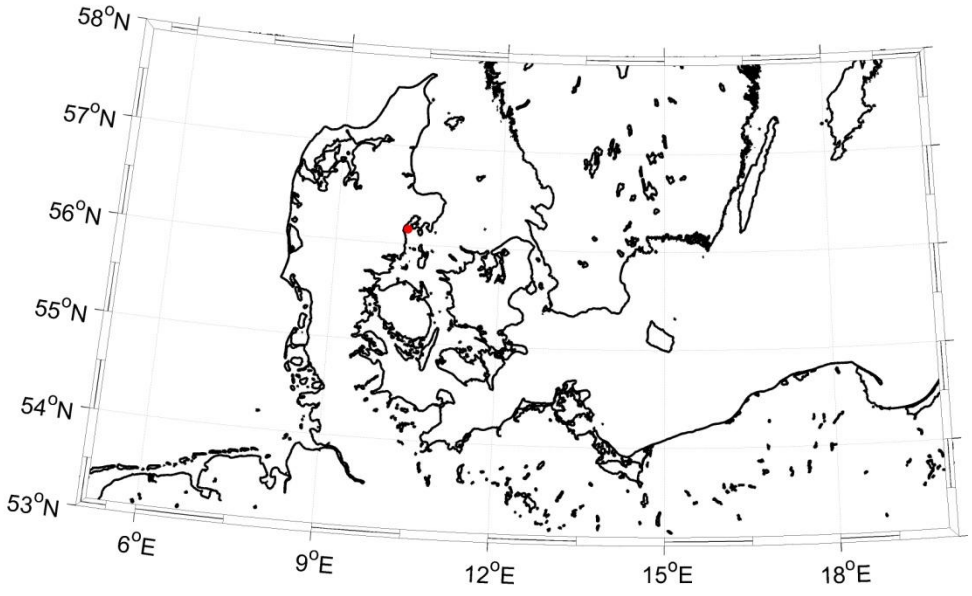

Figure 3.5. Map of the experiment location (red dot) in Aarhus Bay, Denmark.

In Grand Manan, experiments 1-7 were carried out at 6 sites between 8 August and 13 August 2006 (see Figure 3.3 for exact locations of each site; experiments 5-6 were done on the same day at the same site). In Aarhus Bay, measurements were made at the same site in the middle of the bay on 5 September 2006, 29 November 2006, and 16 April 2007 (I will refer to these experiments as experiments 8-10). Table 3.1 gives the exact date of each experiment.

Table 3.1. Dates and locations of transmission loss experiments.

Experiment Number	Date	Location
1	8 August 2006	Grand Manan, NB, Canada
2	10 August 2006	Grand Manan, NB, Canada
3	11 August 2006	Grand Manan, NB, Canada
4	11 August 2006	Grand Manan, NB, Canada
5	12 August 2006	Grand Manan, NB, Canada
6	12 August 2006	Grand Manan, NB, Canada
7	13 August 2006	Grand Manan, NB, Canada
8	5 September 2006	Aarhus Bay, Denmark
9	29 November 2006	Aarhus Bay, Denmark
10	14 April 2007	Aarhus Bay, Denmark

CTD measurements were taken in conjunction with each experiment to allow determination of a sound speed profile for each site, and echosounder measurements were used to characterize the bathymetry at each site. Figures 3.6-3.14 show the sound speed profiles calculated from the CTD data for experiments 1-10. The sound speed profiles for experiments 1, 7, and 9 (Figs. 6, 11 and 13) show nearly isovelocity water columns with minimal variation in sound

speed with depth. In contrast, experiment sites 2-6 and 10 (Figs. 3.7-3.10, 3.14) have downward-refracting sound speed profiles, and site 8 (Fig. 3.12) has a lower-velocity sound channel between about 6-12 meters depth. All sites had relatively flat bathymetry, with a maximum downward slope of about three degrees at sites 5-6. Figure 3.15 shows the bathymetry at the sites of experiments 1-7. Bathymetry plots are not shown for the sites in Aarhus bay, since they had flat bottoms with water depths of about 15 m (experiment 8), 12 m (experiment 9), and 13 m (experiment 10).

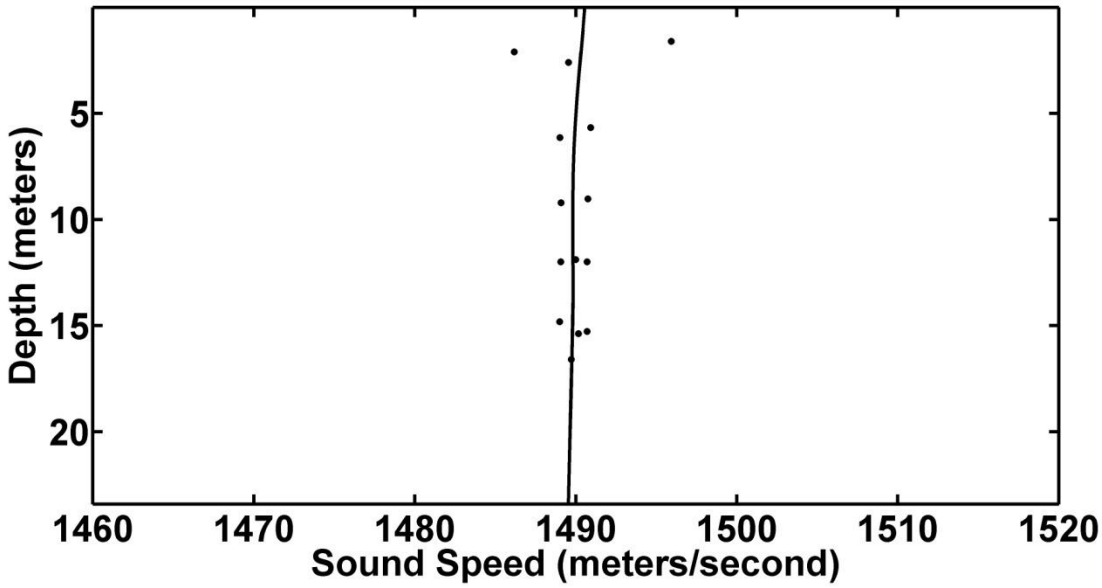

Figure 3.6. Sound speed profile for experiment 1. The black dots indicate raw CTD data, and the solid black line indicates the smoothed sound speed profile used for acoustic modeling.

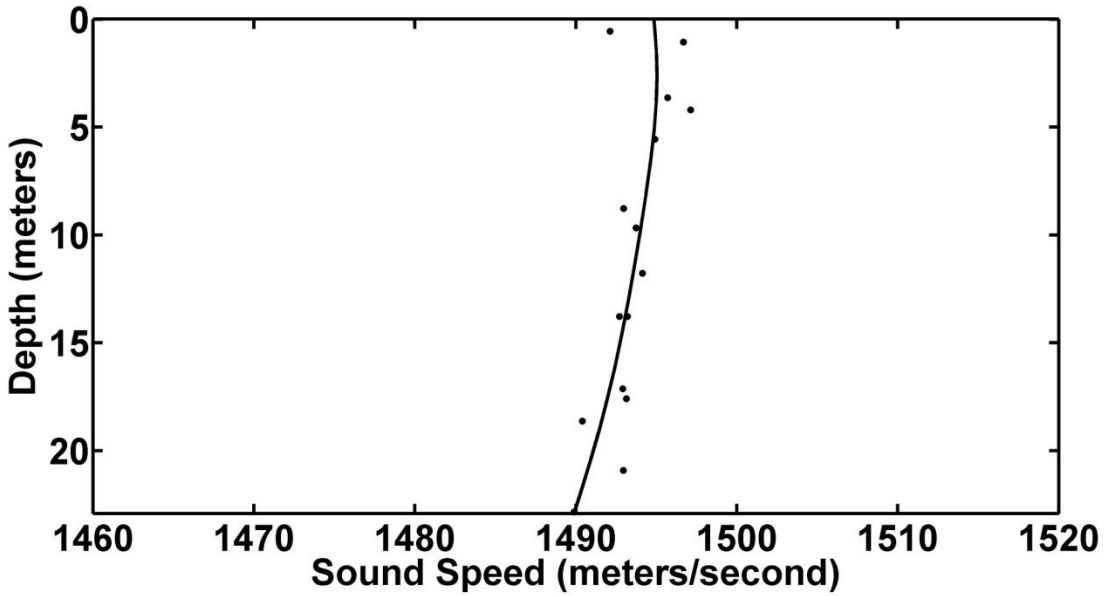

Figure 3.7. Sound speed profile for experiment 2. The black dots indicate raw CTD data, and the solid black line indicates the smoothed sound speed profile used for acoustic modeling.

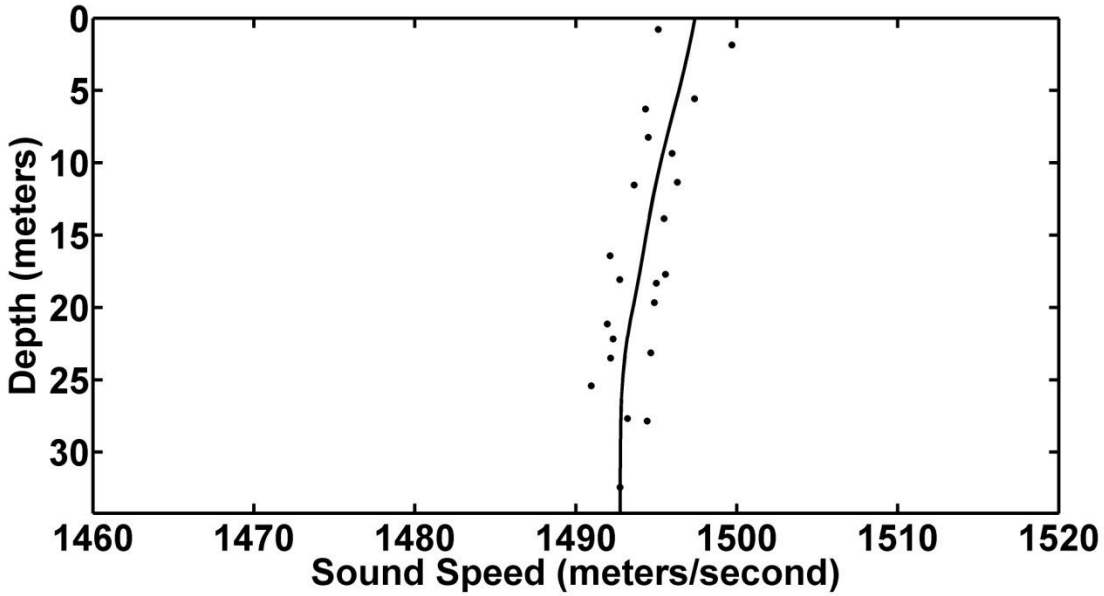

Figure 3.8. Sound speed profile for experiment 3. The black dots indicate raw CTD data, and the solid black line indicates the smoothed sound speed profile used for acoustic modeling.

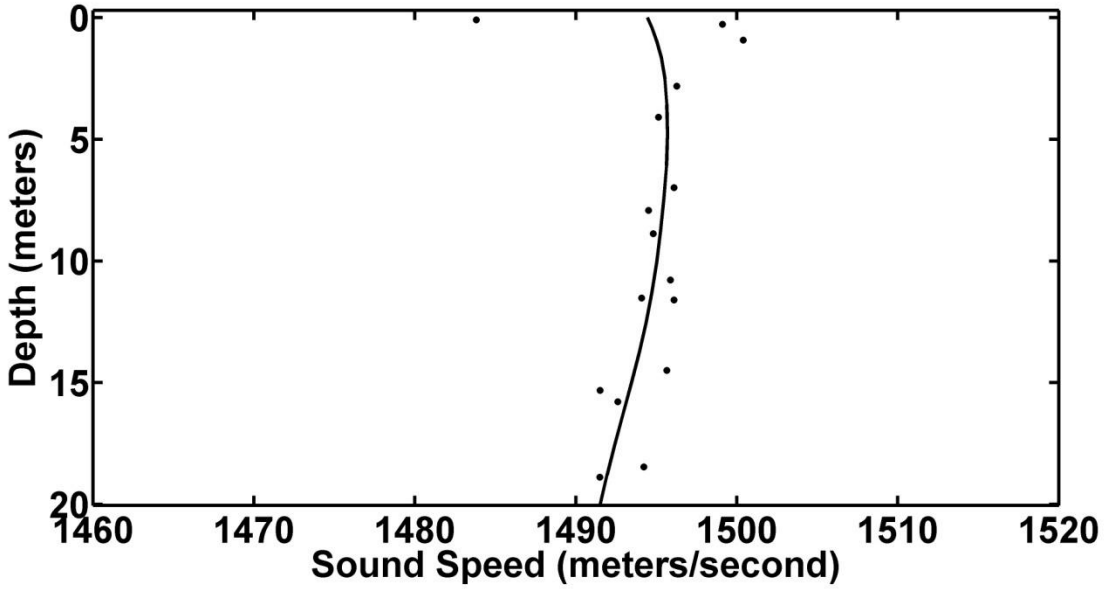

Figure 3.9. Sound speed profile for experiment 4. The black dots indicate raw CTD data, and the solid black line indicates the smoothed sound speed profile used for acoustic modeling.

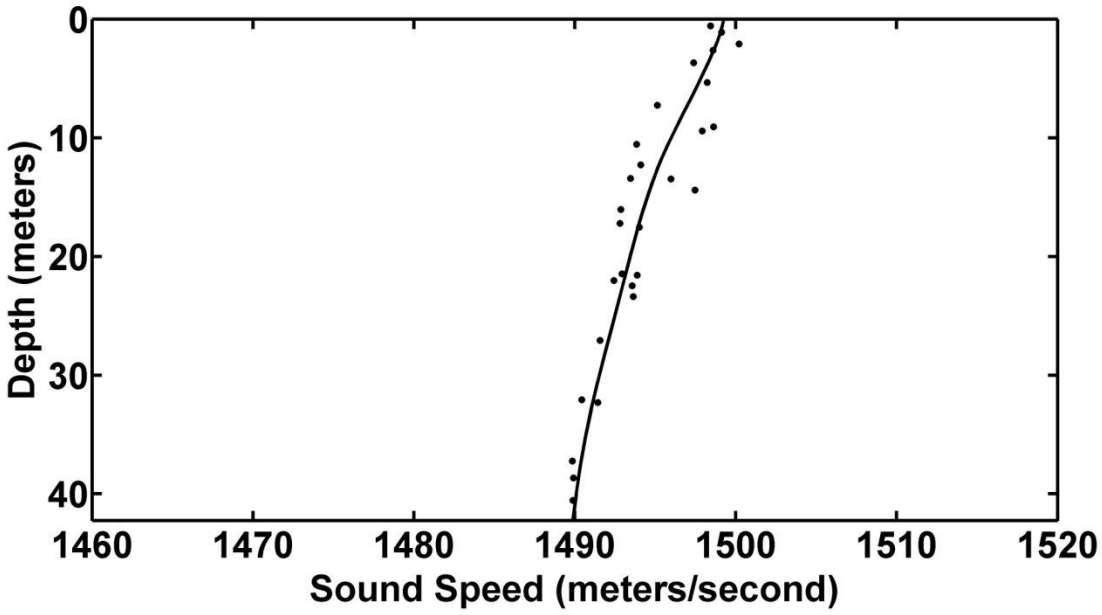

Figure 3.10. Sound speed profile for experiments 5-6. The black dots indicate raw CTD data, and the solid black line indicates the smoothed sound speed profile used for acoustic modeling.

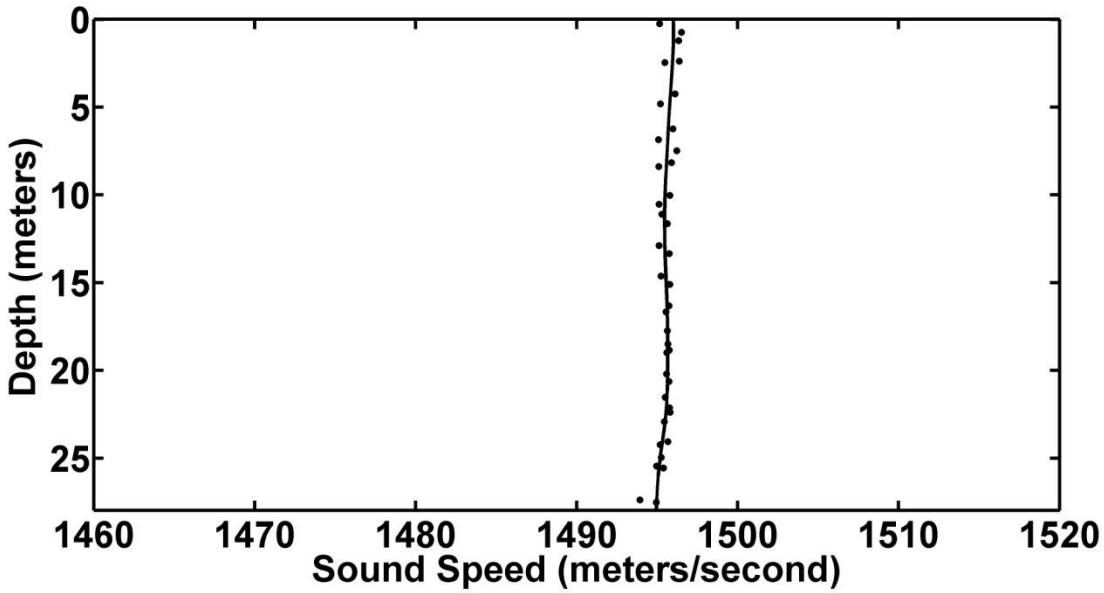

Figure 3.11. Sound speed profile for experiment 7. The black dots indicate raw CTD data, and the solid black line indicates the smoothed sound speed profile used for acoustic modeling.

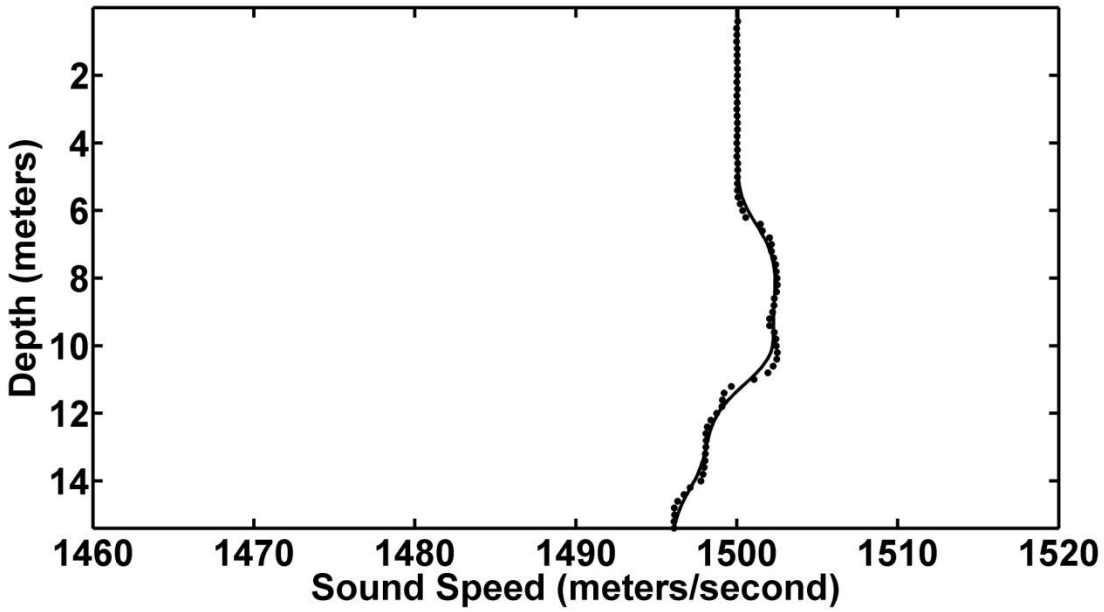

Figure 3.12. Sound speed profile for experiment 8. The black dots indicate raw CTD data, and the solid black line indicates the smoothed sound speed profile used for acoustic modeling.

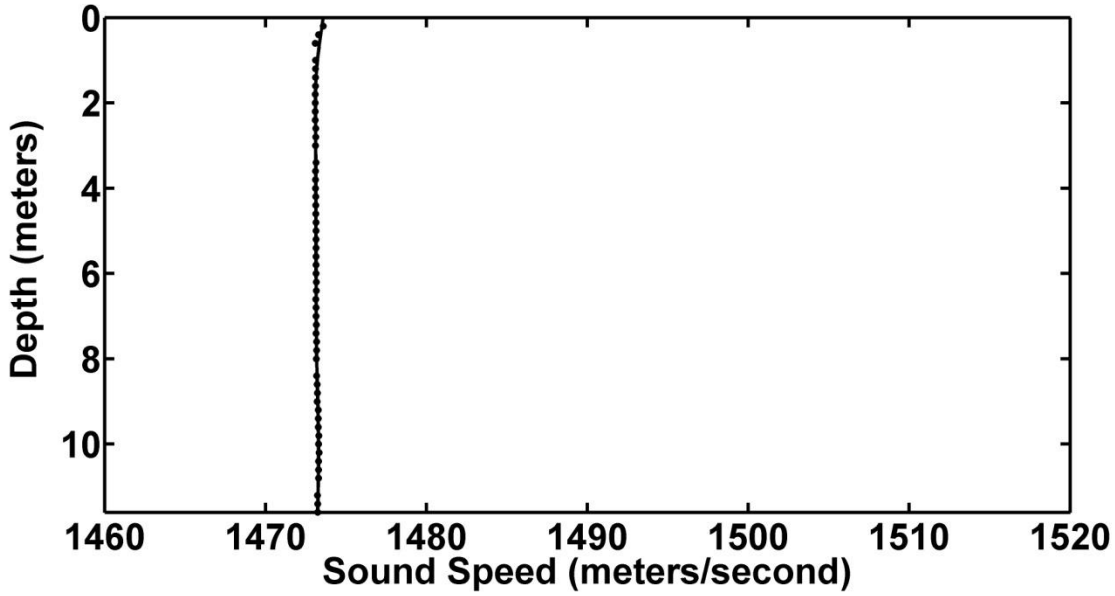

Figure 3.13. Sound speed profile for experiment 9. The black dots indicate raw CTD data, and the solid black line indicates the smoothed sound speed profile used for acoustic modeling.

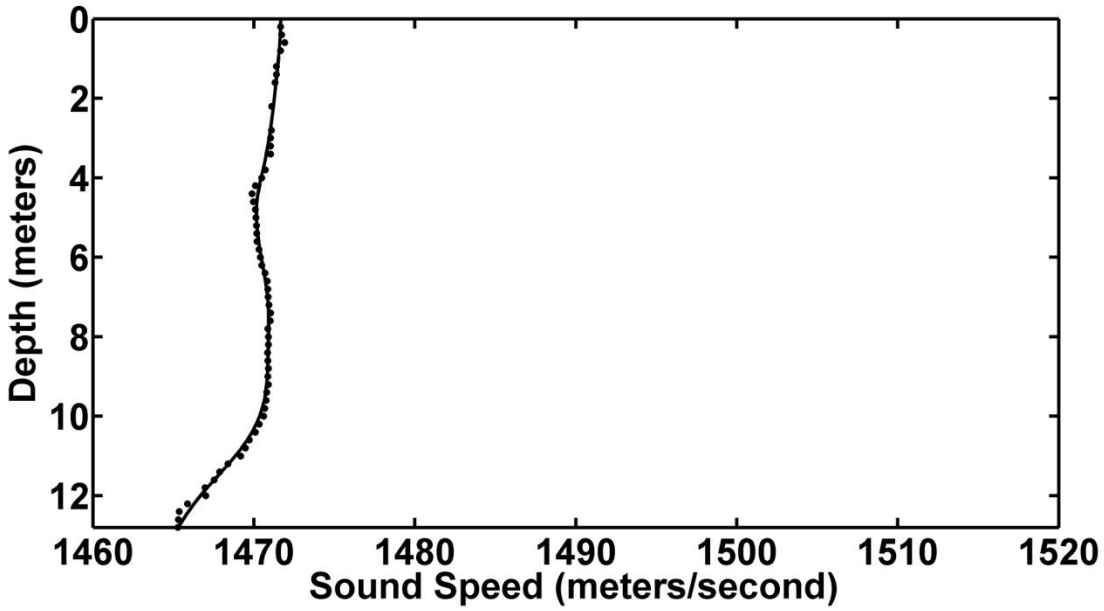

Figure 3.14. Sound speed profile for experiment 10. The black dots indicate raw CTD data, and the solid black line indicates the smoothed sound speed profile used for acoustic modeling.

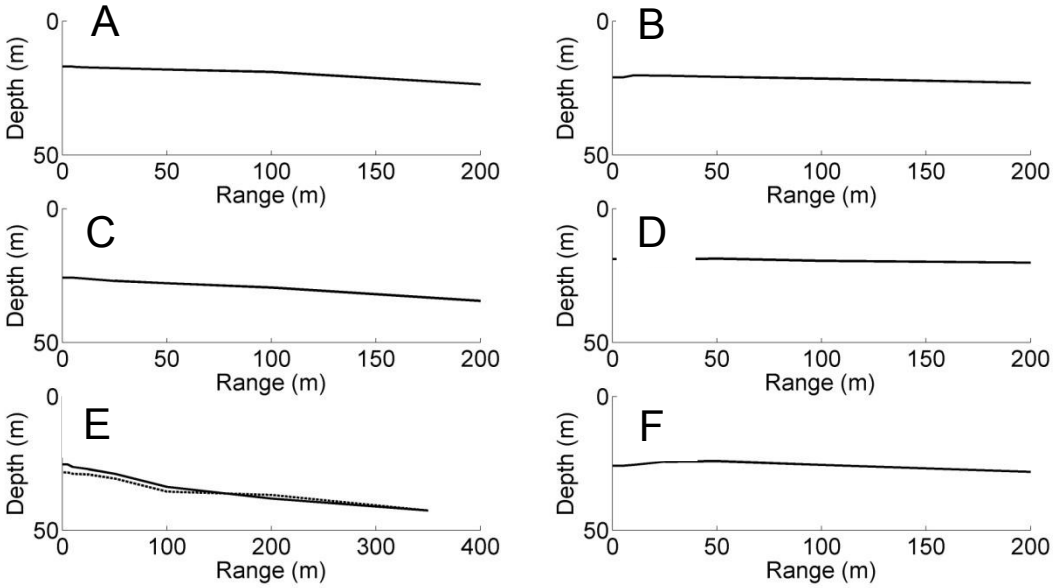

Figure 3.15. Bathymetry at the seven transmission loss experiment sites near Grand Manan Island. Panel A corresponds to experiment 1, B to 2, C to 3, D to 4, E to 5 (solid line) and 6 (dotted line), and F to 7. (Bathymetry is not shown for experiment sites in Denmark, which had flat bottoms with depths of 15.4m (experiment 8), 11.6m (experiment 9), and 12.8m (experiment 10).)

No attempts were made to measure bottom properties during my experiments, but data on bottom properties near my experiment sites are available from several sources. Paskevich et al. (2001) and Poppe et al. (2005) provide sediment grain-size data for sites within about 15 km of the experimental sites, but further from the coast of Grand Manan. Figure 3.2 shows the locations of their sediment samples, which were mainly silty clay with occasional small amounts of sand or shells. The sediments in Aarhus Bay are also mainly silty clay or sandy clay (Lund-Hansen *et al.*, 2002; Røy *et al.*, 2005).

3.2.2. Audio Data Collection

Experimental Setup

The experimental setup for transmission loss measurements required two boats: one to transmit the signals from a fixed location, and one to receive the signals at a variety of ranges. The transmitting boat was anchored or tied up to a fixed object, and the transmitter was deployed over the side of the transmit boat, continuously transmitting synthetic porpoise clicks. The receiving boat was attached to the transmitting boat by a line. The length of the line was adjusted to position the receiving boat at stations 5 m, 10 m, 25 m, 50 m, 100 m, 150 m (experiments 7-10 only), 200 m (experiments 1-7 only), and 350 m (experiments 5-6 only) from the transmitter. Source-receiver ranges were verified by radar when possible. At each station, the receiving boat made one- to five-minute recordings of the transmitted signal on two hydrophones deployed at 3 m and 5 m depth.

Transmitted signal

The transmitted signal in all experiments was a series of synthetic porpoise clicks; each click consisted of 11 cycles (experiments 1-8) or 15 cycles (experiments 9-10) of a 135 kHz pure tone, with a 10 msec pause after each synthetic click. The duration of each synthetic click was about 82 μsec (11 cycles) or 111 μsec (15 cycles). The duration and frequency of the synthetic clicks were similar to the duration (about 75-250 μsec) and peak frequency (120-140 kHz) of typical harbor porpoise echolocation clicks (Au, 1993; Au *et al.*, 1999). We used an Agilent 33220A signal generator (Agilent Technologies, Santa Clara, California) to produce the clicks at a peak-peak amplitude of 1 V, amplified the signal by 46 dB using a custom-built amplifier for a total amplitude of about 200 V peak-peak, and transmitted them into the water with a Brüel & Kjær 8105 spherical hydrophone (Brüel & Kjær Sound & Vibration Measurement A/S, Nærum, Denmark; transmit sensitivity 145 dB relative to 1μPa/V @ 1m)

deployed at either 5 m depth (experiments 1-7, 10) or 3 m depth (experiments 8-9). In contrast to a porpoise, which produces directional echolocation clicks with a -10dB beam width of about 20 degrees in the vertical plane (Au *et al.*, 1999), our transducer was nearly omnidirectional. The measured source level of the transmissions was 184 dB re 1 µPa peak-peak @ 1 m, which is within the expected range for wild harbor porpoise echolocation clicks (178-205 dB re 1µPa peak-peak @ 1 m (Villadsgaard *et al.*, 2007)).

Sound Recordings

Grand Manan (experiments 1-7)

At each station, 1- to 5-minute audio recordings of the signal were collected with hydrophones deployed at 3 m and 5 m depth. The signal at 3 m depth was recorded on a Reson TC4034 hydrophone (Reson, Slangerup, Denmark; receiving sensitivity -220 dB relative to 1V/µPa at 130 kHz), amplified either 40 or 60 dB with a custom-built amplifier and band-pass filtered with an analog filter between 1.7 (1 pole) and 160 kHz (4 pole). The signal at 5 m depth was recorded on a Reson TC4014 hydrophone (receiving sensitivity -186 dB relative to 1V/µPa), amplified 32 dB with an etec amplifier (etec, Frederiksvaerk, Denmark) and high-pass filtered with an analog filter (1 pole) at 1 kHz. All signals from the hydrophones were digitized at 333 kHz sampling rate (16 bits resolution) on a Wavebook 516E analog to digital converter (IOtech, Cleveland, Ohio), and the resulting files were saved on a laptop computer. In order to maximize resolution in the recordings, amplification on the 3 m hydrophone was varied between 40 and 60 dB, and the clip level of the digital recordings was varied between 0.2 and 10 V peak-peak.

Aarhus Bay (experiments 8-10)

At each station, 1- to 5-minute audio recordings of the signal were collected with hydrophones deployed at 3 m and 5 m depth. Both channels were

recorded on Reson TC4034 hydrophones. In order to maximize resolution in the recordings, amplification on the hydrophones was varied between 40 and 60 dB. Signals from the hydrophones were filtered with an analog band-pass filter between 1 (1 pole) and 200 kHz (4 pole) and digitized at 500kHz sampling rate (12 bits resolution) on an ADLINK analog-digital converter (ADLINK Technology Inc., Taipei, Taiwan); the resulting data files were saved to a laptop computer. The peak-peak clip level of the digital recordings was 10 V (experiment 8) or 4 V (experiments 9-10).

3.2.3 Data Processing

The data wave files from each station were band-pass filtered between 100-160 kHz with a 4th order Butterworth filter in Adobe Audition (Adobe, San Jose, California). Using custom-written scripts in Matlab (The MathWorks, Natick, Massachusetts), I applied an envelope-based click detector to extract 100 clicks from each file and calculate the peak-peak amplitude, or received level (RL), of each click. The click detection routine outputs the peak RL of the highest amplitude acoustic arrival only (and not the combined level of several multipath arrivals), as long as the delay in arrival time between the arrivals is greater than about 100 μsec and thus the arrivals do not overlap in time. I subtracted the measured RLs from the transmitter source level, 184 dB re 1μPa peak-peak, to obtain the transmission loss of each click. I recorded the mean, minimum, and maximum transmission loss among the 100 measured clicks at each station for comparison with model predictions.

3.2.4 Transmission Loss Predictions: Spreading Law Calculations

The first model I used to predict transmission loss (TL) was a spherical spreading law ($TL = 20\log_{10}(r)$) with attenuation. At high frequencies like the 135 kHz considered in my experiments, absorption also contributes significantly to the transmission loss, so I included an additional absorption loss of 0.04 dB/m (calculated according to Francois and Garrison (1982a; b)) in the transmission

loss calculation. Therefore, for each source-receiver range *r* (in meters), I calculated the transmission loss *TL* in decibels according to $TL = 20\log_{10}(r) + 0.04r$. I expected this spreading law/attenuation TL approximation to be accurate only in areas where the sound speed was relatively homogeneous and the sound did not interact with the bottom or the sea surface before arriving at the receiver. Because the transmitted signal was very short, one would predict those conditions to hold unless receiver depth was very shallow or source-receiver range was large (Madsen and Wahlberg, 2007).

3.2.5 Transmission Loss Predictions: Bellhop Acoustic Propagation Model

I also applied an acoustic propagation model, which can take into account the sound speed profile, bathymetry, and bottom properties as well as multipath acoustic propagation, to predict transmission loss at each experiment site. Because of the high frequency of the sound source in my experiments, I chose Bellhop, a ray-tracing propagation model written by Michael Porter, for these predictions (Porter and Bucker, 1987). I used the AcTUP Matlab front-end, written by Amos Maggi and Alec Duncan and available at http://www.cmst.curtin.edu.au/products/actoolbox/, to interface with Bellhop. Model inputs included the source and receiver depths, sound speed profiles, and bathymetry of the experimental sites (shown in Figures 3.6-3.15), as well as attenuation in the water column calculated according to Francois and Garrison (1982a; b). I did not gather data on the bottom properties at each site, but as noted earlier, published data indicate that all my experimental sites are dominated by silty clay sediments. In this sediment type, the ratio of sound speed in the surface sediments to sound speed in the water overlying the sediments is generally about 0.984 (Jackson and Richardson, 2007). I combined that ratio with the sound speed at the base of the sound speed profile to calculate a sediment sound speed for each of my experimental sites; I then used Hamilton's (1978) equations to estimate sediment density. Finally, following Jackson and Richardson (2007), I estimated bottom attenuation in my silty clay

sediments to be about 0.45 dB per wavelength. I used the above values to define an isovelocity bottom layer for each of my experiment sites.

Using the inputs described above, I carried out Bellhop model runs specific to each experiment site to determine the incoherent transmission loss and arrival-time delay of each arrival at the appropriate receiver depth/range locations. I used the model output to calculate two transmission loss estimates for each combination of experiment sites and receiver stations. The first, which I will call single-arrival TL, included only the transmission loss of the single highest-amplitude arrival at the receiver (generally the first, direct arrival). The second, which I will call total TL, summed all arrivals at the receiver incoherently. Although the total TL estimate theoretically includes all multipath arrivals at the receiver, in the cases I considered, most of the later arrivals had very high transmission loss, so only the first few arrivals had significant impacts on the total TL value. I expected the single-arrival TL estimate to match the data well whenever arrivals did not overlap in time and I was able to accurately determine the received level of the first arrival in the data; on the other hand, I expected the second estimate to be more accurate in cases where temporal overlap of arrivals did occur.

3.2.6 Comparison of TL data and predictions

I used two measures to compare our observed data TL with the spreading law and Bellhop model predictions. First, I simply calculated the prediction error (for each station in each experiment) by subtracting the data TL from the predicted TL. Second, I calculated a root-mean-squared-error (RMSE) value for each experiment and for the set of 10 experiments according to RMSE = $\sqrt{(\text{mean}(TL_{predicted} - TL_{data})^2)}$. For RMSE calculations, the error values in dB ($TL_{predicted} - TL_{data}$) were converted to linear units, then the resulting RMSE values were converted back into dB.

3.3 Results

3.3.1. Field Data

For most of my experiments, both Bellhop model output and data inspection confirmed that transmission loss increased with range, the first arrival at each receiver had the highest peak-peak amplitude, and it did not overlap in time with other arrivals; therefore, in most cases I compared data TL with spreading law TL and Bellhop single-arrival TL (Figures 3.16-3.19, 3.22-3.24). For experiments 5, 6, and 10, however, I found that the highest-amplitude recorded click was often not the first arrival, but a later arrival that appeared to be composed of several overlapping arrivals. I observed this phenomenon at source-receiver ranges as short as 10 m (experiment 5; 25 m for experiment 6 and 50 m for experiment 10). As an example, Figure 3.26 shows data from experiment 10 for a receiver depth of 3m and a source-receiver range of 50m. The figure includes the waveforms of received arrivals from 100 clicks, as well as the results of a pulse-compression analysis indicating that the largest peak in the data waveform is actually composed of several overlapping arrivals. I also noted that, in experiments 5-6 and 10, transmission loss did not increase as smoothly with range as in the other experiments. Given those observations, I expected that multipath propagation and water-column refraction would significantly affect the measured transmission loss for experiments 5, 6 and 10. Therefore, for those experiments, I compared the data TL with spreading law TL and Bellhop total TL (Figures 3.20-3.21, 3.25).

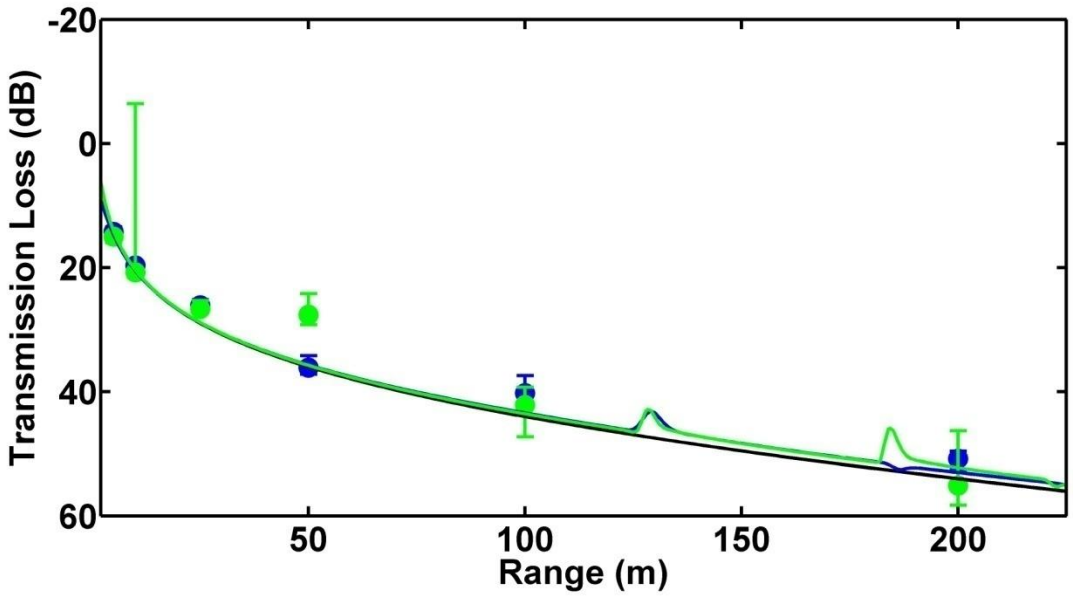

Figure 3.16. Measured and modeled transmission loss as a function of range for experiment 1. Blue circles show data collected at 3m receiver depth (zr = 3m), and green circles show data collected at 5m receiver depth (zr = 5m). Error bars on data points indicate minimum and maximum observed values. The black trace is the transmission loss predicted by a spherical spreading model with attenuation. The colored traces show transmission loss predicted by the Bellhop acoustic propagation model (single-arrival transmission loss; blue for 3m receiver depth, green for 5m receiver depth).

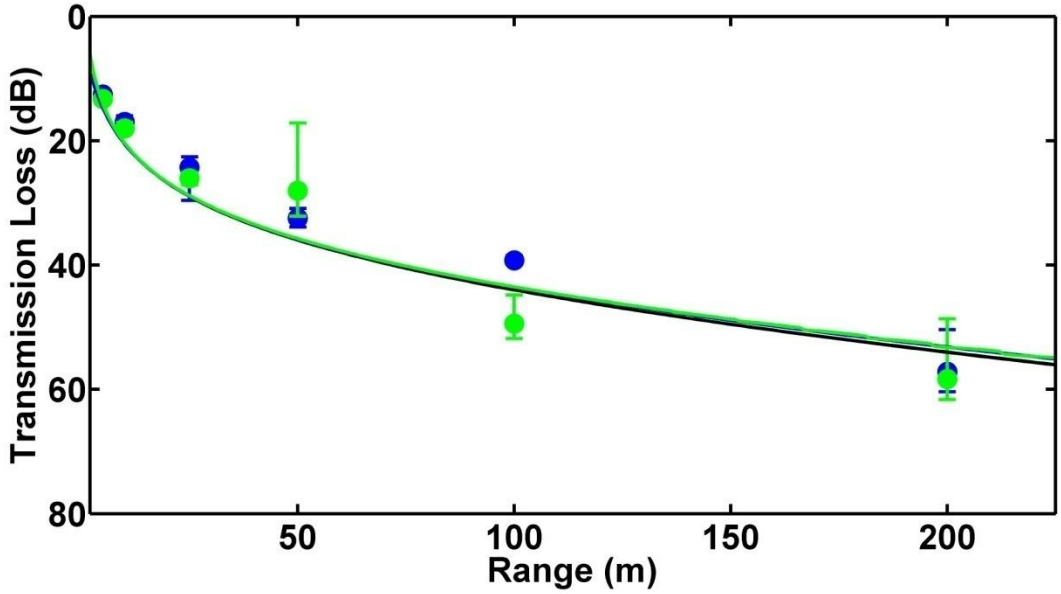

Figure 3.17. Measured and modeled transmission loss as a function of range for experiment 2. Blue circles show data collected at 3m receiver depth (zr = 3m), and green circles show data collected at 5m receiver depth (zr = 5m). Error bars on data points indicate minimum and maximum observed values. The black trace is the transmission loss predicted by a spherical spreading model with attenuation. The colored traces show transmission loss predicted by the Bellhop acoustic propagation model (single-arrival transmission loss; blue for 3m receiver depth, green for 5m receiver depth).

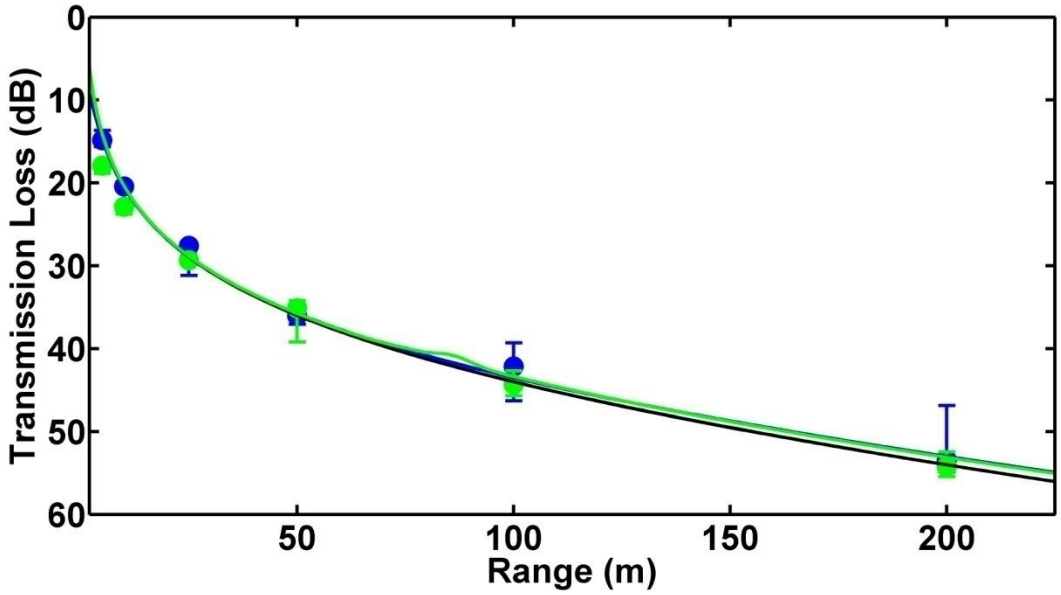

Figure 3.18. Measured and modeled transmission loss as a function of range for experiment 3. Blue circles show data collected at 3m receiver depth (zr = 3m), and green circles show data collected at 5m receiver depth (zr = 5m). Error bars on data points indicate minimum and maximum observed values. The black trace is the transmission loss predicted by a spherical spreading model with attenuation. The colored traces show transmission loss predicted by the Bellhop acoustic propagation model (single-arrival transmission loss; blue for 3m receiver depth, green for 5m receiver depth).

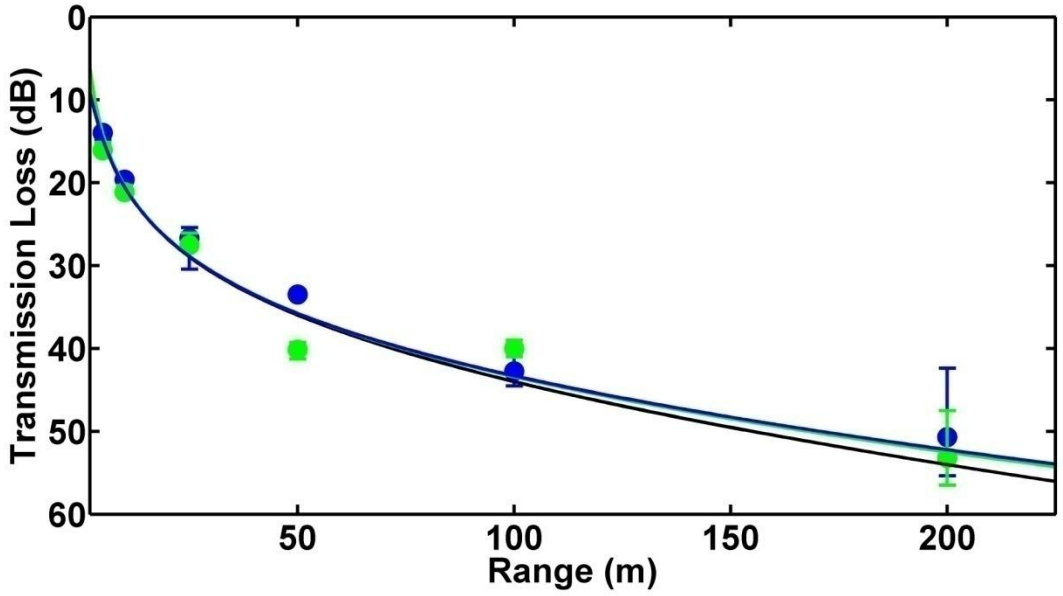

Figure 3.19. Measured and modeled transmission loss as a function of range for experiment 4. Blue circles show data collected at 3m receiver depth (zr = 3m), and green circles show data collected at 5m receiver depth (zr = 5m). Error bars on data points indicate minimum and maximum observed values. The black trace is the transmission loss predicted by a spherical spreading model with attenuation. The colored traces show transmission loss predicted by the Bellhop acoustic propagation model (single-arrival transmission loss; blue for 3m receiver depth, green for 5m receiver depth).

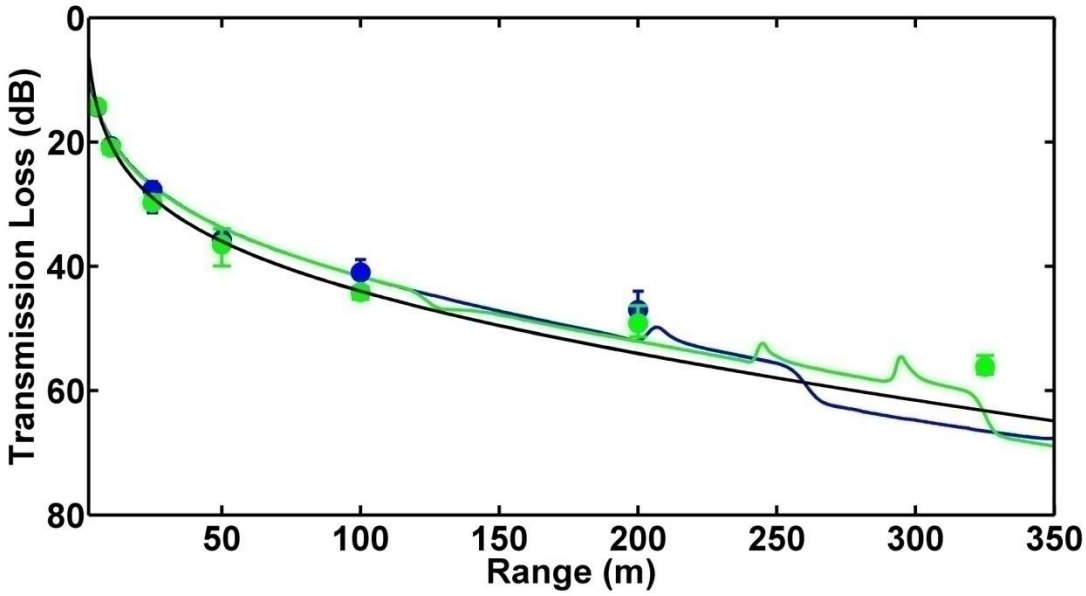

Figure 3.20. Measured and modeled transmission loss as a function of range for experiment 5. Blue circles show data collected at 3m receiver depth (zr = 3m), and green circles show data collected at 5m receiver depth (zr = 5m). Error bars on data points indicate minimum and maximum observed values. The black trace is the transmission loss predicted by a spherical spreading model with attenuation. The colored traces show transmission loss predicted by the Bellhop acoustic propagation model (total transmission loss; blue for 3m receiver depth, green for 5m receiver depth).

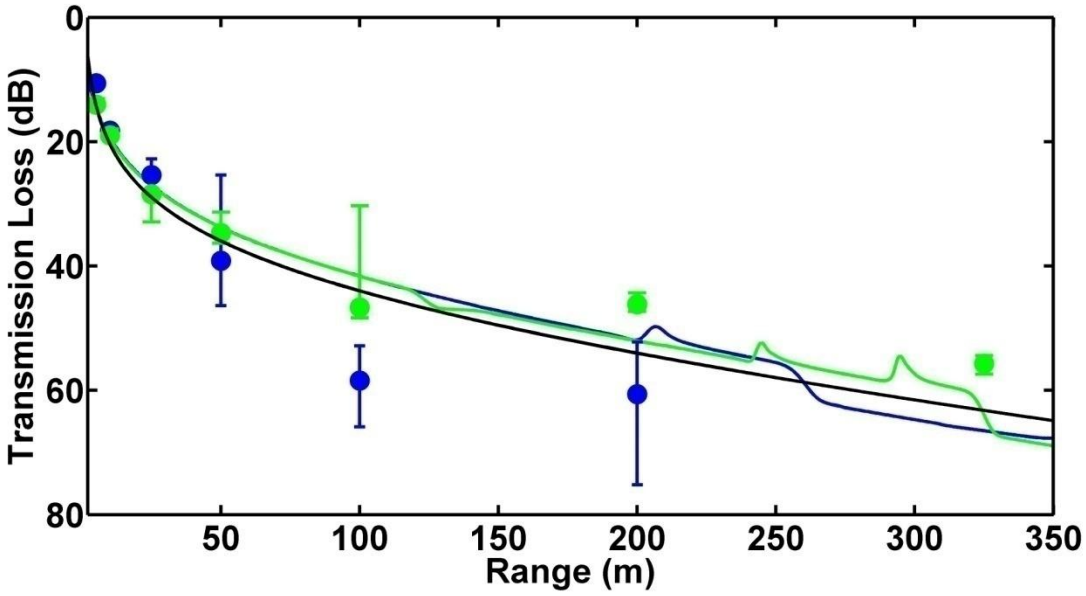

Figure 3.21. Measured and modeled transmission loss as a function of range for experiment 6. Blue circles show data collected at 3m receiver depth (zr = 3m), and green circles show data collected at 5m receiver depth (zr = 5m). Error bars on data points indicate minimum and maximum observed values. The black trace is the transmission loss predicted by a spherical spreading model with attenuation. The colored traces show transmission loss predicted by the Bellhop acoustic propagation model (total transmission loss; blue for 3m receiver depth, green for 5m receiver depth).

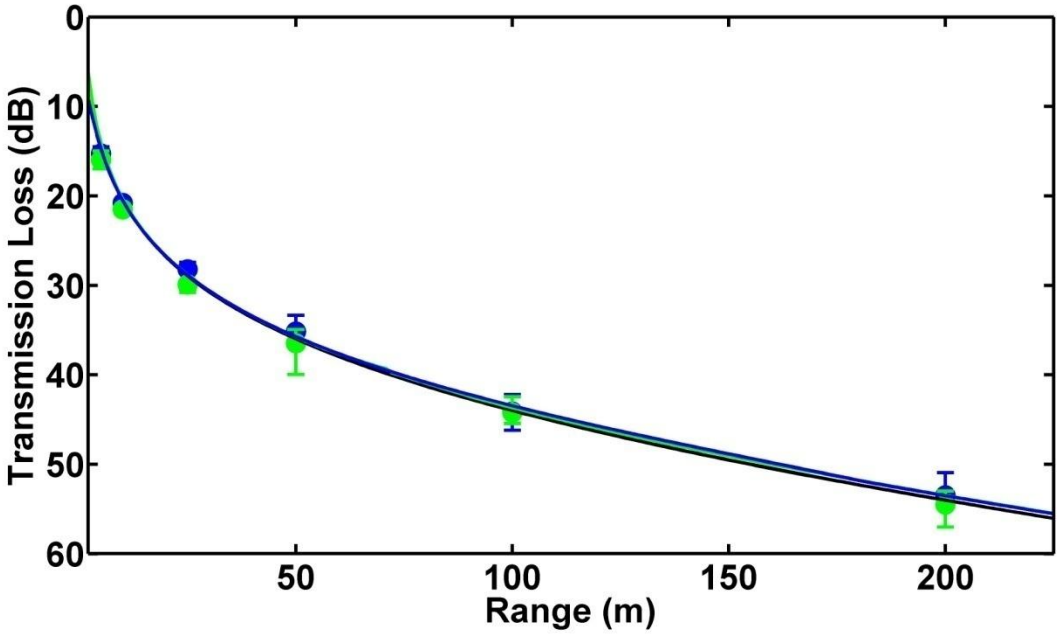

Figure 3.22. Measured and modeled transmission loss as a function of range for experiment 7. Blue circles show data collected at 3m receiver depth (zr = 3m), and green circles show data collected at 5m receiver depth (zr = 5m). Error bars on data points indicate minimum and maximum observed values. The black trace is the transmission loss predicted by a spherical spreading model with attenuation. The colored traces show transmission loss predicted by the Bellhop acoustic propagation model (single-arrival transmission loss; blue for 3m receiver depth, green for 5m receiver depth).

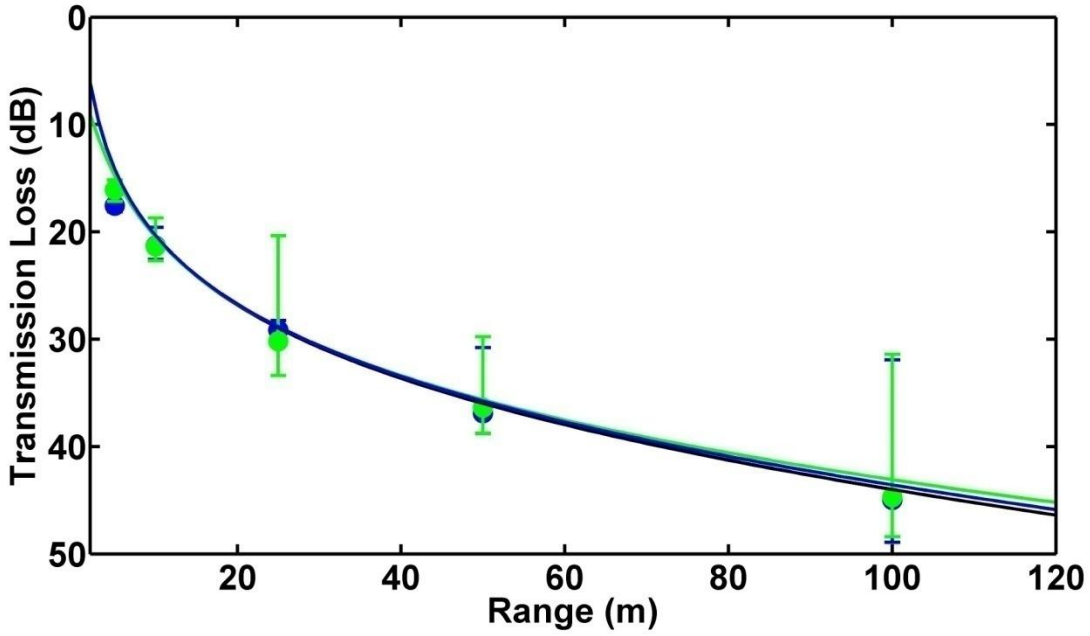

Figure 3.23. Measured and modeled transmission loss as a function of range for experiment 8. Blue circles show data collected at 3m receiver depth (zr = 3m), and green circles show data collected at 5m receiver depth (zr = 5m). Error bars on data points indicate minimum and maximum observed values. The black trace is the transmission loss predicted by a spherical spreading model with attenuation. The colored traces show transmission loss predicted by the Bellhop acoustic propagation model (single-arrival transmission loss; blue for 3m receiver depth, green for 5m receiver depth).

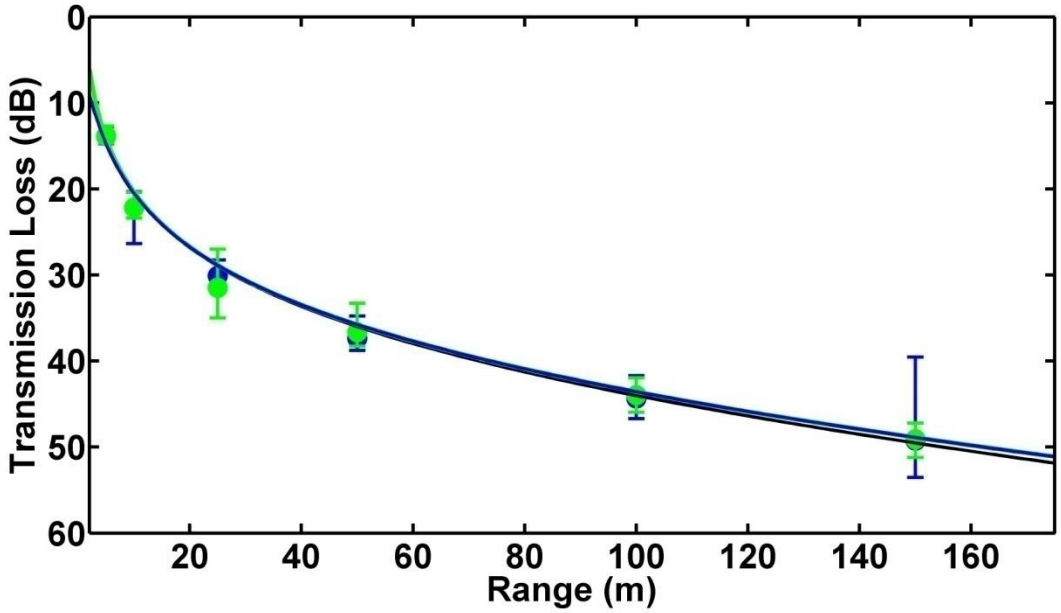

Figure 3.24. Measured and modeled transmission loss as a function of range for experiment 9. Blue circles show data collected at 3m receiver depth (zr = 3m), and green circles show data collected at 5m receiver depth (zr = 5m). Error bars on data points indicate minimum and maximum observed values. The black trace is the transmission loss predicted by a spherical spreading model with attenuation. The colored traces show transmission loss predicted by the Bellhop acoustic propagation model (single-arrival transmission loss; blue for 3m receiver depth, green for 5m receiver depth).

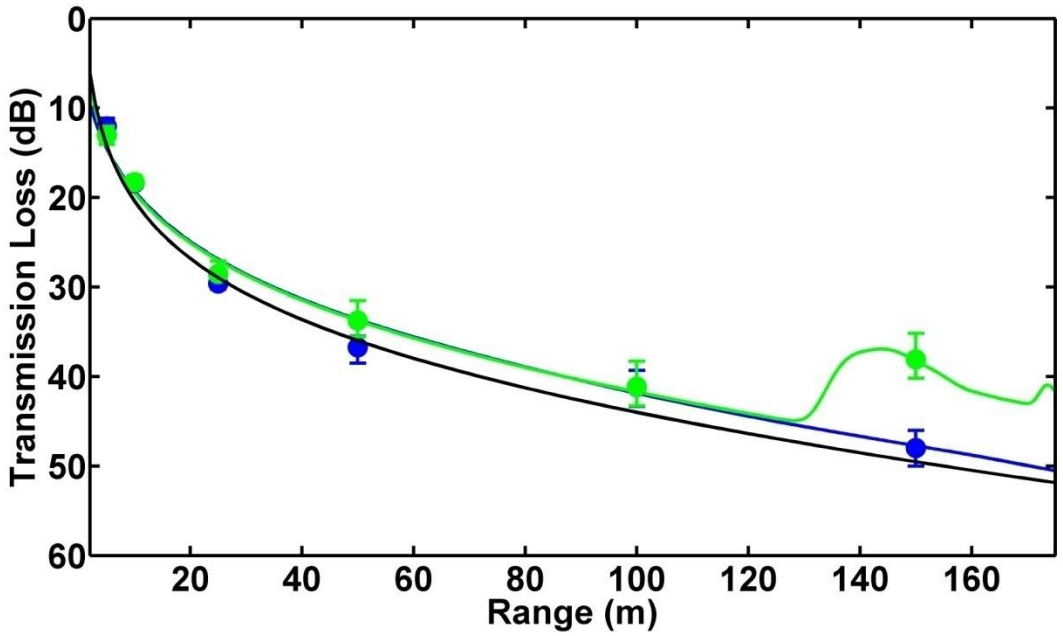

Figure 3.25. Measured and modeled transmission loss as a function of range for experiment 10. Blue circles show data collected at 3m receiver depth (z_r = 3m), and green circles show data collected at 5m receiver depth (z_r = 5m). Error bars on data points indicate minimum and maximum observed values. The black trace is the transmission loss predicted by a spherical spreading model with attenuation. The colored traces show transmission loss predicted by the Bellhop acoustic propagation model (total transmission loss; blue for 3m receiver depth, green for 5m receiver depth).

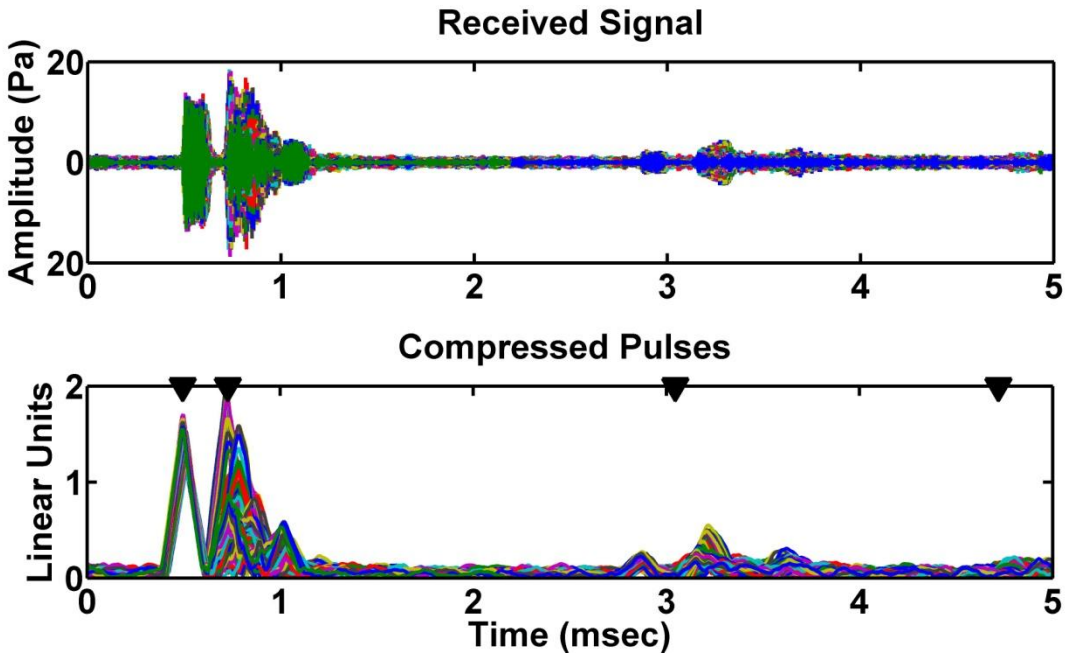

Figure 3.26. This figure contains data from experiment 10, for a receiver depth of 3 m and a source-receiver range of 50 m. Top panel: Received signal waveforms from 100 outgoing clicks. (The position of 0 on the time axis is arbitrary, since the transmitter and receivers were not time synchronized.) Bottom panel: results of pulse compression, generated by applying a matched filter (15 cycles of a 135 kHz signal sampled at 500 kHz) to the received signal waveforms. Black arrows on the upper x axis indicate Bellhop-predicted arrival times for the first (direct), second (surface reflected), third (bottom reflected), and fourth (bottom then surface reflected) acoustic arrivals. In this particular case, Bellhop does not predict the observed pattern of multiple arrivals around the time of the second, surface reflected arrival; since the arrival delay and amplitude of the additional arrivals varies gradually over time, I suspect they are from some scattering object moving between the source and receiver.

3.3.2. Comparison of Measured and Modeled Transmission Loss

Figures 3.27-3.29 summarize my results regarding the relative accuracy of the spreading law and Bellhop TL predictions. Figure 3.27, which plots the error of both types of TL prediction as a function of source-receiver range, shows that the prediction error did tend to increase with range. However, the error points remain relatively evenly scattered around zero at all ranges, indicating that neither model has a tendency to consistently over- or under-estimate TL as range increases. Error is plotted separately for each experiment in Figure 3.28, and Figure 3.29 shows the RMSE for each experiment. The two plots show that both models predicted TL quite accurately (errors not exceeding 6 dB, RMSE less than 3 dB) for experiments 3 and 7-9 and somewhat accurately for experiments 1-2 and 4 (errors not exceeding 10 dB, RMSE less than 5 dB). They both performed poorly for experiment 6, though the spreading law model performed somewhat better than the Bellhop model. The spreading law also performed well for experiment 5, where the Bellhop model performed less well. However, for experiment 10, the Bellhop model performed accurately while the spreading law did not. According to Figure 3.29, The RMSE for the whole set of ten experiments was between 3-4 dB for both the spreading law prediction and the Bellhop model, with the spreading law predictions performing slightly better than the Bellhop model predictions.

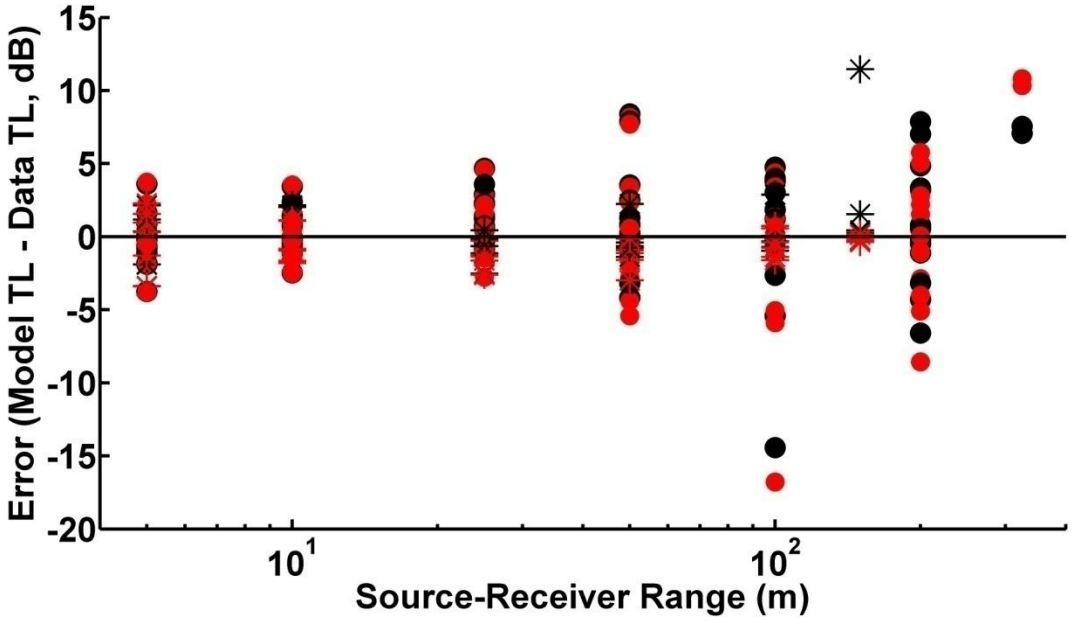

Figure 3.27. Error of the Bellhop and spherical spreading models as a function of range. Asterisks mark data points from Grand Manan experiments (experiments 1-7), and circles mark datapoints from Danish experiments (experiments 8-10). Black asterisks and circles show the error of the spherical spreading/attenuation model, while red asterisks and circles show the error of the Bellhop model.

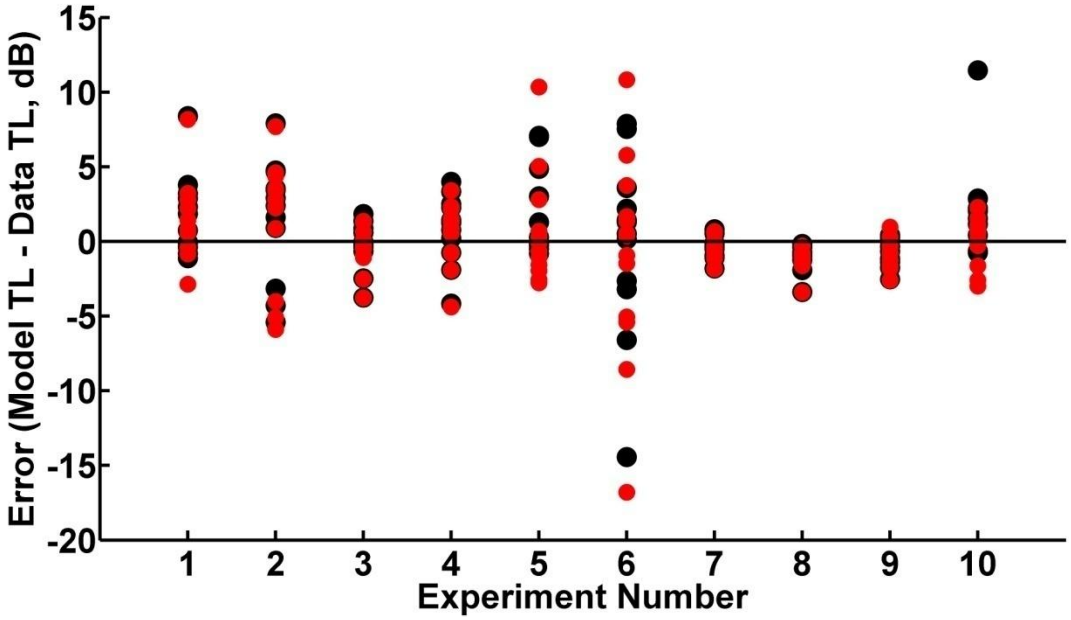

Figure 3.28. Error of the Bellhop and spherical spreading models by experiment. Data are shown for both Grand Manan experiments (experiments 1-7) and Danish experiments (experiments 8-10). One data point is shown for each source-receiver range. Black circles show the error of the spherical spreading/attenuation model, while red circles show the error of the Bellhop model.

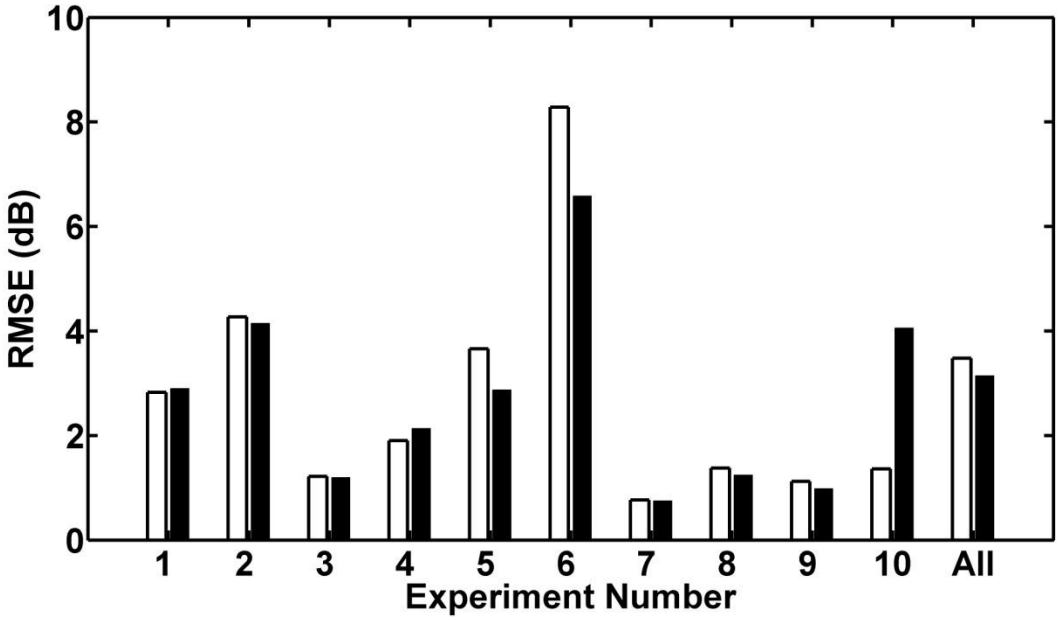

Figure 3.29. Comparison of the accuracy of the Bellhop and spherical spreading transmission loss predictions. For each experiment and each model, we calculated the RMSE between mean observed transmission loss and model-predicted transmission loss. White bars show the RMSE of the Bellhop model, while black bars show the RMSE of the spreading/attenuation model. (RMSE was averaged over all ranges and over both 3m and 5m receiver depths for each experiment. To calculate the RMSE, we calculated error (in dB) at each range and receiver depth, converted the error values to linear units, calculated RMSE, and finally converted back to dB.)

3.4 Discussion

Both of the modeling approaches I tried were able to predict transmission loss with overall RMS error of less than about 4 dB. I consider this to be relatively good model performance overall, and would not necessarily expect a perfect match between data and model, as there were several potential sources of error and inaccuracy in my dataset. First, I estimate that error in the measurements of source-receiver range at each station could have been off by

as much as 10%, especially at the longer ranges, due to the effects of wind and currents on the rope linking the transmit and receive boats. Second, especially at Grand Manan where tidal currents are very strong, the source and receiver depths may be slightly inaccurate because the hydrophone cables were not hanging exactly vertically.

In this paper, I have compared Bellhop model predictions of transmission loss with a simple spherical spreading law with attenuation. This spreading law is the one most commonly applied in predictions of transmission loss related to marine mammal echolocation and communication, which is why I chose it. In some cases, it might be more accurate to invoke a hybrid spherical/cylindrical spreading law, such as the following: at short ranges, transmission loss increases as the square of range (spherical spreading); as range increases to the point where the sound could be expected to interact with the surface and bottom, a transition from spherical spreading to cylindrical spreading (in which TL increases linearly with range) occurs (Urick, 1975). I chose not to include such a model in this analysis for simplicity, given that most of the arrivals I considered did not interact with the surface or bottom (so spherical spreading did not systematically overestimate TL at larger ranges).

At the sites I studied, the spherical spreading law with attenuation was able to predict transmission loss with an average error of just over 3 dB at source-receiver ranges up to 325 m, with less error at ranges of 50 m or less (Fig. 3.27). This result makes sense given the very short duration of the signal I used and the methods I used to calculate transmission loss from the data. I quantified the level of only the highest-amplitude arrival at each station. The highest-amplitude arrival was generally a direct (not surface- or bottom-interacting) arrival that underwent minimal refraction in the water column, in which case most of the assumptions underlying the spreading law assumption were upheld and the spreading law could accurately predict transmission loss for

that arrival. In addition, for the sites and ranges I considered, the direct arrival did not overlap temporally with any other arrivals, so multipath propagation and surface/bottom interactions did not affect its transmission loss.

The results of this study should be relevant to estimation of porpoise communication ranges and echolocation detection ranges as long as the set of source-receiver ranges I considered match the distances over which porpoises actually communicate and echolocate. Direct observations of such distances have not been made, but it is possible to calculate rough estimates as follows.

Consider a porpoise producing echolocation clicks with source levels of 191 dB re 1 μPa peak-to-peak at 1 m (Villadsgaard *et al.*, 2007), equivalent to an energy flux density of 140 dB re 1 μPa^2s (Kastelein *et al.*, 1999). Assume that the porpoise echolocates on a herring with a target strength of -37 dB (Ona, 2003), and listens for returning echoes with a detection threshold of about 27 dB re 1 μPa^2s (Kastelein *et al.*, 1999). Echoes with one-way transmission loss of 38 dB or less would be detectable to the porpoise (calculated according to received level = detection threshold = source level – 2(one-way transmission loss) + target strength). At the sites examined in this study, transmission losses first exceeded 38 dB at ranges of 50 or 100 m (Figs. 3.16-3.25), with observed losses of less than 38 dB at a range of 150 m in one case (Fig. 3.25).

For a similar calculation of communication call detection ranges, assume that the threshold for detection of communication sounds is the same as that for echoes (27 dB re 1 μPa^2s (Kastelein *et al.*, 1999)), and that the source level of communication clicks is about 180 dB re 1 μPa peak-to-peak at 1 m (Clausen *et al.*, 2008), equivalent to 129 dB re 1 μPa^2s (Kastelein *et al.*, 1999). In that case, communication sounds with transmission losses of 102 dB or less would be detectable to conspecifics (calculated according to received level = detection threshold = source level – transmission loss). 102 dB is much higher than the largest transmission loss value observed in the current study (61 dB), indicating

that porpoises can detect conspecific calls at the ranges considered in this study (5-325 m) and greater ranges.

Previous work has shown that click source levels of free-ranging porpoises average 191 dB re 1 µPa peak-to-peak @ 1 m (Villadsgaard *et al.*, 2007), and that T-POD porpoise detectors can detect porpoise clicks at levels as low as 114-123 dB re 1 µPa peak-equivalent RMS (Kyhn, 2006), or 123-132 dB re 1 µPa peak-to-peak. Given those values, on-axis porpoise clicks with transmission loss on the order of about 68 dB may be detectable on T-PODs. Off-axis clicks with transmission loss as great as about 28 dB may be detectable, since off-axis click source levels can be upwards of 40 dB lower than those of on-axis clicks (Hansen, 2007). Transmission losses on the order of 30-70 dB are within or slightly greater than the range measured and modeled in this study. At the study sites, measured transmission loss first exceeded 28 dB at 25 or 50 m range, and I never measured transmission loss of more than 68 dB (at maximum ranges of 100-325m). The results of my experiments therefore suggest that, in areas similar to my study sites, using a spreading law-based model of transmission loss in T-POD detection range estimates should result in relatively low error on average for off-axis clicks detected at ranges of 50m or less (Fig. 3.27). For on-axis clicks, which are likely to be detected at much greater ranges, error in spreading-law-based calculations is likely to be greater (Fig. 3.27).

It is important to note that in some particular cases, spreading-law-based transmission loss estimates may not perform well. The spherical spreading law did not predict transmission loss as accurately for experiment 10, while the Bellhop model was able to do so. I believe that the spreading law prediction failed because the loudest arrivals in the experiment 10 data were not always the first, direct arrivals; often a subsequent arrival peak comprised of several overlapping arrivals was louder. In addition, multiple ray paths pass through a focus near the receiver at 5 m depth and 150 m range (Figure 3.30), significantly

reducing the transmission loss at that location. In this case, it was unsurprising that the Bellhop model (which accounts for multipath propagation and water column refraction) outperformed the spreading law calculation (which does not). The spreading law model cannot be relied upon in cases such as experiment 10, where surface/bottom interactions and/or refraction in the water column significantly affect transmission loss between the source and the receiver.

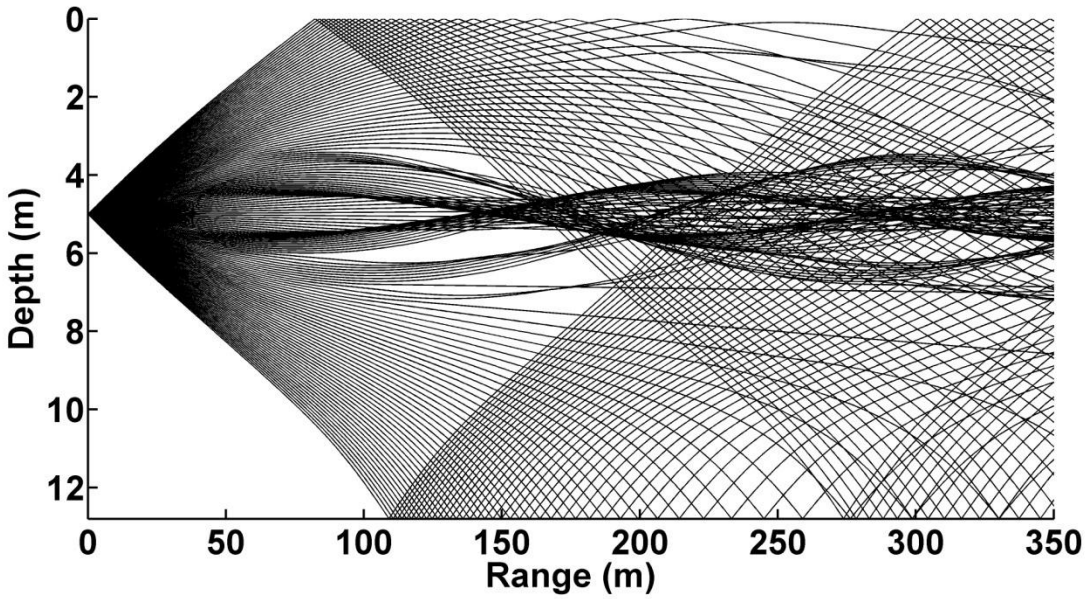

Figure 3.30. Bellhop ray trace output for the experiment 10 site. For clarity, only rays with launch angles between +/- 4 degrees from the horizontal are shown. Some rays pass through a focus at about 5 m depth and 150 m range.

One might argue that surface and bottom interacting propagation paths are unlikely to influence the transmission loss of real porpoise clicks because porpoises, unlike the transducer used in our experiments, produce highly directional clicks with a -10 dB beam width of about 20 degrees in the vertical plane (Au *et al.*, 1999). It is likely that, given this narrower beam and given the porpoise's ability to scan and point its sonar in a desired direction, the amount of acoustic energy in higher-launch-angle, surface- and bottom-interacting arrivals

would be attenuated and the direct arrival would dominate. However, given the porpoise beam width, this reduction would only occur at relatively short source-receiver ranges. For example, Figure 3.31 shows a Bellhop ray trace for a porpoise-like source (transmitting a 135 kHz signal at launch angles between -20 and 20 degrees from the horizontal) at 5 m depth at the experiment 10 site. In that case, surface- and bottom-interacting arrivals will reach receivers at 3 and 5 m depth at source-receiver ranges of 50 m or less.

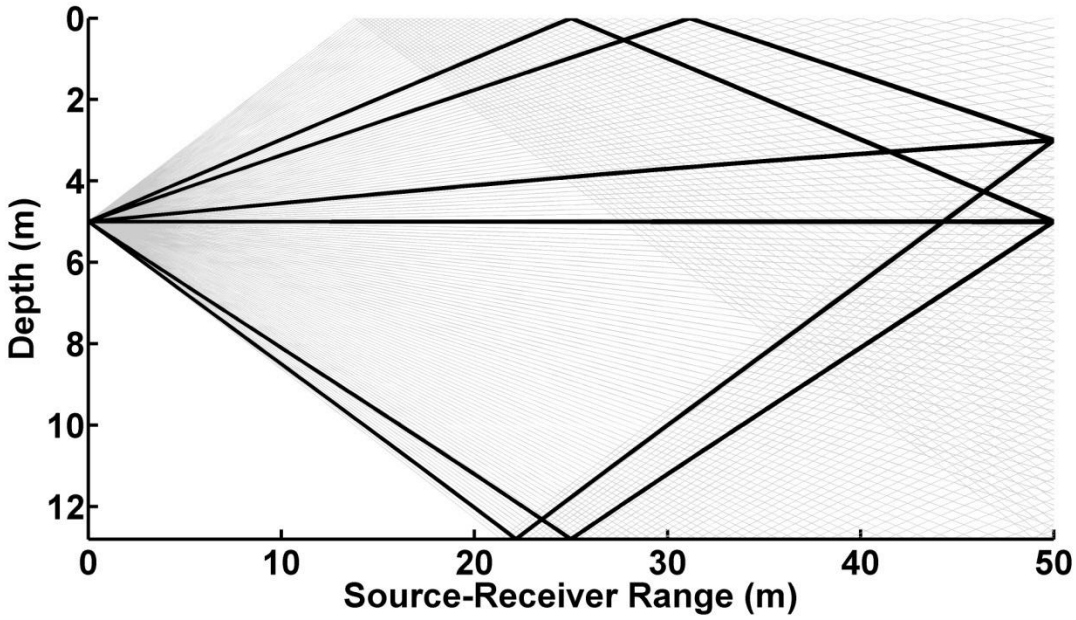

Figure 3.31. Bellhop ray trace output for a porpoise-like source (transmitting a 135 kHz signal at launch angles between -20 and 20 degrees from the horizontal) at the experiment 10 site. Grey traces show all the ray paths, while black traces show eigenrays between the source and receivers at 50 m range and 3 or 5 m depth.

The experiment 10 case also illustrates that refraction in the water column can strongly affect transmission loss in some cases; in experiment 10, a minimum in the sound speed profile at around 5 m depth channeled and focused the sound and resulted in reduced transmission loss at certain ranges and

depths (including the receiver at 150 m range, 5 m depth; Figs. 3.14 and 3.30). Porpoises may be able to exploit such sound channels to increase the range at which they can detect prey or other targets with their echolocation, or to increase the active space of their communication calls. For example, assume that communication calls remain detectable until transmission loss exceeds 102 dB (see earlier calculation of communication call detection ranges). In a habitat where transmission loss can be approximated by a spherical spreading law with attenuation, the active space of an on-axis porpoise communication call would be about 1 km or 4.2 km^3. In the same situation, an off-axis call with 40 dB lower source level would have an active space of about 300m or 0.1 km^3. By taking advantage of a sound channel like the one at the experiment 10 site, porpoises could dramatically increase their active space: the active space of an on-axis call could increase to 1.5 km or 14 km^3, and that of an off-axis call to 600 m or 0.9 km^3 (calculated using Bellhop output transmission loss for the experiment 10 site). Future studies could test the hypothesis that porpoises exploit sound channels for communication by looking for a relationship between sound-speed profiles and the depth distribution of porpoise acoustic activity[1].

Variability in transmission loss as a function of depth also has implications for passive acoustic monitoring, since in a habitat where such variation occurs, detection probabilities and distances will vary with animal depth and detector depth. For example, assuming that T-PODs can detect porpoise clicks that undergo transmission loss of 68 dB or less (see earlier calculations), and assuming that spherical spreading with attenuation accurately estimates

[1] In any habitat where sound channels were present, such a study would have to take into account the following: porpoises clicks produced in a sound channel would likely be detectable at greater ranges, so the amount of acoustic activity in the channel might appear to be greater even if porpoise sound production depths were randomly distributed.

[2] If the whale is in a certain state *j*, it will remain in that state for a certain "waiting time" before changing to the next state; each observed waiting time is generally assumed to be a random sample from a state-specific probability distribution.

[3] The -3dB bandwidth of a porpoise click is about 15 kHz (Au et al. 1999, Villadsgaard et al. 2007). In absolute terms, this bandwidth is not dramatically different from the -3dB bandwidth of

transmission loss, one would expect a T-POD to detect porpoises over an area of 0.5 km^2. However, in a habitat like the experiment 10 site with a sound channel, a T-POD in the sound channel would actually be able to detect porpoises in the sound channel over an area of 1.5 km^2 (area estimate calculated using Bellhop output for the experiment 10 site). If not accounted for, variability of this magnitude could easily result in very large errors in estimates of animal density. Therefore, variability in transmission loss as a function of depth should be considered when selecting detector deployment depths and reviewing passive acoustic monitoring data.

Neither the spherical spreading law predictions nor the Bellhop model predictions were particularly accurate for experiments 5 and 6; they were particularly poor for experiment 6, especially at longer ranges. I believe that the spreading law model performed poorly because multipath propagation and surface/bottom interactions played an important role in determining the transmission loss, as was the case for experiment 10. However, for experiments 5-6, the Bellhop model predictions were also inaccurate. I suspect that the environment model we used as Bellhop input was incomplete for the experiment 5-6 site. Specifically, I suspect that the area around the site may have contained boulders and a rocky ledge or outcropping (A.J. Westgate, personal communication to S.D.R., May 27, 2008). These features were not accounted for in my environmental model, and they would reflect sound much more strongly than the silty clay bottom I specified for Bellhop model runs.

For most of the cases I considered, spherical spreading with attenuation provided relatively accurate estimates of transmission loss in porpoise habitats. However, its accuracy depended on the fact that the dominant acoustic arrival at the receiver did not interact with the sea surface or bottom, did not overlap temporally with other arrivals, and was not dramatically affected by refraction in the water column. The existence of those conditions depends on site-specific

source-receiver geometry, bathymetry, sediment properties, and sound speed profile, so spherical spreading may not accurately describe transmission loss in porpoise habitats that differ significantly from the sites considered here. When adequate data on the acoustic environment are available, a more detailed model such as Bellhop can be a useful tool to investigate the effects of environmental conditions on transmission loss at a particular site in greater detail.

Acknowledgements

I am very grateful to Michael Hansen, as well as Heather Koopman, Andrew Westgate, and everyone else at the Grand Manan Whale and Seabird Research Station, for their advice and their assistance collecting data in the field in Canada. Michael and others from Aarhus University, Denmark, collected all the Danish field data. I am grateful to Peter Madsen and Aarhus University for loaning me equipment needed to make the field recordings; Peter Madsen also provided the original versions of some Matlab scripts modified to determine TL from the field data. Ying-Tsong Lin, James Lynch, and Arthur Newhall provided very helpful advice related to data interpretation and acoustic propagation modeling, and Ying-Tsong Lin also provided a Matlab script used as the basis of the pulse compression analysis. Peter Tyack, Peter Madsen, and Regina Campbell-Malone also provided helpful comments on the analysis and this manuscript. Field data collection was partially supported by a Student Research Award from the WHOI Ocean Life Institute (grant number 25051351).

References

Akamatsu, T., Teilmann, J., Miller, L. A., Tougaard, J., Dietz, R., Wang, D., Wang, K. X., Siebert, U., and Naito, Y. (**2007**). "Comparison of echolocation behaviour between coastal and riverine porpoises," Deep-Sea Research Part II -Topical Studies in Oceanography **54**, 290-297.

Akamatsu, T., Wang, D., Wang, K. X., and Naito, Y. (**2005**). "Biosonar behaviour of free-ranging porpoises," Proceedings of the Royal Society B - Biological Sciences **272**, 797-801.

Au, Floyd, R. W., Penner, R. H., and Murchison, A. E. (**1974**). "Measurement of echolocation signals of the Atlantic bottlenose dolphin, *Tursiops truncatus* Montagu, in open waters," Journal of the Acoustical Society of America **56**, 1280-1290.

Au, W. W. L. (**1993**). *The sonar of dolphins* (Springer-Verlag, New York, NY).

Au, W. W. L., and Benoit-Bird, K. J. (**2003a**). "Acoustic backscattering by Hawaiian lutjanid snappers. II. Broadband temporal and spectral structure," Journal of the Acoustical Society of America **114**, 2767-2774.

Au, W. W. L., and Benoit-Bird, K. J. (**2003b**). "Automatic gain control in the echolocation system of dolphins," Nature **423**, 861-863.

Au, W. W. L., Benoit-Bird, K. J., and Kastelein, R. A. (**2007**). "Modeling the detection range of fish by echolocating bottlenose dolphins and harbor porpoises," Journal of the Acoustical Society of America **121**, 3954-3962.

Au, W. W. L., Ford, J. K. B., Horne, J. K., and Allman, K. A. N. (**2004**). "Echolocation signals of free-ranging killer whales (*Orcinus orca*) and modeling of foraging for chinook salmon (*Oncorhynchus tshawytscha*)," Journal of the Acoustical Society of America **115**, 901-909.

Au, W. W. L., and Jones, L. (**1991**). "Acoustic reflectivity of nets - Implications concerning incidental take of dolphins," Marine Mammal Science **7**, 258-273.

Au, W. W. L., Kastelein, R. A., Rippe, T., and Schooneman, N. M. (**1999**). "Transmission beam pattern and echolocation signals of a harbor porpoise (*Phocoena phocoena*)," Journal of the Acoustical Society of America **106**, 3699-3705.

Benoit-Bird, K. J., Au, W. W. L., and Kelley, C. D. (**2003**). "Acoustic backscattering by Hawaiian lutjanid snappers. I. Target strength and swimbladder characteristics," Journal of the Acoustical Society of America **114**, 2757-2766.

Bowen, D., Brodie, P., Conway, J., Gearin, P., Hammill, M., Hood, C. C., Kingsley, M. C., Lesage, V., Lien, J., Metuzals, K., Palka, D., Potter, D., Read, A. J., Rosel, P., Simon, P., and Stenson, G. (**2001**). "Proceedings of the International Harbour Porpoise Workshop," in *International Harbour Porpoise Workshop*, edited by G. Stenson (Canadian Science Advisory Secretariat, Bedford Institute of Oceanography, Dartmouth, Nova Scotia, Canada).

Carstensen, J., Henriksen, O. D., and Teilmann, J. (**2006**). "Impacts of offshore wind farm construction on harbour porpoises: acoustic monitoring of echolocation activity using porpoise detectors (T-PODs)," Marine Ecology-Progress Series **321**, 295-308.

Clausen, K. T., Madsen, P. T., and Wahlberg, M. (**2008**). "Click communication in harbour porpoises, *Phocoena phocoena* [poster presentation]," European Cetacean Society 2008 Conference, Egmond aan Zee, The Netherlands, 10-12 March 2008.

Cox, T. M., Read, A. J., Solow, A., and Tregenza, N. (**2001**). "Will harbour porpoises (*Phocoena phocoena*) habituate to pingers?," Journal of Cetacean Research and Management **3**, 81-86.

Culik, B. M., Koschinski, S., Tregenza, N., and Ellis, G. M. (**2001**). "Reactions of harbor porpoises *Phocoena phocoena* and herring *Clupea harengus* to acoustic alarms," Marine Ecology Progress Series **211**, 255-260.

Dawson, S. M., Read, A. J., and Slooten, E. (**1998**). "Pingers, porpoises and power: Uncertainties with using pingers to reduce bycatch of small cetaceans," Biological Conservation **84**, 141-146.

Francois, R. E., and Garrison, G. R. (**1982a**). "Sound absorption based on ocean measurements: Part I: Pure water and magnesium sulfate contributions," Journal of the Acoustical Society of America **72**, 896-907.

Francois, R. E., and Garrison, G. R. (**1982b**). "Sound absorption based on ocean measurements: Part II: Boric acid contribution and equation for total absorption," Journal of the Acoustical Society of America **72**, 1879-1890.

Hamilton, E. L. (**1978**). "Sound velocity-density relations in sea-floor sediments and rocks," Journal of the Acoustical Society of America **63**, 366-377.

Hansen, M. (**2007)**. "High and low frequency components in harbour porpoise (*Phocoena phocoena*) clicks for echolocation and communication - facts or artefacts?," M.Sc. Thesis, Zoophysiology Department, Faculty of Science, University of Aarhus.

Hemilä, S., Nummela, S., and Reuter, T. (**2001**). "Modeling whale audiograms: effects of bone mass on high-frequency hearing," Hear Res **151**, 221-226.

Jackson, D. R., and Richardson, M. D. (**2007**). *High-Frequency Seafloor Acoustics* (Springer Science+Business Media, L.L.C., New York, NY).

Jensen, F. B., Kuperman, W. A., Porter, M. B., and Schmidt, H. (**1994**). *Computational Ocean Acoustics* (AIP Press, Woodbury, NY).

Kaschner, K. (**2003**). "Review of small cetacean bycatch in the ASCOBANS area and adjacent waters – current status and suggested future actions," (Report to ASCOBANS).

Kastelein, R. A., Au, W. W. L., and De Haan, D. (**2000**). "Detection distances of bottom-set gillnets by harbour porpoises (*Phocoena phocoena*) and bottlenose dolphins (*Tursiops truncatus*)," Marine Environmental Research **49**, 359-375.

Kastelein, R. A., Au, W. W. L., Rippe, H. T., and Schooneman, N. M. (**1999**). "Target detection by an echolocating harbor porpoise (*Phocoena phocoena*)," Journal of the Acoustical Society of America **105**, 2493-2498.

Kastelein, R. A., Bunskoek, P., Hagedoorn, M., Au, W. W. L., and de Haan, D. (**2002**). "Audiogram of a harbor porpoise (*Phocoena phocoena*) measured with narrow-band frequency-modulated signals," Journal of the Acoustical Society of America **112**, 334-344.

Kastelein, R. A., Hagedoorn, M., Au, W. W. L., and de Haan, D. (**2003**). "Audiogram of a striped dolphin (*Stenella coeruleoalba*)," Journal of the Acoustical Society of America **113**, 1130-1137.

Kastelein, R. A., Janssen, M., Verboom, W. C., and de Haan, D. (**2005a**). "Receiving beam patterns in the horizontal plane of a harbor porpoise (*Phocoena phocoena*)," Journal of the Acoustical Society of America **118**, 1172-1179.

Kastelein, R. A., Verboom, W. C., Muijsers, M., Jennings, N. V., and van der Heul, S. (**2005b**). "The influence of acoustic emissions for underwater data transmission on the behaviour of harbour porpoises (*Phocoena phocoena*) in a floating pen," Marine Environmental Research **59**, 287-307.

Ketten, D. R. (**1997**). "Structure and function in whale ears," Bioacoustics **8**, 103-135.

Koschinski, S., Culik, B. M., Henriksen, O. D., Tregenza, N., Ellis, G., Jansen, C., and Kathe, G. (**2003**). "Behavioural reactions of free-ranging porpoises and seals to the noise of a simulated 2 MW windpower generator," Marine Ecology Progress Series **265**, 263-273.

Kyhn, L. A. (**2006)**. "Detection of harbour porpoises using T-PODs," M. Sc. Thesis, Zoophysiology Department, Aarhus University.

Leeney, R. H., Berrow, S., McGrath, D., O'Brien, J., Cosgrove, R., and Godley, B. J. (**2007**). "Effects of pingers on the behaviour of bottlenose dolphins," Journal of the Marine Biological Association of the United Kingdom **87**, 129-133.

Lund-Hansen, L. C., Laima, L. C., Mouritsen, K. N., Lam, Y., and Hai, A. (**2002**). "Effects of benthic diatoms, fluff layer, and sediment conditions on critical shear stress in a non-tidal coastal environment," Journal of the Marine Biological Association of the United Kingdom **82**, 1-8.

Madsen, P. T., Kerr, I., and Payne, R. (**2004a**). "Echolocation clicks of two free-ranging, oceanic delphinids with different food preferences: false killer whales *Pseudorca crassidens* and Risso's dolphins *Grampus griseus*," Journal of Experimental Biology **207**, 1811-1823.

Madsen, P. T., Kerr, I., and Payne, R. (**2004b**). "Source parameter estimates of echolocation clicks from wild pygmy killer whales (*Feresa attenuata*) (L)," Journal of the Acoustical Society of America **116**, 1909-1912.

Madsen, P. T., and Wahlberg, M. (**2007**). "Recording and quantification of ultrasonic echolocation clicks from free-ranging toothed whales," Deep-Sea Research Part I-Oceanographic Research Papers **54**, 1421-1444.

Medwin, H., and Clay, C. S. (**1998**). *Fundamentals of Acoustical Oceanography* (Academic Press, Boston, MA).

Møhl, B., Wahlberg, M., Madsen, P. T., Heerfordt, A., and Lund, A. (**2003**). "The monopulsed nature of sperm whale clicks," Journal of the Acoustical Society of America **114**, 1143-1154.

Møhl, B., Wahlberg, M., Madsen, P. T., Miller, L. A., and Surlykke, A. (**2000**). "Sperm whale clicks: Directionality and source level revisited," Journal of the Acoustical Society of America **107**, 638-648.

Mooney, T. A., Au, W. W. L., Nachtigall, P. E., and Trippel, E. A. (**2007**). "Acoustic and stiffness properties of gillnets as they relate to small cetacean bycatch," ICES Journal of Marine Science **64**, 1324-1332.

Mooney, T. A., Natchigall, P. E., and Au, W. W. L. (**2004**). "Target strength of a nylon monofilament and an acoustically enhanced gillnet: Predictions of biosonar detection ranges," Aquatic Mammals **30**, 220-226.

Nachtigall, P. E., Yuen, M. M. L., Mooney, T. A., and Taylor, K. A. (**2005**). "Hearing measurements from a stranded infant Risso's dolphin, *Grampus griseus*," Journal of Experimental Biology **208**, 4181-4188.

Ona, E. (**2003**). "An expanded target-strength relationship for herring," ICES Journal of Marine Science **60**, 493-499.

Paskevich, V. F., Poppe, L. J., Hastings, M. E., and Hathaway, J. C. (**2001**). "Sea floor photography from the continental margin program: A pictorial survey of benthic character and habitats along the U.S. east coast (Open File Report 01-154)," (United States Geological Survey Woods Hole, MA).

Philpott, E., Englund, A., Ingram, S., and Rogan, E. (**2007**). "Using T-PODs to investigate the echolocation of coastal bottlenose dolphins," Journal of the Marine Biological Association of the United Kingdom **87**, 11-17.

Popov, V. V., Ladygina, T. F., and Supin, A. Y. (**1986**). "Evoked potentials of the auditory cortex of the porpoise, *Phocoena phocoena*," Journal of Comparative Physiology A **158**, 705-711.

Popov, V. V., Supin, A. Y., Wang, D., Wang, K. X., Xiao, J. Q., and Li, S. H. (**2005**). "Evoked-potential audiogram of the Yangtze finless porpoise *Neophocaena phocaenoides asiaeorientalis* (L)," Journal of the Acoustical Society of America **117**, 2728-2731.

Poppe, L. J., Williams, S. J., and Paskevich, V. F. (**2005**). "U.S.G.S. East-coast sediment analysis: Procedures, database and G.I.S. data (Open File Report 05-1001)," (U.S. Geological Survey, Woods Hole, MA).

Porter, M. B., and Bucker, H. P. (**1987**). "Gaussian beam tracing for computing ocean acoustic fields," Journal of the Acoustical Society of America **82**, 1349-1359.

Rasmussen, M. H., Miller, L. A., and Au, W. W. L. (**2002**). "Source levels of clicks from free-ranging white-beaked dolphins (*Lagenorhynchus albirostris* Gray 1846) recorded in Icelandic waters," Journal of the Acoustical Society of America **111**, 1122-1125.

Read, A. J., Kraus, S. D., Bisack, K. D., and Palka, D. (**1993**). "Harbor porpoises and gill nets in the Gulf of Maine," Conservation Biology **7**, 189-193.

Reeder, D. B., Jech, J. M., and Stanton, T. K. (**2004**). "Broadband acoustic backscatter and high-resolution morphology of fish: Measurement and modeling," Journal of the Acoustical Society of America **116**, 747-761.

Rose, G. A. (**1998**). "Acoustic target strength of capelin in Newfoundland waters," ICES Journal of Marine Science **55**, 918-923.

Røy, H., Huettel, M., and Jørgensen, B. B. (**2005**). "The influence of topography on the functional exchange surface of marine soft sediments, assessed from sediment topography measured *in situ*.," Limnology and Oceanography **50**, 106-112.

Sauerland, M., and Dehnhardt, G. (**1998**). "Underwater audiogram of a tucuxi (*Sotalia fluviatilis guianensis*)," Journal of the Acoustical Society of America **103**, 1199-1204.

Schulkin, M., and Marsh, H. W. (**1962**). "Sound absorption in sea water," Journal of the Acoustical Society of America **42**, 864-865.

Szymanski, M. D., Bain, D. E., Kiehl, K., Pennington, S., Wong, S., and Henry, K. R. (**1999**). "Killer whale (*Orcinus orca*) hearing: Auditory brainstem response and behavioral audiograms," Journal of the Acoustical Society of America **106**, 1134-1141.

Thomas, J., Chun, N., Au, W., and Pugh, K. (**1988**). "Underwater Audiogram of a False Killer Whale (*Pseudorca crassidens*)," Journal of the Acoustical Society of America **84**, 936-940.

Thomsen, F., van Elk, N., Brock, V., and Piper, W. (**2005**). "On the performance of automated porpoise-click-detectors in experiments with captive harbor porpoises (*Phocoena phocoena*) (L)," Journal of the Acoustical Society of America **118**, 37-40.

Thorp, W. H. (**1965**). "Deep ocean sound attenuation in the sub and low kilocycle-per-second region," Journal of the Acoustical Society of America **38**, 648-654.

Thorp, W. H. (**1967**). "Analytic description of the low-frequency attenuation coefficient," Journal of the Acoustical Society of America **42**, 270.

Trippel, E. A., Holy, N. L., Palka, D. L., Shepherd, T. D., Melvin, G. D., and Terhune, J. M. (**2003**). "Nylon barium sulphate gillnet reduces porpoise and seabird mortality," Marine Mammal Science **19**, 240-243.

Urick, R. J. (**1975**). *Principles of Underwater Sound for Engineers* (McGraw-Hill Book Company, New York, NY).

Verfuss, U. K., Honnef, C. G., Meding, A., Dahne, M., Mundry, R., and Benke, H. (**2007**). "Geographical and seasonal variation of harbour porpoise (*Phocoena phocoena*) presence in the German Baltic Sea revealed by passive acoustic monitoring," Journal of the Marine Biological Association of the United Kingdom **87**, 165-176.

Villadsgaard, A., Wahlberg, M., and Tougaard, J. (**2007**). "Echolocation signals of wild harbour porpoises, *Phocoena phocoena*," Journal of Experimental Biology **210**, 56-64.

Wenz, G. M. (**1962**). "Acoustic ambient noise in the ocean: Spectra and sources," Journal of the Acoustical Society of America **34**, 1936-1956.

Yuen, M. M. L., Nachtigall, P. E., Breese, M., and Supin, A. Y. (**2005**). "Behavioral and auditory evoked potential audiograms of a false killer whale (*Pseudorca crassidens*)," Journal of the Acoustical Society of America **118**, 2688-2695.

Chapter 4. Modeling acoustic propagation of airgun array pulses recorded on tagged sperm whales (*Physeter macrocephalus*)

The following paper (full citation below) was previously published in the Journal of the Acoustical Society of America, and is reprinted here with permission from the publishers.

DeRuiter, S. L., Tyack, P. L., Lin, Y. T., Newhall, A. E., and Lynch, J. F. (**2006**). "Modeling acoustic propagation of airgun array pulses recorded on tagged sperm whales (*Physeter macrocephalus*)," Journal of the Acoustical Society of America **120**, 4100-4114.

Modeling acoustic propagation of airgun array pulses recorded on tagged sperm whales (*Physeter macrocephalus*)[a)]

Stacy L. DeRuiter[b)] and Peter L. Tyack
Biology Department, Woods Hole Oceanographic Institution, Woods Hole, Massachusetts 02543

Ying-Tsong Lin, Arthur E. Newhall, and James F. Lynch
Department of Applied Ocean Physics and Engineering, Woods Hole Oceanographic Institution, Woods Hole, Massachusetts 02543

Patrick J. O. Miller
Sea Mammal Research Unit, University of St. Andrews, Fife KY16 8LB, Scotland

(Received 26 January 2006; revised 1 September 2006; accepted 13 September 2006)

In 2002 and 2003, tagged sperm whales (*Physeter macrocephalus*) were experimentally exposed to airgun pulses in the Gulf of Mexico, with the tags providing acoustic recordings at measured ranges and depths. Ray trace and parabolic equation (PE) models provided information about sound propagation paths and accurately predicted time of arrival differences between multipath arrivals. With adequate environmental information, a broadband acoustic PE model predicted the relative levels of multipath arrivals recorded on the tagged whales. However, lack of array source signature data limited modeling of absolute received levels. Airguns produce energy primarily below 250 Hz, with spectrum levels about 20–40 dB lower at 1 kHz. Some arrivals recorded near the surface in 2002 had energy predominantly above 500 Hz; a surface duct in the 2002 sound speed profile helps explain this effect, and the beampattern of the source array also indicates an increased proportion of high-frequency sound at near-horizontal launch angles. These findings indicate that airguns sometimes expose animals to measurable sound energy above 250 Hz, and demonstrate the influences of source and environmental parameters on characteristics of received airgun pulses. The study also illustrates that on-axis source levels and simple geometric spreading inadequately describe airgun pulse propagation and the extent of exposure zones. © *2006 Acoustical Society of America.* [DOI: 10.1121/1.2359705]

PACS number(s): 43.80.Nd, 43.20.Mv, 43.30.Dr [WWA] Pages: 4100–4114

I. INTRODUCTION

Airgun arrays are often used as sources of low-frequency underwater sound for geophysical research and exploration, especially by the oil industry. Airguns generate sound by rapidly releasing compressed air from an airgun cylinder, creating an oscillating air bubble that acts as a source of loud, broadband impulsive sound. The oscillating air bubble also produces a sequence of exponentially decaying bubble pulses following the initial pulse (Parkes and Hatton, 1986). Airguns are generally deployed as horizontal planar towed arrays, minimizing the bubble pulses and directing the main beam of low-frequency sound toward the seafloor (Parkes and Hatton, 1986). Airgun arrays are reported to have theoretical on-axis (directly downward) signatures with peak energy in the 10–200 Hz range, and far-field measurements yield typical peak-to-peak source levels in the range 222–261 dB re 1 μPa when corrected to a source range of 1 m, treating the full array as a point source (Richardson *et al.*, 1995). During seismic surveys, a streamer of hydrophones is also generally towed to record sound reflected from below the seafloor, and characteristics of these reflections are used to invert for bottom properties and map subseafloor features (Barger and Hamblen, 1980; Caldwell and Dragoset, 2000; Dragoset, 2000; Richardson *et al.*, 1995). Although much of the acoustic energy produced by an airgun array is in the frequency range below 250 Hz, both field recordings and models of source spectra illustrate that airguns can produce significant energy at frequencies up to at least 1 kHz [source energy at 1 kHz is about 40 dB re 1 μPa^2/Hz less than at 50 Hz (Blackman *et al.*, 2004; Caldwell and Dragoset, 2000; Goold and Fish, 1998)]. Due to their high source levels and their low frequency content, airgun array transmissions in suitable ocean environments have been detected above background noise at distances of up to 3000 km (Nieukirk *et al.*, 2004).

The source level and frequency range of airgun pulses have generated concern that they may adversely affect fish and marine mammals. Airgun noise could produce adverse effects by direct injury, for example by damaging the animals' ears, or by less direct mechanisms, such as by masking

[a)]Portions of this work were presented in "Preliminary modeling of Dtag acoustic arrivals from the Gulf of Mexico in 2002 and 2003," Proceedings of the Twenty-Third Gulf of Mexico Information Transfer Meeting, U.S. Department of the Interior Minerals Management Service, Gulf of Mexico OCS Region, 2005, and "Quantification and Acoustic Propagation Modeling of Airgun Noise Recorded on Dtag-tagged Sperm Whales in the Gulf of Mexico," Proceedings of the 16th Biennial Conference on the Biology of Marine Mammals, San Diego, CA, December 2005.

[b)]Author to whom correspondence should be addressed. Electronic mail: sderuiter@whoi.edu

sounds or disrupting behavior. In terms of wildlife conservation, the primary concern regarding these alterations involves questions about whether they could affect populations by reducing survival, reproductive success, or foraging effectiveness. Experiments have documented that exposure to airgun pulses at close range can damage fish ears (McCauley *et al.*, 2003), that fish catches are reduced during airgun surveys in an area (Engås *et al.*, 1996), and that some marine mammals may change their behavior in response to airgun exposure (Engås *et al.*, 1996; McCauley *et al.*, 2003; Richardson *et al.*, 1995).

One method for determining whether, and how, airgun transmissions might affect marine mammals involves controlled exposure experiments (CEEs), in which animals are observed pre-exposure and then exposed to a controlled level of sound. A set of CEEs to measure the response of sperm whales to airgun sounds took place during the Sperm Whale Seismic Study (SWSS) in the Gulf of Mexico during September 2002 and June 2003 (Jochens and Biggs, 2003, 2004). During the experiments, sperm whales were tagged with a Dtag, an archival tag that records acoustic, depth, and orientation information (Johnson and Tyack, 2003). Tagged whales were exposed to airgun array transmissions at ranges from 1 to 13 km. The tags recorded whale movements and vocalizations during the exposure as well as airgun sound arrivals at a variety of source-whale ranges and whale depths. Analysis of the effects of airgun exposure on sperm whale foraging behavior in the Gulf of Mexico and determination of airgun received levels at the whales during these two studies will be presented in two other papers [Miller *et al.* (unpublished) and Madsen *et al.* (2006)]. In this paper, we study the acoustic propagation of airgun signals recorded on Dtags with standard acoustic propagation models. We show that seasonally and spatially variable environmental characteristics play critical roles in determining spectra and levels of airgun arrivals at the whales. Our results also show how source directivity and a surface ducting effect may proportionally increase the high-frequency content of airgun signals arriving at whales near the surface compared to on-axis airgun spectra.

To put the discussion of our modeling techniques and results in context, we have structured this article as follows. Before addressing the CEEs of the Sperm Whale Seismic Study (SWSS) in the Gulf of Mexico, we will begin by discussing the sound sources and receivers employed during the experiments and the acoustic environment in which the CEEs took place. We reiterate that there were two components to the experiment, one that took place in September 2002 and one in June 2003, and we outline differences and similarities between the 2 years. Next, we describe the field experimental techniques and the acoustic models used to analyze the data. We then present the modeling results for each year. Finally, we discuss the implications and significance of our work, emphasizing that near-surface receivers may detect significant sound energy above 250 Hz in certain conditions and that geometric spreading approximations, which have traditionally been used to determine the extent of marine animal exposure zones, are inadequate to describe transmission loss in our study environments.

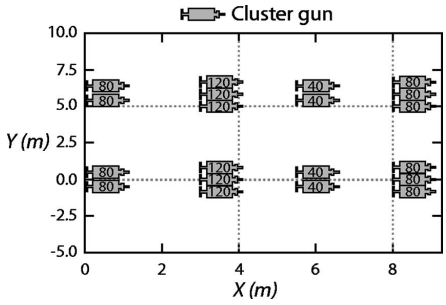

FIG. 1. Configuration of the M/V *Speculator* airgun array, used in the 2002 experiment. Numbers inside individual airguns indicate the displacement (in cubic inches) of each gun.

II. ACOUSTIC SOURCES, RECEIVERS, AND ENVIRONMENT

A. Sound sources: Airgun arrays

In 2002, tagging operations were based on the R/V *Gyre*, and the airgun source vessel was the M/V *Speculator* (the coastal vessel *Speculator* was mounted aboard the deep-water service vessel M/V *Rylan T* to allow work in deep-water research areas). The *Speculator* airgun array was a tuned array 8 m long and 6 m wide, including 20 external sleeve type airguns of various volumes for a total volume of 1680 in^3. Figure 1 shows the configuration of the *Speculator* array. During CEEs, the airgun array was towed at a nominal depth of 6 m and fired every 15 s, with a ramp-up at the start of each firing period during which the number of airguns fired was gradually increased. In this study, we analyzed only recordings of full-array airgun arrivals. The equivalent point-source source level of the array, backcalculated from the on-axis (directly downwards) theoretical far-field signature [shown in Fig. 2(a)], was reported to be 258 dB re 1 μPa@1 m (peak-peak) in the 3–800 Hz frequency band (Jochens and Biggs, 2003). Frequency notches in the spectrum of the theoretical far-field signature, which is shown in Fig. 2(b), indicate a Lloyd's mirror effect.

Because sound from an airgun array will reflect at the ocean surface (which is approximately a pressure-release boundary), a Lloyd's mirror effect will occur, and airgun pulse arrivals at distant (far-field) receivers will include, in addition to the direct arrival, a 180-degree-phase-shifted, surface-reflected arrival (Frisk, 1994). This reflected arrival is equivalent to the sound that would be received from a virtual mirror image source located above the sea surface, with approximately the same source amplitude as the airgun array but with opposite polarity [the exact mirror source amplitude depends on sea-surface roughness and source frequency (Jovanovich *et al.*, 1983)]. Interference between the direct pulse and the surface reflection affects the time and frequency structure of pulses recorded at distant receivers, lengthening the pulse and introducing frequency nulls into the source spectrum (Caldwell and Dragoset, 2000; Parkes and Hatton, 1986). The effect varies with airgun array tow depth: as tow depth increases, frequency nulls occur at more

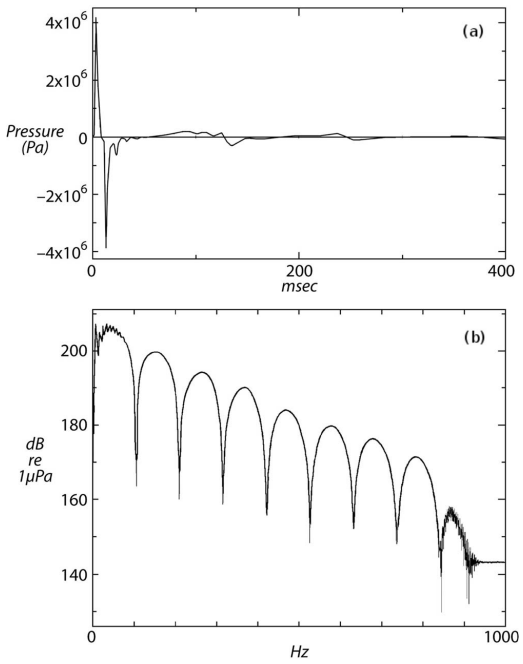

FIG. 2. (a) On-axis theoretical source signature of the M/V *Speculator* airgun array and (b) its amplitude spectrum. Both plots are extracted from Jochens and Biggs (2003).

closely spaced intervals in the source spectrum, and source pressure amplitude increases at frequencies below 100 Hz (Parkes and Hatton, 1986).

The beampattern of a planar array composed of identical point sources has grating lobes when the spacing between array elements, d, is greater than $\lambda/2$ (where λ is source wavelength). The grating lobes are centered at angles θ from the acoustic axis such that $n\lambda = d\sin(\theta)$ (where $n = 1, 2, 3, \ldots$) (Tipler and Llewellyn, 2003). For the *Speculator* array, the spacing between airgun clusters was about 3 m in the x dimension (along the bow-stern axis of the source vessel) and about 6 m in the y dimension (perpendicular to the bow-stern axis of the source vessel). Therefore, the array beampattern should have grating lobes for source frequencies above approximately 250 Hz in the x-z plane and approximately 125 Hz in the y-z plane (assuming a sound speed of 1500 m/s), although array shading will affect the pattern of grating lobes somewhat (Urick, 1975). The presence of grating lobes in the array beampattern at higher frequencies increases the proportion (but not the absolute amount) of higher-frequency energy transmitted by the array at launch angles close to parallel to the sea surface. Detailed modeling of the *Speculator* array beampattern will be presented later in the paper, and will include the Lloyd's mirror effect from sea-surface reflection as well as the effects of array geometry mentioned here.

The Fresnel zone or near field of an acoustic array extends to a range of about D^2/λ, where D is the array dimension (length or width) and λ is sound wavelength (Clay and Medwin, 1977). Assuming a sound speed of 1500 m/s, the far field of the *Speculator* array begins about 2 m from the source at 50 Hz and about 85 m from the source at 2 kHz. All airgun pulses used in this study were recorded in the far field.

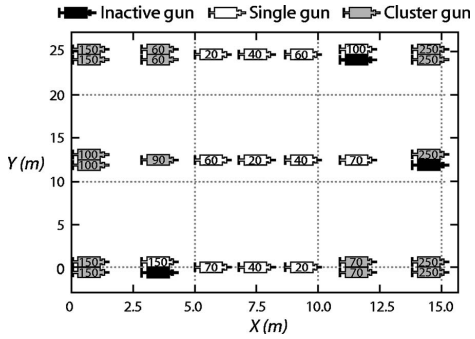

FIG. 3. Configuration of the M/V *Kondor* airgun array, used in 2003 experiment. Numbers inside individual airguns indicate the displacement (in cubic inches) of each gun.

In 2003, tagging operations and visual and acoustic monitoring were based on the R/V *Maurice Ewing*, and the airgun source vessel was the M/V *Kondor Explorer*. The *Kondor* array was a tuned array, 15 m long and 10 m wide, with 31 guns of various sizes for a total volume of 3090 in^3. Only 28 of the guns were active during the experiment, making the total volume of the active guns 2590 in^3. Figure 3 shows the configuration of the array. The private geoservice firm PGS Exploration (Walton-on-Thames, Surrey, UK) provided the on-axis theoretical far-field signature of the array (shown in Fig. 4). Backcalculating from the signature, the equivalent point-source source level was 261 dB re 1 μPa@1 m (peak-peak) in the 3–218 Hz frequency band. During CEEs, the airgun array was towed at a nominal depth of 7.5 m and fired every 15 s, with a ramp-up at the start of each firing period during which the number of guns fired was gradually increased to 28. In this study, we analyzed only recordings of full-array airgun arrivals. Like the *Speculator* array, the *Kondor* array source signature is also affected by a Lloyd's mirror effect. The *Kondor* array beampattern should also have grating lobes for source frequencies above approximately 375 Hz in the x-z plane and approximately 75 Hz in the y-z plane (calculated as explained earlier for the *Speculator* array, only using airgun cluster spacings of 2 m in the x dimension and 10 m in the y dimension), again increasing the proportion of higher-frequency energy transmitted by the array at launch angles close to parallel to the sea surface. The Fresnel near field of the Kondor array begins at about 8 m from the array at 50 Hz and 300 m from the array at 2 kHz (calculated as above for the *Speculator* array). Again, all airgun pulses used in this study were recorded in the far field.

B. Receivers: Dtags

Sperm whales (*Physeter macrocephalus*) were tagged with Dtags, digital archival tags that record acoustic, depth,

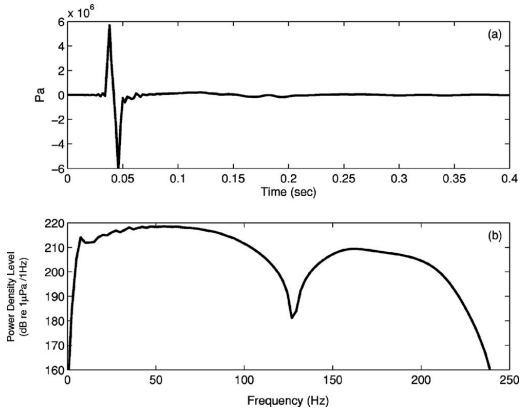

FIG. 4. (a) On-axis theoretical source signature of the M/V *Kondor* airgun array and (b) its amplitude spectrum (0–250 Hz). Both plots were provided by PGS Exploration (Walton-on-Thames, Surrey, UK).

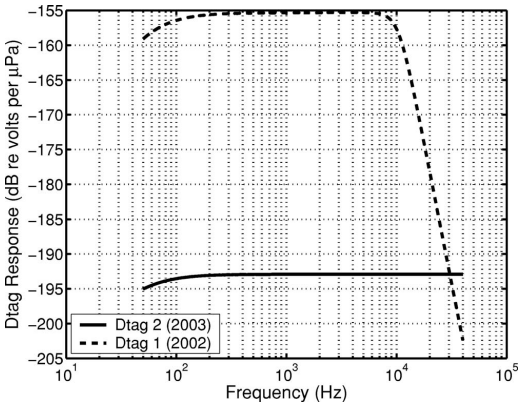

FIG. 5. Frequency response of acoustic sampling of Dtags 1 and 2.

and animal orientation data (Johnson and Tyack, 2003). Orientation data recorded by the tag can be combined with visual tracks to derive an estimate of the position of the tagged whale (Zimmer *et al.* 2005). Two versions of the Dtag were used in the experiments. In 2002, Dtagl tags were used. Dtagl recorded audio at a sampling rate of 32 kHz (12 bit resolution), with flat frequency response (±3 dB) between 400 Hz and 10 kHz and clip level of 155 dB re 1 μPa (0-peak). Filtering was applied to postemphasize the audio recordings at low frequencies. With postemphasis, the frequency response was flat (±1.5 dB) from 60 Hz to 12 kHz. Dtagl also recorded data from three-axis accelerometers and magnetometers, ambient pressure (depth), and temperature at a sampling rate of 48 Hz. In 2003, both Dtagl and Dtag2 tags were used, but only Dtag2 data were analyzed in this study. Dtag2 recorded audio at a sampling rate of 96 kHz (16 bit resolution), with flat (±1.5 dB) frequency response between 400 Hz and 45 kHz and clip level of 193 dB re 1 μPa (0-peak). Filtering was applied to postemphasize the audio recordings at low frequencies. With postemphasis, the frequency response was flat (±1.5 dB) from 50 Hz to 45 kHz. Dtag2 also recorded data from three-axis accelerometers and magnetometers, ambient pressure (depth), and temperature at 50 Hz. Figure 5 shows the sensitivity curves of Dtagl and Dtag2. Both Dtagl and Dtag2 measured temperature near the crystal used to control clock speed of the tag. Their thermistors did not measure ambient water temperature.

C. Ocean and ocean acoustic environment

The CEE components of the SWSS in the Gulf of Mexico were performed in September 2002 and July 2003, and we analyzed data from one exposed whale per year. Figure 6 shows the study areas where the data modeled in this study were collected. On September 11, 2002, the modeled CEE took place on a bathymetric slope of about 1.5° in the west Mississippi Canyon region, in an area where the water depth varies from 400 to 800 m. On June 13, 2003, the modeled CEE took place in the Mississippi Canyon, in an area where the bathymetry is locally flat and the water depth is about 800 m.

During the CEE cruises in both years, CTD (conductivity, temperature, depth) and XBT (expendable bathythermograph) casts were made periodically to estimate the sound speed profile (Jochens and Biggs, 2003, 2004). For acoustic modeling of 2002 airgun pulses, we chose one XBT profile from the 2002 data set, closest to the experiment site and the airgun exposure time. The profile [Fig. 7(a)] indicates a 40 m thick mixed layer below the sea surface, which created a strong surface duct that trapped high-frequency sound and allowed it to propagate with little transmission loss (Urick, 1975). All sound speed profiles taken from the CTD and XBT casts in 2002 showed a similar surface duct. For acoustic modeling of 2003 airgun pulses, we averaged data from two CTD profiles taken near the experiment site to obtain our sound speed profile. Unlike the 2002 sound speed profile, the 2003 profile did not include a strong surface duct [Fig. 7(b)].

No bottom surveys were conducted during the CEE cruises, but marine geology and geoacoustic reports near the experiment areas are available to help establish the geoacoustic bottom model. According to the NGDC Seafloor Surficial Sediment (Deck41) Database (http://www.ngdc.noaa.gov), the dominant lithological component of the surficial seafloor in the CEE areas is clay, and the secondary lithological component is silt. The ratio of bottom sound speed to water sound speed at the seafloor should be about 0.995, a typical value for silty-clay sediments (Hamilton, 1980).

A chirp sonar subbottom survey during the Littoral Acoustic Demonstration Center experiment in August 2001 (Turgut *et al.*, 2002) was conducted in the same area as the 2002 modeled CEE, and sound speed and density profiles from that report are reproduced in Fig. 8(a). Comparing the ocean bottom sound speed to the water sound speed, as shown in Fig. 7(a), confirms that the sound speed ratio at the 2002 study site matches the ratio typical of silty-clay sedi-

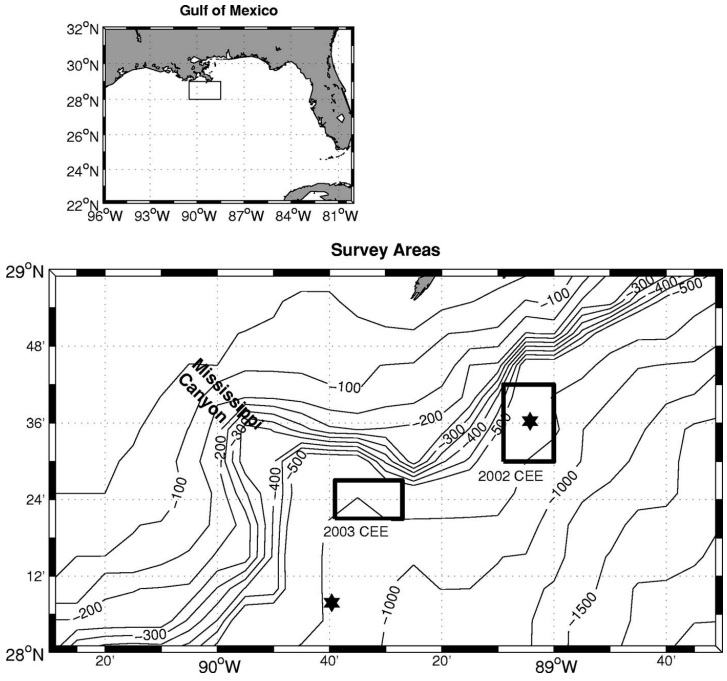

FIG. 6. Sites of airgun operations measured in 2002 and 2003. Upper panel: Location of the study areas. Lower panel: Detail of the 2002 and 2003 study sites (boxes) and locations where data on bottom properties were collected by Turgut *et al.* (2002) and Geresi *et al.* (2005) (stars).

ments. Figure 8(b) shows reflection coefficient versus grazing angle on the seafloor at the site of the 2002 modeled CEE, calculated with the acoustic modeling package OASES (Schmidt, 2004) using data on bottom properties from Turgut *et al.* (2002). For acoustic modeling of the 2002 CEE, we adopted a smoothed version of Turgut's seafloor sound speed and density profiles.

We did not find data on the bottom properties at the site of the 2003 modeled CEE in the literature; the closest detailed studies of the sea floor were conducted in 2003 on Mississippi Canyon Block 798 (about 20 km from the 2003 CEE site, but on the opposite side of the canyon; see Fig. 6)

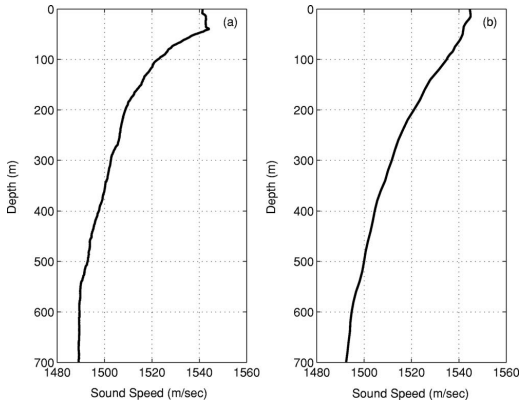

FIG. 7. Sound speed profiles for 2002 (left) and 2003 (right) used for acoustic modeling.

(McGee *et al.*, 2003). Geresi *et al.* (2005) applied a migration velocity analysis to McGee and colleagues' seismic reflection data and obtained the bottom sound speed to 600 m depth, which is reproduced in Fig. 9(a). The sound speed ratio between the top layer of the bottom and deep water [shown in Fig. 7(b)], 0.993, is typical of silty-clay sediments. Figure 9(b) shows the bottom reflection coefficient as a function of frequency and grazing angle on the seafloor at the site of the 2003 modeled CEE, calculated with the acoustic modeling package OASES (Ocean Acoustics and Seismic Exploration Synthesis) (Schmidt, 2004) using bottom properties from Geresi *et al.* (2005). We used Geresi's seafloor sound speed profiles to model the 2003 CEE data.

We applied Hamilton's regression equations to the selected bottom profiles to estimate the bottom density (Hamilton, 1978) at the 2003 study site and the bottom attenuation (Hamilton, 1972) at both sites.

III. METHODS

A. Experiments

Dtags were deployed by approaching sperm whales at the surface in a small inflatable boat, then using a long pole to place the tag atop a whale's back, where it attached with suction cups. The tags were positively buoyant and programmed to release from the whales after a maximum recording time of 12 h (Dtagl) or 16 h (Dtag2), at which point they floated to the surface and were located and recovered with the help of a built-in radio beacon. Since the tags were attached to the whales, it is possible that shadowing by the whales' bodies might have affected recorded airgun pulses.

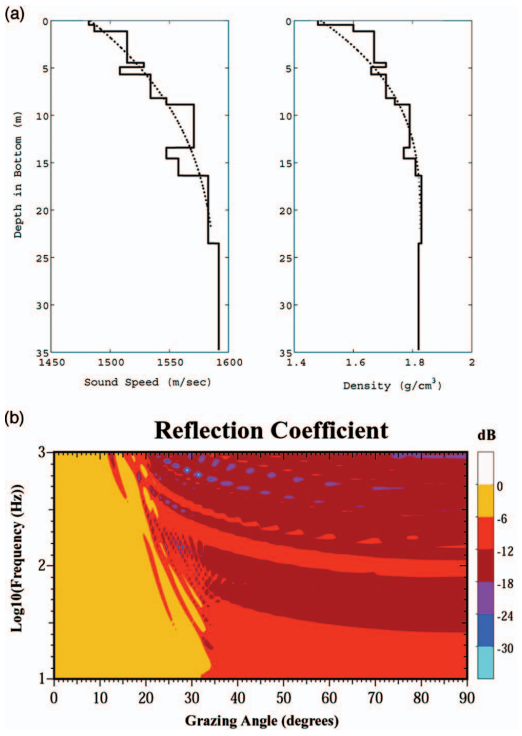

FIG. 8. (a) Bottom sound speed and density profiles for the 2002 study area. The solid lines are the geoacoustic inversion results from wideband (2–12 kHz) chirp sonar data obtained from a Littoral Acoustic Demonstration Center experiment on the east of the Mississippi Canyon in 2001 (Turgut *et al.*, 2003). The dotted lines are fitted curves. (b) Corresponding reflection coefficient contour (grazing angle vs frequency) for the 2002 study area. The corresponding density and attenuation profiles were calculated using Hamilton's regression equations (Hamilton, 1972, 1978).

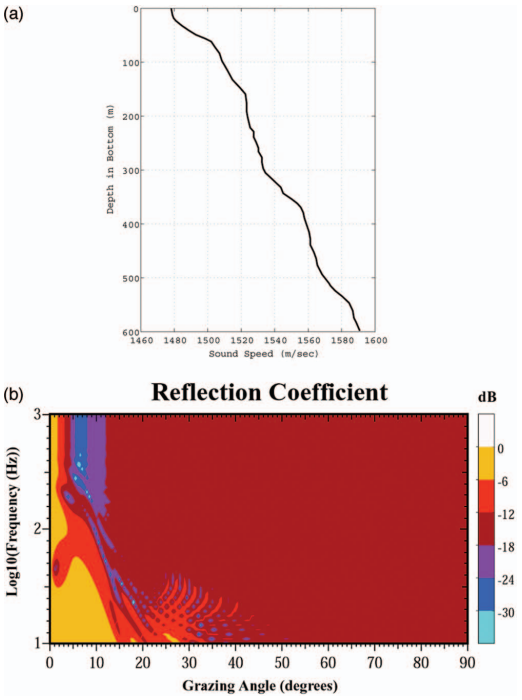

FIG. 9. (a) Bottom sound speed profile for the 2003 study area. The sound speeds were obtained by applying the migration velocity analysis to reflection seismic data on Mississippi Canyon Block 798 (Geresi *et al.*, 2005). (b) Corresponding reflection coefficient contour (grazing angle vs frequency) for the 2003 study area. The corresponding density and attenuation profiles were calculated using Hamilton's regression equations (Hamilton, 1972, 1978).

However, body shadowing should have negligible impact on the timing of pulse arrivals, and only minor influence on relative levels at the frequencies we studied. In fact, body shadowing would have a greater effect in reducing high frequencies than low, which would only reduce the surface ducting effect described in this study. In 2002, one whale underwent a CEE on September 10, and three simultaneously tagged whales underwent a CEE on September 11. In 2003, CEEs were performed on individual tagged whales on June 13 and 22, and two simultaneously tagged whales underwent a CEE on June 14. Each CEE lasted about 1 h, and was preceded and followed by tagged control periods with no airgun exposure. Visual observers on the observation vessel tracked the tagged whales using reticle-binoculars and the radio-beacon in the tag. A derived three-dimensional (3D) track for the entire tag attachment period, estimated to be accurate to ±0.5 km, was calculated using dead-reckoning based on the orientation sensors and the visual locations [Johnson and Tyack, 2003; Madsen *et al.* (2006)]. Horizontal ranges between the airgun arrays and the whales were calculated to the nearest 0.1 km using the derived tracks.

In this study, we modeled airgun arrivals recorded on one tagged whale each year (whale sw02_254b, tagged on September 11, 2002, and whale sw03_164a, tagged on June 13, 2003). Table I presents the exact durations and timing of the tag deployments that included the modeled CEEs. During the 2002 exposure, source-whale range varied from 5.4 to 12.0 km, and water depth varied from 600 to 800 m. During the 2003 exposure, source-whale range varied from 11.0 to 12.0 km, and water depth was about 800 m. Figure 10 shows the locations of the airgun source vessels and tagged whales during the modeled exposures, along with the bathymetry of each study area.

B. Acoustic models

1. Normal mode model for determination of the cutoff frequency

Surface ducts are shallow (generally less than 100 m deep), so only higher-frequency (shorter-wavelength) sound

TABLE I. Duration and timing of modeled tag deployments and CEEs in 2002 and 2003.

Date	Whale ID	Tagged time	Airgun exposure time
9/11/2002	sw02_254b	10:28–22:52	12:16–14:20
6/13/2003	sw03_164a	09:48–23:20	18:26–19:26

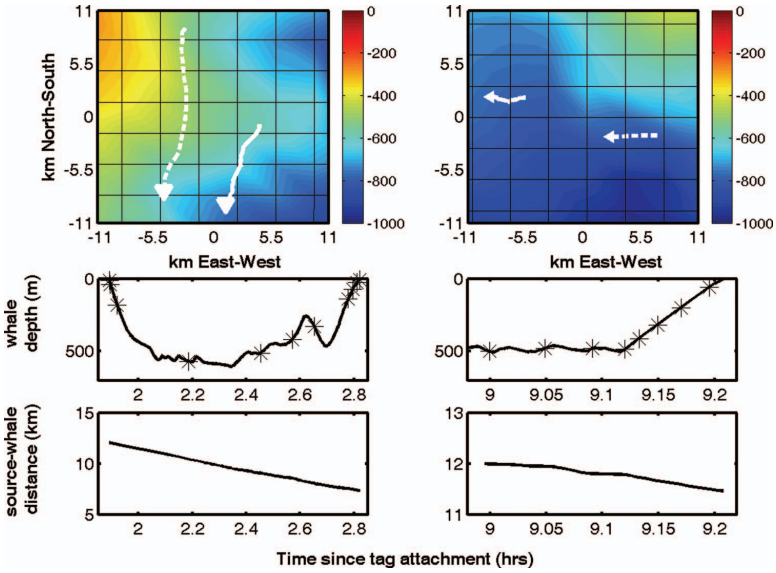

FIG. 10. The left column contains information related to the controlled exposure experiment on September 11, 2002, and the right column contains information on the controlled exposure experiment on June 13, 2003. Top panels: Airgun array source vessel (dotted lines) and tagged sperm whale (solid lines) locations during the two modeled airgun exposures. Arrowheads indicate direction of travel. The x and y axis values indicate distance in km from approximate centers of the study locations: 28.600°N, 89.070°W (2002) and 28.380°N, 89.520°W (2003). Middle panels: Dive profiles of the tagged whales during the modeled exposures. Asterisks indicate the time of firing of modeled airgun pulses. Lower panels: Range from the airgun source vessels to the tagged whales during the modeled exposures.

is trapped and propagates efficiently in surface ducts (Urick, 1975). The cutoff frequency of a surface duct is the approximate frequency below which sound is not trapped in the duct. Cutoff frequency is approximate because sound below the cutoff frequency may be only partially trapped in the duct (a "leaky duct"), and sound may need to be significantly above the cutoff frequency for maximal trapping to occur. To estimate the cutoff frequency of the surface duct in our 2002 study area, we performed a series of KRAKEN normal mode model runs (Porter, 1995) at five frequencies ranging from 50 to 1600 Hz. We used the model output to determine the mode number n and modal eigenvalue k_n for the lowest-numbered mode trapped in the duct at each frequency (a mode was considered trapped if it had high intensity in the duct, and exponentially decaying intensity below the duct). Then, to determine whether mode n would propagate, we calculated its mode-propagation cutoff frequency, ω_n (the frequency above which at least n modes will propagate). Trapped modes with ω_n less than the frequency of the KRAKEN model run that generated them would propagate. We estimated ω_n according to Frisk (1994):

$$\omega_n = k_{zn} c, \tag{1}$$

where

$$k_{zn} = \sqrt{\left(\frac{\omega}{c}\right)^2 - k_n^2}, \tag{2}$$

ω is radian frequency and c is sound speed. We used 1543 m/s for sound speed in the calculations [see Fig. 7(a)]. This procedure determined whether or not the trapped modes would propagate in the duct at each frequency tested, and therefore allowed us to estimate the cutoff frequency of the surface duct as the lowest frequency at which the trapped modes would propagate.

2. Airgun array beampattern model

An airgun array usually contains airgun elements with different volumes, which produce sound pulses with different amplitudes, damping rates and bubble pulse periods (Ziolkowski, 1970). This variability makes airgun array signature modeling complex and difficult. One can estimate the signature from near-field measurements of an airgun array (Ziolkowski *et al.*, 1982, 1997; Laws *et al.*, 1998), but during the CEEs we studied, no near-field measurements of airgun pulses were made. An alternative way to estimate the signature of an airgun array is to treat each element as a monopole source and consider the geometric configuration of the array. The volume of every element in the *Speculator* and *Kondor* arrays was known, and since the amplitude of an airgun element is approximately proportional to the cube-root of its volume, we could estimate the relative amplitude of the elements in each array (Caldwell and Dragoset, 2000). We modeled the array according to the following normalized formulation in a free space bounded by the sea surface

$$S(\vec{x},\omega) = \sum_i \nu_i^{1/3} \frac{e^{-jk_w R_i}}{R_i} + \sum_i (-1)\nu_i^{1/3} \frac{e^{-jk_w R_i'}}{R_i'}, \tag{3}$$

where $\vec{x}$ is the position of the receiver, ω is the acoustic frequency, $k_w = \omega/c$ is the acoustic wave number in water

(where c is the sound speed, 1500 m/s), v_i is the volume of ith airgun element, and R_i is the distance from the receiver to the ith airgun element. In the second term, the (-1) indicates the contribution from the virtual "mirror image source" due to the Lloyd's mirror effect of the sea surface (modeled as a pressure release boundary), and R_i' is the distance from the receiver to the image source of the ith airgun element. Therefore, our airgun array beampattern model includes both the effects of array geometry and the Lloyd's mirror effect caused by sea-surface reflection. Using this model, we calculated the acoustic pressure at a certain radius from the array and normalized it to obtain an estimate of the source beampattern. The airgun elements in this model were treated as monopole sources with a single impulse, while real airgun pulses include a series of bubble pulses (Ziolkowski, 1970). However, the model could still predict the locations of spatial and frequency notches in the airgun array beampattern, since notch locations are mainly determined by the geometric configuration of the array (Parkes and Hatton 1986, Tipler and Llewellyn 2003).

3. Acoustic ray-tracing model

In this study, we modeled range-dependent acoustic propagation but considered only reflection from the sea-floor and sea-surface boundaries and refraction due to soundspeed variations. We used the ray-tracing program RAY (Bowlin *et al.*, 1992), which can deal with a range-dependent environment, to calculate sound propagation paths and travel times of the airgun pulses recorded during the modeled CEEs. The fundamental theory underlying RAY is well known; the reader interested in more detail is referred to the relevant literature (e.g., Bowlin *et al.*, 1992; Jensen *et al.*, 1994).

4. Broadband acoustic propagation modeling

To model the transient airgun pulse signals recorded on Dtags in the CEEs, we developed a two-dimensional (2D) broadband range-dependent acoustic propagation program based on Fourier synthesis (Jensen *et al.*, 1994). The model, described below, can compute received sound pulses over a specified bandwidth at a single position.

The Fourier pulse synthesis technique is based on the Fourier transform of the continuous wave frequency-domain response multiplied by the spectrum

$$p(r,z,t) = \frac{1}{2\pi}\int_{-\omega_{\max}}^{\omega_{\max}} S(\bar{\omega})H(r,z,\omega)e^{-j\omega t}d\omega, \tag{4}$$

where $p(r,z,t)$ is the pressure signal of a sound source received at the position (r,z) on a vertical plane, which also includes the source; r is horizontal range; and z is depth. $S(\omega)$ is the source spectrum with a finite bandwidth $2\omega_{\max}$, and $H(r,z,\omega)$ is the frequency response of a monopole source at a frequency ω. In our program, $H(r,z,\omega)$ is calculated by the existing time-harmonic acoustic model RAM (range-dependent acoustic model), a parabolic equation (PE) model developed by Michael D. Collins at the Naval Research Laboratory in Washington, DC (Collins, 1993). Discretizing the transform Eq. (4), we obtain

$$\sum_{m=-\infty}^{\infty} p(r,z,k\Delta t + mT) = \frac{\Delta\omega}{2\pi}\sum_{n=-(N/2-1)}^{N/2}[S(\omega)H(r,z,n\Delta\omega) \times e^{-jt_0 n\Delta\omega}]e^{-j(2\pi nk)/N}, \tag{5}$$

where on the right hand side, the frequency within a finite bandwidth is discretized as N samples with values $n\Delta\omega$, with $n=(N/2-1)\sim N/2$. On the left-hand side, the time within a finite window $T(=1/\Delta\omega)$ is sampled at $k\Delta t$, with $k=1,2,3\ldots N$. The sampling rate must obey the Nyquist criterion, or aliasing will occur in the frequency domain. Similarly, discretization in the frequency domain can cause wrap-around in the time domain if $\Delta\omega$ is too large, with m (on the left-hand side of the equation) being the index of the periodicity of the discretized time-domain signal. To minimize the wrap-around effect while keeping $\Delta\omega$ large enough for reasonable computation time, we applied complex frequency integration (Malick and Frazer, 1987; Jensen *et al.*, 1994). If N is an integer power of two, the fast Fourier transform algorithm is efficient for evaluating the summation.

For all model runs, we placed an artificial absorbing layer in the sediments to prevent sound energy from being reflected or refracted back to the water from the deep bottom. The sound source in our model runs was a bell-shaped single pulse, containing most of its energy in the frequency band from 0 Hz to three times its central frequency. Mathematically, this pulse can be represented as

$$s(t) = 0.75 - \cos 2\pi f_c t + 0.25\cos 4\pi f_c t, \quad 0 \leqslant t \leqslant T = 1/f_c, \tag{6}$$

where f_c is the center frequency. We used $f_c=250$ Hz. The model source does not accurately represent the output of an airgun array, but the resulting model output can still predict the arrival time pattern measured at the receiver. Because the low-frequency flow noise is very high in the 2002 Dtag record, and the model source produces 95% of its energy in the 0–600 Hz frequency band, we bandpass filtered the 2002 data and model results from 100 to 600 Hz before comparing them.

IV. RESULTS

A. 2002 experiment and model results

Figure 11 shows the wave form and spectrogram of two airgun pulses from the 2002 experiment, recorded on the same whale near the surface (at 24 m depth) and in deep water (at 420 m depth). There are three clear arrivals in the pulse recorded at 24 m depth. The spectrogram shows that the first arrival contains significant high-frequency energy but almost no energy below 250 Hz. In the pulse recorded at 420 m depth, two strong whale clicks appear at 0.12 and 0.56 s (reduced arrival time), followed by their echoes. Five arrivals from the airgun pulse also can be seen. The first two weak arrivals at 0.25 and 0.32 s contain only high frequency

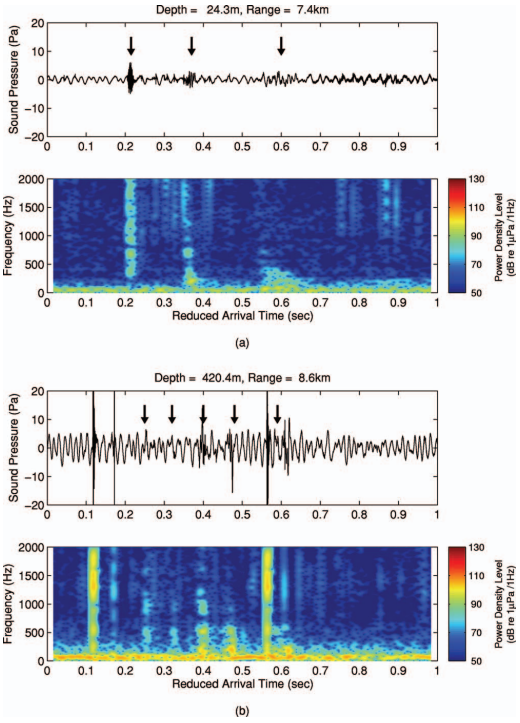

FIG. 11. The wave form and spectrogram of two airgun pulses recorded on the Dtag when the tagged whale was at (a) 24 m depth and (b) 420 m depth during the 2002 experiment. Arrows indicate the airgun arrivals. The intense broadband signals at about 0.12 s and about 0.56 s (both followed by their echoes) are clicks produced by the tagged whale.

energy. The last arrival, at 0.6 s, overlaps with the echo of the second whale click. Spectrograms from both depths also show high level, low frequency flow noise.

The first airgun arrivals recorded when the whale was near the surface lacked low-frequency energy because of the high-pass filtering effect of the surface duct (Fig. 7). Figure 12 shows a plot of RAM parabolic equation model output (transmission loss as a function of range and depth for a 600 Hz source), illustrating the surface ducting effect. Based on our normal mode model runs, we estimated that the cutoff frequency of the surface duct in the 2002 sound speed profile was about 250 Hz, which agrees well with the cutoff frequency shown in the data (Fig. 11). Grating lobes in the airgun array beampattern can also channel energy to near-horizontal launch angles from the array, and thus into the surface duct. Modeling the beampattern of the *Speculator* source array at 7 m depth showed that grating lobes (due to both array geometry and sea-surface reflection) start emerging at 120 Hz, an octave below the duct cutoff frequency. Figure 13 shows examples of the *Speculator* airgun array beampattern at six frequencies from 50 to 650 Hz. Our beampattern model predicts frequency notches occurring in the downward direction at 107 and 214 Hz, in good agreement with the predicted amplitude spectrum of the on-axis airgun array signature [see Fig. 2(b)]. At 650 Hz, the energy

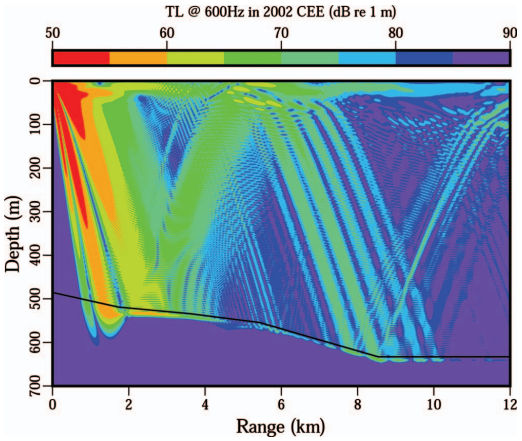

FIG. 12. Transmission loss as a function of range and depth for a 600 Hz omnidirectional point source at 7 m depth in the 2002 study environment. The sea floor is indicated by a solid black line.

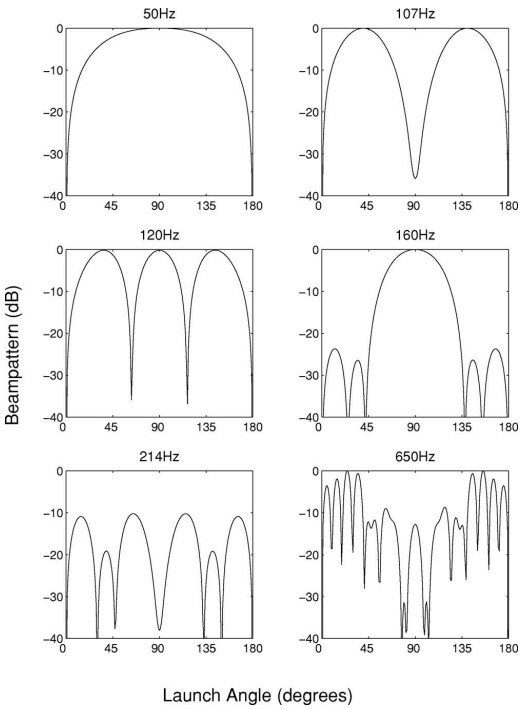

FIG. 13. The modeled beampattern of the M/V *Speculator* airgun array at several frequencies, in a vertical plane along the towing direction. Modeled beampattern includes the effects of sea-surface reflection as well as array geometry, as noted in the text. The airgun array was 7 m below the sea surface for consistency with the modeled source signature (Fig. 2). Launch angles were measured relative to a line extending from bow to stern, and a 3D normalized beampattern was calculated at each frequency. (Because the figure shows 2D beampatterns, the maximum plotted beampattern levels may be less than 0 dB if the maximum-amplitude lobe of the beampattern occurred outside the plane plotted in this figure.)

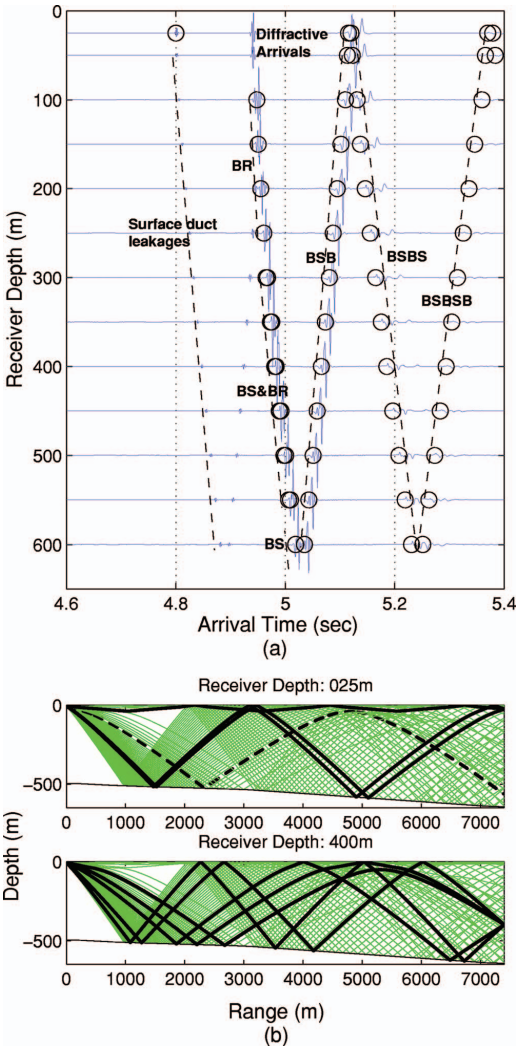

FIG. 14. (a) Modeled wave forms (blue traces) and eigenray arrival times (highlighted by black circles) at 7.4 km range and various depths in 2002. Ray labels are as follows: B indicates a bottom reflection, S indicates a surface reflection, and R indicates refraction in the water column. (b) Modeled eigenray paths (thick black lines) to receivers at 25 m and 400 m depth and sound propagation paths (thin green lines) for the 2002 experiment. The dashed line in the 25 m depth panel is the ultimate BR ray with the shallowest turning point.

emitted by the array at near-horizontal launch angles is even greater than in the downward direction. The model also illustrates that, even at frequencies where the greatest proportion of sound is directed toward the sea floor (e.g., 160 Hz), sound carried by the sidelobes (at launch angles closer to the horizontal) is only 20 dB lower than that in the main, downward-directed lobe [see Fig. 2(b)].

The modeling of the pulse arrivals, including the eigenray arrival time at 7.4 km range and various depths, is shown in Fig. 14(a). The corresponding ray labels are also included; the labels consist of a "B" for every bottom reflection, an "S" for each reflection at the sea surface, and an "R" to indicate refraction in the water column. For example, a BS ray leaves the source, bounces off the bottom, reflects at the surface, and finally arrives at the receiver, and a BSB ray is like a BS ray with one more bottom bounce before arriving at the receiver. The pulse arrivals calculated from the broadband model arrive exactly when the ray-tracing model predicts, except in the case of the diffractive arrivals near the surface and the surface duct leakages, where ray theory fails (Frisk, 1994). The eigenray paths are also calculated and shown in Fig. 14(b) for two selected depths, 25 and 400 m. The first arrival at the 25 m-depth receiver travels in the surface duct, in concordance with our observation that the first arrival has little low-frequency energy. The BSB and BSBS eigenray paths also produce pulses at the 25 m receiver depth; however, they arrive almost at the same time and combine into a single pulse. Figure 14(a) also shows that as the receiver goes deeper, the pulses traveling along BSB and BSBS ray paths separate, and the grazing angles of the bottom bounces of these two rays also change. The reflection coefficient contour for 2002 [Fig. 8(b)] shows that the BSBS ray (grazing angle 24°) has more bottom loss than the BSB ray (grazing angle of 18°), explaining the difference in amplitudes of the BSB and BSBS rays [Figs. 14(a) and 15]. A plot of eigenrays to the 400 m receiver is shown in Fig. 14(b); as shown in Fig. 14(a), the BR ray path arrives at the receiver almost at the same time as the BS ray. Ray trace output also shows that BR rays can arrive at a receiver at 7.4 km range only above 560 m depth. Below that, only BS rays can reach. Conversely, BR and not BS rays arrive at receivers at depths shallower than 330 m.

Figure 14(a) also shows surface duct leakage and the diffractive arrivals. Sound energy leaks from the surface duct due to diffraction and scattering at the boundaries of the duct (Weston *et al.*, 1991). Since the propagation model we used does not account for interface roughness at the boundaries of the duct, the leakage seen in our modeling results is due only to diffraction. Sound energy trapped in a surface duct and subject to leakage has been previously described, from a modal sound propagation perspective, as a virtual mode (Labianca, 1972). When such a virtual mode occurs, some surface ducted energy continuously seeps from the duct, but remains trapped in the waveguide as a whole. The leakages eventually return to the duct after bouncing off the bottom or refracting in the water column (Porter and Jensen, 1993). Figure 14(a) shows two arrivals resulting from surface duct leakages; the second of those arrivals actually leaks from the duct first, but undergoes a bottom bounce before arriving at the whale. The broadband PE model also predicts that a receiver in the surface duct will detect diffractive arrivals [Fig. 14(a); Murphy and Davis, 1974]. Unlike the surface duct leakages, diffractive arrivals in the duct are from an upward-directed ray that is below the duct. As shown in Fig. 14(b), the ray in question is the ultimate BR ray, which has a turning point closer to the base of the surface duct than any other BR ray. The ray turns down at the lower bound of the surface duct (a local maximum in the sound speed profile), and some of its energy enters the duct.

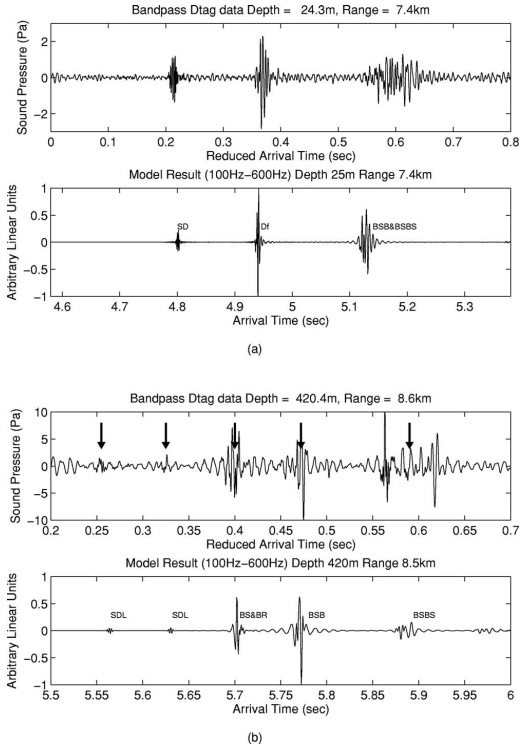

FIG. 15. Wave form comparison between the 2002 Dtag recordings and broadband model results for a receiver at (a) 7.4 km range and 24.3 m depth and (b) 8.5 km range and 420 m depth. All wave forms were bandpass filtered between 100–600 Hz, as described in Sec. III. Ray path labels are as follows: B indicates a bottom reflection, S indicates a surface reflection, SD indicates a surface ducted arrival, SDL indicates a surface duct leakage, and Df indicates diffraction in the water column.

A comparison of wave forms from the Dtag records and the broadband model results is shown in Fig. 15. As shown in Fig. 15(a), the timing and relative amplitudes of modeled arrivals match the data very well for a receiver at 7.4 km range and 24.3 m depth. The broadband model also provides very good results compared with the Dtag data at 8.6 km range and 420 m depth, where the relative differences between the surface duct leakages and the single bottom bounce pulses are especially well described.

B. 2003 experiment and model results

Figure 16 shows the wave form and spectrogram of a typical airgun pulse recorded on a tagged whale 11.2 km from the source at 450 m depth (the intense broadband signals at about 0.4 and 0.9 s are clicks produced by the tagged whale). The spectrogram illustrates that, in contrast to the 2002 data, all arrivals from the airgun pulse contain mainly low-frequency energy (below 500 Hz, and concentrated below 200 Hz). Because the sound speed profile for the modeled 2003 CEE did not include a significant surface duct, high-frequency sound did not undergo ducted propagation to

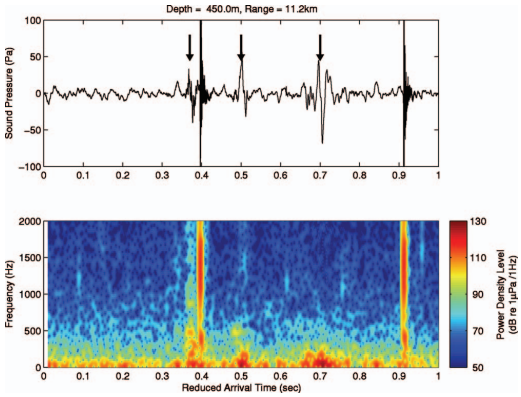

FIG. 16. The wave form and spectrogram of an airgun pulse recorded on the Dtag when the tagged whale was at 450 m depth and 11.2 km range during the 2003 experiment. Arrows indicate airgun arrivals. The intense broadband signals at about 0.4 and 0.9 s are clicks produced by the tagged whale.

the tagged whale near the surface, but rather reached the whale after reflecting from the bottom and the sea surface [see Fig. 17(b)].

The modeled pulse arrivals and eigenray arrival times at 11.2 km range and various depths are shown in Fig. 17(a). The eigenray paths for receivers at 150 and 450 m depth are also shown in Fig. 17(b). As they did in the 2002 model runs, the ray and broadband models predicted nearly identical airgun pulse arrival times. The modeled arrival times match fairly well with the data (Figs. 18 and 19). Figure 17(a) shows that the first airgun arrival at 150 m depth is a BR ray, while that at 450 m depth is a BS ray, because no BR rays arrive at receivers below about 200 m depth at 11.2 km range. Figure 17 also indicates that the third-arriving rays undergo one more surface reflection than the second-arriving rays, which explains why the third arrivals (shown in Fig. 18) are about 180° out of phase with the second arrivals (Frisk, 1994).

Figure 19 shows a wave form comparison between the Dtag records and the broadband PE model results for a receiver at 450 m depth and 11.2 km range. These model results did not match the data as well as the 2002 model results because our information about bottom characteristics was less precise for the 2003 site, as will be clarified further in the discussion section.

V. DISCUSSION AND CONCLUSIONS

Most reviews on the effects of airgun array pulses on marine life have accepted the assumption that airgun noise is limited to low frequencies, and have concentrated on species thought to have good low-frequency hearing (Caldwell, 2002; Popper *et al.*, 2004; Richardson *et al.*, 1995). We found that animals located near the surface when surface-ducting conditions are present may be exposed to measurable levels of airgun sound above 500 Hz. The surface ducting effect described here means that even animals with poor low-frequency hearing (for example, dolphins and other small odontocetes) could potentially detect and be affected by air-

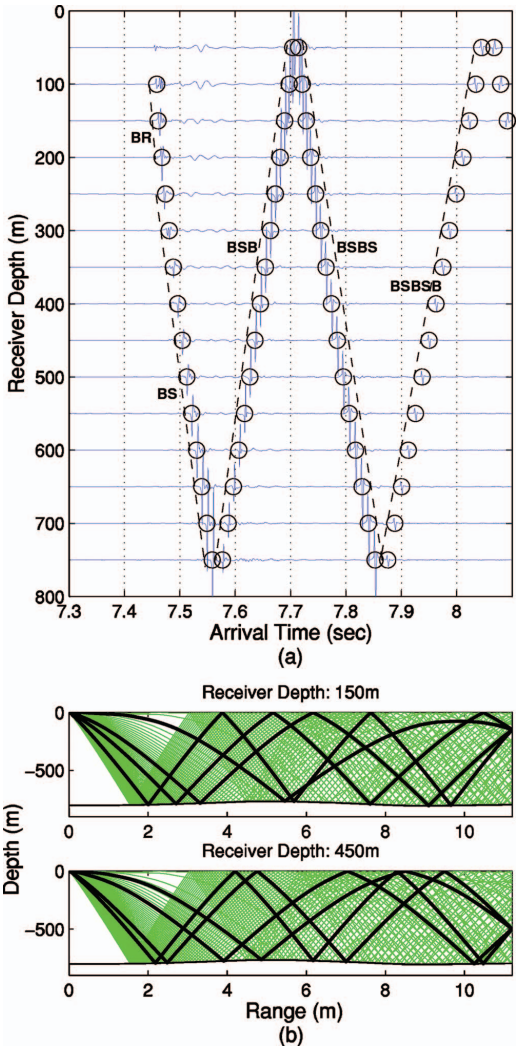

FIG. 17. (a) Modeled wave forms (blue traces) and eigenray arrival times (highlighted by black circles) at 11.2 km range and different depths in 2003. Ray path labels are as follows: B indicates a bottom reflection, S indicates a surface reflection, and R indicates refraction in the water column. (b) Modeled eigenray paths (thick black lines) to receivers at 150 and 450 m depth and sound propagation paths (thin green lines) for the 2003 experiment.

gun noise. However, we did not observe the surface ducting effect in all environmental settings, which underscores the influence of temporally and spatially variable oceanographic conditions on acoustic propagation. The received level of airgun pulses clearly depends not only on source-receiver range and on-axis airgun array source level, but also on array beampattern, sound speed profile, bathymetry, and bottom properties.

Our ability to model the absolute intensity of airgun pulses at the whales was limited by incomplete data in a few key areas. First, we did not have an adequate measurement of the source signatures of the airgun arrays (at all launch

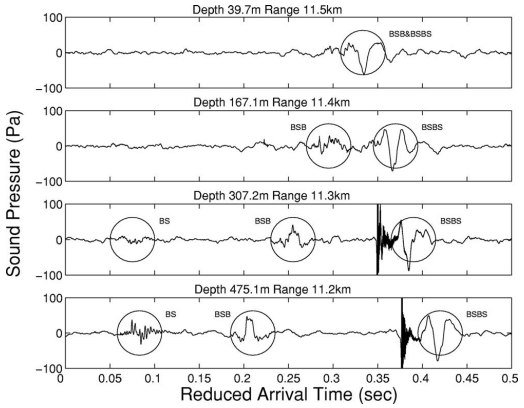

FIG. 18. Wave forms of airgun arrivals recorded on Dtags at different depths and about 11 km range in 2003. Black circles highlight the time of each airgun arrival. Ray path labels are as follows: B indicates a bottom reflection, and S indicates a surface reflection.

angles). Also, the lack of suitably detailed information on environmental properties in the 2003 study area explains the mismatch between 2003 model and data wave forms (Fig. 19). First, the 2003 bottom property data was taken about 20 km from the 2003 CEE site, on the opposite side of the Mississippi Canyon, and errors in bottom parameters result in inaccurate modeling of sound amplitude. Second, in 2003, sound speed data were collected temporally and spatially further from the study area than in 2002. Consequently, inaccuracies in the 2003 sound speed profile resulted in differences between modeled and observed relative arrival times; any errors in bathymetry could also have caused arrival-time discrepancies. Finally, the numerical source used in the models is a point source, which acts like a dipole at low frequencies and emits less energy at launch angles close to the horizontal than does an airgun array. This difference helps explain why airgun arrivals that left the source at near-horizontal launch

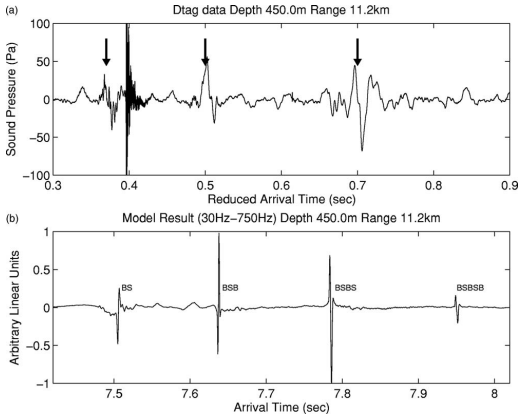

FIG. 19. Wave form comparison between (a) the 2003 Dtag recording and (b) broadband model results for a receiver at 11.2 km range and 450 m depth.

angles have more energy than the model predicts. The observed mismatch between 2003 data and model results emphasizes the fact that accurate modeling of airgun pulse arrivals is impossible without adequate environmental data and source information.

Surface ducted propagation increased the proportion of high-frequency content compared to the seismic (low frequency) content of some airgun arrivals recorded on whales at shallow depths (<50 m) in 2002, but not in 2003, when no surface duct was observed. A reasonable "ducting gain" estimate for the reduction in transmission loss for sound trapped in a surface duct can be obtained by a simple physical argument. The surface duct confines the low-angle trapped energy to its thickness h, as opposed to the full water column depth H, so that there is an H/h geometric ducting gain for the trapped energy. Also, the ducted energy does not interact with the bottom and suffer bottom loss, so the ducted rays will "gain" the amount of energy they would have lost in bottom interaction if the duct did not exist. Thus we can predicate a "surface duct gain" G in dB of

$$G = 10\log(H/h) + \mathrm{TL}(f, r, \theta) \tag{7}$$

for the portion of the rays trapped in the duct, where TL is the transmission loss for a nonducted ray of source angle θ. Of course, exact model calculations are preferable, and we would recommend that any calculations requiring precision be based on such models.

The exact levels notwithstanding, the data from the 2002–2003 Dtag controlled exposure studies do show that airgun arrays produce significant energy at frequencies well above those actually utilized for geophysical surveys (Caldwell and Dragoset, 2000; see Madsen *et al.* (2006) for quantification of received levels). Our model results and source beampattern analysis explain why there was more energy in the 500–2500 Hz frequency band in the airgun signals recorded at a whale near the surface when a surface duct was present.

We recommend that future research should include both modeling and measurement of airgun array source signatures at a full range of angles and at frequencies up to several kilohertz. Collecting (and publishing) accurate and detailed data on airgun array sources would allow for correspondingly accurate and detailed predictions of airgun sound propagation in the ocean. Failure to properly quantify the acoustic source properties of airgun arrays presently limits our ability to predict, test for, and mitigate any potential negative effects they may have. In addition, the ability to predict received levels of airgun pulses as a function of source-receiver range depends on having detailed, current information about the ocean and seabed environment in which the sounds are propagating.

The data we used were collected as part of a controlled exposure experiment designed to study the effect of airgun activity on sperm whale behavior (Miller *et al.*, unpublished). Even assuming behavioral effects can be well-described, there are several major obstacles to the interpretation of such controlled exposure data and their integration into policies designed to mitigate adverse effects of airgun sounds on marine life. First, one must quantify received levels of airgun noise in a manner that accurately relates to the animals' perception of the sound; ideally, this measured level should be directly proportional to the risk of physical damage or adverse behavioral modifications (Madsen, 2005). Second, most management guidelines for mitigating potential airgun effects on marine mammals define maximum allowable exposure levels and then design regulations to protect animals from exposure to unacceptable sound levels. One popular framework for current discussions on potential effects of human-made sounds on marine species, proposed by Richardson *et al.* (1995), suggests that a sound source is surrounded by several zones of potential influence on receiving animals: at very close ranges, animals may be injured by a very loud sound; at greater ranges, their behavior or fitness may be affected by the sound; at even greater ranges, they can detect the sound but are not affected by it; and finally, beyond some range, the animals cannot detect the sound at all. While conceptually useful, the model assumes that sound exposure decreases monotonically with range from the source. Accordingly, an allowable exposure level is generally translated to a range from the airgun array within which potentially impacted marine mammals must not occur during airgun operation (Barlow and Gentry, 2004; Richardson *et al.*, 1995). This range is usually estimated from the maximum allowable exposure level using the backcalculated, broadband, on-axis source level of the airgun array. Most allowable range estimates also assume a geometric spreading transmission loss or a range-independent acoustic model with an omnidirectional sound source (Barlow and Gentry, 2004; Gordon *et al.*, 2004). Since most airgun array source levels are calculated only on-axis and for frequencies below 250 Hz (Gausland, 2000), the range estimation described above does not account for the full frequency range produced by the array or the directionality of the array [although some regulatory approaches include a correction for array beampattern effects (NMFS, 2003)]. Moreover, the detailed aspects of the multipath acoustic propagation, such as the existence of convergence zones and shadow zones, surface ducts, etc., are disregarded.

Our ray trace and PE model results show a convergence zone at 6–8 km range (2003) or 4–6 km range (2002) (shown in Fig. 12), which is further confirmed by data on received levels in the Dtag recordings (for details, see Madsen *et al.*, 2006). These results illustrate that in many cases airgun received levels will not decrease monotonically with increasing range, so that a simple spherical or cylindrical spreading law will not accurately predict the observed pattern of received levels. Regulation based on inappropriate application of a geometric spreading law to calculate the extent of exposure zones could result in exposing animals to higher-than-intended noise levels. For example, using a geometric-spreading based calculation method to estimate the range from an airgun array at which a near-surface sperm whale in the Gulf of Mexico would be exposed to a potentially harmful received level of 180 dB re 1 μPa [root-mean-squared (rms)] results in a range of 295 m (NMFS, 2003). However, received airgun array levels of 180 dB re 1 μPa (rms) at 18 m depth in the Gulf of Mexico have been mea-

sured at ranges up to ~3.5 km from the source—over ten times the range predicted by the geometric spreading calculation (Tolstoy *et al.*, 2004).

Regulations defining allowable ranges between airgun array sound sources and marine species must take into account the potentially complicated relationship between source-receiver range and depth, acoustic frequency, and received sound level. Other mitigation actions, such as ramp-up, assume that potentially affected animals will swim away from a source during ramp-up. Our results show, however, that animals may experience increased exposure levels as they swim away from a source under some conditions, and decreased levels as they approach. In this case, an animal seeking to reduce exposure in the short-term may actually approach the source. Source beampattern may also vary dramatically during ramp-up, resulting in variation in received levels and frequency spectra over time at a given location. There is clearly an urgent need better to define the acoustic signatures of airgun arrays and how sound propagates from them. Any efforts to reduce the risk of airguns to marine mammals must include accurate predictions of exposure.

ACKNOWLEDGMENTS

The authors thank the crews and science parties of the research cruises on which data for this study were collected. Funding for this work was provided by the Office of Naval Research, the U.S. Department of the Interior Minerals Management Service Cooperative Agreements Nos. 1435-01-02-CA-85186 and NA87RJ0445, and the Industry Research Funding Coalition. S.L.D.R. was supported by a National Science Foundation Graduate Research Fellowship. Peter Madsen performed airgun pulse extraction, and Peter Madsen and Mark Johnson provided helpful comments on the manuscript. All approaches to animals for tagging were made following the conditions of NMFS research permits 981-1578 and 981-1707. The Woods Hole Oceanographic Institution Animal Care and Use Committee approved this research.

Barger, J. E., and Hamblen, W. R. (**1980**). "The air gun impulsive underwater transducer," J. Acoust. Soc. Am. **68**, 1038–1045.

Barlow, J., and Gentry, R. (**2004**). "Report of the NOAA Workshop on Anthropogenic Sound and Marine Mammals, 19–20 February 2004," NOAA Technical Memorandum NMFS-SWFSC-361.

Blackman, D. K., de Groot-Hedlin, C., Harben, P., Sauter, A., and Orcutt, J. A. (**2004**). "Testing low/very low frequency acoustic sources for basin-wide propagation in the Indian Ocean," J. Acoust. Soc. Am. **116**, 2057–2066.

Bowlin, J. B., Spiesberger, J. L., Duda, T. F., and Freitag, L. F. (**1992**). *Ocean Acoustic Ray-Tracing Software RAY*, WHOI Technical Report, WHOI-93-10 (Woods Hole Oceanographic Institution, Woods Hole, MA).

Caldwell, J. (**2002**). "Does air-gun noise harm marine mammals?," The Leading Edge **21**, 75–78.

Caldwell, J., and Dragoset, W. (**2000**). "A brief overview of seismic air-gun arrays," The Leading Edge **19**, 898–902.

Clay, C. S., and Medwin, H. (**1977**). *Acoustical Oceanography: Principles and Applications* (Wiley, New York).

Collins, M. D. (**1993**). "A split-step Padé solution for the parabolic equation method," J. Acoust. Soc. Am. **93**, 1736–1742.

Dragoset, W. (**2000**). "Introduction to air guns and air-gun arrays," The Leading Edge **19**, 892–897.

Engås, A., Løkkeborg, S., Ona, E., and Soldal, A. V. (**1996**). "Effects of seismic shooting on local abundance and catch rates of cod (*Gadus morhua*) and haddock (*Melanogrammus aeglefinus*)," Can. J. Fish. Aquat. Sci. **53**, 2238–2249.

Frisk, G. V. (**1994**). *Ocean and Seabed Acoustics* (P.T.R. Prentice-Hall, Upper Saddle River, NJ).

Gausland, I. (**2000**). "Impact of seismic surveys on marine life," The Leading Edge **19**, 903–905.

Geresi, E., Chapman, N. R., McGee, T., and Woolsey, J. R. (**2005**). "Gas hydrate geohazard assessment in the northern Gulf of Mexico using a vertical line array," *Proceedings of the AAPG Annual Convention*, Calgary, Alberta.

Goold, J. C., and Fish, P. J. (**1998**). "Broadband spectra of seismic survey air-gun emissions, with reference to dolphin auditory thresholds," J. Acoust. Soc. Am. **103**, 2177–2184.

Gordon, J., Gillespie, D., Potter, J., Frantzis, A., Simmonds, M. P., Swift, R., and Thompson, D. (**2004**). "A review of the effects of seismic surveys on marine mammals," Mar. Technol. Soc. J. **37**, 16–34.

Hamilton, E. L. (**1972**). "Compressional-wave attenuation in marine sediments," Geophysics **37**, 620–646.

Hamilton, E. L. (**1978**). "Sound velocity-density relations in sea-floor sediments and rocks," J. Acoust. Soc. Am. **63**, 366–377.

Hamilton, E. L. (**1980**). "Geoacoustic modeling of the sea floor," J. Acoust. Soc. Am. **68**, 1313–1340.

Jensen, F. B., Kuperman, W. A., Porter, M. B., and Schmidt, H. (**1994**). *Computational Ocean Acoustics* (AIP, Woodbury, NY).

Jochens, A. E., and Biggs, D. C. (**2003**). *Sperm Whale Seismic Study in the Gulf of Mexico, Annual Report: Year 1* (U.S. Department of the Interior Minerals, Management Service, Gulf of Mexico OCS Region, New Orleans, LA).

Jochens, A. E., and Biggs, D. C. (**2004**). *Sperm Whale Seismic Study in the Gulf of Mexico, Annual Report: Year 2* (U.S. Department of the Interior Minerals, Management Service, Gulf of Mexico OCS Region, New Orleans, LA).

Johnson, M. P., and Tyack, P. L. (**2003**). "A digital acoustic recording tag for measuring the response of wild marine mammals to sound," IEEE J. Ocean. Eng. **28**, 3–12.

Jovanovich, D. B., Sumner, R. D., and Akins-Easterlin, S. L. (**1983**). "Ghosting and marine signature deconvolution: a prerequisite for detailed seismic interpretation," Geophysics **48**, 1468–1485.

Labianca, F. M. (**1972**). "Normal modes, virtual modes, and alternative representations in the theory of surface-duct sound propagation," J. Acoust. Soc. Am. **53**, 1137–1147.

Laws, R., Landrø, M., and Amundsen, L. (**1998**). "An experimental comparison of three direct methods of marine source signature estimation," Geophys. Prospect. **46**, 353–389.

Madsen, P. T. (**2005**). "Marine mammals and noise: Problems with root mean square sound pressure levels for transients," J. Acoust. Soc. Am. **117**, 3952–3957.

Madsen, P. T., Johnson, M., Miller, P. J. O., Aguilar de Soto, N., Lynch, J., and Tyack, P. L. (**2006**). "Quantitative measures of air gun pulses recorded on sperm whales (*Physeter macrocephalus*) using acoustic tags during controlled exposure experiments,"J. Acoust. Soc. Am. **120**, 2366–2379

Mallick, S., and Frazer, L. N. (**1987**). "Practical aspects of reflectivity modeling," Geophysics **52**, 1355–1364.

McCauley, R. D., Fewtrell, J., and Popper, A. N. (**2003**). "High intensity anthropogenic sound damages fish ears," J. Acoust. Soc. Am. **113**, 638–642.

McGee, T., Geresi, E., Lutken, C., Woolsey, B., Higley, P., and Sharpe, S. (**2003**). Operation Report: The 8–14 October, 2003, Cruise of the R/V PELICAN, to deploy the CMRET vertical line array in Mississippi Canyon 798 and Atwater Valley 14, northern Gulf of Mexico, MMRI/CMRET, University of Mississippi.

Miller, P. J. O., Johnson, M. P., Madsen, P. T., Quero, M. E., Biassoni, N., King, R., and Tyack, P. L. (unpublished). "At-sea experiments provide preliminary evidence that airguns affect the foraging behavior of sperm whales in the Gulf of Mexico."

Murphy, E. L., and Davis, J. A. (**1974**). "Modified ray theory for bounded media," J. Acoust. Soc. Am. **56**, 1747–1760.

National Marine Fisheries Service (NMFS) (**2003**). "Taking and importing marine mammals; Taking marine mammals incidental to conducting oil and gas exploration activities in the Gulf of Mexico," Federal Register **68**, 9991–9996.

Nieukirk, S. L., Stafford, K. M., Mellinger, D. K., Dziak, R. P., and Fox, C. G. (**2004**). "Low-frequency whale and seismic airgun sounds recorded in the mid-Atlantic Ocean," J. Acoust. Soc. Am. **115**, 1832–1843.

Parkes, G., and Hatton, L. (**1986**). *The Marine Seismic Source* (D. Reidel, Dordrecht, Holland).
Popper, A. N., Fewtrell, J., Smith, M. E., and McCauley, R. D. (**2004**). "Anthropogenic sound: Effects on the behavior and physiology of fishes," Mar. Technol. Soc. J. **37**, 35–40.
Porter, M. B. (**1995**). *The KRAKEN Normal Mode Program* (SACLANT Undersea Research Center, La Spezia, Italy).
Porter, M. B., and Jensen, F. B. (**1993**). "Anomalous parabolic equation results for propagation in leaky surface ducts," J. Acoust. Soc. Am. **94**, 1510–1516.
Richardson, W. J., Greene, Jr., C. R., Malme, C. I., and Thompson, D. H. (**1995**). *Marine Mammals and Noise* (Academic, San Diego, CA).
Schmidt, H. (**2004**). OASES version 3.1 User Guide and Reference Manual; http://acoustics.mit.edu/faculty/henrik/oases.html. Last accessed 10/30/2006.
Tipler, P. A., and Llewellyn, R. (**2003**). *Modern Physics* (W.H. Freeman and Company, New York).
Tolstoy, M., Diebold, J. B., Webb, S. C., Bohnenstiehl, D. R., Chapp, E., Holmes, R. C., and Rawson, M. (**2004**). "Broadband calibration of R/V *Ewing* seismic sources," Geophys. Res. Lett. **31**, L14310.
Turgut, A., McCord, M., Newcomb, J., and Fisher, R. (**2002**). "Chirp sonar sediment characterization at the northern Gulf of Mexico Littoral Acoustic Demonstration Center experimental site," Oceans '02 MTS/IEEE **4**, 2248–2252.
Urick, R. J. (**1975**). *Principles of Underwater Sound for Engineers* (McGraw-Hill, New York).
Weston, D. E., Esmond, C. G., and Ferris, A. (**1991**). "The duct leakage relation for the surface sound channel," J. Acoust. Soc. Am. **89**, 156–164.
Zimmer, W. M. X., Tyack, P. L., Johnson, M. P., and Madsen, P. T. (**2005**). "Three-dimensional beam pattern of regular sperm whale clicks confirms bent-horn hypothesis," J. Acoust. Soc. Am. **117**, 1473–1485.
Ziolkowski, A. (**1970**). "A method for calculating the output pressure waveform from an air gun," Geophys. J. R. Astron. Soc. **21**, 137–161.
Ziolkowski, A., Parkes, G., Hatton, L., and Haugland, T. (**1982**). "The signature of an airgun array: Computation from near-field measurements including interactions," Geophysics **47**, 1413–1421.
Ziolkowski, A., and Johnston, R. G. K. (**1997**). "Marine seismic sources: QC of wavefield computation from near-field pressure measurements," Geophys. Prospect. **45**, 611–639.

Chapter 5. Modeling Sperm Whale Response to Airgun Sounds

5.1 Introduction

Despite strong public concern about potential adverse effects of sonars, airguns and other anthropogenic sounds on marine mammals, relatively few controlled exposure experiments have been carried out to describe and quantify those effects (Richardson *et al.*, 1995; Miller *et al.*, 2000; Nowacek *et al.*, 2004; Tyack, 2008). Even when there is anecdotal evidence of behavioral reactions to a certain stimulus, careful experiments testing responses of marine mammals to noise are relatively few. Such experiments are difficult to design and carry out, and the resulting data difficult to analyze, for several reasons. Because of the cost and logistical difficulties involved with field work, most studies of marine mammal behavior involve relatively few individual animals. To avoid potential injury, temporary hearing threshold shift, or significant disruption of behavior, controlled exposures are usually conducted at relatively low sound levels compared to the maximum levels animals might encounter if the sound source were operating at close range and at full power. Consequently, behavioral responses to controlled exposures are likely to be subtle and difficult to detect; statistical power to detect such small effects is limited when the number of animals exposed is relatively small and traditional statistical methods are applied. Among published studies, when statistical analysis of behavioral rate data is presented, it generally entails binning the time-series behavior observations into pre-exposure, exposure, and post-exposure periods, then applying ANOVA or similar statistical tests to detect differences in mean behavioral rates between periods. Richardson and colleagues review marine mammal examples (1995); many examples of general animal behavior rate studies also exist (Cherry, 1989; Mooring, 1995; Paredes *et al.*, 2005; Fernández-Juricic and Tran, 2007). When relatively low-power tests are employed and expected impacts are subtle, the failure to detect an impact does not imply that no impact exists, so results can be disappointingly inconclusive. Careful experimental design (including adequate

sample size and a range of sound exposure levels) may limit this problem for future marine mammal sound exposure studies, but appropriate and more powerful statistical methods can also help.

To overcome some of the data analysis limitations described above, I have developed several statistical methods applicable to whale behavior data, and I have applied them to data from an experiment in which sperm whales were exposed to airgun sounds. To assess whether sperm whale foraging behavior changed during airgun exposure, I applied two main types of statistical analysis. The first test was the rotation test, a randomization technique designed to detect changes in the rate of a behavioral point process even if the behavioral time-series is auto-correlated, contains bouts or clumps of events, or is otherwise sequentially dependent. The second method involved use of a continuous-time semi-Markov chain model to describe whale behavior, combined with a likelihood ratio test for significant differences in behavior between control and exposure time-periods.

Although similar models can be applied to any point-process time series or defined set of behavioral states, I chose to model foraging behavior in particular for several reasons. First, I wanted to test for changes in behavior that were biologically significant, not just statistically significant; since foraging rate and foraging success are important determinants of individual fitness, adverse effects of noise on individual foraging may have population-level consequences. Second, the experiment provided especially extensive and detailed data on foraging behavior. Sperm whales use echolocation to find prey, and audio/dive records from the dataset allowed me to determine when each animal was foraging and which stage of foraging they occupied (echolocating to search for prey, attempting to capture prey item(s), or silent/not actively echolocating). The whales in the study spent the majority of their time foraging.

The methods presented in this chapter have several advantages over the more traditional methods described above, including: 1) increased statistical power (because the power of our tests scales with the number of events observed rather than the number of whales tested); 2) ability to conduct analyses both at the level of the individual animal and at the group level; and 3) potential to allow for or average over individual variation in baseline behavior and behavioral response. In the following sections, I will describe the experimental data collection, development and application of the semi-Markov chain model, and results of the data analysis.

5.2 Methods

5.2.1 Experimental Methods and Data Collection

In the 2002 and 2003 Sperm Whale Seismic Study (SWSS) experiments in the Gulf of Mexico, eight sperm whales underwent controlled exposure to airgun pulses. A brief description of the experiments follows here, and detailed descriptions of the experimental set-up and acoustic data collected are available in the literature (Jochens and Biggs, 2003; Miller *et al.*, 2003; Jochens and Biggs, 2004; DeRuiter *et al.*, 2006; Madsen *et al.*, 2006). During the experiments, eight sperm whales were tagged with a dtag, an archival tag that records acoustic, depth, and orientation information (Johnson and Tyack, 2003). Tagged whales were exposed to transmissions from airgun arrays, fired every 15 seconds at source-whale ranges from 1 to13 km. Table 5.1 presents details on the timing and duration of tagging and airgun exposure, as well as the sex of the tagged whales when known. The tags recorded whale movements and vocalizations during the exposure, as well as airgun sound arrivals at a variety of source-whale ranges and whale depths. Of the eight whales tested, seven foraged during the airgun exposure; the animal that did not forage was not included in my analysis.

Whale ID	Date	Tag on	Tag off	CEE start	CEE duration	RL	Sex
sw02_253a	10/9/2002	16:38	20:58	17:59	104 min	120-146	?
sw02_254a	11/9/2002	10:13	21.45	12:16	70 min	116-143	F
sw02_254b	11/9/2002	10:28	22.52	12:16	70 min	121-142	F
sw02_254c	11/9/2002	10:34	22.56	12:16	70 min	125-143	?
sw03_164a	13/6/03	9:48	23.2	18:26	60 min	125-146	F
sw03_165a	14/6/03	13:35	6:19	17:01	120 min	123-146	F
sw03_165b	14/6/03	13:38	6:05	17:01	120 min	119-147	F

Table 5.1. Timing and duration of whale tagging during controlled exposure experiments in 2002 and 2003. The RL column gives *m*-weighted rms (root-mean-squared) received levels of airgun arrivals with signal-to-noise levels sufficient to allow quantification (from Madsen *et al.*, 2006; see paper for details on the level calculations). CEE = Controlled Exposure Experiment. The sex of some animals was determined genetically using sloughed skin samples (Dan Engelhaupt, personal communication); F means female, and ? means no sample was analyzed.

5.2.2 Rotation Test for Changes in Buzz Rates

Using the rate of echolocation buzzes recorded on the dtags (which indicate attempted or successful prey capture events) as a proxy for foraging rate (Miller *et al.*, 2004a), I was able to construct a time-series of attempted prey captures for each whale in the study. One of my major analysis goals for the sperm whale dataset was to determine whether the whale foraging rate changed during airgun exposure relative to control periods (in this case, I hypothesized that airgun exposure would lead to decreased foraging rates as airgun pulses masked prey echoes or acted as a nuisance to the whales). This type of problem

is common in behavioral ecology and ethology, as researchers often wish to determine whether the rate at which a certain behavioral event occurs is affected by an environmental or other factor. In the case I considered, the event is a vocalization by an individual sperm whale and the factor is the operation or non-operation of an airgun array. A typical experiment to test for such effects involves observing animals during control and treatment periods and determining the average rate of certain behaviors under each condition. This type of behavioral rate data is often analyzed as binned counts (e.g., Cherry, 1989; Mooring, 1995; Paredes *et al.*, 2005; Fernández-Juricic and Tran, 2007). Analyzing point process data in this way entails a loss of statistical power (Dean and Balshaw, 1997), and since maximizing power is critical for my seven-whale dataset, I have instead pursued a more powerful approach.

In some cases, under the null hypothesis of no treatment effect, behavioral events can be assumed to follow a stationary Poisson process, and a statistical test to determine whether event rate changes during treatment can be based on the binomial distribution, as described in more detail in DeRuiter and Solow (in press). However, if the Poisson assumption is not correct – for example, if behavioral events occur in bouts – then the binomial test can give misleading results. In such cases, one option is to find a test that is valid under a particular alternative to the Poisson model. Unfortunately, while it is often easy to demonstrate that a point process is not Poisson, it can be difficult to specify an appropriate alternative model. Because the sperm whale echolocation buzz time series have a low but significant amount of autocorrelation, and because it is reasonable to expect that sperm whale foraging events occur in bouts as the whale encounters patches of prey, I believe that the Poisson assumption may be incorrect for my data.

The rotation test is a simple nonparametric method that can be used to analyze behavioral point process data even if the process generating the data is

unknown, and if the dataset is auto-correlated, contains bouts or clumps of events, or is otherwise sequentially dependent. The general approach of the rotation test was originally proposed by Harkness & Isham (1983) for testing association between two two-dimensional point processes observed on a rectangle. The method has also been applied to one-dimensional point process data (behavioral time-series, Miller *et al.*, 2004a; Miller *et al.*, 2004b). However, no formal description of the test (including assessment of its validity and power) has been published to date; with Andy Solow, I have submitted such a description for publication (DeRuiter and Solow, in press; see Appendix A for full text). Here, I describe the rotation test more informally by detailing a specific application: detection of changes in sperm whale buzz rate in response to airguns.

To apply the rotation test to the sperm whale buzz rate data, I began by calculating my test statistic, the observed number of buzzes during control conditions (N_c), for each individual whale. N_c is higher if buzz rate is elevated during control conditions relative to experimental conditions. To estimate the distribution of N_c under the null hypothesis of no change in buzz rate, I used the rotation test method to resample the data. The rotation test is similar to other randomization procedures in that it involves resampling the dataset to determine a distribution (or confidence bounds) for a parameter of interest; however, it preserves the sequential order of data points, so it can be used for datasets with sequential dependence. For each rotation of the dataset, I kept the time-series of buzzes intact, and held the duration of the airgun exposure constant, but randomly shifted the nominal start time of the exposure to a random time within the experiment. I then calculated $N_{c,rotated}$ for the rearranged dataset. I repeated the process 10,000 times to construct a distribution of $N_{c,rotated}$ and to calculate the p-value of the test (the probability of $N_{c,rotated}$ being at least as large as the N_c value observed in the data). I applied the test to each of the seven whales studied, then used Fisher's method to account for multiple statistical tests and

obtain a combined p-value indicating whether at least one of the seven whales showed a statistically significant reduction in foraging rate during airgun exposure (Fisher, 1948). I also tested the hypothesis that all seven whales showed a concerted reduction in foraging rate during airgun exposure; for that test I used the sum of N_c (for all whales) as my test statistic, and again determined its distribution with a rotation test.

I also estimated the power of the rotation test for the individual-whale hypothesis tests by testing synthetic datasets whose durations and event rates were approximately equal to the mean dataset duration and event rate. The model underlying the sperm whale buzz rate process is of course unknown, so the synthetic datasets I used were simulated using a variety of point process models with varying degrees of event "clumpiness" and autocorrelation: a stationary Poisson process, a one-dimensional Thomas process (Thomas, 1949), and an exponential autoregressive (EAR) model (Lawrance and Lewis, 1979).

5.2.3 Markov Chain Models: Background

Markov chain models are a subset of matrix models, a group of mathematical models that describe changes between states of some quantity of interest over time (for example, the number of individuals in a population that are in various developmental states, or the behavioral state of an animal). Discrete-time matrix models are generally formulated as a system of linear equations, $\vec{N}_{t+1} = \mathrm{P}\vec{N}_t$, where N is a vector of the number or proportion of individuals in each state, subscripts indicate time, and P is a matrix containing the probabilities of transition between states per unit time. Markov chain models differ from matrix models in general because they include the additional assumption that the current state of a model depends only on previous states. The order of a Markov chain is defined as the number of previous states required to determine the current state (so the current state depends on the immediately previous state in a

first-order Markov chain, the two previous states in a second-order Markov chain, and so on).

In ecology, matrix models (usually discrete-time, discrete-state models) have been used extensively to characterize the population size, spatial distribution, or life history of many species, and the related mathematical theory is well developed (Tuljapurkar and Caswell, 1997; Caswell, 2001; Kot, 2001; Keyfitz and Caswell, 2005; Madsen *et al.*, 2006). However, such models have only rarely been applied to behavioral time series. One study advocated Markov chain matrix models as an alternative method for determination of animal time budgets, constructing a discrete-time, discrete-state model of beaver behavior as a case study (Rugg and Buech, 1990). Another set of experiments fit a discrete-time, discrete-state Markov chain model to dolphin behavior data collected in the presence and absence of tourist boats to analyze the effects of tourist boats on dolphin behavior at two New Zealand field sites (Lusseau, 2003; 2004). Finally, Haccou and Meelis (1992) described statistical techniques to select and fit discrete- and continuous-time Markov and semi-Markov models of animal behavior data, including examples of model application to data on rats and rhesus monkeys. In each case, researchers were able to draw statistically sound conclusions from studies of relatively few individuals. These few examples illustrate the efficacy of matrix modeling techniques for analysis of animal behavior data, while highlighting the opportunity for increased application of such analyses. I have fit a continuous-time semi-Markov chain model to sperm whale foraging behavior, and used the model to assess changes in foraging behavior in response to airgun exposure.

5.2.4 Sperm Whale sMC Model Construction

Female and immature sperm whales perform stereotyped dive behavior. They consistently spend about 40 minutes of each hour doing deep dives (to 400-1000m depth), and about 20 minutes resting near the sea surface. While

they are underwater, after they have reached 200-300m depth, they begin to make regular clicks – powerful, relatively regularly spaced echolocation clicks (Watwood *et al.*, 2006). For the purposes of this study, I defined the foraging portion of a sperm whale dive as the time between initial onset and final end of regular clicking, and considered only data from foraging periods in all analyses (Fig. 4.1).

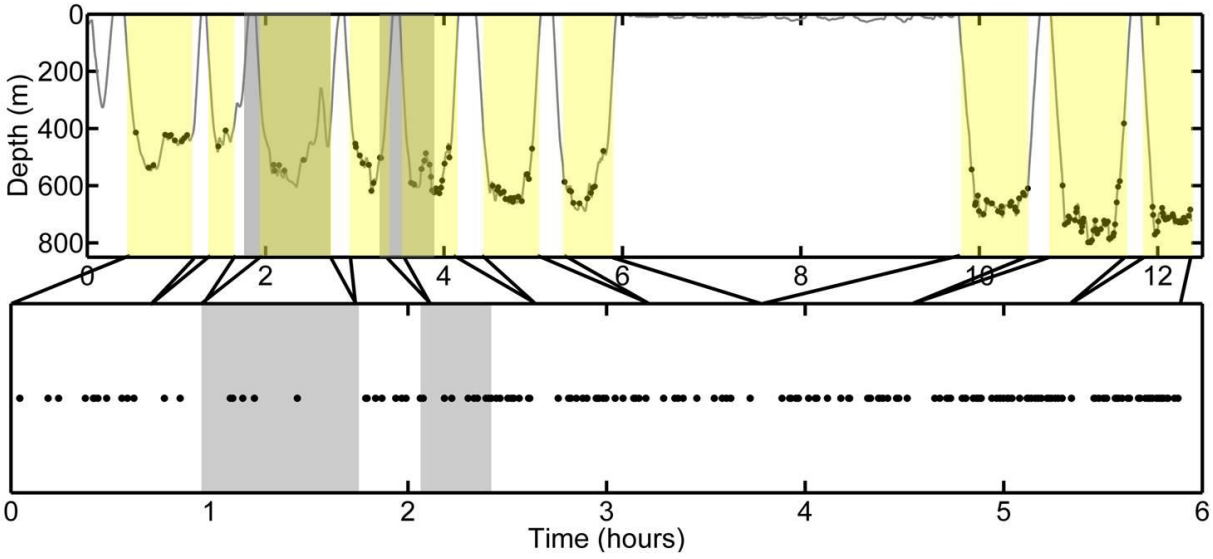

Figure 5.1. Top panel: Dive profile of the tagged sperm whale. The grey line indicates whale depth, and black circles indicate the times of echolocation buzzes. Airgun exposure periods are shaded gray. Black lines connecting the top and bottom panels illustrate how dive ascents, descents and surface periods were cut from the dataset to produce the foraging behavior time-series we analyzed. Only foraging periods (indicated by yellow shading) were included in the foraging behavior time-series. Bottom Panel: Time-series of echolocation buzzes produced by the sperm whale during foraging periods. Black dots indicate the times of buzzes, and gray shaded areas indicate airgun exposure periods.

Sperm whale foraging can be divided into three distinct phases, each of which is characterized by distinctive sounds:

- *Search Phase* The whale is echolocating, but has not yet begun a capture attempt. The whale produces regularly spaced, high-level echolocation clicks.
- *Capture Phase* The whale captures or attempts to capture a prey item, and produces an echolocation buzz. Buzzes are series of clicks with a much faster repetition rate than search clicks; to human ears they sound like a buzz or creak that varies in pitch over a few (1-10 or so) seconds.
- *Pause Phase* During pauses, the whale is silent for a period of a few seconds (and thus is not actively echolocating).

I modeled sperm whale foraging behavior as a continuous-time three-state semi-Markov process, in which whales can occupy three possible behavioral states (Search, Capture, and Pause); I converted the field data for each whale into a time-series of state-to-state transitions based on the dtag audio records.

The order of a Markov process is defined as the number of previous states required to determine the current state (so the current state depends on the immediately previous state in a first-order Markov chain, the two previous states in a second-order Markov chain, and so on). In this study, I considered only first-order processes. There was no obvious evidence for higher-order sequential dependence in the behaviors I analyze (data not shown). My first-order model assumed that the next behavioral state depended only on the current state, so I defined a time-independent state-to-state transition probability matrix as follows. Given that a transition from behavioral state j occurs at a certain time, the probability that the transition is from state j to another state k is a_{jk} (the row j, column k element of the transition matrix A).

The dtag audio sampling frequency is orders of magnitude greater than the frequency with which whales change behavioral states, so my data are effectively sampled in near-continuous time; in addition, there is no obvious

discrete time-step size to use that would be behaviorally relevant for a foraging sperm whale. Therefore, I chose to model foraging behavior in continuous time rather than discrete time. Standard continuous-time Markov chains use exponential distributions for the waiting times[2], but I chose to use state-specific gamma distributions, as exponential distributions fit my data poorly (e.g., Fig. 5.2). (This change in waiting time distributions means that my model is technically a semi-Markov chain (sMC) rather than a Markov chain.) In summary, the foraging behavior model includes

1) A transition matrix of probabilities of transitions from each state to the others, and

2) state-specific probability distributions that describe the "waiting times," or the expected time a whale will spend in a given state before switching states.

[2] If the whale is in a certain state *j*, it will remain in that state for a certain "waiting time" before changing to the next state; each observed waiting time is generally assumed to be a random sample from a state-specific probability distribution.

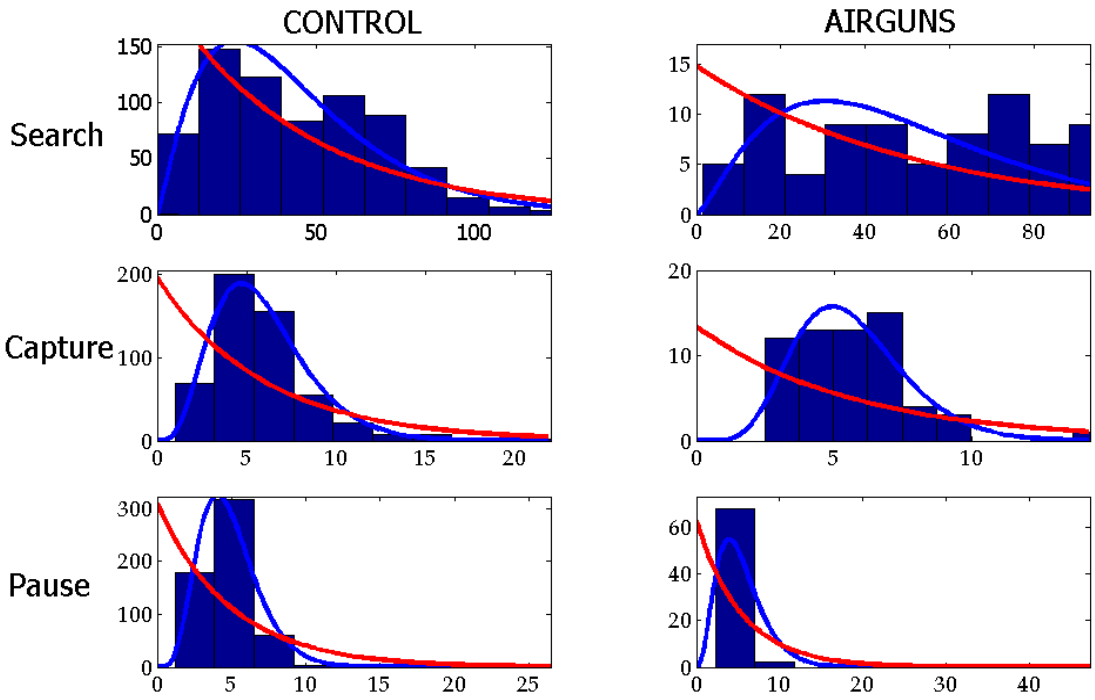

Figure 5.2. Waiting time histograms for a representative whale (165b) with exponential (red) and gamma (blue) distributions fit to the data. All x axes indicate time in seconds, while y axes indicate number of observations.

5.2.5 Fitting the sMC Model and Checking Model Goodness-of-Fit

I fit the model to the data for each whale by calculating the maximum likelihood estimates of: 1) the gamma distribution parameters that best fit the data waiting time distributions (using the function gamfit in Matlab) and 2) the transition probabilities ($a_{jk} = \frac{N_{jk}}{N_j}$, where N_{jk} is the number of transitions from state j to state k, and Nj is the total number of times a whale is in state j; Haccou and Meelis, 1992).

I fit the model described above to the data under the null hypothesis that the same Markov chain underlies the behavior of all whales during all conditions, and also under several nested alternate hypotheses:

H_{A1}) The sMC underlying whale behavior varies from whale to whale (inter-individual variation is significant).

H_{A2}) The sMC underlying whale behavior changes during airgun exposure.

I used several approaches to check the model's goodness of fit to the data before carrying out hypothesis tests. First, I used graphical methods to check for time-homogeneity of waiting times and transition probabilities (waiting times: cumulative bout-length plots and log-bout-length plots (Haccou and Meelis, 1992); transition probabilities: time-series of transition probabilities determined from blocks of 50 observed states). I also compared the maximized log likelihoods of our datasets to the distributions of maximized log likelihoods of equal-duration datasets simulated under the best-fit sMC models; if the model fit the data poorly, one would expect the data likelihoods to be small in comparison to the simulated data likelihoods.

5.2.6 sMC Model Hypothesis Tests and Significance Assessment

I next used likelihood ratio tests to determine whether the null hypothesis should be rejected in favor of the alternates, assessing the significance of the result with both a parametric bootstrap and a rotation test (DeRuiter and Solow, in press). For the parametric bootstrap, I simulated data under the null

hypothesis to construct a probability distribution for the likelihood ratio test statistic, which allowed me to assign a p-value to the observed test statistic. I first tested whether there was significant inter-individual variation (by comparing a model in which parameters were identical for the group of seven whales to a model in which each whale had individual-specific model parameters) (H_{A1}). Then I tested for effects of airgun exposure (by comparing a model with one set of parameters for all time periods to a model that allowed the parameters to be different during airgun exposure) (H_{A2}). I carried out the test for each whale individually (to look for individual effects), and also for concerted change by the set of seven whales (by summing the likelihood ratios for all whales).

A major assumption of the sMC model is that sperm whale foraging behavior is homogeneous in time (that is, the state-to-state transition probabilities and waiting times do not vary as functions of time) in the absence of any treatment effect. That assumption is probably true on average, and my model goodness-of-fit tests provided qualitative checks for some possible types of deviation from the assumption. However, I expect that the homogeneity assumption is not strictly true. Waiting times and especially transition probabilities may change cyclically or episodically (diurnally, over the course of a foraging dive, or as a whale encounters prey patches of different species or densities). Such fluctuations are difficult to detect, and difficult or impossible to parameterize explicitly in the model. If one occurred during an airgun exposure period, the parametric-bootstrap test described above might incorrectly conclude that airgun exposure caused a significant change in behavior. Rather than assuming that effects of such behavior fluctuations on the results were insignificant, I carried out a second round of analyses in which I replaced the parametric bootstrap with the rotation test described earlier in this paper. The rotation test is a more conservative, nonparameteric randomization technique that controls for fluctuations in the time-series parameters, but it has somewhat lower power than the parametric bootstrap. In the absence of model-data

mismatch, the rotation test and parametric bootstrap tests should return the same p-values (as long as both tests have sufficient power to detect the observed effect size).

Finally, in order to check the validity of my hypothesis tests, I applied them to dtag datasets from six sperm whales that were not part of the airgun exposure experiment. I selected a random one-hour period in each of the six datasets as the sham "airgun exposure" period, then applied the sMC model and hypothesis tests to each dataset exactly as for the airgun exposure datasets. I expected that if the tests were valid, they would not return significant p-values.

5.3 Results

5.3.1 Rotation Test Results

Table 5.2 shows the p-values of all rotation tests for changes in buzz rates; Figure 5.3 shows the results in graphical form, including 95% confidence intervals for the expected buzz rate during airgun exposure (based on the distribution of values obtained by applying the rotation test). Applying Fisher's (1948) method to the rotation test results for the seven individual whales indicated that at least one of the seven whales reduced its foraging rate by about 60% during airgun exposure ($p = 0.036$). However, I did not find strong evidence for a concerted reduction in foraging rate during airgun exposure by all seven whales ($p=0.19$). Figure 5.4 shows the power of the test to detect changes in foraging rate in response to airgun exposure, for simulated datasets with numbers of events similar to the individual sperm whale records. (The different types of synthetic datasets displayed have varying types and amounts of sequential dependency; it is not known which, if any, most closely approximates the sperm whale data.) For the data types shown in Figure 5.4, the test does not have high power to detect very small changes in foraging rate (power > ~0.8 only for >~15% reduction by all seven whales or >~40% reduction by a single whale).

Individual Whales	p-value (rotation test)
1 (253a)	0.70
2 (254a)	0.54
3 (254b)	0.069
4 (254c)	0.0021
5 (164a)	0.92
6 (165a)	0.72
7 (165b)	0.13
Group of 7 whales	
Fisher's method	0.036
Concerted change	0.19

Table 5.2. Results of rotation tests. The null hypothesis is that buzz rate was the same during airgun exposure and control conditions, while the alternate hypothesis was that the buzz rate decreased during airgun exposure. The Fisher's method p-value accounts for multiple statistical tests, indicating whether at least one of the seven whales tested showed a statistically significant reduction in foraging rate during airgun exposure. The concerted change p-value tests the hypothesis that all seven whales reduced their buzz rate during airgun exposure.

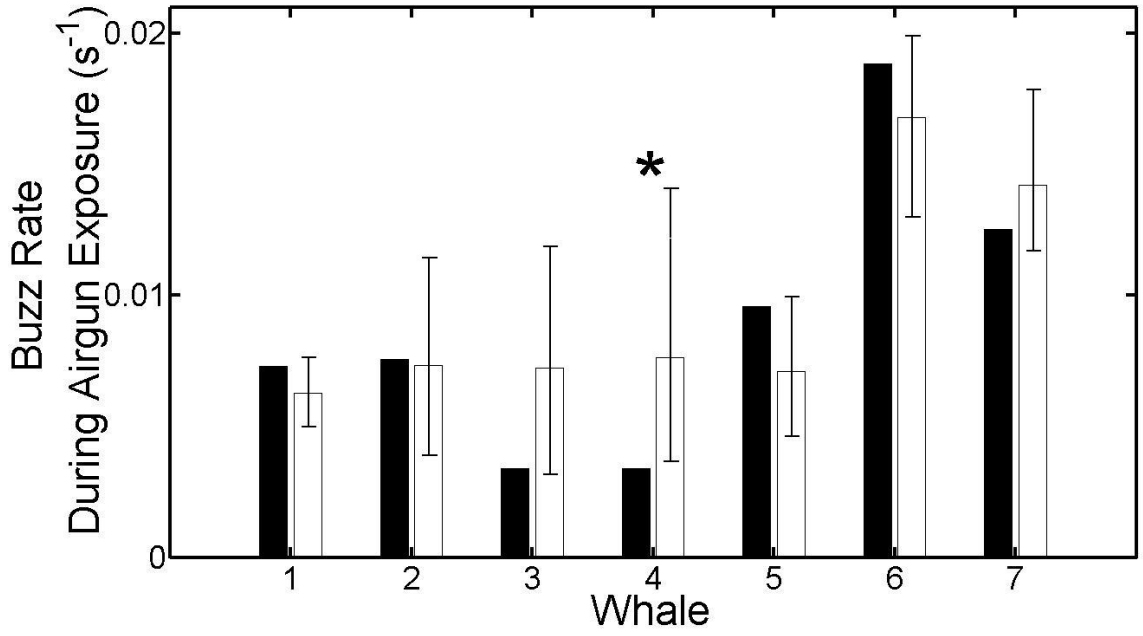

Figure 5.3. Rate of buzz production during airgun exposure. Black columns show observed buzz rate during airgun exposure for each whale. White columns show expected buzz rate during airgun exposure under the null hypothesis that exposure did not reduce buzz rate (column height is mean value from rotation tests, and error bars indicate 2.5% and 97.5% percentiles). An asterisk indicates the result that is statistically significant at the $p<0.05$ level.

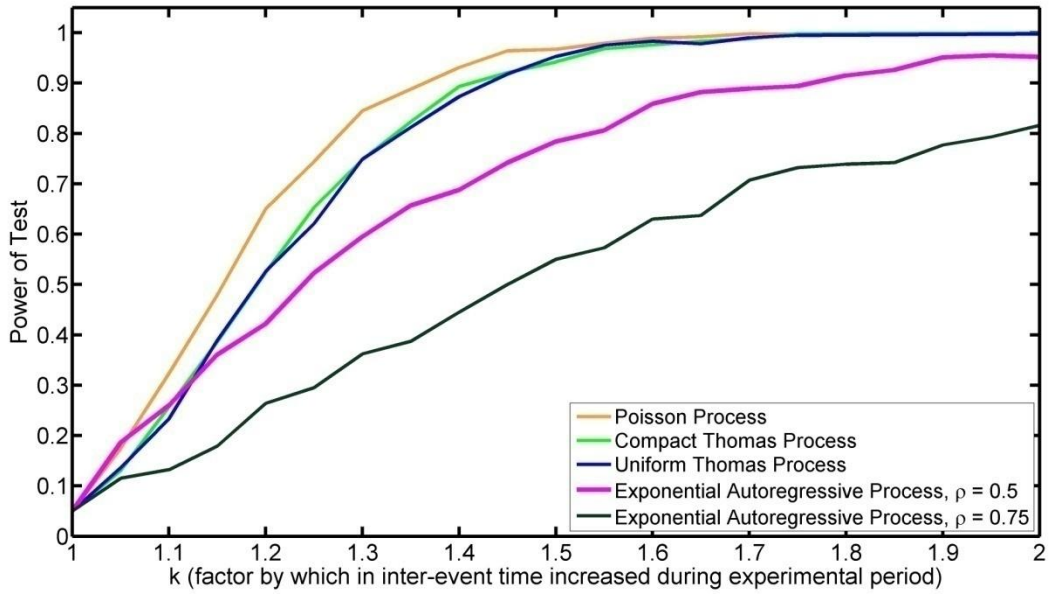

Figure 5.4. Power of the rotation test to detect reductions in buzz rate at the $p<0.05$ level for synthetic datasets with duration and event rate similar to those of the sperm whale datasets.

5.3.2 sMC Model Goodness-of-Fit Assessment

Figures 5.5 – 5.12 plot cumulative waiting times versus event number for all seven whales combined (Fig. 5.5) and for each whale individually. Changes in the slope of a cumulative waiting time plots indicate change points in the time-series of waiting times (Haccou and Meelis, 1992). Such changes in slope are present, though rather subtle, in the figure containing data for all seven whales (Fig. 5.5); the variation is clearest in the search waiting times. This observation provided initial evidence that individual variability in foraging behavior must be taken into account in the model fitting and analysis. As shown in Figures 5.6 – 5.12, the slopes of the cumulative waiting time plots for individual whales did not vary much with event number, supporting the idea that the waiting time distributions were time homogeneous.

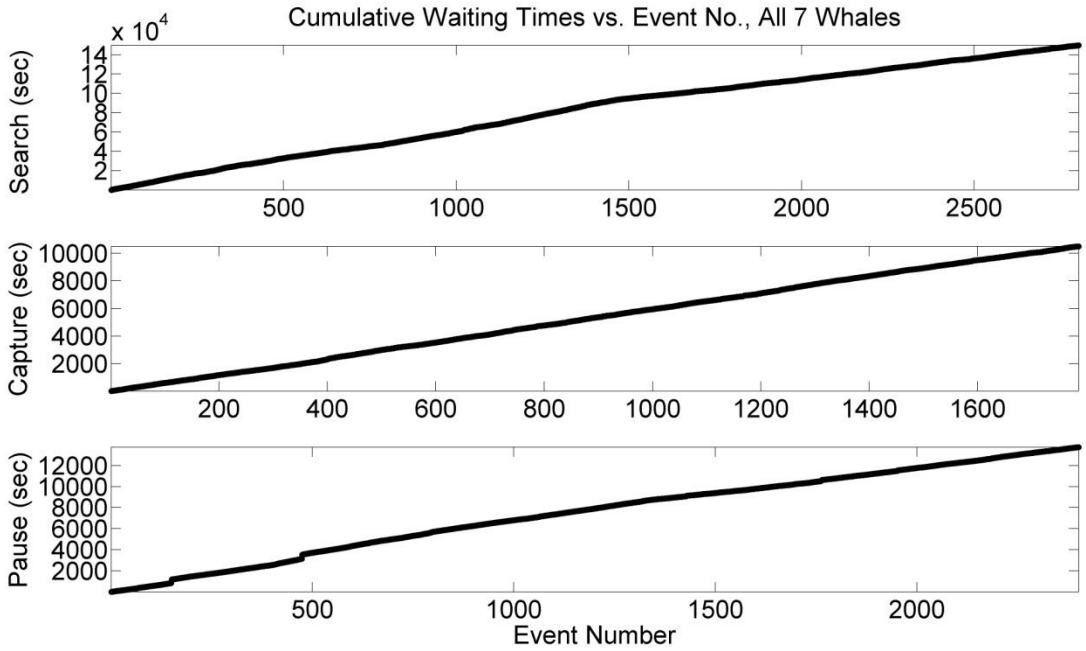

Figure 5.5. Cumulative waiting time vs. event number for the set of seven whales. Abrupt changes in the slope of the line would indicate changes in the waiting times.

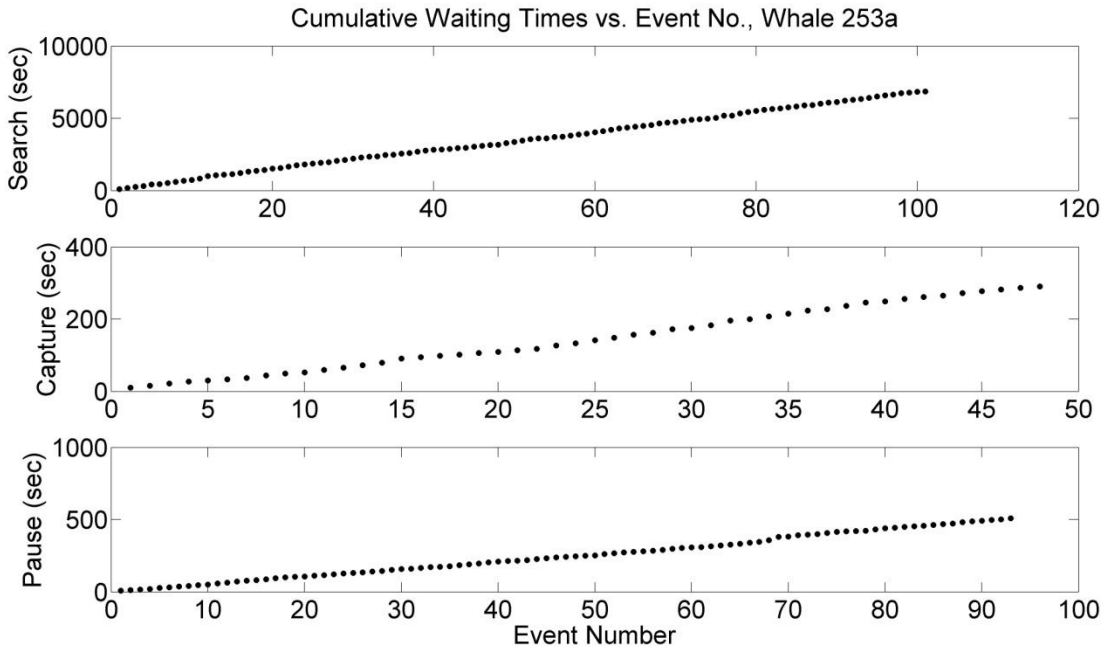

Figure 5.6. Cumulative waiting time vs. event number for whale 253a. Abrupt changes in the slope of the line would indicate changes in the waiting times.

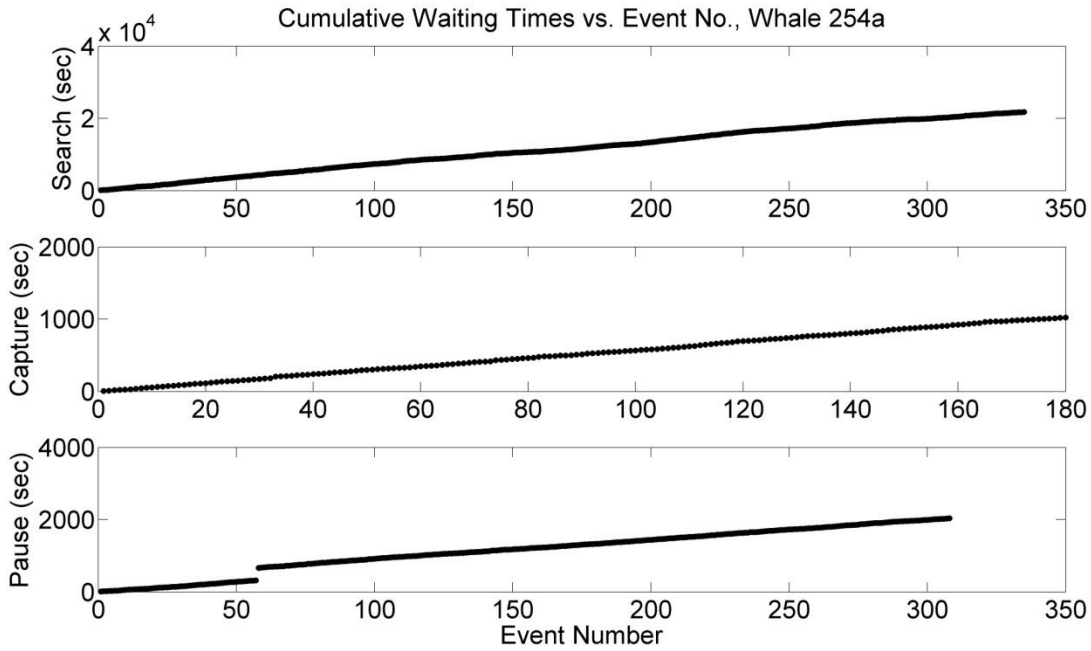

Figure 5.7. Cumulative waiting time vs. event number for whale 254a. Abrupt changes in the slope of the line would indicate changes in the waiting times.

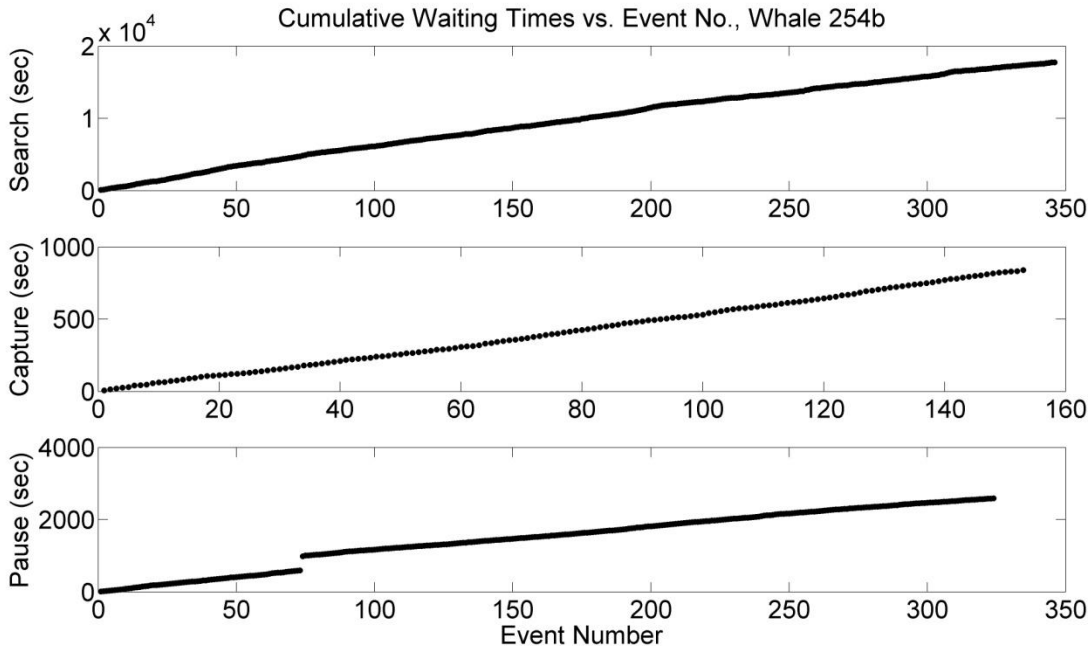

Figure 5.8. Cumulative waiting time vs. event number for whale 254b. Abrupt changes in the slope of the line would indicate changes in the waiting times. The vertical jump around event 75 in the pause data is the result of one extraordinarily long pause.

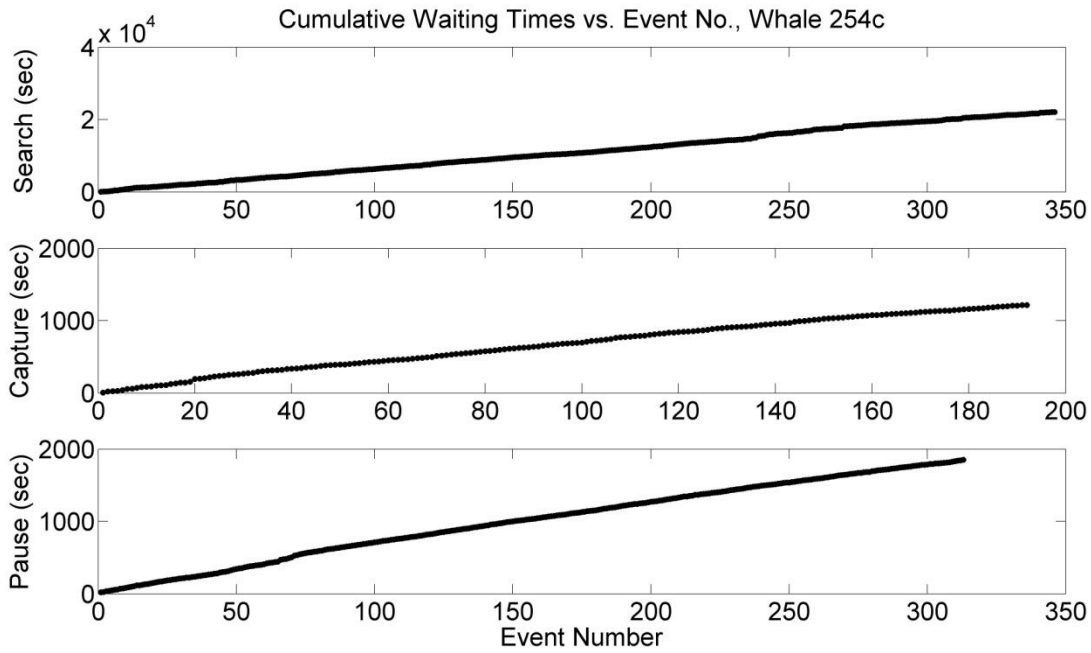

Figure 5.9. Cumulative waiting time vs. event number for whale 254c. Abrupt changes in the slope of the line would indicate changes in the waiting times.

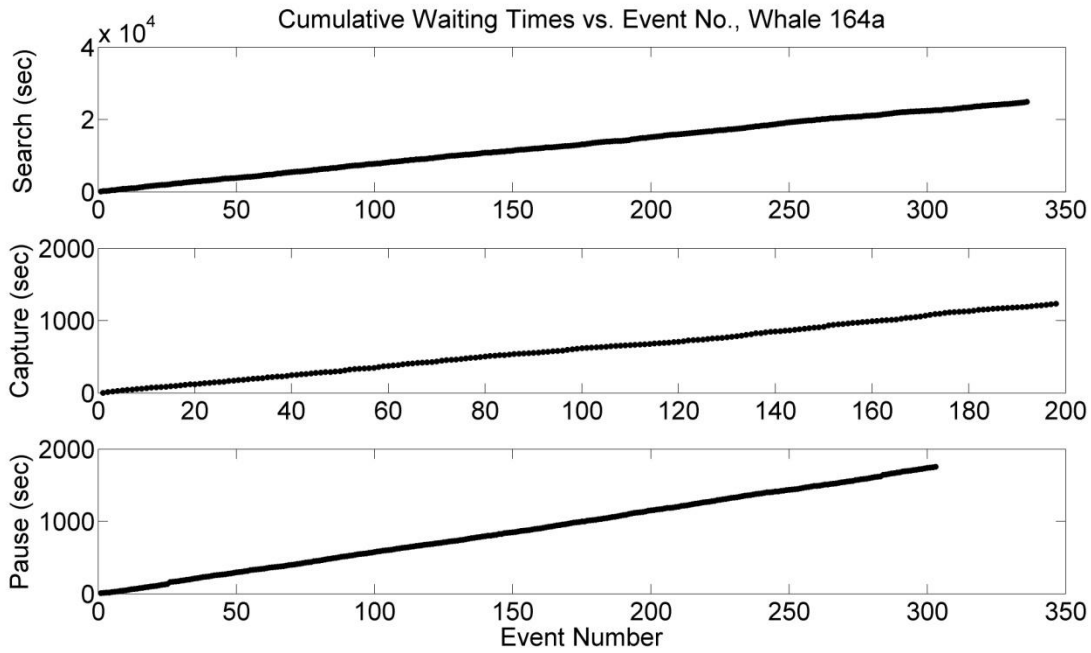

Figure 5.10. Cumulative waiting time vs. event number for whale 164a. Abrupt changes in the slope of the line would indicate changes in the waiting times.

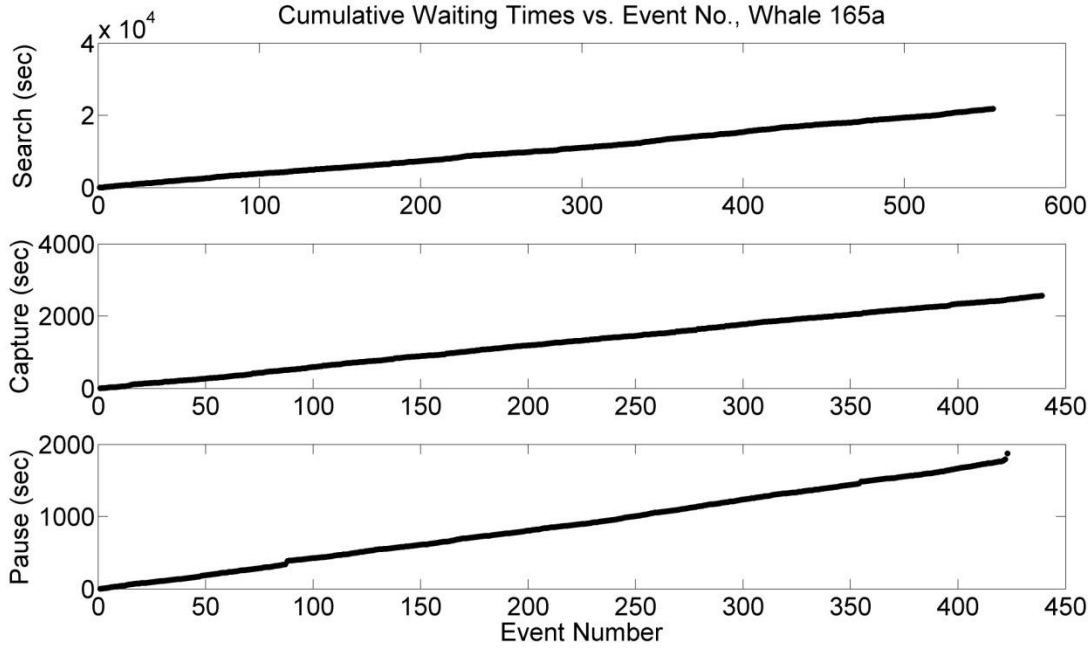

Figure 5.11. Cumulative waiting time vs. event number for whale 165a. Abrupt changes in the slope of the line would indicate changes in the waiting times.

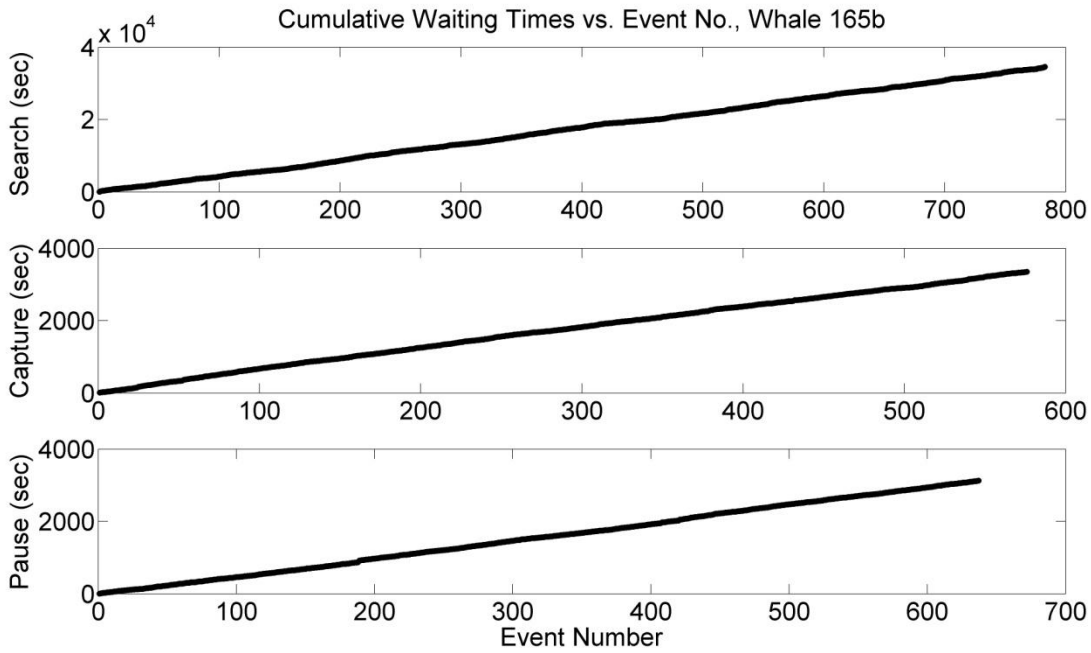

Figure 5.12. Cumulative waiting time vs. event number for whale 165b. Abrupt changes in the slope of the line would indicate changes in the waiting times.

I also plotted the logarithm of waiting time vs. event time for the set of seven whales (Fig. 5.13) and for each whale individually (Figs. 5.14 – 5.20). In Figures 5.13 – 5.20, a change in the distribution of waiting times would be indicated by a vertical shift in the positions of successive data points (Haccou and Meelis, 1992). Several of those shifts are visible in Figure 5.13; for example, search waiting times seem to be slightly higher between 15-30 hours, and pause waiting times are slightly lower from 30-35 hours. These shifts indicate that there is significant whale-to-whale variation in waiting times. No shifts are apparent in Figures 5.14-5.20, again supporting the idea that state-specific waiting times are constant with time for any individual whale.

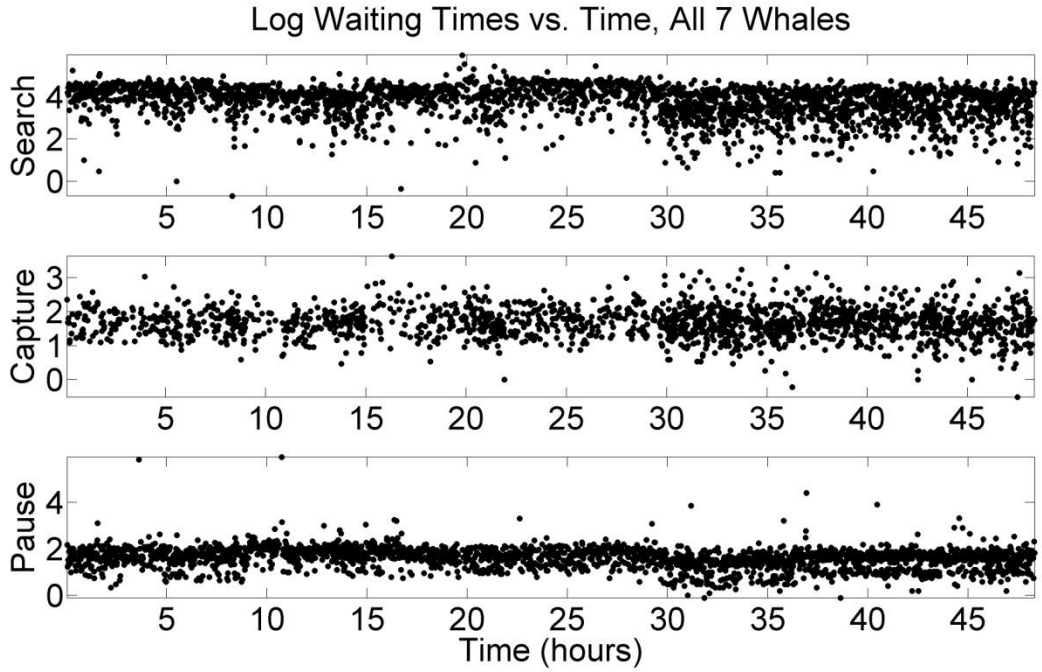

Figure 5.13. Logarithm of waiting time as a function of event time for the set of seven whales. Vertical shifts in the data points would indicate temporal shifts in waiting time distribution.

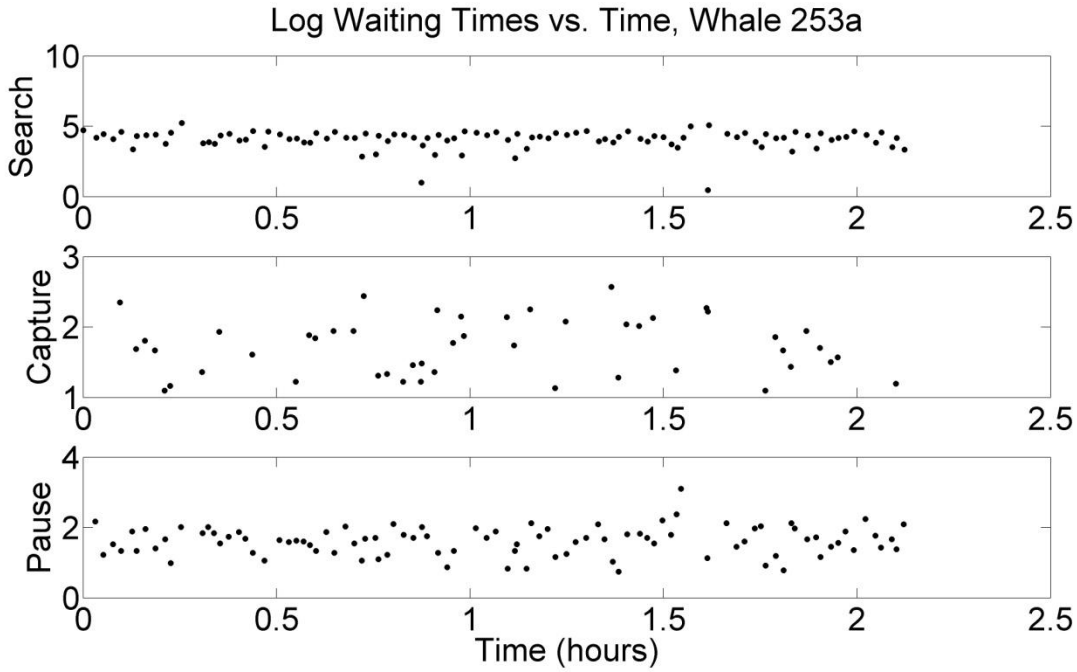

Figure 5.14. Logarithm of waiting time as a function of event time for whale 253a. Vertical shifts in the data points would indicate temporal shifts in waiting time distribution.

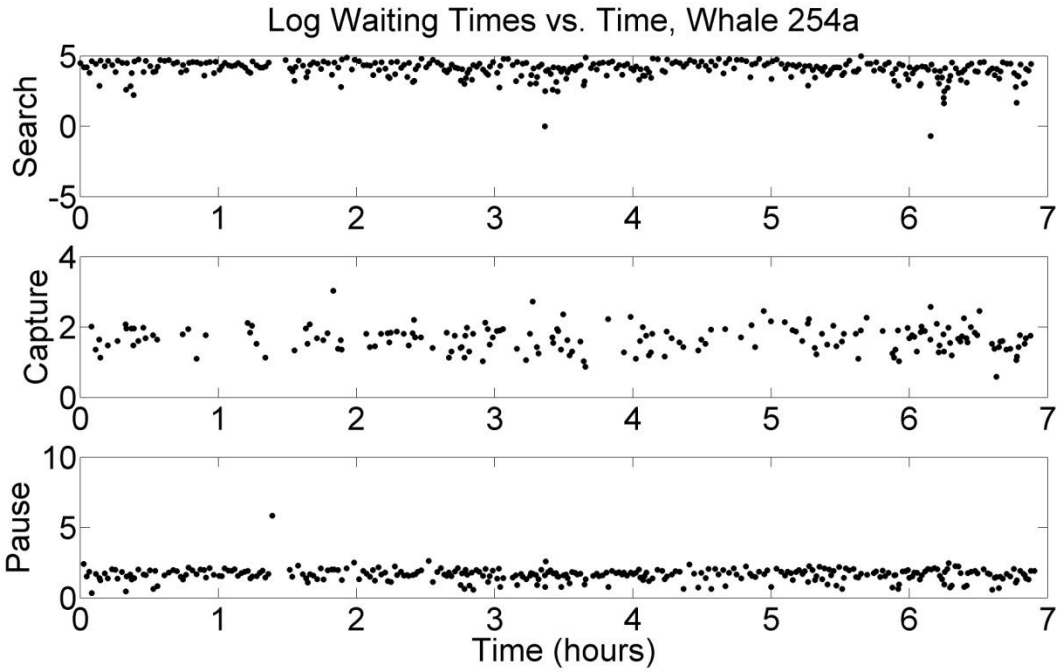

Figure 5.15. Logarithm of waiting time as a function of event time for whale 254a. Vertical shifts in the data points would indicate temporal shifts in waiting time distribution.

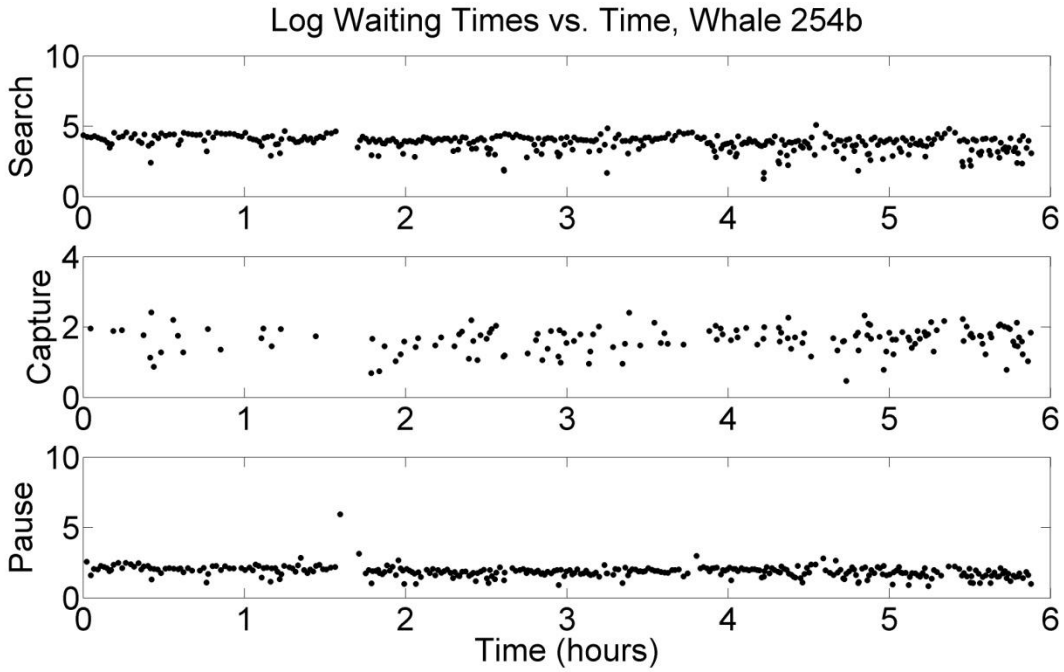

Figure 5.16. Logarithm of waiting time as a function of event time for whale 254b. Vertical shifts in the data points would indicate temporal shifts in waiting time distribution.

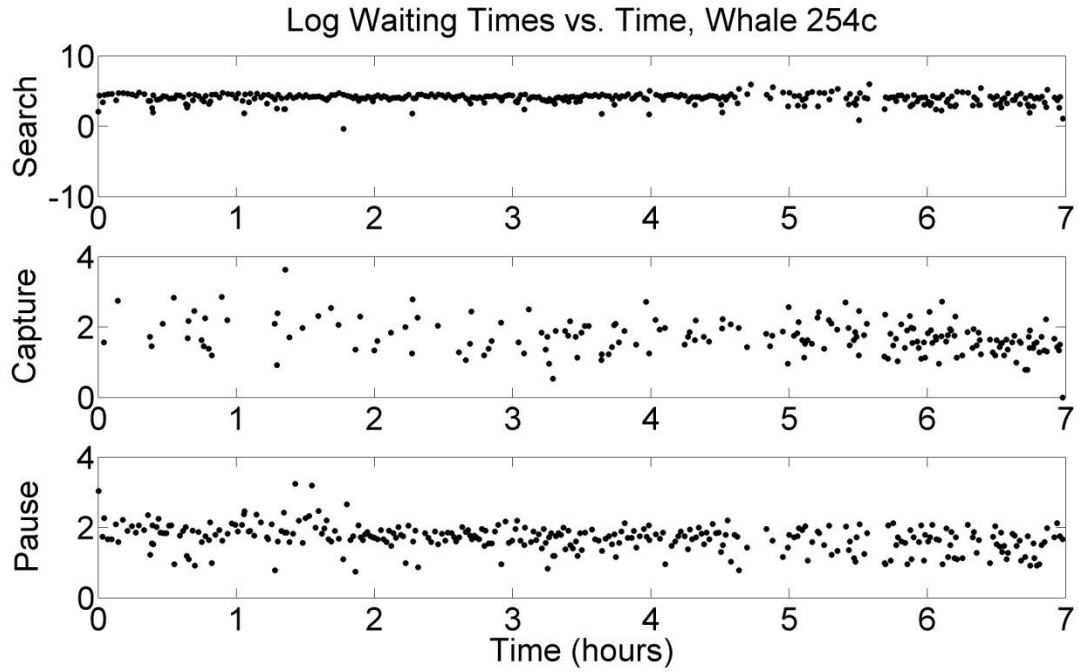

Figure 5.17. Logarithm of waiting time as a function of event time for whale 254c. Vertical shifts in the data points would indicate temporal shifts in waiting time distribution.

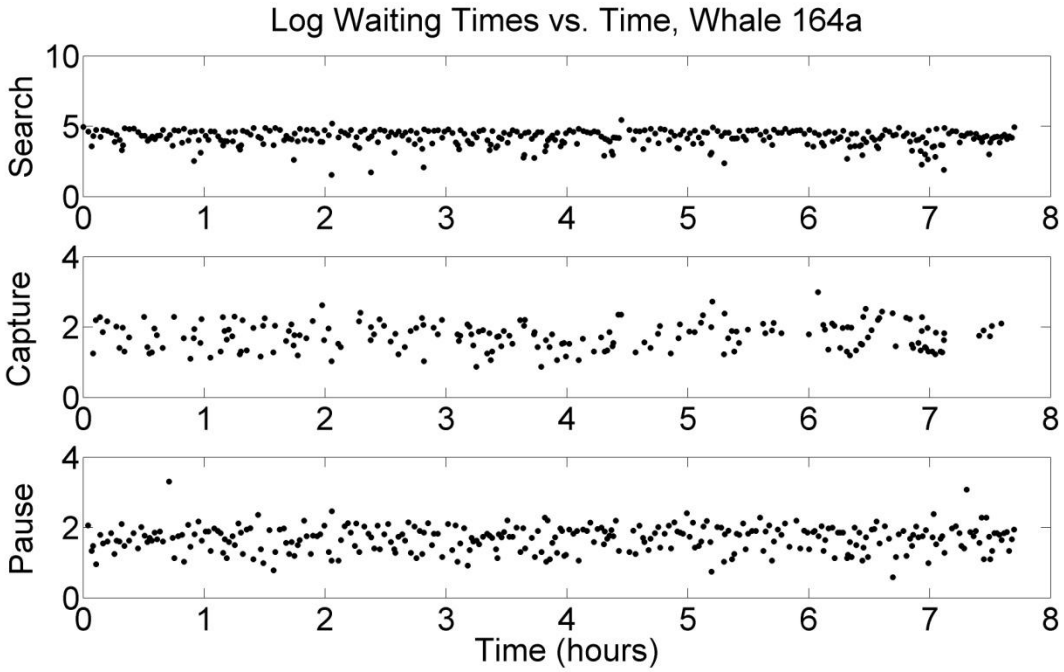

Figure 5.18. Logarithm of waiting time as a function of event time for whale 164a. Vertical shifts in the data points would indicate temporal shifts in waiting time distribution.

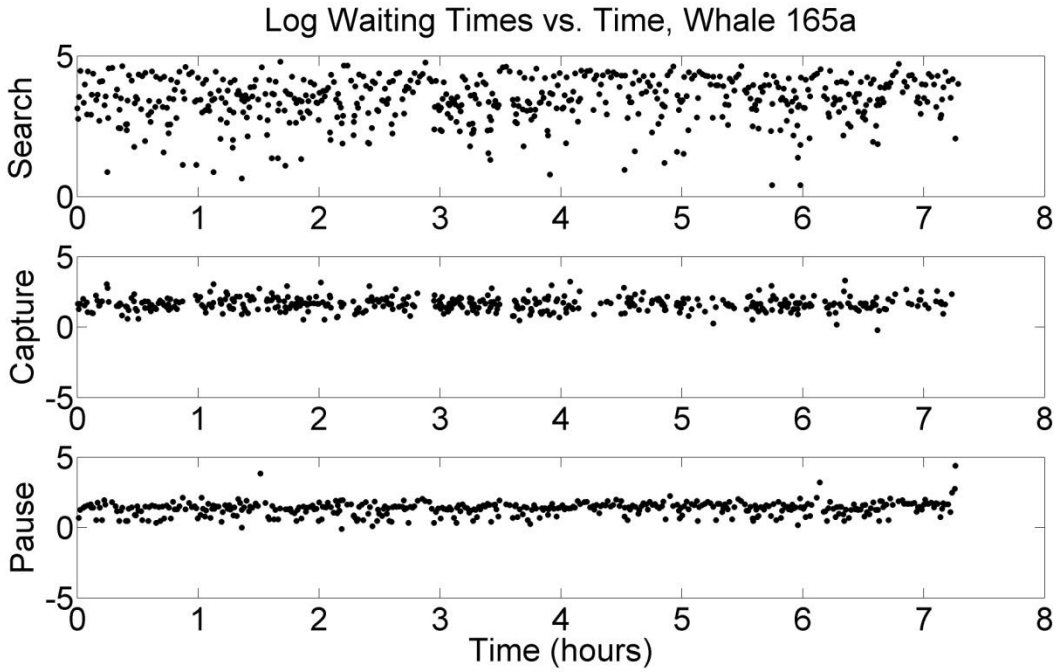

Figure 5.19. Logarithm of waiting time as a function of event time for whale 165a. Vertical shifts in the data points would indicate temporal shifts in waiting time distribution.

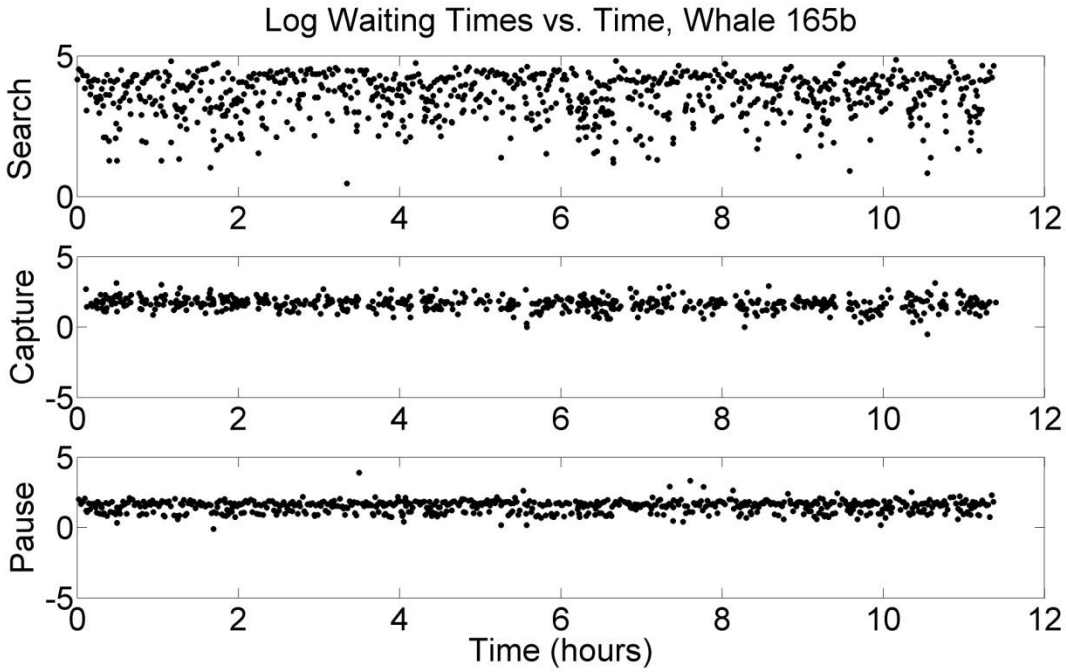

Figure 5.20. Logarithm of waiting time as a function of event time for whale 165b. Vertical shifts in the data points would indicate temporal shifts in waiting time distribution.

Figures 5.21 – 5.23 show the temporal variability in between-state transition probabilities. The figures show data from the seven analyzed whale datasets, all seven whales (considered as one dataset), and two simulated datasets synthesized under the sMC model. (The synthetic datasets had durations of seven hours, similar to the aggregate duration of the real datsets, and the model parameters used for the simulations were average values from the real datasets). In each figure, the main data points are the transition probabilities from the whole datasets. Error bars were determined by analyzing subsets of the data, and indicate the minimum and maximum values obtained by calculating transition probabilities for each possible subset of 50 consecutive states. (The choice of 50 events is arbitrary.) Figure 5.21 shows variability in transitions from search state, Figure 5.22 transitions from capture state, and Figure 5.23

transitions from pause state. In all cases, the observed temporal variability in data transition probabilities does not greatly exceed the variability observed in the synthetic datasets. These data qualitatively support the sMC model assumption that the data transition probabilities are constant with time. However, it is difficult to assess the validity of that assumption more quantitatively. Of the seven whales studied, whales 254b, 254c, and 165a show temporal variability in transition probabilities that matches or slightly exceeds than that seen in the more variable of the two simulated datasets. The assumption of time-homogeneous transition probabilities is not as well-supported for those three whales.

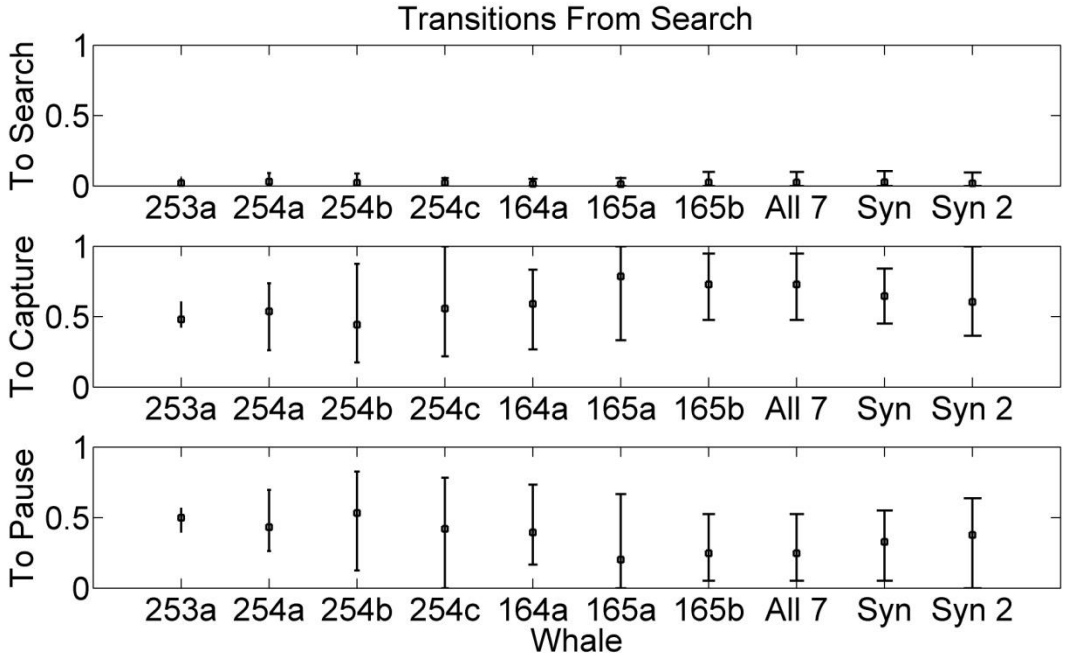

Figure 5.21. Variability in the probability of transition from search state to search, capture, or pause states. Data are shown for the seven individual whale datasets analyzed, all seven whales considered as one dataset, and two synthetic datasets of similar duration synthesized under the sMC model.

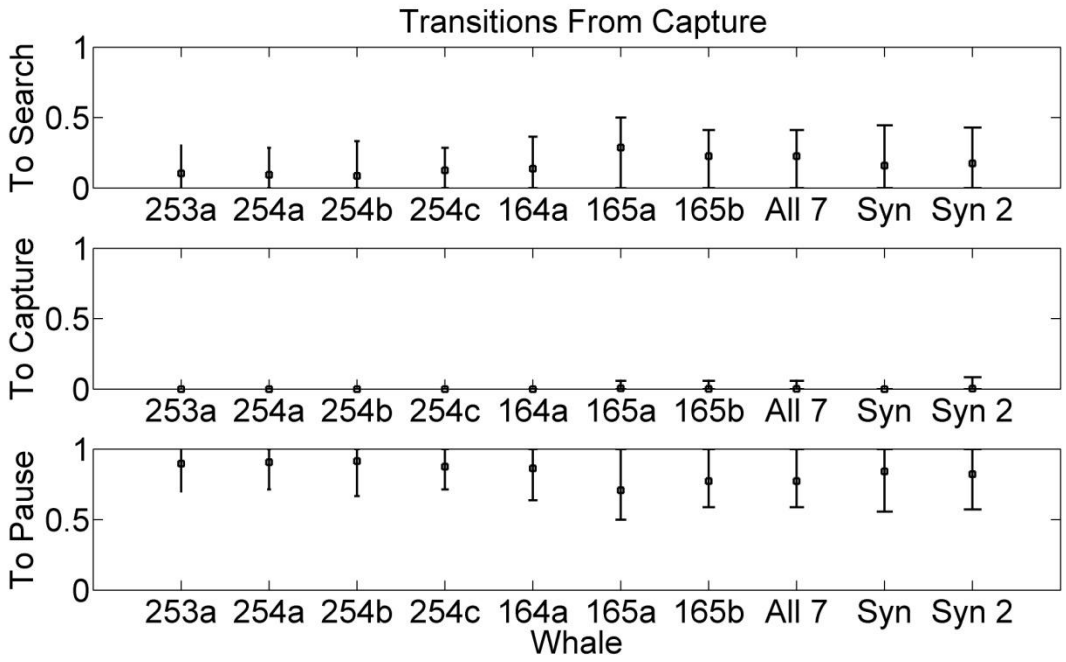

Figure 5.22. Variability in the probability of transition from capture state to search, capture or pause states. Data are shown for the seven individual whale datasets analyzed, all seven whales considered as one dataset, and two synthetic datasets of similar duration synthesized under the sMC model.

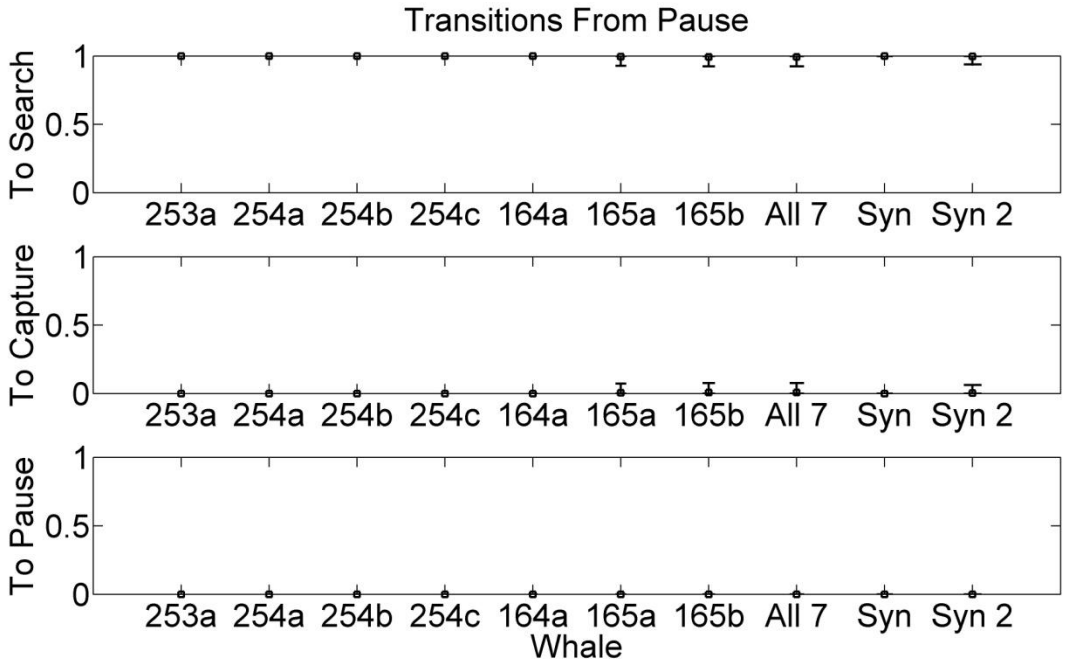

Figure 5.23. Variability in the probability of transition from pause state to search, capture, or pause states. Data are shown for the seven individual whale datasets analyzed, all seven whales considered as one dataset, and two synthetic datasets of similar duration synthesized under the sMC model. (Pause to pause transition probability is always zero, in both real and simulated datasets.)

Table 5.2 shows the maximized log-likelihoods of the seven datasets under the null hypothesis that whale behavior is the same during airgun exposure and control conditions. The table also indicates the percentile occupied by the data log-likelihoods in a distribution of log-likelihoods of synthetic sMC datasets synthesized for the parametric bootstrap significance assessment. If the sMC model fit the data poorly, the observed data log-likelihoods would probably be much lower than most of the synthetic-data likelihoods, occupying low percentiles (or being smaller than all the synthetic likelihoods). In fact, the data likelihoods are in the center of the synthetic likelihood distributions, indicating a relatively good fit between the sMC model and the datasets.

Whale	Log-Likelihood (null)	Percentile
1 (253a)	-892.7	56
2 (254a)	-3177	50
3 (254b)	-3143	54
4 (254c)	-3204	54
5 (164a)	-3075	53
6 (165a)	-5087	51
7 (165b)	-7168	50

Table 5.2. Maximized log-likelihoods of the seven datasets under the null hypothesis (whale behavior is the same during airgun exposure and control conditions) and percentiles occupied by the data log-likelihoods in distributions of log-likelihoods of synthetic sMC datasets synthesized for the parametric bootstrap significance assessment. If the sMC model fit the data poorly, the observed data log-likelihoods would be much lower than most of the synthetic-data likelihoods, occupying low percentiles.

5.3.3 sMC Model Results

Table 5.3 shows the p-values obtained using the sMC model/likelihood ratio test method, both for the parametric bootstrap and the rotation test. The tests indicated very clearly ($p = 0.0016$ or less) that foraging behavior varied from individual to individual, and that mean model parameters (determined by averaging over data from all 7 whales) described individual behavior very poorly compared to parameters fit for each individual whale. Consequently, I tested for effects of airgun exposure using a model that allowed model parameters to vary from whale to whale.

All group tests indicated that whale behavior was significantly different during airgun exposure and control periods. The p-values for the rotation tests were all higher than those obtained with the parametric bootstrap. Even referring

to the rotation test results, however, two of the seven whales (254b, p = 0.040 and 254c, p = 0.025) showed a significant change in foraging behavior during airgun exposure, and one more showed a marginally significant response (whale 165b, p = 0.082). Application of Fisher's test indicated that at least one of the observed significant results remains significant at the p = 0.05 level after correcting for the effects of applying multiple statistical tests (p = 0.028). In addition, the test for a concerted change by all seven whales returned a significant p-value of 0.046.

Hypothesis Tested	**p-value (parametric bootstrap)**	**p-value (rotation)**
Individual Variation between 7 whales?	0	0.0016
Individual Whales: Changes during airgun exposure?		
1 (253a)	0.08	0.44
2 (254a)	0.005	0.37
3 (254b)	0	0.04
4 (254c)	0	0.025
5 (164a)	0.22	0.29
6 (165a)	0.042	0.65
7 (165b)	0.0012	0.082
Group of 7 whales		
Fisher's Method	0	0.028
Concerted Change	0	0.046

Table 5.3. Results of hypothesis tests (significance assessed by likelihood ratio test/parametric bootstrap).

Figures 5.24 – 5.30 show the gamma distributions that best fit the waiting time data for each whale during airgun exposure and control conditions, along with the range of those distributions expected under the null hypothesis (as determined by the parametric bootstrap). Figures 5.31 – 5.37 show the same data, but with expected distributions determined by the rotation method. For whales 254b, 254c, and 165b, which showed significant or marginally significant behavior changes in response to airguns, the most notable changes in waiting times were increases in waiting times in search and capture states, reductions in pause waiting times (especially 254b), and increased variability in capture and pause waiting times.

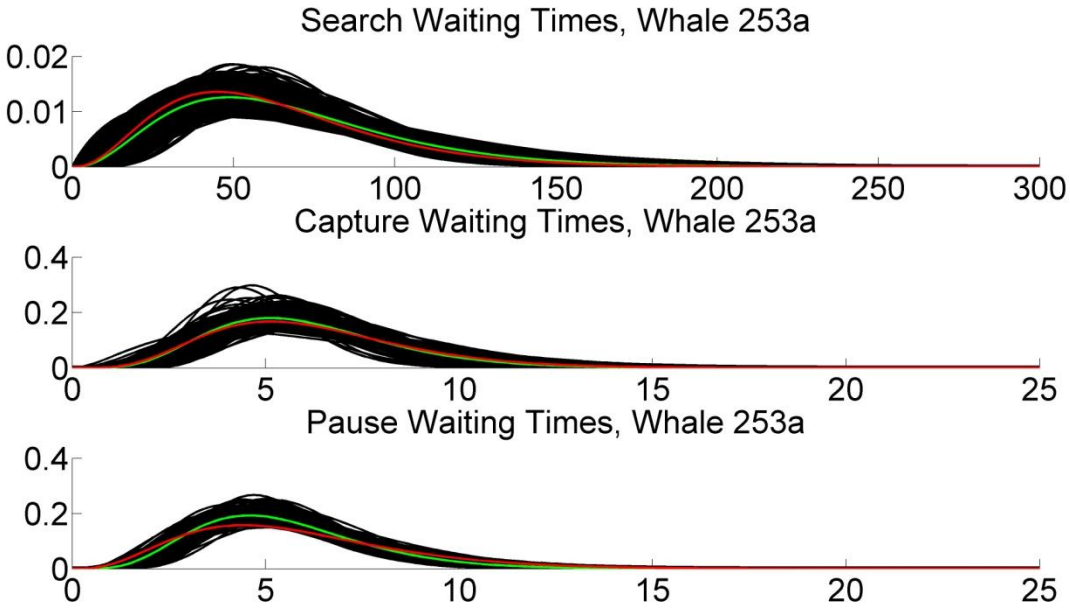

Figure 5.24. Changes in waiting times during airgun exposure for whale 253a. All x axes show time in seconds, and y axes probability. Green lines are the gamma distributions that best fit the waiting time data under the null hypothesis, and red lines are those that best fit the data from the airgun exposure period. Black lines show the expected variability of the airgun exposure line under the null hypothesis of no airgun effect, as determined by parametric bootstrap simulations (1000 of 10,000 simulation results plotted).

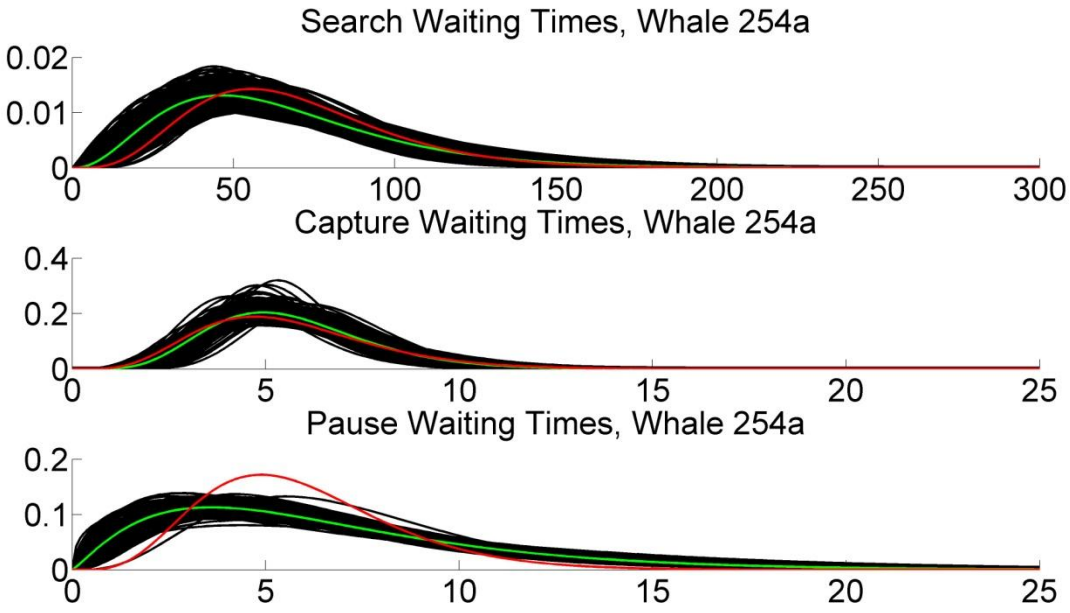

Figure 5.25. Changes in waiting times during airgun exposure for whale 254a. All x axes show time in seconds, and y axes probability. Green lines are the gamma distributions that best fit the waiting time data under the null hypothesis, and red lines are those that best fit the data from the airgun exposure period. Black lines show the expected variability of the airgun exposure line under the null hypothesis of no airgun effect, as determined by parametric bootstrap simulations (1000 of 10,000 simulation results plotted).

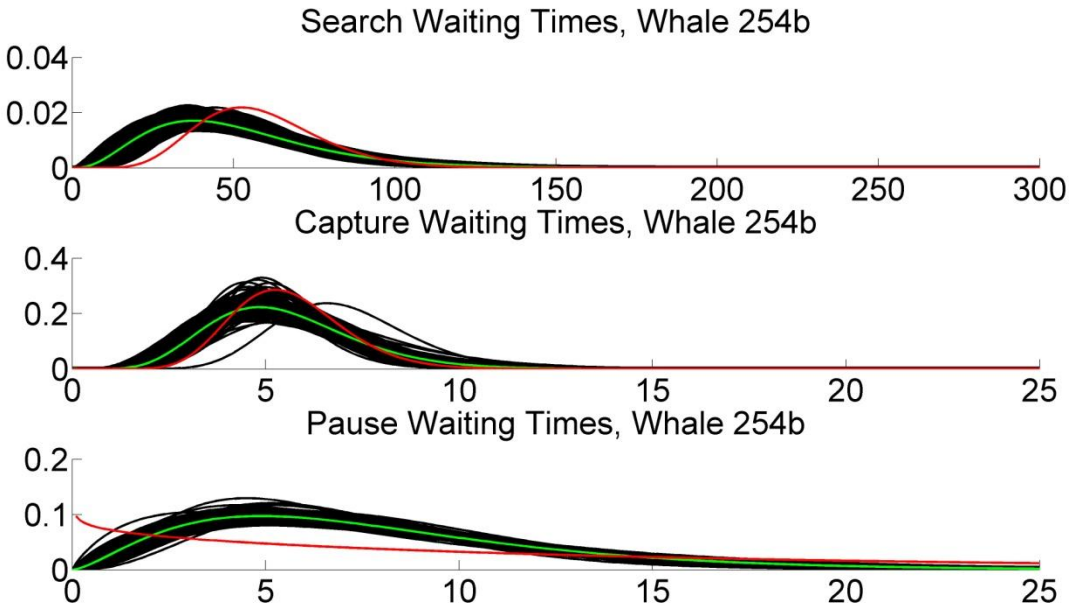

Figure 5.26. Changes in waiting times during airgun exposure for whale 254b. All x axes show time in seconds, and y axes probability. Green lines are the gamma distributions that best fit the waiting time data under the null hypothesis, and red lines are those that best fit the data from the airgun exposure period. Black lines show the expected variability of the airgun exposure line under the null hypothesis of no airgun effect, as determined by parametric bootstrap simulations (1000 of 10,000 simulation results plotted).

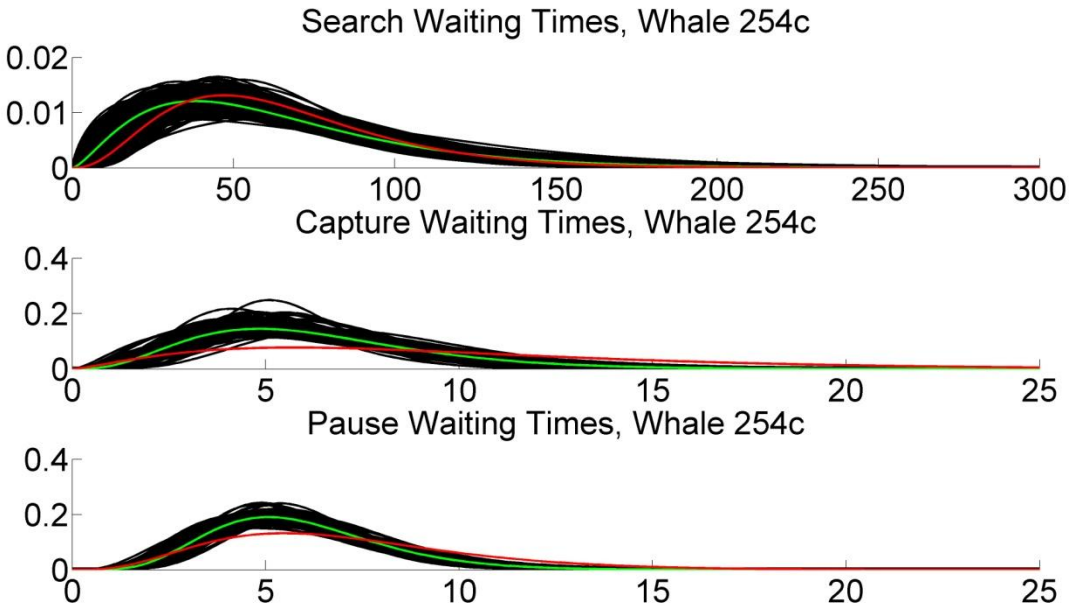

Figure 5.27. Changes in waiting times during airgun exposure for whale 254c. All x axes show time in seconds, and y axes probability. Green lines are the gamma distributions that best fit the waiting time data under the null hypothesis, and red lines are those that best fit the data from the airgun exposure period. Black lines show the expected variability of the airgun exposure line under the null hypothesis of no airgun effect, as determined by parametric bootstrap simulations (1000 of 10,000 simulation results plotted).

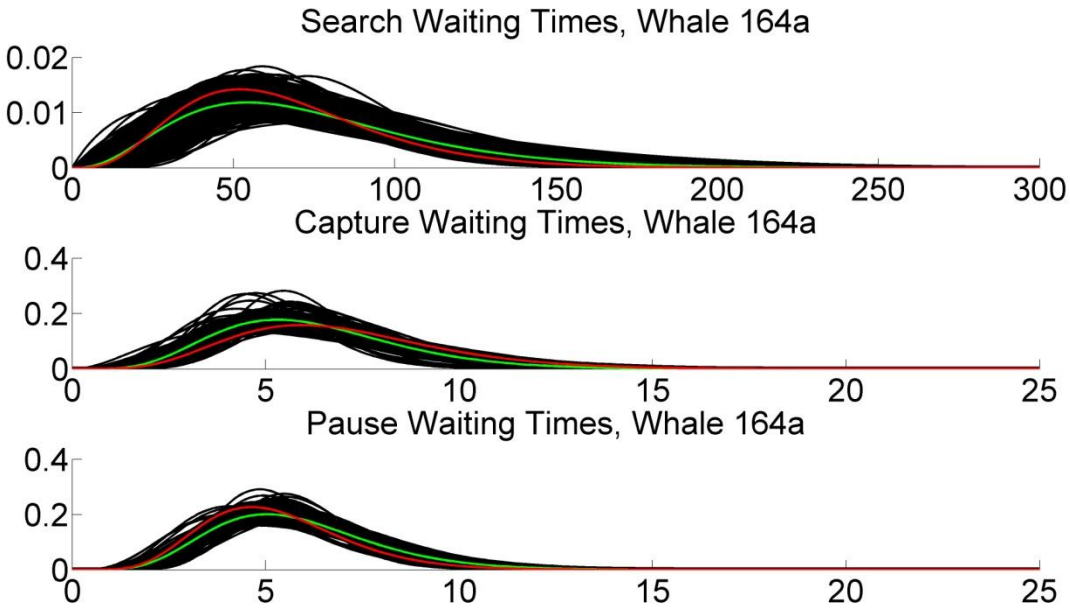

Figure 5.28. Changes in waiting times during airgun exposure for whale 164a. All x axes show time in seconds, and y axes probability. Green lines are the gamma distributions that best fit the waiting time data under the null hypothesis, and red lines are those that best fit the data from the airgun exposure period. Black lines show the expected variability of the airgun exposure line under the null hypothesis of no airgun effect, as determined by parametric bootstrap simulations (1000 of 10,000 simulation results plotted).

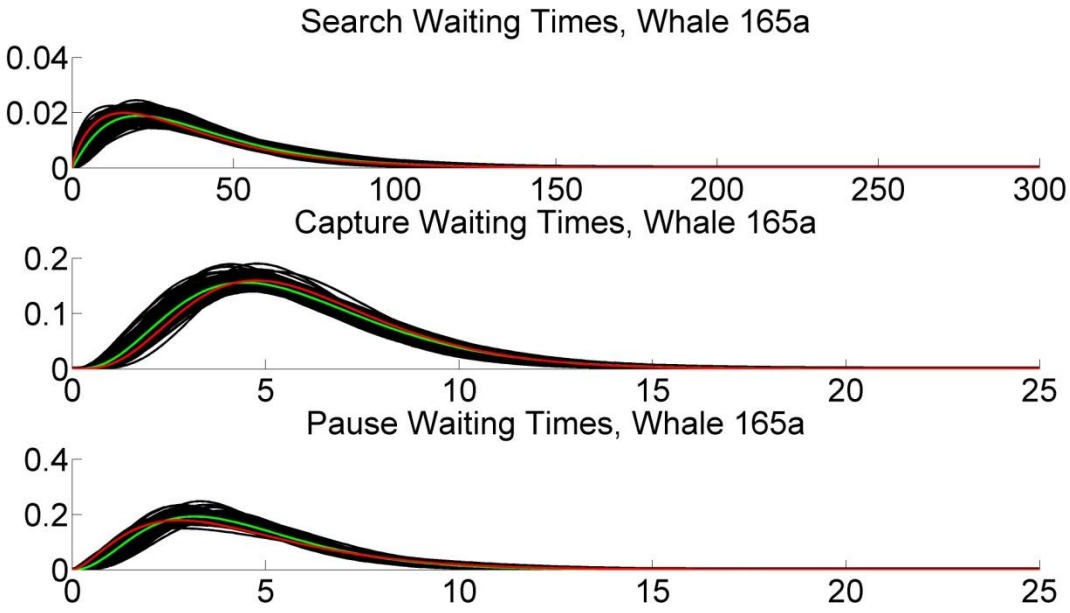

Figure 5.29. Changes in waiting times during airgun exposure for whale 165a. All x axes show time in seconds, and y axes probability. Green lines are the gamma distributions that best fit the waiting time data under the null hypothesis, and red lines are those that best fit the data from the airgun exposure period. Black lines show the expected variability of the airgun exposure line under the null hypothesis of no airgun effect, as determined by parametric bootstrap simulations (1000 of 10,000 simulation results plotted).

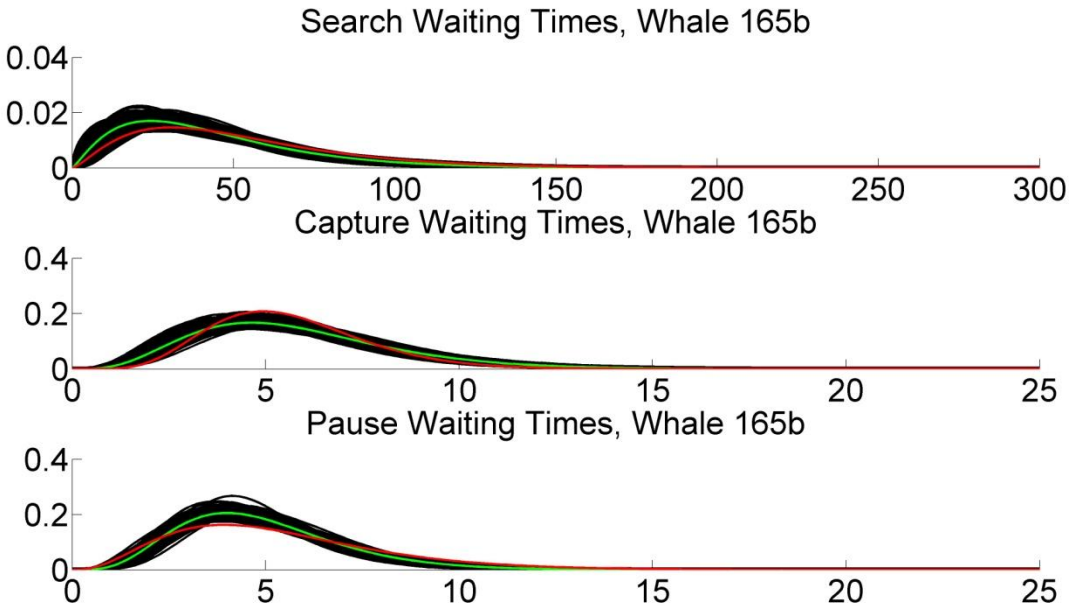

Figure 5.30. Changes in waiting times during airgun exposure for whale 165b. All x axes show time in seconds, and y axes probability. Green lines are the gamma distributions that best fit the waiting time data under the null hypothesis, and red lines are those that best fit the data from the airgun exposure period. Black lines show the expected variability of the airgun exposure line under the null hypothesis of no airgun effect, as determined by parametric bootstrap simulations (1000 of 10,000 simulation results plotted).

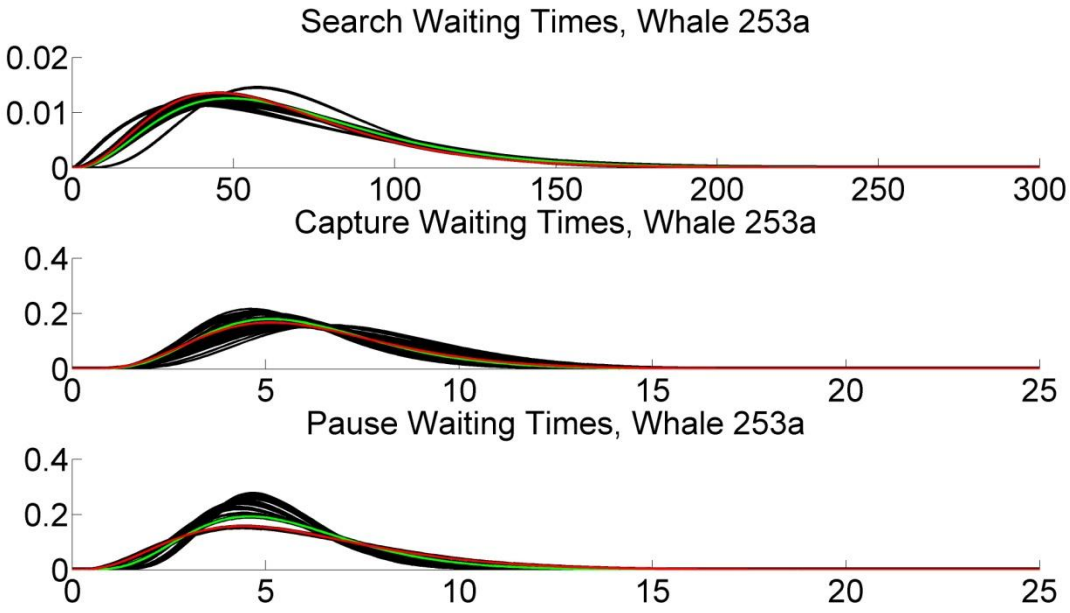

Figure 5.31. Changes in waiting times during airgun exposure for whale 253a. All x axes show time in seconds, and y axes probability. Green lines are the gamma distributions that best fit the waiting time data under the null hypothesis, and red lines are those that best fit the data from the airgun exposure period. Black lines show the expected variability of the airgun exposure line under the null hypothesis of no airgun effect, as determined by rotation test data resampling (1000 of 10,000 simulation results plotted).

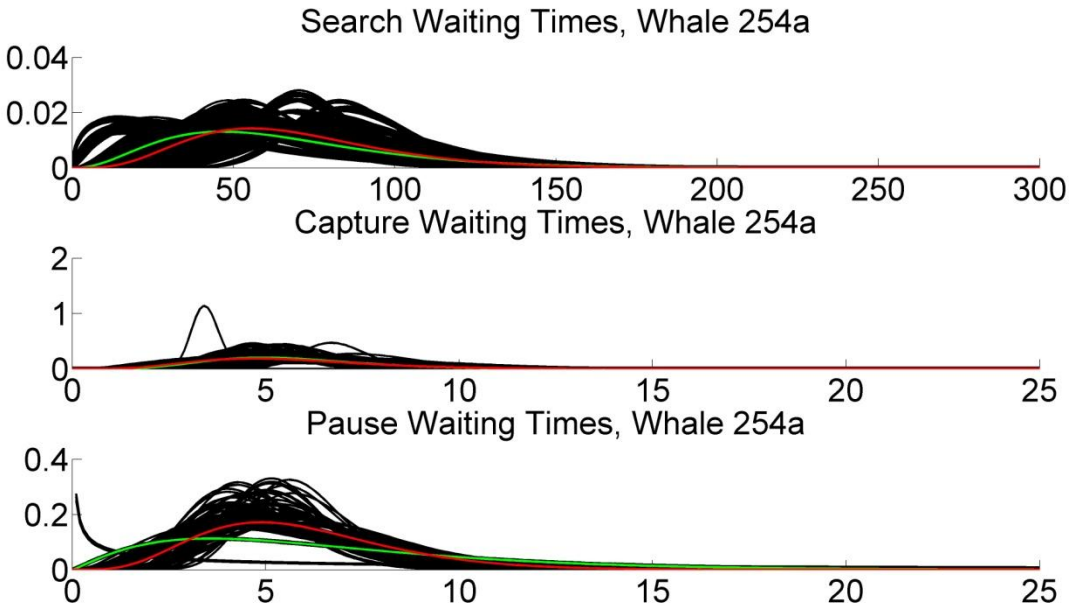

Figure 5.32. Changes in waiting times during airgun exposure for whale 254a. All x axes show time in seconds, and y axes probability. Green lines are the gamma distributions that best fit the waiting time data under the null hypothesis, and red lines are those that best fit the data from the airgun exposure period. Black lines show the expected variability of the airgun exposure line under the null hypothesis of no airgun effect, as determined by rotation test data resampling (1000 of 10,000 simulation results plotted).

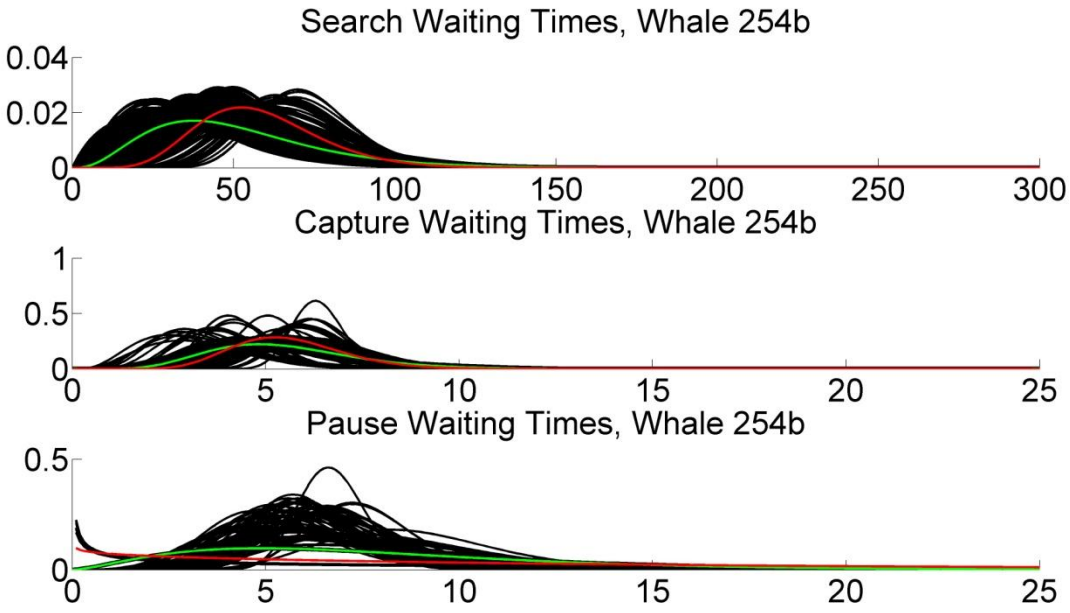

Figure 5.33. Changes in waiting times during airgun exposure for whale 254b. All x axes show time in seconds, and y axes probability. Green lines are the gamma distributions that best fit the waiting time data under the null hypothesis, and red lines are those that best fit the data from the airgun exposure period. Black lines show the expected variability of the airgun exposure line under the null hypothesis of no airgun effect, as determined by rotation test data resampling (1000 of 10,000 simulation results plotted).

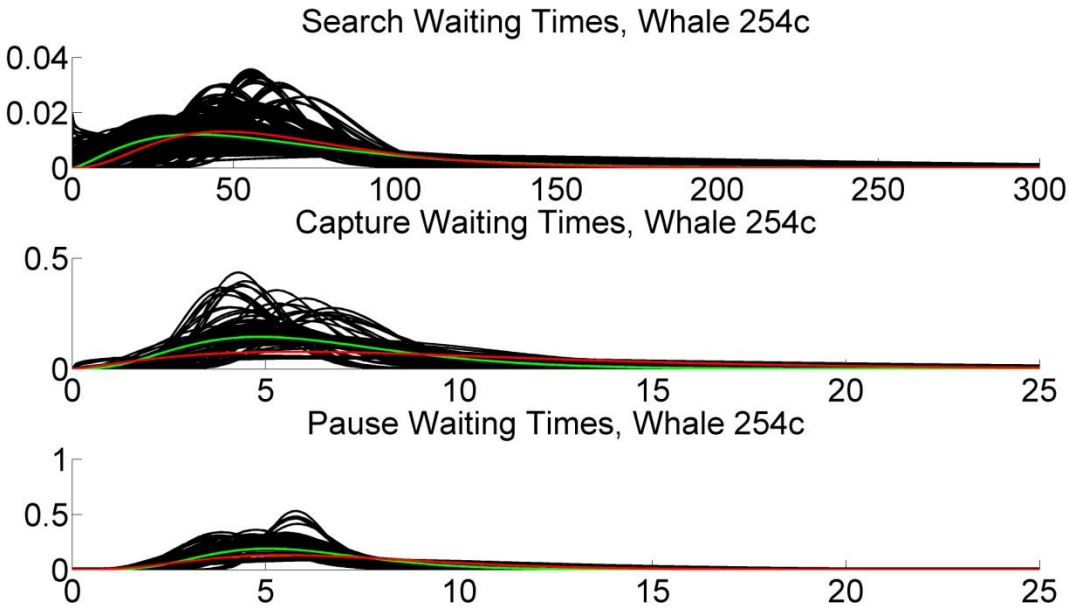

Figure 5.34. Changes in waiting times during airgun exposure for whale 254c. All x axes show time in seconds, and y axes probability. Green lines are the gamma distributions that best fit the waiting time data under the null hypothesis, and red lines are those that best fit the data from the airgun exposure period. Black lines show the expected variability of the airgun exposure line under the null hypothesis of no airgun effect, as determined by rotation test data resampling (1000 of 10,000 simulation results plotted).

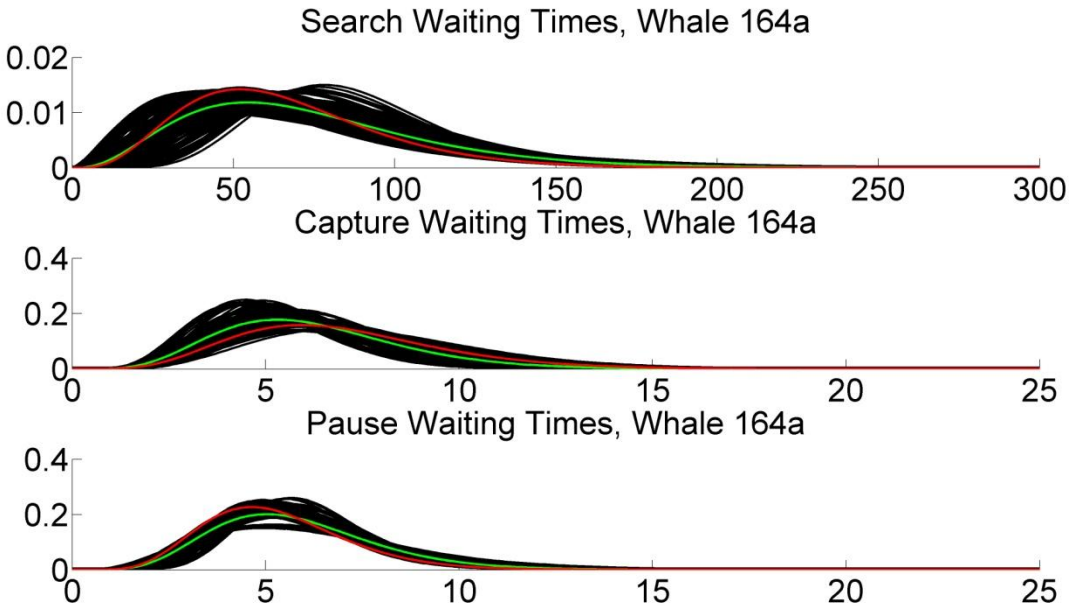

Figure 5.35. Changes in waiting times during airgun exposure for whale 164a. All x axes show time in seconds, and y axes probability. Green lines are the gamma distributions that best fit the waiting time data under the null hypothesis, and red lines are those that best fit the data from the airgun exposure period. Black lines show the expected variability of the airgun exposure line under the null hypothesis of no airgun effect, as determined by rotation test data resampling (1000 of 10,000 simulation results plotted).

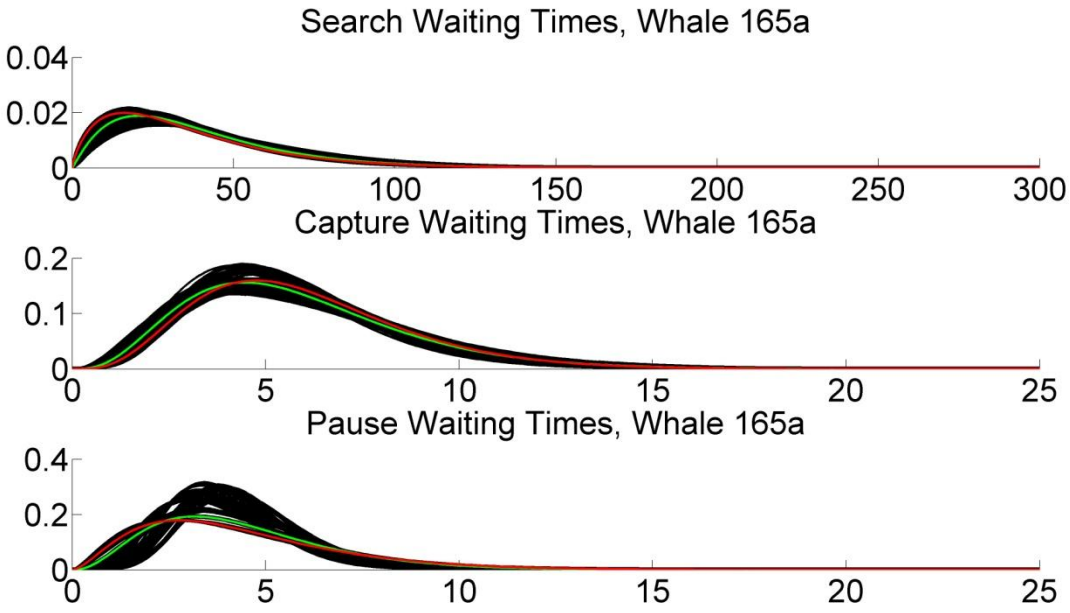

Figure 5.36. Changes in waiting times during airgun exposure for whale 165a. All x axes show time in seconds, and y axes probability. Green lines are the gamma distributions that best fit the waiting time data under the null hypothesis, and red lines are those that best fit the data from the airgun exposure period. Black lines show the expected variability of the airgun exposure line under the null hypothesis of no airgun effect, as determined by rotation test data resampling (1000 of 10,000 simulation results plotted).

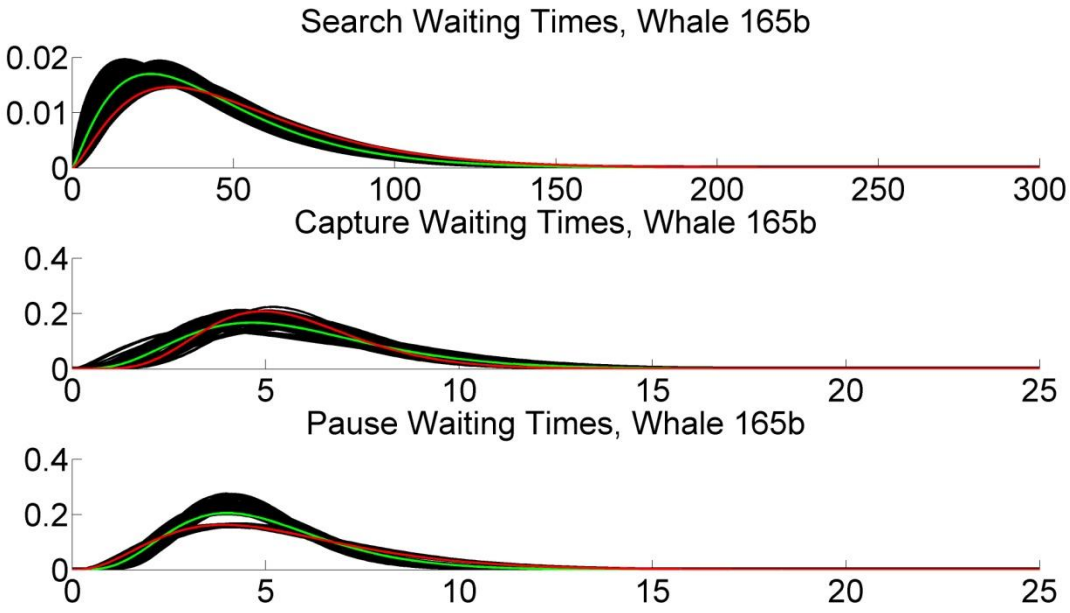

Figure 5.37. Changes in waiting times during airgun exposure for whale 165b. All x axes show time in seconds, and y axes probability. Green lines are the gamma distributions that best fit the waiting time data under the null hypothesis, and red lines are those that best fit the data from the airgun exposure period. Black lines show the expected variability of the airgun exposure line under the null hypothesis of no airgun effect, as determined by rotation test data resampling (1000 of 10,000 simulation results plotted).

Figures 5.38 – 5.44 and 5.45 – 5.51 plot the observed changes in transition probabilities during airgun exposure periods, with error bars indicating expected values under the null hypothesis as determined by the parametric bootstrap and rotations, respectively. For whales 254b, 254c, and 165b, which responded significantly or marginally significantly to airgun exposure, the most notable changes in transition probabilities were as follows: capture to search transitions were replaced by capture to pause transitions during exposure, and search to capture transitions were replaced by search to pause transitions.

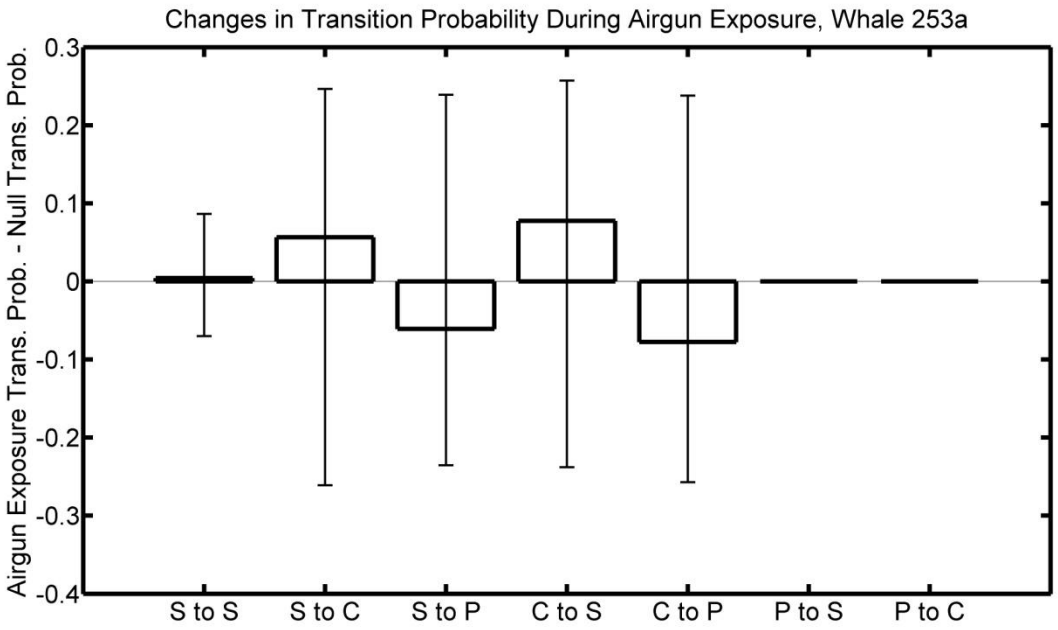

Figure 5.38. Changes in transition probabilities during airgun exposure for whale 253a. S stands for search, C for capture, and P for pause. Bar heights indicate observed difference between transition probabilities calculated for the airgun exposure period only and for the entire experiment (under the null hypothesis). Error bars show the maximum and minimum observed differences obtained in 10,000 parametric bootstrap simulations under the null hypothesis of no airgun effect.

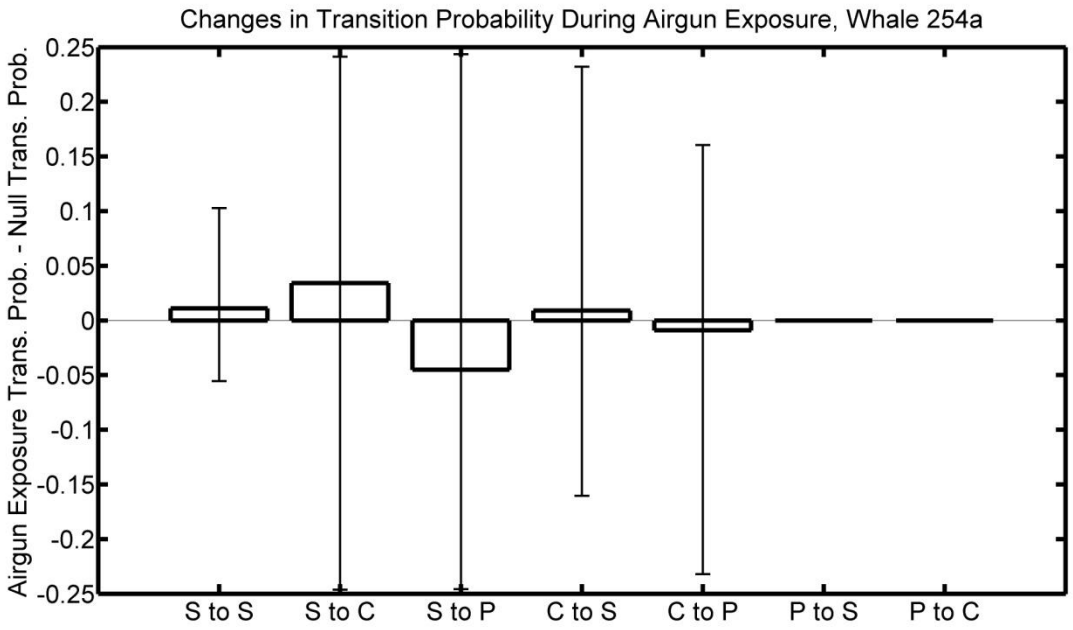

Figure 5.39. Changes in transition probabilities during airgun exposure for whale 254a. S stands for search, C for capture, and P for pause. Bar heights indicate observed difference between transition probabilities calculated for the airgun exposure period only and for the entire experiment (under the null hypothesis). Error bars show the maximum and minimum observed differences obtained in 10,000 parametric bootstrap simulations under the null hypothesis of no airgun effect.

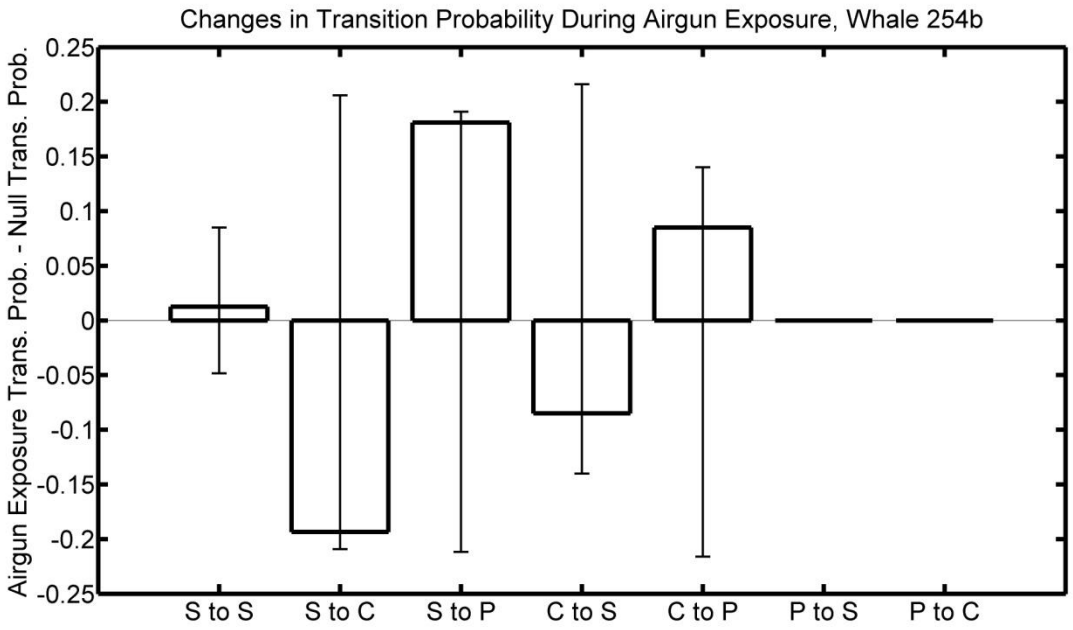

Figure 5.40. Changes in transition probabilities during airgun exposure for whale 254b. S stands for search, C for capture, and P for pause. Bar heights indicate observed difference between transition probabilities calculated for the airgun exposure period only and for the entire experiment (under the null hypothesis). Error bars show the maximum and minimum observed differences obtained in 10,000 parametric bootstrap simulations under the null hypothesis of no airgun effect.

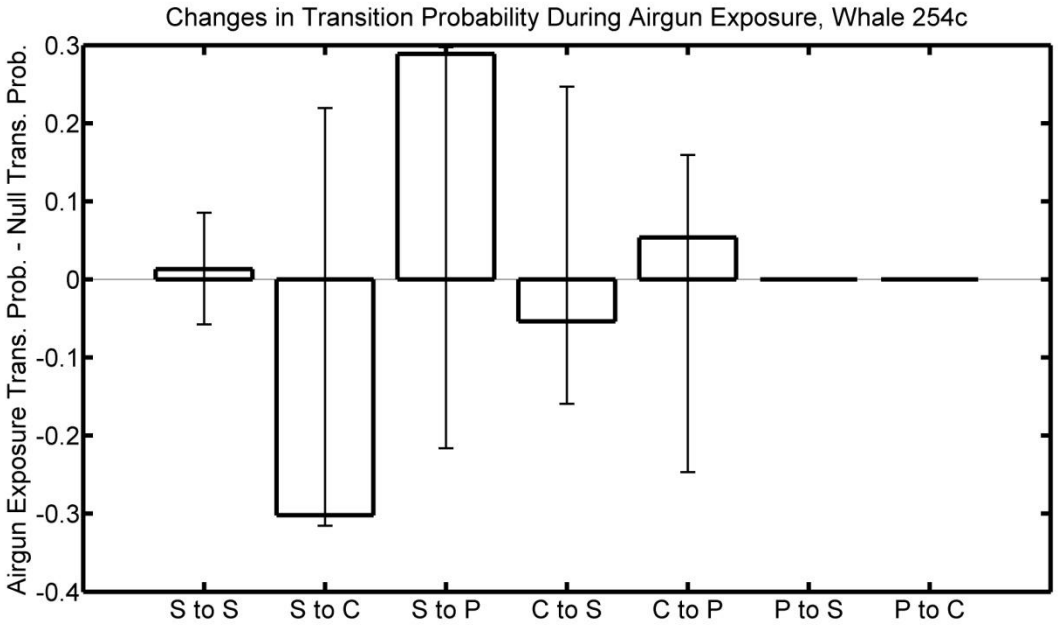

Figure 5.41. Changes in transition probabilities during airgun exposure for whale 254c. S stands for search, C for capture, and P for pause. Bar heights indicate observed difference between transition probabilities calculated for the airgun exposure period only and for the entire experiment (under the null hypothesis). Error bars show the maximum and minimum observed differences obtained in 10,000 parametric bootstrap simulations under the null hypothesis of no airgun effect.

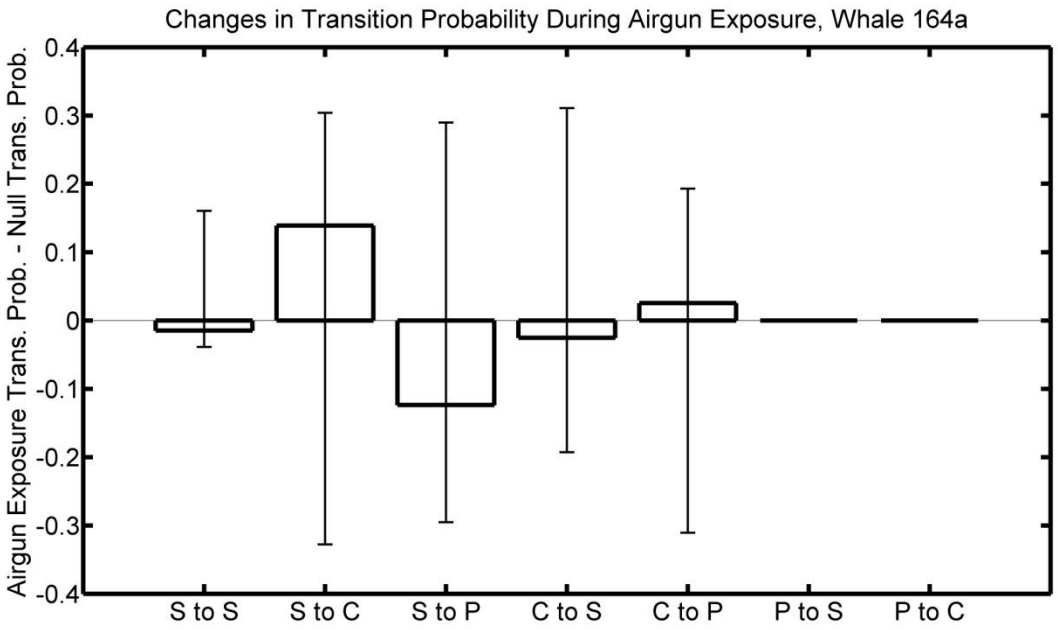

Figure 5.42. Changes in transition probabilities during airgun exposure for whale 164a. S stands for search, C for capture, and P for pause. Bar heights indicate observed difference between transition probabilities calculated for the airgun exposure period only and for the entire experiment (under the null hypothesis). Error bars show the maximum and minimum observed differences obtained in 10,000 parametric bootstrap simulations under the null hypothesis of no airgun effect.

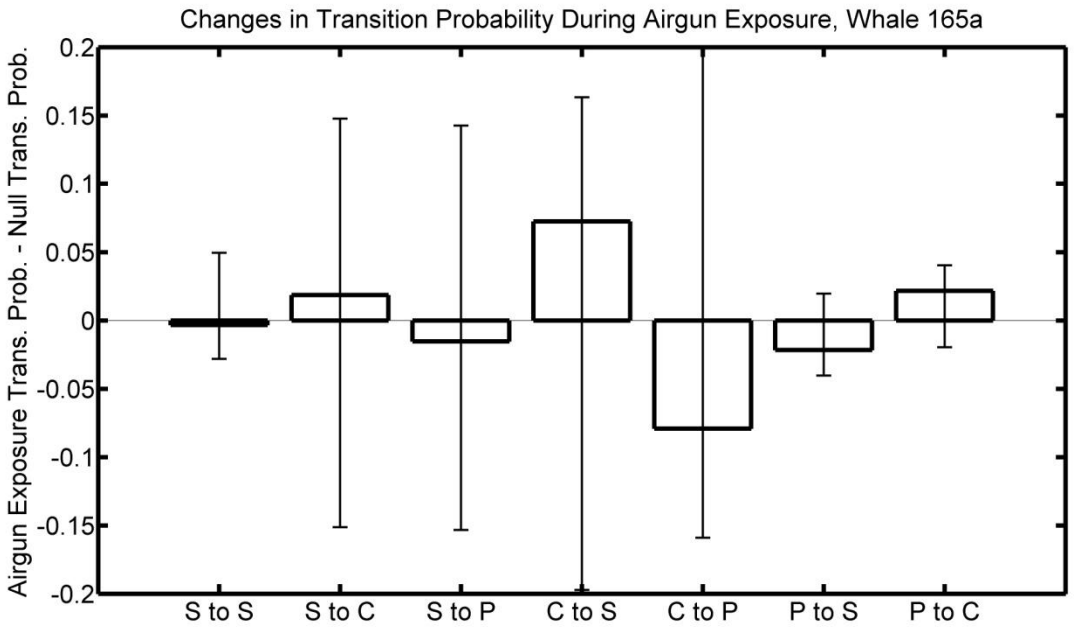

Figure 5.43. Changes in transition probabilities during airgun exposure for whale 165a. S stands for search, C for capture, and P for pause. Bar heights indicate observed difference between transition probabilities calculated for the airgun exposure period only and for the entire experiment (under the null hypothesis). Error bars show the maximum and minimum observed differences obtained in 10,000 parametric bootstrap simulations under the null hypothesis of no airgun effect.

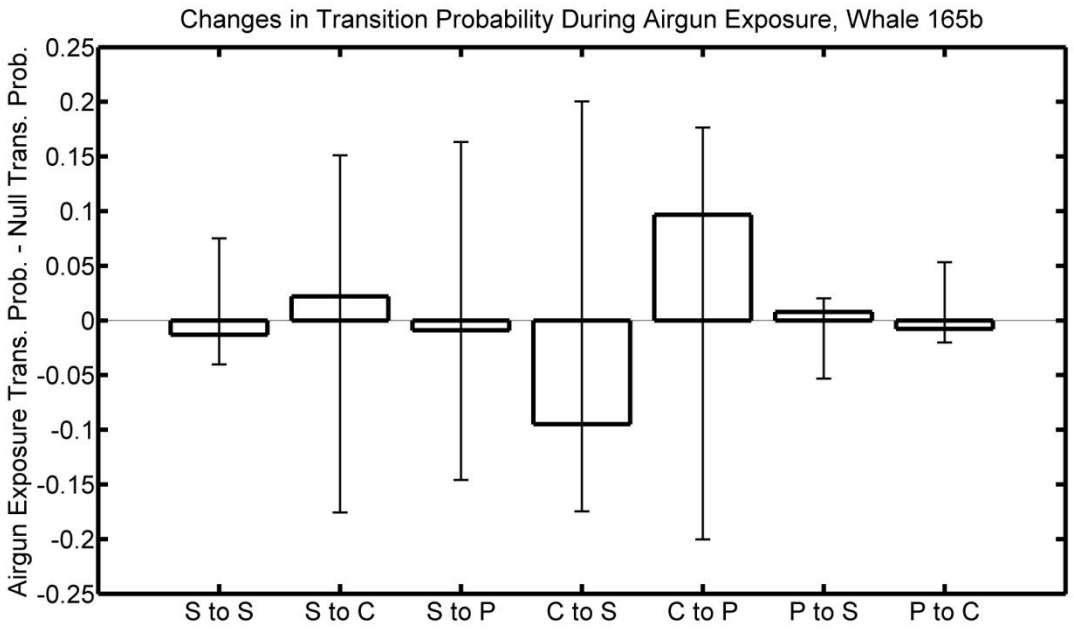

Figure 5.44. Changes in transition probabilities during airgun exposure for whale 165b. S stands for search, C for capture, and P for pause. Bar heights indicate observed difference between transition probabilities calculated for the airgun exposure period only and for the entire experiment (under the null hypothesis). Error bars show the maximum and minimum observed differences obtained in 10,000 parametric bootstrap simulations under the null hypothesis of no airgun effect.

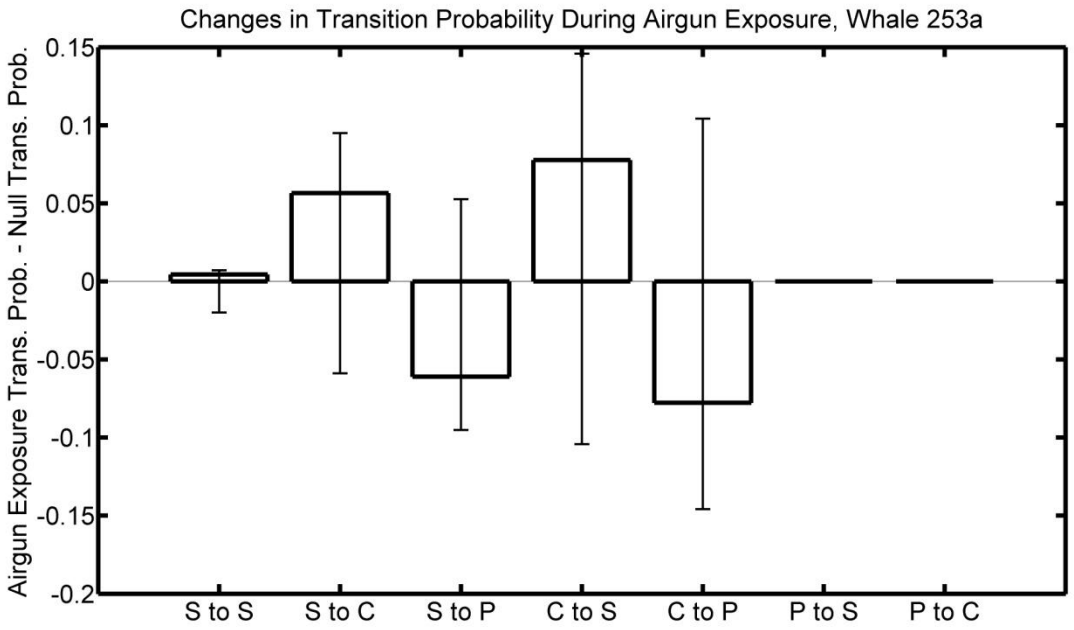

Figure 5.45. Changes in transition probabilities during airgun exposure for whale 253a. S stands for search, C for capture, and P for pause. Bar heights indicate observed difference between transition probabilities calculated for the airgun exposure period only and for the entire experiment (under the null hypothesis). Error bars show the maximum and minimum observed differences obtained in 10,000 rotation test runs under the null hypothesis of no airgun effect.

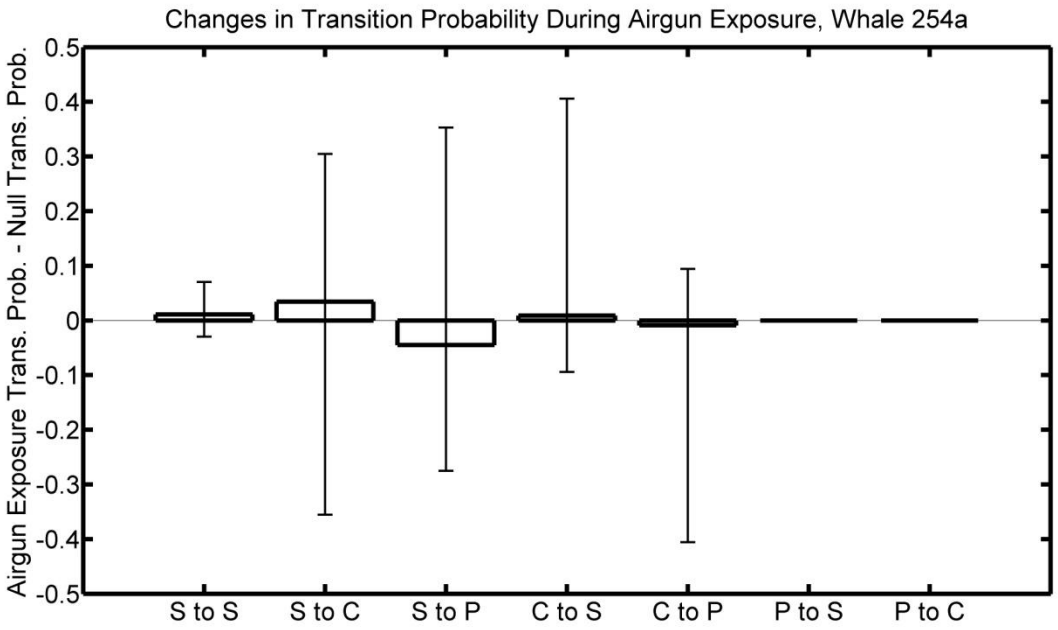

Figure 5.46. Changes in transition probabilities during airgun exposure for whale 254a. S stands for search, C for capture, and P for pause. Bar heights indicate observed difference between transition probabilities calculated for the airgun exposure period only and for the entire experiment (under the null hypothesis). Error bars show the maximum and minimum observed differences obtained in 10,000 rotation test runs under the null hypothesis of no airgun effect.

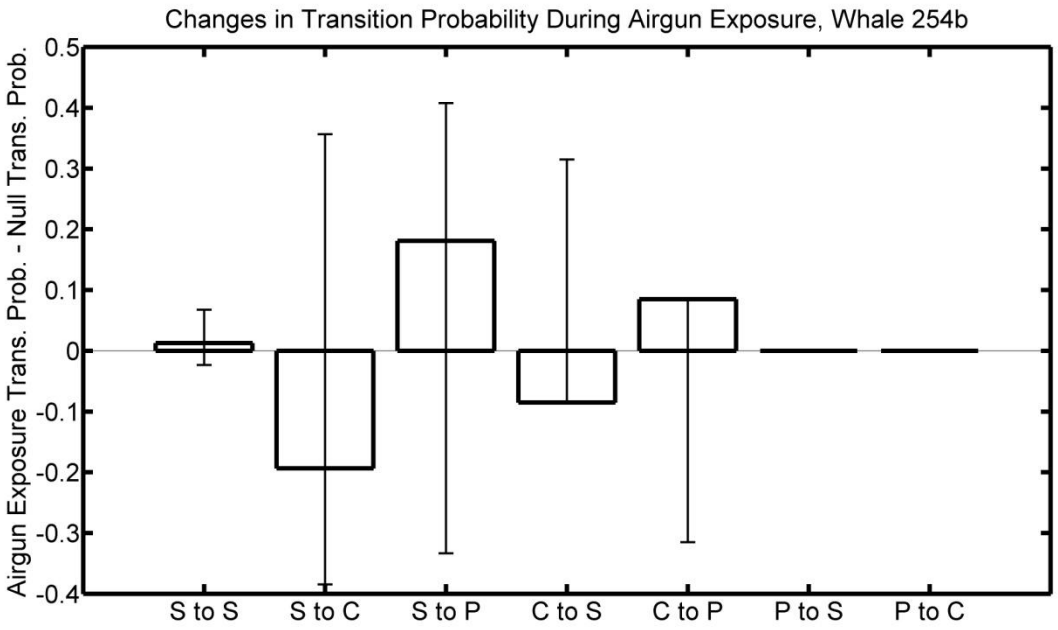

Figure 5.47. Changes in transition probabilities during airgun exposure for whale 254b. S stands for search, C for capture, and P for pause. Bar heights indicate observed difference between transition probabilities calculated for the airgun exposure period only and for the entire experiment (under the null hypothesis). Error bars show the maximum and minimum observed differences obtained in 10,000 rotation test runs under the null hypothesis of no airgun effect.

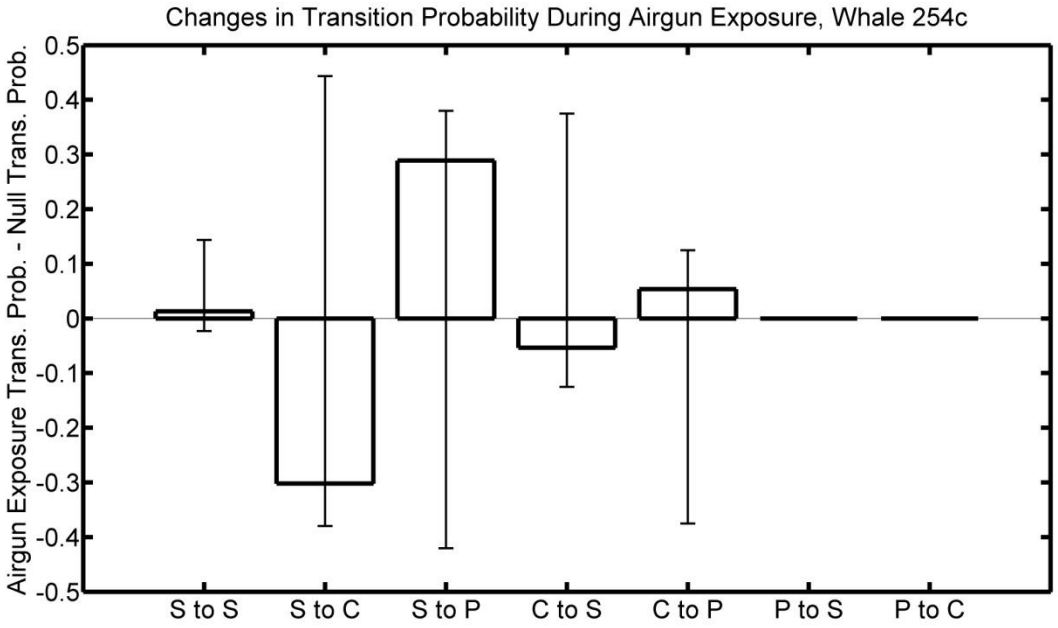

Figure 5.48. Changes in transition probabilities during airgun exposure for whale 254c. S stands for search, C for capture, and P for pause. Bar heights indicate observed difference between transition probabilities calculated for the airgun exposure period only and for the entire experiment (under the null hypothesis). Error bars show the maximum and minimum observed differences obtained in 10,000 rotation test runs under the null hypothesis of no airgun effect.

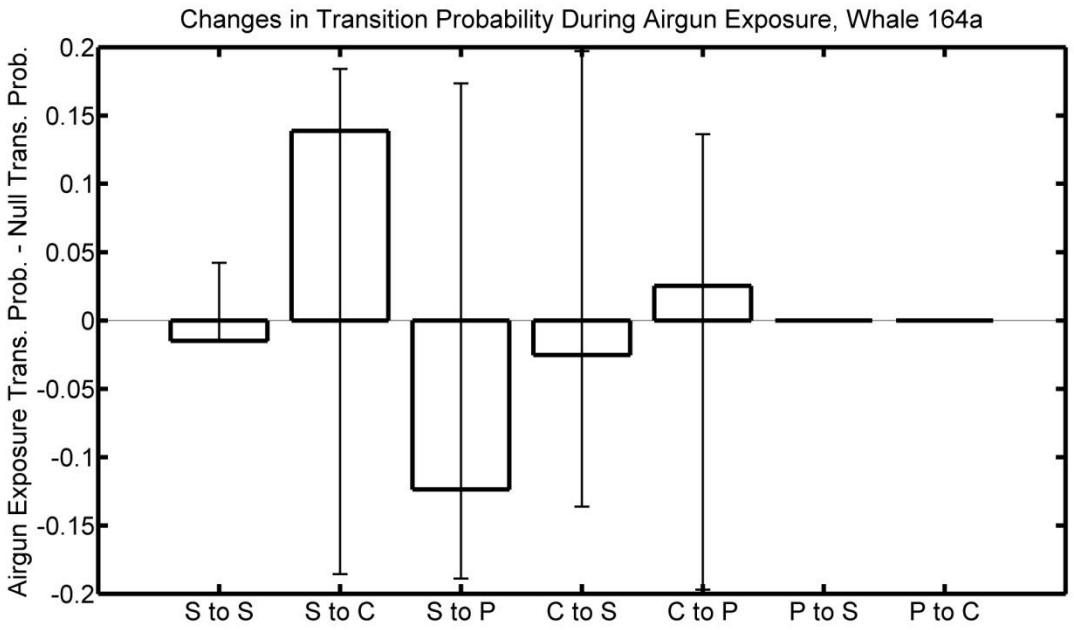

Figure 5.49. Changes in transition probabilities during airgun exposure for whale 164a. S stands for search, C for capture, and P for pause. Bar heights indicate observed difference between transition probabilities calculated for the airgun exposure period only and for the entire experiment (under the null hypothesis). Error bars show the maximum and minimum observed differences obtained in 10,000 rotation test runs under the null hypothesis of no airgun effect.

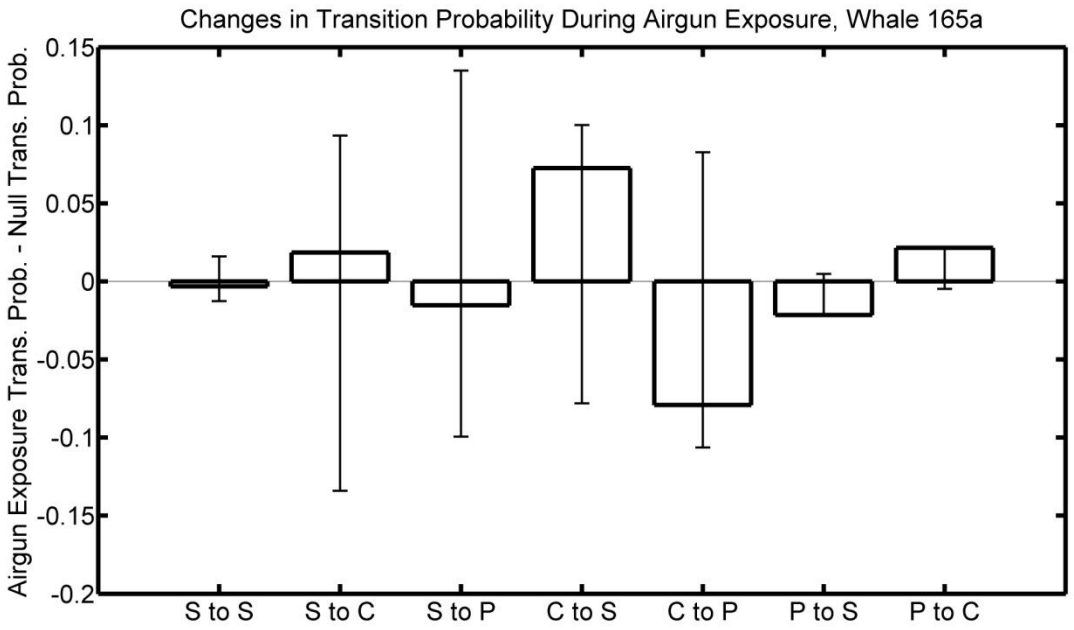

Figure 5.50. Changes in transition probabilities during airgun exposure for whale 165a. S stands for search, C for capture, and P for pause. Bar heights indicate observed difference between transition probabilities calculated for the airgun exposure period only and for the entire experiment (under the null hypothesis). Error bars show the maximum and minimum observed differences obtained in 10,000 rotation test runs under the null hypothesis of no airgun effect.

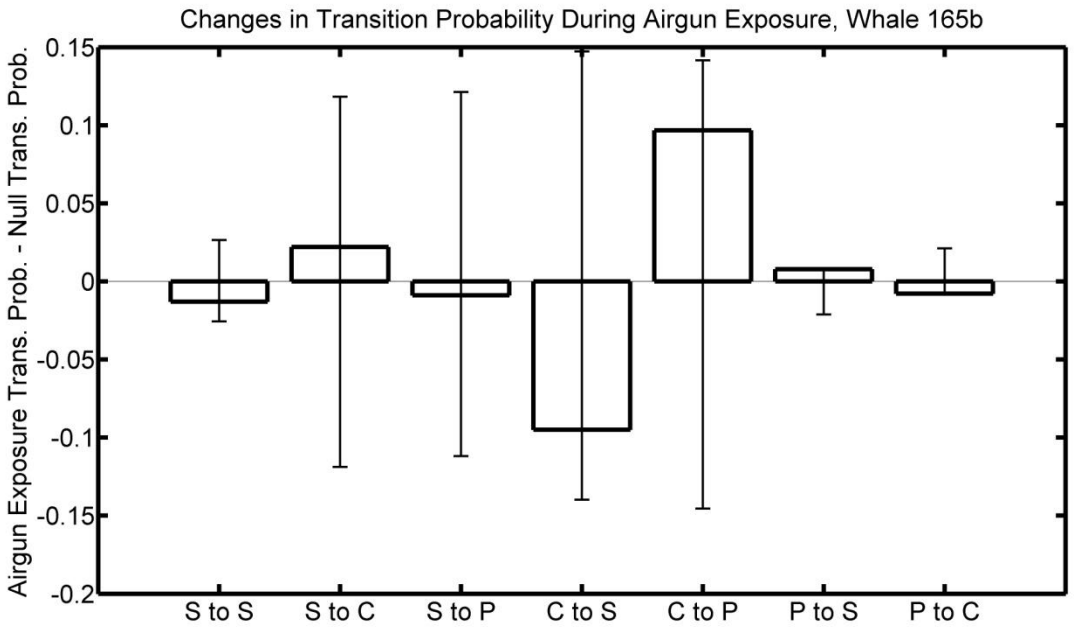

Figure 5.51. Changes in transition probabilities during airgun exposure for whale 165b. S stands for search, C for capture, and P for pause. Bar heights indicate observed difference between transition probabilities calculated for the airgun exposure period only and for the entire experiment (under the null hypothesis). Error bars show the maximum and minimum observed differences obtained in 10,000 rotation test runs under the null hypothesis of no airgun effect.

Table 5.4 shows the p-values obtained by likelihood ratio tests (with parametric bootstrap or rotation), carried out on data from sham-exposed sperm whales (which were never actually exposed to airgun sounds). The parametric bootstrap method detected significant “airgun” effects on four of six whales tested, and applying Fisher’s test ($p = 0$) indicated that the significant results were unlikely to have been simply a consequence of multiple statistical tests. On the other hand, the rotation test results were marginally significant for one of the six whales tested ($p = 0.095$), and that result could likely have been a side effect of multiple hypothesis tests (Fisher’s test, $p = 0.24$).

Whale	p-value (parametric bootstrap)	p-value (rotation test)
200a	0.0001	0.095
204a	0.49	0.82
265a	0.24	0.53
275b	0.0005	0.17
239a	0	0.16
240c	0.018	0.48
Fisher's test	0	0.24

Table 5.4. Results of significance tests (for changes in individual-whale foraging behavior in response to sham airgun exposure) on non-exposed sperm whales.

5.4 Discussion

My results indicate that airgun exposure – even at the low exposure levels observed in this experiment – can result in large reductions in foraging (buzz) rate for some individual sperm whales. A more detailed analysis of foraging behavior also indicated behavioral changes during airgun exposure, most notably increased duration of search and capture states, increased variability of capture and pause state durations, replacement of capture to search transitions with capture to pause transitions, and replacement of search to capture transitions with search to pause transitions. Overall, these changes suggest increased time and effort spent searching for and attempting to capture each prey item, and increased occurrence of pauses. Post-capture pauses during echolocation may be used for prey-handling in some bat species (Acharya and Fenton, 1992; Britton and Jones, 1999; Surlykke *et al.*, 2003). If the same is true for sperm whales, the increased number of transitions into pause state during airgun exposure may indicate increased time spent manipulating and handling prey or possibly increased prey capture success rate. However, as described in Chapter 2 of this thesis, post-buzz pauses do not seem to play a critical role in post-

capture prey handling for porpoises; they handle and swallow prey while producing echolocation buzzes in some cases, and not all successful captures are followed by pauses.

The two whales whose behavior changed most radically during airgun exposure (254b and 254c) were also the two who were most closely approached by the airgun source vessel during the experiments (although the range of airgun sound levels they received overlapped significantly with those of most of the other whales; see Table 5.3). Although the two whales were tagged and underwent airgun exposure together, they were tagged in a large aggregation of whales, and they were not observed traveling together at any point while they were tagged (Miller *et al.*, 2003, P.J.O. Miller, Pers. Comm.).

Although all available indicators suggested relatively good fit of the sMC model to the sperm whale datasets, testing the parametric bootstrap and rotation significance tests on data from non-exposed whales indicated that the parametric bootstrap detected significant differences in behavior between sham airgun exposure and control periods much more frequently than expected by chance, assuming that no real behavior-changing stimulus was present. The rotation test, on the other hand, seemed to perform much better as a significance-assessment tool for the sMC model. For this reason, I believe that the rotation test results are superior to the parametric bootstrap results, and I have based my conclusions and interpretations on the rotation test results.

The rotation test and sMC modeling approaches I employed are quite versatile, applicable at the individual or group level. Here, I used them to test for effects of the presence of an airgun noise source, but if behavioral noise response datasets that include reliable data on exposure level become available, both methods could be extended to model effect size as a function of exposure level. Because of this versatility, my methods may prove useful in studies with the long term goal of predicting the effect of long-term changes in foraging on population parameters. The ability to detect reductions in foraging rates may be

of particular interest, since reduced foraging rates could result in lower energy stores and consequent reductions in individual reproductive fitness and population growth rates.

In addition to testing hypotheses about airgun exposure, my sMC analysis confirmed that there are significant differences in foraging behavior between individual sperm whales. This result highlights the utility of using methods like those described in this paper (which can account for variations between animals) to detect small effects that might be masked by inter-individual variability if analysis required pooling data from many individuals.

My failure to detect changes in foraging rate or in response to airgun exposure for the majority of the whales studied does not necessarily indicate that exposure has no population impacts, for several reasons. First, some whales displayed an apparent change in behavior (detected by the sMC analysis) that did not correspond to a detectable reduction in buzz rate. In addition, I detected significant inter-individual variability in foraging behavior among the whales in our study; it is possible that response to noise may similarly vary from whale to whale. For example, if the reduction in foraging tends to occur in reproductive females, it could have a larger impact on reproduction than if it occurs among males; female reproductive success requires large energetic investments in pregnancy and lactation, so female fitness is more closely linked to physical condition. It is also reasonable to expect that different age or sex classes, and individual whales with different histories of exposure, would have different patterns of behavioral response to airgun sounds. The sex of five of the seven individuals in this study was determined by genetic analysis (see Table 5.1), and they were all female, so the results of this study do not allow me to draw any conclusions about sex differences in airgun response.

The sperm whales in this study were exposed to relatively low levels of airgun noise (maximum 147 dB re 1uPa rms; most airgun source levels are >230dB), well below the regulated exposure level (National Marine Fisheries

Service, 2003), so it is somewhat surprising that any effects at all were detectable. Therefore, the results presented here may suggest that current regulation requirements should be reconsidered.

Although the tests I employed have far greater power than methods that require converting behavioral time-series to a mean event rate for each animal, the power of our statistical tests to detect small changes in individual whales' foraging behavior was still lower than optimal. In future experiments, increasing the duration of the experiment (both control and airgun exposure periods), increasing the exposure levels, and increasing the number of animals involved would further increase available power to detect behavioral changes.

Acknowledgements

I thank the crews and science parties of the research cruises on which data for this study were collected. Funding for this work was provided by the Office of Naval Research, the U.S. Department of the Interior Minerals Management Service Cooperative Agreements numbers 1435-01-02-CA-85186 and NA87RJ0445, and the Industry Research Funding Coalition. During part of this work, I was supported by a National Science Foundation Graduate Research Fellowship. I am grateful to Andy Solow (WHOI Marine Policy Center), Hal Caswell, Mike Neubert, and Sanjay Tiwari (all of the WHOI Biology department) for their encouragement and helpful advice on model development and statistical analyses for this project. Peter Tyack (WHOI Biology Department), Patrick Miller (Sea Mammal Research Unit, University of St. Andrews) and Ari Shapiro (MIT/WHOI Joint Program) also provided helpful comments on this work.

References

Acharya, L., and Fenton, M. B. (**1992**). "Echolocation behavior of Vespertilionid bats (*Lasiurus cinereus* and *Lasiurus borealis*) attacking airborne targets including Arctiid moths," Canadian Journal of Zoology **70**, 1292-1298.

Britton, A. R. C., and Jones, G. (**1999**). "Echolocation behaviour and prey-capture success in foraging bats: Laboratory and field experiments on *Myotis Daubentonii*," Journal of Experimental Biology **202**, 1793-1801.

Caswell, H. (**2001**). *Matrix Population Models* (Sinauer, New York, NY).

Cherry, J. A. (**1989**). "Ultrasonic vocalizations by male hamsters - parameters of calling and effects of playbacks on female behavior," Animal Behaviour **38**, 138-153.

Dean, C. B., and Balshaw, R. (**1997**). "Efficiency lost in analyzing counts rather than event times in Poisson and over-dispersed Poisson regression models," Journal of the American Statistical Association **92**, 1387-1398.

DeRuiter, S. L., and Solow, A. (**in press**). "A rotation test for behavioural point-process data," Animal Behaviour.

DeRuiter, S. L., Tyack, P. L., Lin, Y. T., Newhall, A. E., and Lynch, J. F. (**2006**). "Modeling acoustic propagation of airgun array pulses recorded on tagged sperm whales (*Physeter macrocephalus*)," Journal of the Acoustical Society of America **120**, 4100-4114.

Fernández-Juricic, E., and Tran, E. (**2007**). "Changes in vigilance and foraging behaviour with light intensity and their effects on food intake and predator detection in house finches," Animal Behaviour **74**, 1381-1390.

Fisher, R. A. (**1948**). "Combining independent tests of significance," The American Statistician **2**, 30-31.

Haccou, P., and Meelis, E. (**1992**). *Statistical Analysis of Behavioural Data: An approach based on time-structured models* (Oxford University Press, Oxford, U.K.).

Harkness, R. D., and Isham, V. (**1983**). "A bivariate spatial point pattern of ants' nests," Applied Statistics **32**, 293-303.

Jochens, A. E., and Biggs, D. C. (**2003**). "Sperm Whale Seismic Study in the Gulf of Mexico: Annual Report: Year 1," (U.S. Department of the Interior Minerals Management Service, Gulf of Mexico OCS Region, New Orleans, LA).

Jochens, A. E., and Biggs, D. C. (**2004**). "Sperm Whale Seismic Study in the Gulf of Mexico, Annual Report: Year 2," (U.S. Department of the Interior Minerals Management Service, Gulf of Mexico OCS Region, New Orleans, LA).

Johnson, M. P., and Tyack, P. L. (**2003**). "A digital acoustic recording tag for measuring the response of wild marine mammals to sound," IEEE Journal of Oceanic Engineering **28**, 3-12.

Keyfitz, N., and Caswell, H. (**2005**). *Applied Mathematical Demography* (Springer Science+Business Media, Inc., New York, NY).

Kot, M. (**2001**). *Elements of Mathematical Ecology* (Cambridge University Press, Cambridge, U.K.).

Lawrance, A. J., and Lewis, P. A. W. (**1979**). "Simulation of some autoregressive Markovian sequences of positive random variables," in *Proceedings of the IEEE 11th Conference on Winter Simulation* (IEEE, San Diego, CA).

Lusseau, D. (**2003**). "Effects of tour boats on the behavior of bottlenose dolphins: Using Markov chains to model anthropogenic impacts," Conservation Biology **17**, 1785-1793.

Lusseau, D. (**2004**). "The hidden cost of tourism: Detecting long-term effects of tourism using behavioral information," Ecology and Society **9**, 2-16.

Madsen, P. T., Johnson, M., Miller, P. J. O., Soto, N. A., Lynch, J., and Tyack, P. (**2006**). "Quantitative measures of air-gun pulses recorded on sperm whales (*Physeter macrocephalus*) using acoustic tags during controlled exposure experiments," Journal of the Acoustical Society of America **120**, 2366-2379.

Miller, P. J., Biassoni, N., Samuels, A., and Tyack, P. L. (**2000**). "Whale songs lengthen in response to sonar," Nature **405**, 903.

Miller, P. J., Johnson, M. P., Aguilar, N., Grund, M., Teloni, V., Quero, M., Beier, A., Engelhaupt, D., Thode, A., and Diebold, J. (**2003**). "Cruise Report for EW0303: SWSS year two, DTAG component," (Woods Hole Oceanographic Institution; Lamont-Doherty Earth Observatory; Sea Mammal Research Unit, University of St. Andrews).

Miller, P. J., Johnson, M. P., and Tyack, P. L. (**2004a**). "Sperm whale behavior indicates the use of echolocation click buzzes 'creaks' in prey capture," Proceedings of the Royal Society B - Biological Sciences **271**, 2239-2247.

Miller, P. J. O., Shapiro, A. D., Tyack, P. L., and Solow, A. R. (**2004b**). "Call-type matching in vocal exchanges of free-ranging resident killer whales, *Orcinus orca*," Animal Behaviour **67**, 1099-1107.

Mooring, M. S. (**1995**). "The effect of tick challenge on grooming rate by impala," Animal Behaviour **50**, 377-392.

National Marine Fisheries Service (**2003**). "Taking and importing marine mammals; Taking marine mammals incidental to conducting oil and gas exploration activities in the Gulf of Mexico," Federal Register **68**, 9991–9996.

Nowacek, D. P., Johnson, M. P., and Tyack, P. L. (**2004**). "North Atlantic right whales (*Eubalaena glacialis*) ignore ships but respond to alerting stimuli," Proceedings of the Royal Society B - Biological Sciences **271**, 227-231.

Paredes, R., Jones, I. L., and Boness, D. J. (**2005**). "Reduced parental care, compensatory behaviour and reproductive costs of thick-billed murres equipped with data loggers," Animal Behaviour **69**, 197-208.

Richardson, W. J., Greene, C. R., Jr., Malme, C. I., and Thompson, D. H. (**1995**). *Marine Mammals and Noise* (Academic Press, San Diego, CA).

Rugg, D. J., and Buech, R. R. (**1990**). "Analyzing time budgets with Markov chains," Biometrics **46**, 1123-1131.

Surlykke, A., Futtrup, V., and Tougaard, J. (**2003**). "Prey-capture success revealed by echolocation signals in pipistrelle bats (*Pipistrellus pygmaeus*)," Journal of Experimental Biology **206**, 93-104.

Thomas, M. (**1949**). "A generalization of Poisson's binomial limit for use in ecology," Biometrika **36**, 18-25.

Tuljapurkar, S., and Caswell, H. (eds). (**1997**). *Structured-Population Models in Marine, Terrestrial, and Freshwater Systems* (Chapman & Hall, New York, NY).

Tyack, P. L. (**2008**). "Implications for marine mammals of large-scale changes in the marine acoustic environment," Journal of Mammalogy **89**, 549–558.

Watwood, S. L., Miller, P. J. O., Johnson, M., Madsen, P. T., and Tyack, P. L. (**2006**). "Deep-diving foraging behaviour of sperm whales (*Physeter macrocephalus*)," Journal of Animal Ecology **75**, 814-825.

Chapter 6. Conclusions

6.1 Implications of the Thesis

The preceding chapters of this thesis have explored quantitative descriptions of toothed whale echolocation and foraging behavior (Chapters 2 and 5), including assessment of the effects of noise on foraging behavior (Chapter 5) and the potential influence of ocean acoustic propagation conditions on biosonar detection ranges (Chapter 3) and whale noise exposure (Chapter 4). In addition to presenting some novel basic science findings, the case studies presented in this thesis have implications for future work and for management.

In Chapter 2, I presented results that described how porpoises vary the rate and level of their echolocation clicks during prey capture events; detailed the differences in echolocation behavior between different animals and in response to differences in prey fish; and showed that, unlike bats, porpoises continue their echolocation buzz after the moment of prey capture.

Chapters 3-4 provided case studies that emphasized the importance of applying realistic models of ocean acoustic propagation in marine mammal studies. These chapters illustrated that, although using geometric spreading approximations to predict communication/target detection ranges or noise exposure levels is appropriate in some cases, it can result in large errors in other cases, particularly in situations where refraction in the water column or multi-path acoustic propagation are significant.

Finally, in Chapter 5, I applied a rotation test and a semi-Markov chain model to test for changes in sperm whale foraging behavior in response to airgun noise exposure. Test results indicated that, despite the low-level exposures experienced by the whales in the study, some (but not all) of them reduced their

buzz production rates and altered other foraging behavior parameters in response to the airgun exposure.

6.2 Future Work

The results presented in this thesis suggest several promising directions for future work. Many of them are mentioned in the discussion sections of the preceding chapters, but priorities are summarized briefly below.

6.2.1 Porpoise Tag Data Analysis

The porpoise prey capture tag experiments examined in Chapter 2, supplemented by additional prey capture trials carried out in April 2008 with increased tag audio gain, will provide a rich dataset for continued analysis.

I have not yet investigated the tag movement data; analyzing it should complement the work to date on the acoustic data.

In addition, preliminary analysis of the April 2008 data indicate that prey echoes may be detectable in the audio recordings. If they are, I should be able to use the timing of echoes to calculate porpoise-prey range over the course of prey capture. Echo timing data will also allow me to test the hypothesis that porpoises avoid temporal overlap between prey echoes and non-target echoes (or outgoing clicks, though such overlap is unlikely given the short duration of porpoise clicks). In addition, it may be possible to estimate minimum prey detection ranges. Study of prey echoes may also help elucidate the echo characteristics available to porpoises as they decide whether or not to select a particular prey item. Finally, if I can measure the relative levels of prey echoes as porpoises approach prey fish, it will be possible to test the hypothesis that porpoises use transmit-side automatic gain control to maintain relatively constant echo levels as porpoise-fish range decreases.

In addition to analysis of movement and echo data, further investigation of the acoustic data from the prey capture experiments will be possible. Analysis to

date indicates that the off-axis clicks recorded on the tag comprise several overlapping, reverberant arrivals. It is therefore likely that the frequency spectra of the recorded clicks do not accurately represent that of clicks recorded in the far field. However, it may be worthwhile to examine the temporal and frequency characteristics of clicks produced before, during and after prey capture in hopes of identifying an acoustic indicator of successful prey capture. If such an indicator exists, it would facilitate calculation of prey capture rates (rather than just buzz production rates) from field recordings of foraging behavior.

I have also collected several tag datasets at the Fjord & Baelt Center that contain concurrent data on porpoise movements and social communication sounds, including adult-adult interactions, mother-calf interactions, and interactions between an adult male and a female calf. Although it is known that porpoises use clicks for intraspecific communication as well as echolocation, and the individual clicks used in their communication signals are thought to be acoustically indistinguishable from their echolocation clicks, neither the clicks nor the communications sounds have been well described in the peer-reviewed literature (but see Amundin, 1991; DeRuiter and Tyack, 2007; Clausen *et al.*, 2008). Analysis and publication of the tag datasets could thus contribute significantly to the information available on this topic.

6.2.2 Depth Distribution of Echolocating Porpoises

The acoustic propagation model analysis in Chapter 3 indicated that porpoises might be able to take advantage of the effects of refraction in the water column to increase the range at which they can communicate and detect echolocation targets. Field experiments to collect hydrophone array and CTD data would allow me to test the prediction that porpoises adjust their depth distribution to take advantage of sound propagation channels in the water column.

6.2.3 Whale Foraging Behavior and Population Modeling

Although the techniques applied in Chapter 5 were able to address the question of whether sperm whales changed their foraging behavior in response to airgun sound exposure, they were not sufficient to determine whether the observed behavior changes (if any) were large enough to affect whale population dynamics. In the future, I hope to use literature data and established modeling methods to relate changes in whale foraging rate to changes in reproductive success, and finally to relate individual reproductive success rates to population growth rates. Such modeling will facilitate a noise-management approach in which managers can regulate noise exposure levels based on the predicted effects of noise exposure on population growth rate.

In the study presented in Chapter 5, I compared airgun exposure periods to control periods because exposure levels were so low that they were in many cases difficult to quantify (Madsen *et al.*, 2006). However, realistically, one would expect the intensity of sperm whale response to be a function of noise exposure level, as higher exposure levels would result in increased masking or annoyance. If future noise exposure experiments provided whale behavior data coupled with more extensive noise exposure level data, it would be possible to carry out similar analyses that would quantify the relationship between whale response magnitude and noise exposure intensity. Specifically, I could test the hypothesis that, between some minimum threshold level and some maximum effect level, sperm whale foraging rates are inversely related to noise exposure level.

In addition to the controlled exposure experiments described in Chapters 4-5, the Johnson-Tyack laboratory group has deployed Dtags on many other sperm whales in the Gulf of Mexico, the Atlantic Ocean, and the Mediterranean. Those recordings would provide a uniquely extensive dataset on which to carry out an analysis analogous to that described above for airgun exposure data. In this case, however, I would attempt to quantify the relationship between

background noise exposure level and sperm whale buzz rates, foraging behavior, and ultimately reproductive success and population dynamics.

6.2.4 Comparative Studies of Toothed Whale Echolocation Signals & Strategies

Although the work presented in this thesis is insufficient to allow detailed comparison of toothed whale echolocation signals and strategies, it does contribute basic biological data on the echolocation behavior of harbor porpoises as they locate and consume prey fish. Continued collection of this kind of data for various species, both in captivity and in the wild, will eventually form the basis for future interspecific comparative studies. At present, based on current knowledge of toothed whale echolocation signals and behavior, it is possible to compare the echolocation signals of harbor porpoises and sperm whales and speculate as to whether differences in echolocation signals, behavior, and physiology may relate to niche adaptation by these species. Hypotheses suggested by such speculation may be tested in future work related to interspecific comparative studies of toothed whale echolocation.

Various types of echolocation signals have been recorded from toothed whales. Examples include the lower-frequency, broadband, multi-pulsed clicks of sperm whales (Zimmer *et al.*, 2005b), the high-frequency, broadband, impulsive clicks of bottlenose dolphins (Au *et al.*, 1974), the high-frequency, frequency-modulated clicks of Cuvier's beaked whales *Ziphius cavirostris* (Zimmer *et al*., 2005a), and the very high-frequency, narrowband clicks of porpoises (Au *et al.*, 1999). The natural history, echolocation signals, and behavior of harbor porpoises and sperm whales are discussed in further detail in Section 1.2.

Researchers have noted some connections between the ecological niches of cetaceans and their echolocation signals. For example, small near-shore and riverine species that hunt small prey in acoustically cluttered habitats tend to use higher-frequency (>100kHz), more narrow-band echolocation signals (Ketten,

2000). Harbor porpoises are a good example. In contrast, larger offshore species like sperm whales hunt larger prey in open water (a potentially less cluttered habitat) and use lower-frequency, broadband signals (Ketten, 2000). However, exceptions to this pattern exist; for example, pygmy sperm whales *Kogia breviceps*, which forage in deeper waters for squid, also produce narrowband echolocation signals centered at about 130 kHz (Madsen *et al.*, 2005).

The center frequency of porpoise clicks, 130 kHz (Au *et al.*, 1999), is much higher than that of sperm whale clicks, 15 kHz (Madsen *et al.*, 2002a). Sperm whale clicks also have higher levels than those of porpoises (235 dB re 1 µPa root-mean-squared (Møhl *et al.*, 2003) vs 179 dB re 1 µPa root-mean-squared (Villadsgaard *et al.*, 2007)). These differences may be explained simply by the much larger size of the sperm whale. Vocalization frequencies of terrestrial animals generally scale with body size; hypotheses to explain this phenomenon range from anatomical (larger sound generators and/or vocal tracts produce lower frequency sound) to evolutionary (lower-frequency calls allow larger communication distances, and larger animals with larger ranges must communicate over longer ranges, so evolutionary optimization of call frequency leads to lower-frequency calls by larger animals) (Fletcher, 2004). These same patterns seem to hold for whale tonal calls: recent taxon-specific work on cetacean tonal sounds has shown that the minimum and center frequencies of calls increase with decreasing body size, even when expected similarity in call frequency due to common ancestry is taken into account (May-Collado *et al.*, 2007b). In addition, for relatively solitary cetacean species with smaller social groups, minimum tonal call frequency is lower and call duration is higher (May-Collado *et al.*, 2007a). Both features could be adaptive for longer-range social communication (May-Collado *et al.*, 2007a). Thus, it seems likely that the arguments presented above to explain scaling of acoustic frequency with terrestrial animal size may also apply to cetacean tonal sounds. Similar

arguments probably also apply to toothed whale echolocation clicks, since the size of whale sound generators also scales roughly with body size, and since larger species tend to forage at greater depth and over larger areas.

Another hypothesis to explain the observed relationship between whale body size and echolocation click frequency relates to click directionality. Echolocation clicks are directional (e.g., Au, 1993; Au *et al.*, 1999; Zimmer *et al.*, 2005b), and sound reflection and refraction caused by features of head and melon anatomy is thought to play a key role in producing this directionality (Au, 1993; Zimmer *et al.*, 2005b; Cranford *et al.*, 2008). Such effects cannot occur unless the wavelength of sound produced is significantly smaller than the size scale of the anatomical features, so very small whales would not be able to produce low-frequency directional clicks.

It has also been suggested that squid, a major prey item of sperm whales, have very low acoustic target strength and thus sperm whale clicks must have very high levels to ensure that prey are detectable at reasonable ranges (Madsen *et al.*, 2002b). As an alternate explanation for the very high source levels of sperm whale clicks, researchers have hypothesized that the clicks stun or acoustically debilitate prey, making them easier to catch (Norris and Mohl, 1983). However, recent work has shown that at least one squid species, *Loligo pealeii*, shows no discernable reaction to simulated sperm whale clicks (Wilson *et al.*, 2007).

The harbor porpoise's use of higher-frequency, lower-level calls may also be adaptive for the niche it occupies. Relatively few marine predators are thought to hear well at the high frequencies used by porpoises, and high frequency sound is rapidly attenuated in the ocean, so even animals that can detect it are unlikely to do so at long ranges. High frequency clicks are thus relatively unlikely to attract predators, which could be an advantage for the small, rather solitary harbor porpoise. The low levels and high frequency of porpoise

clicks greatly limit the ranges at which they may detect targets compared to other toothed whales (Au *et al.*, 2007). This limited detection range may not be a disadvantage for porpoises. First, the extent of the surrounding area that is behaviorally relevant to a porpoise may be proportional to their own relatively small size. In addition, their foraging habitat is likely to include numerous clutter targets including strong reflectors like the sea surface and sea floor (not only sediments, but also rocks and other features); minimizing echoes from such targets may facilitate detection of desirable targets. Finally, considering echolocation for navigation rather than foraging purposes, navigational landmarks are probably relatively dense in the coastal habitats used by porpoises, so shorter-range echolocation may be adequate for accurate navigation.

Porpoise clicks are longer and more narrowband[3] than those of other odontocetes, making their signal characteristics more analogous to those of CF bats, which employ Doppler compensation of outgoing signals (Simmons, 1974). In addition, anatomical study of the porpoise inner ear (cochlea) provides some evidence for an acoustic fovea at around 110 kHz in the porpoise auditory system, meaning porpoises have increased sensitivity and more acute frequency discrimination in the frequency range of their biosonar clicks (and prey echoes) (Ketten, 2000; Popov *et al.*, 2006). A similar anatomical adaptation exists in CF-FM Doppler bats (*Rhinolophus* spp. and *Pteronotus parnellii*) (Vater, 2004).

[3] The -3dB bandwidth of a porpoise click is about 15 kHz (Au et al. 1999, Villadsgaard et al. 2007). In absolute terms, this bandwidth is not dramatically different from the -3dB bandwidth of a sperm whale click (10-15 kHz, Madsen et al. 2002). However, the center frequency of a porpoise click is about 130 kHz (Au et al. 1999), while that of a sperm whale is only 8-25 kHz (Madsen et al. 2002); the porpoise click bandwidth is much narrower when considered as a proportion of click center frequency. In other words, the porpoise click has a higher Q value, where Q = center frequency/bandwidth. For comparison, a bottlenose dolphin click has -3 dB bandwidth ~ 40 kHz and center frequency ~ 115 kHz (Au 1993).

Given those similarities and porpoises' observed capacity for detecting very small frequency differences, it has been hypothesized that porpoises too may use some form of Doppler processing (Bibikov, 2004). However, given the typical swimming speeds of porpoises and their prey and the speed of sound in water, porpoises would have to detect very small frequency shifts (on the order of a few hundred Hz) to take advantage of the Doppler effect. A simple calculation based on swimming speeds and porpoise frequency discrimination capabilities suggests that they may (just barely) be able to do so (see Appendix C for calculations), but strong evidence against the porpoise-Doppler hypothesis also exists. First, Doppler-sensitive bats adjust the frequency of their outgoing clicks to maintain constant frequency spectra in returning echoes. If porpoises did the same, they would have to precisely control the center frequencies of their outgoing clicks to within a few hundred Hz. It seems unlikely that they do so, given the wide scatter (10-20 kHz) observed in center frequencies of clicks produced by individual porpoises (Au *et al.*, 1999); in fact, the available data suggest that they do not have such fine control over the frequency content of their clicks. Second, porpoise clicks (~150 μsec (Au *et al.*, 1999)) are much shorter than the cries of Doppler bats (*e.g. Rhinolophus* spp., ~50 msec (Jones and Rayner, 1989)), which limits frequency resolution during processing of returning echoes. Thorpe and colleagues (1991) carried out an ambiguity-diagram-based analysis of clicks produced by Hector's dolphin (*Cephalorhynchus hectori*), which are similar in duration and frequency spectrum to those of porpoises. They concluded that the clicks were poorly suited to Doppler range discrimination, and could not resolve changes in relative target velocity of less than 20 m/sec (much larger than the expected relative velocity of dolphin or porpoise prey). However, it should be noted that their estimate of dolphin range discrimination ability depends on the assumption that dolphins use matched-filter-like processing on echolocation target echoes.

Harbor porpoises inhabit temperate and subarctic waters and use echolocation for foraging and navigation. They tend to forage in shallow, coastal waters (less than a few hundred meters deep) (Westgate *et al.*, 1995; Reynolds and Rommel, 1999), and they consume some species of fish that tend to be found at or near the sea floor (Fontaine *et al.*, 1994; Santos *et al.*, 2004). Consequently, their foraging environment is highly cluttered, and sensitivity to Doppler shifts in returning echoes or Doppler compensation like that of CF-Doppler bats could help porpoises more easily detect moving prey against a background of stationary clutter. One way to test the Doppler compensation hypothesis would involve collection of data on the frequency of outgoing clicks and echoes during a prey capture task, during which velocity of the porpoise relative to the prey was also monitored. It may be possible to begin to address this question using data from the prey capture experiments (with higher-gain tag) described earlier in this chapter. However, off-axis tag audio recordings are not ideal for determination of outgoing click frequencies, and audio sampling rates higher than 400 kHz would also aid processing, so further experiments would be required to explore the question fully.

References

Amundin, M. (**1991)**. "Sound production in Odontocetes with emphasis on the harbour porpoise *Phocoena phocoena*," PhD Thesis, Department of Zoology, Division of Functional Morphology, University of Stockholm.

Au, Floyd, R. W., Penner, R. H., and Murchison, A. E. (**1974**). "Measurement of echolocation signals of the Atlantic bottlenose dolphin, *Tursiops truncatus* Montagu, in open waters," Journal of the Acoustical Society of America **56**, 1280-1290.

Au, W. W. L. (**1993**). *The sonar of dolphins* (Springer-Verlag, New York, NY).

Au, W. W. L., Benoit-Bird, K. J., and Kastelein, R. A. (**2007**). "Modeling the detection range of fish by echolocating bottlenose dolphins and harbor porpoises," Journal of the Acoustical Society of America **121**, 3954-3962.

Au, W. W. L., Kastelein, R. A., Rippe, T., and Schooneman, N. M. (**1999**). "Transmission beam pattern and echolocation signals of a harbor porpoise (*Phocoena phocoena*)," Journal of the Acoustical Society of America **106**, 3699-3705.

Bibikov, N. G. (**2004**). "What do evoked potentials tell us about the auditory system of the harbor porpoise?," Acoustical Physics **50**, 295-304.

Clausen, K. T., Madsen, P. T., and Wahlberg, M. (**2008**). "Click communication in harbour porpoises, *Phocoena phocoena* [poster presentation]," European Cetacean Society 2008 Conference, Egmond aan Zee, The Netherlands, 10-12 March 2008.

Cranford, T. W., McKenna, M. F., Soldevilla, M. S., Wiggins, S. M., Goldbogen, J. A., Shadwick, R. E., Krysl, P., St Leger, J. A., and Hildebrand, J. A. (**2008**). "Anatomic geometry of sound transmission and reception in Cuvier's beaked whale (*Ziphius cavirostris*)," The Anatomical Record **291**, 353-378.

DeRuiter, S. L., and Tyack, P. L. (**2007**). "Contact recordings of buzz-like calls of a harbor porpoise (*Phocoena phocoena*) [oral presentation]," 5th Annual Boston Behavior Club Symposium, Woods Hole, MA, 26 May 2007.

Fletcher, N. H. (**2004**). "A simple frequency-scaling rule for animal communication," Journal of the Acoustical Society of America **115**, 2334-2338.

Fontaine, P. M., Hammill, M. O., Barrette, C., and Kingsley, M. C. (**1994**). "Summer diet of the harbor porpoise (*Phocoena phocoena*) in the estuary and the northern Gulf of St. Lawrence," Canadian Journal of Fisheries and Aquatic Sciences **51**, 172-178.

Jones, G., and Rayner, J. M. V. (**1989**). "Foraging behavior and echolocation of wild horseshoe bats *Rhinolophus ferrumequinum* and *Rhinolophus hipposideros* (Chiroptera, Rhinolophidae)," Behavioral Ecology and Sociobiology **25**, 183-191.

Ketten, D. R. (**2000**). "Cetacean Ears," in *Hearing by Whales and Dolphins*, edited by W. W. L. Au, A. N. Popper, and R. R. Fay (Springer, New York, NY), pp. 43-108.

Madsen, P. T., Carder, D. A., Bedholm, K., and Ridgway, S. H. (**2005**). "Porpoise clicks from a sperm whale nose - Convergent evolution of 130 kHz pulses in toothed whale sonars?," Bioacoustics **15**, 195-206.

Madsen, P. T., Johnson, M., Miller, P. J. O., Soto, N. A., Lynch, J., and Tyack, P. (**2006**). "Quantitative measures of air-gun pulses recorded on sperm whales (*Physeter macrocephalus*) using acoustic tags during controlled exposure experiments," Journal of the Acoustical Society of America **120**, 2366-2379.

Madsen, P. T., Payne, R., Kristiansen, N. U., Wahlberg, M., Kerr, I., and Møhl, B. (**2002a**). "Sperm whale sound production studied with ultrasound time/depth recording tags," Journal of Experimental Biology **205**, 1899-1906.

Madsen, P. T., Wahlberg, M., and Møhl, B. (**2002b**). "Male sperm whale (*Physeter macrocephalus*) acoustics in a high-latitude habitat: implications for echolocation and communication," Behavioral Ecology and Sociobiology **53**, 31-41.

May-Collado, L., Agnarsson, I., and Wartzok, D. (**2007a**). "Phylogenetic review of tonal sound production in whales in relation to sociality," BMC Evolutionary Biology **7**, 136.

May-Collado, L. J., Agnarsson, I., and Wartzok, D. (**2007b**). "Reexamining the relationship between body size and tonal signals frequency in whales: A comparative approach using a novel phylogeny," Marine Mammal Science **23**, 524-552.

Møhl, B., Wahlberg, M., Madsen, P. T., Heerfordt, A., and Lund, A. (**2003**). "The monopulsed nature of sperm whale clicks," Journal of the Acoustical Society of America **114**, 1143-1154.

Norris, K. S., and Mohl, B. (**1983**). "Can odontocetes debilitate prey with sound?," The American Naturalist **122**, 85-104.

Popov, V. V., Supin, A. Y., Wang, D., and Wang, K. (**2006**). "Nonconstant quality of auditory filters in the porpoises, *Phocoena phocoena* and *Neophocaena phocaenoides* (Cetacea, Phocoenidae)," Journal of the Acoustical Society of America **119**, 3173-3180.

Reynolds, J. E. I., and Rommel, S. A. (eds). (**1999**). *Biology of Marine Mammals* (Smithsonian Institution Press, Washington, D.C.).

Santos, M. B., Pierce, G. J., Learmonth, J. A., Reid, R. J., Ross, H. M., Patterson, I. A. P., Reid, D. G., and Beare, D. (**2004**). "Variability in the diet of harbor porpoises (*Phocoena phocoena*) in Scottish waters 1992-2003," Marine Mammal Science **20**, 1-27.

Thorpe, C. W., Bates, R. H. T., and Dawson, S. M. (**1991**). "Intrinsic echolocation capability of Hector's dolphin, *Cephalorhynchus hectori*," Journal of the Acoustical Society of America **90**, 2931-2934.

Vater, M. (**2004**). "Chapter 13: Cochlear anatomy related to bat echolocation," in *Echolocation in Bats and Dolphins*, edited by J. A. Thomas, C. F. Moss, and M. Vater (University of Chicago Press, Chicago, IL), pp. 99-104.

Villadsgaard, A., Wahlberg, M., and Tougaard, J. (**2007**). "Echolocation signals of wild harbour porpoises, *Phocoena phocoena*," Journal of Experimental Biology **210**, 56-64.

Westgate, A. J., Read, A. J., Berggren, P., Koopman, H. N., and Gaskin, D. E. (**1995**). "Diving Behavior of Harbor Porpoises, *Phocoena phocoena*," Canadian Journal of Fisheries and Aquatic Sciences **52**, 1064-1073.

Wilson, M., Hanlon, R. T., Tyack, P. L., and Madsen, P. T. (**2007**). "Intense ultrasonic clicks from echolocating toothed whales do not elicit anti-predator responses or debilitate the squid *Loligo pealeii*," Biology Letters **3**, 225-227.

Zimmer, W. M., Johnson, M. P., Madsen, P. T., and Tyack, P. L. (**2005a**). "Echolocation clicks of free-ranging Cuvier's beaked whales (*Ziphius cavirostris*)," Journal of the Acoustical Society of America **117**, 3919-3927.

Zimmer, W. M. X., Tyack, P. L., Johnson, M. P., and Madsen, P. T. (**2005b**). "Three-dimensional beam pattern of regular sperm whale clicks confirms bent-horn hypothesis " Journal of the Acoustical Society of America **117**, 1473-1485.

Appendix A: A Rotation Test for Behavioural Point Process Data

The following manuscript (full citation below) has been accepted for publication in Animal Behaviour and is reprinted with permission from the publishers.

DeRuiter, S. L., and Solow, A. (**in press**). "A rotation test for behavioural point-process data," Animal Behaviour.

A ROTATION TEST FOR BEHAVIOURAL POINT PROCESS DATA

Running Headline: DeRuiter and Solow, Rotation Test for Behavioral Data

STACY L. DERUITER & ANDREW R. SOLOW

Woods Hole Oceanographic Institution

Woods Hole, MA

Addresses for Correspondence:
Stacy DeRuiter
Biology Department, MS #50
Woods Hole Oceanographic Institution
Woods Hole, MA 02543
USA
Email: sderuiter@whoi.edu

Andrew Solow
Marine Policy Center, MS #41
Woods Hole Oceanographic Institution
Woods Hole, MA 02543
USA

Word Count: 3079

Key Words: behavioural point process, statistical analysis, time-series analysis

A common problem in animal behavior is determining whether the rate at which a certain behavioural event occurs is affected by an environmental or other factor. In the example considered later in this paper, the event is a vocalization by an individual sperm whale and the factor is the operation or non-operation of an underwater sound source. A typical experiment to test for such effects involves observing animals during control and treatment periods and recording the times of the events that occur in each. In statistical terminology, the data arising from such an experiment – the times at which events of a specified type occur – represent a point process (Cox & Lewis 1978). Events in a point process are treated as having no duration. Although this is not strictly correct for behavioural events, the approximation is reasonable when the duration of events is small in relation to the interval between them.

In some cases, under the null hypothesis of no treatment effect, behavioural events can be assumed to follow a stationary Poisson process. Under this model, the intervals between successive events are independent and, conditional on their number, the events are uniformly distributed over the observation period. As described below, when the Poisson assumption is valid, a statistical test to determine whether event rate changes under treatment can be based on the binomial distribution. In many cases, however, the Poisson model has been shown to be invalid for behavioural events. This is the case, for example, when events occur in bouts (Slater & Lester 1982; Sibly et al. 1990; Haccou & Meelis 1992). As illustrated below, when behavioural events do not follow a Poisson process, the binomial test can give misleading results. A number of methods are available to test whether a point process is Poisson based on the uniformity result mentioned above (Stephens 1986). If a point process cannot be assumed to be Poisson, one option is to use a test that is valid under a particular alternative to the Poisson model. Unfortunately, while it is often easy to show that a point process is not Poisson, it can be difficult to specify an appropriate alternative model. The purpose of this paper is to

describe and illustrate the use of a simple nonparametric method that can be used to analyze behavioural point process data even if the process generating the data is unknown.

A Rotation Test

Suppose that events are observed over the period (0, *T*), and that the total times under control and treatment conditions are T_C and T_T, respectively (with $T = T_C + T_T$). Assume that, under control conditions, events follow a stationary Poisson process with rate λ_C and that, under treatment conditions, events follow an independent Poisson process with rate λ_T. Under this model, interest centers on testing the null hypothesis $H_o : \lambda_C = \lambda_T$ of no treatment effect. Let the random variables N_C and N_T be the numbers of events occurring under control and treatment conditions, respectively, and let $N = N_C + N_T$ be the total number of events. Conditional on the observed value *n* of *N*, under H_o, N_C has a binomial distribution with *n* trials and success probability T_C / T. The null hypothesis can be rejected at significance level α if the observed value of N_C is below the lower $(\alpha / 2)$ quantile or above the upper $(\alpha / 2)$ quantile of this binomial distribution. Provided *n* is not too small and T_C / T is not too close to 0 or 1, the binomial distribution can be approximated by a normal distribution with mean $n T_C / T$ and variance $n T_C T_T / T^2$, so that H_o can be rejected at approximate significance level α if:

$$\left| \frac{TN_C - nT_C}{\sqrt{nT_C T_T}} \right| > \Phi^{-1}(\alpha/2) \qquad (1)$$

where $\Phi^{-1}(\alpha/2)$ is the upper $(\alpha/2)$ quantile of the standard normal distribution.

Behavioral events often exhibit clustering in time beyond what is expected under a Poisson process. As illustrated below, the binomial test may fail in such cases because the underlying randomization scheme – distributing *n* events at random over the observation period – fails to capture internal structure in the events that is present even under the null hypothesis. A randomization procedure that does preserve this internal structure can be visualized in the following way. Transform the observation period into a circle by joining its end to its beginning. This is sometimes referred to as imposing a periodic boundary condition. Keeping the partition of the observation period into control and treatment segments fixed, displace the events by the same random rotation. Let t_j be the time of the *j*th event. Its time under this rotation scheme is given by:

$$t_j^* = \begin{array}{ll} t_j + U & t_j + U < T \\ t_j + U - T & t_j + U > T \end{array} \qquad (2)$$

where *U* is a uniform random variate over the interval (0, *T*). By displacing each event by the same random angle, this procedure preserves the internal structure of the events except at the beginning of the original observation period, where events originally near *T* are now in proximity to events originally near 0. Provided

n is not too small, the effect of this concatenation is negligible. The test proceeds by approximating the distribution of N_C under the null hypothesis from values produced by a large number of random rotations. The null hypothesis is then rejected at significance level α if the observed value of N_C lies below the lower or above the upper $\alpha/2$ quantile of this distribution. This general approach was originally proposed by Harkness & Isham (1983) for testing association between two two-dimensional point processes observed on a rectangle. The test has been applied by Miller et al (2004a, b), but a detailed description of the test including assessment of its validity and power has not previously been published.

To summarize, the steps involved in the rotation test are:

1. Express the data as a set of behavioral event times over the observation period (0, T).
2. Calculate the number N_c of events occurring during the control period.
3. Generate a rotated set of behavioural event times according to (6).
4. Calculate the number N_{c_rot}, of events in the rotated set falling in the original control time period.
5. Repeat steps 3-5 many times to obtain a distribution for N_{c_rot} and assess significance by comparing the the observed value of N_C to the quantiles of this distribution.

Test Performance

In this section, we assess the performance of the binomial and rotation tests under three point process models: the stationary Poisson process, the one-dimensional Thomas process (Thomas 1949), and an exponential autoregressive (EAR) model (Lawrance & Lewis 1979). The Thomas process is a classical model of clustering in point process data, while the EAR model gives rise to clustering through positive autocorrelation in the intervals between events. No claim is made that either of these models is necessarily appropriate for a particular behavioural point process. Instead, they are used here as plausible alternatives to the Poisson process.

In a Thomas process, initiating events follow a stationary Poisson process with rate μ. Each initiating event gives rise to an additional number of offspring events. The numbers of these offspring are independent Poisson random variables with mean θ. Let s_o be the time of an initiating event and suppose that it gives rise to k offspring. The times of these offspring are given by $s_j = s_o + \delta_j$, *j* = 1, 2, …, *k*, where $\delta_1, \delta_2, ..., \delta_k$ are independent random intervals with common distribution function *F*. The process consists of the union of the initiating events and their offspring. The Thomas process is stationary with overall rate $\mu(1+\theta)$. However, it is over-dispersed in relation to the Poisson process with the same rate. For example, for the Thomas process, the variance of the number of events occurring in a unit interval is $\mu(1+3\theta+\theta^2)$ instead of $\mu(1+\theta)$ for the Poisson process with the same overall rate.

In contrast to the Thomas process, which is a model of the event times, the EAR process is a model for the intervals between events. Let $d_j = t_j - t_{j-1}$ be the interval between events j – 1 and *j*. Under the Poisson model, the intervals

d_1, d_2,...are independent exponential random variables. In contrast, under the EAR model, the sequence of intervals follows the autoregressive process:

$$d_j = \rho d_{j-1} + \varepsilon_j \qquad (3)$$

where ε_j is equal to 0 with probability ρ and equal to an exponential random variable with mean $1/\lambda$ with probability $1-\rho$. The EAR process is stationary with overall rate λ and autocorrelation function $Corr(d_j, d_{j-h}) = \rho^h$. The positive dependence between successive intervals gives rise to clustering of events.

Although it is possible to make some progress analytically, for the purpose of this paper we present some results from a small simulation study. The goal of the first part of this study was to assess the validity of the nominal significance levels of the binomial and rotation tests under the three point process models outlined above. This involved repeatedly simulating point process data from these models under the null hypothesis and applying both tests at the nominal 0.05 significance level. For a valid test, the null hypothesis should be rejected at a rate equal to the nominal significance level. In the study described here, the observation period was taken to be the unit interval, with the first half corresponding to the control period and the second half to the treatment period. Results are presented in Table 1 for overall mean rates of 500 and 1000. For the Thomas process, the parameter θ was fixed at 1 while for the EAR process the parameter ρ was fixed at 0.5. Each entry in Table 1 was based on 1000 simulated data sets and each rotation test was based on 1000 random rotations. In the case of the Thomas process, we assumed that offspring events fell into the

same sub-period as their initiating event. In practical terms, this amounts to the assumption that the displacements between offspring and initiating events are negligible in relation to the length of the periods of control and treatment conditions.

Turning to Table 1, it is clear that the binomial test is invalid for point process data generated by the Thomas and EAR processes. For these models, the estimated true rate at which the null hypothesis is falsely rejected is well above the nominal significance level. In contrast, the estimated true significance level for the rotation test is not significantly different from the nominal level for all three point process models.

The goal of the second part of the simulation study was to assess the power of the rotation test. Power is defined as the probability of rejecting the null hypothesis when the alternative hypothesis is correct. This probability will depend on the nature and magnitude of the departure from the null hypothesis, as well as on the amount of data. As a rough guide, a test has good power if this probability is at least 0.8. The power study was based on the same general simulation procedure outlined above except that, for each of the point process models, the overall rate under treatment conditions was increased by a multiplicative factor *f* over its value under control. For the Thomas process, this was accomplished by increasing the rate μ of initiating events. As before, let λ_C and λ_T be the rates under control and treatment conditions, respectively. For the case here where the observation period is evenly divided between control and treatment, the overall rate λ is simply the average of λ_C and λ_T. Throughout

this power study, this overall rate was held fixed by taking $\lambda_C = 2\lambda/(1+f)$ and $\lambda_T = f\,\lambda_C$.

The results of the power study are shown in Table 2. Results are presented for overall rates 500 and 1000 with the parameter θ of the Thomas process fixed at 1, the parameter ρ of the EAR process fixed at 0.5, and *f* = 1.5, 2, and 3. . As before, each entry in this table was based on 1000 simulated data sets and for each data set the rotation test was based on 1000 random rotations. For the Poisson case, results are presented for both the binomial test and the rotation test. In this case, the rotation test is less powerful than the binomial test, although it achieves good power in most of the cases considered here. As the binomial test is not valid for the Thomas and EAR processes, for these processes results are presented only for the rotation test. The power of the rotation test is quite similar for the two cluster processes. In general, the rotation test achieves good power provided the magnitude of the treatment effect and the overall rate of events are not too small.

In addition to the results presented in Table 2, we determined by simulation the minimum detectable effect size $f_{\min}$ – defined as the value of *f* for which the test at 0.05 significance level achieves a power of 0.8 – for the cases considered in Table 2. Results are presented in Table 3. In overall terms, the rotation test has good power once *f* reaches approximately 2.

An Application to Sperm Whale Response to Airgun Sounds

In this section, we apply the rotation test to some experimental data involving the exposure of a sperm whale to airgun sounds. Airguns are a source of loud, impulsive low-frequency underwater sound. They are generally deployed in towed arrays for geophysical exploration (Richardson et al. 1995). Airgun arrays have very high source levels (Richardson et al. 1995; Caldwell & Dragoset 2000) and there is a concern that exposing sperm whales and other marine mammals to airgun noise may have adverse impacts on their behavior (Gordon et al. 2003).

As sperm whales use echolation to locate prey, one hypothesized behavioral impact of airgun sound is a reduction in whale foraging rate. Sperm whales produce regular echolocation clicks almost continuously while foraging, interrupted only by short pauses and buzzes (short series of rapid echolocation clicks indicative of attempted prey capture (Whitehead 2003, Miller et al. 2004a)). Whales begin producing echolocation clicks during the descent phase of deep dives, stop clicking during or just prior to ascent, and do not generally produce series of regular echolocation clicks while at the surface or during shallow dives (Watwood et al. 2006). We therefore defined foraging periods as the portions of deep dives between the start and end of regular echolocation clicks. The behavioral event of interest was the production of echolocation buzzes, which serve as a proxy for foraging rate.

The data used here were collected during controlled exposure experiments conducted on the 2002 and 2003 Sperm Whale Seismic Study cruises. During the experiments, dtags (Johnson & Tyack 2003) were attached to individual whales to record sound and movement data during control conditions (no airgun sound exposure) and treatment conditions (airgun sound exposure).

Airguns were fired every 15 seconds during the treatment period. Detailed information on these experiments can be found in Jochens & Biggs (2003, 2004) and Madsen et al. (2006). Here, we present data from a single individual.

The behavioural record is shown in Figure 1. For this whale, the total time spent foraging during the observation period was T = 5.89 hours, of which $T_C = 4.74$ hours was under control conditions (the airgun array was not operating) and $T_T = 1.15$ hours was under treatment conditions (the airgun array was in operation). A total of n = 153 echolocation buzzes were recorded, of which $N_C = 139$ occurred during control conditions and $N_T = 14$ occurred during treatment conditions. The empirical rate of events during control conditions was 29.3 events h^{-1} and the corresponding rate during treatment conditions was only 12.2 events h^{-1}. The value of the binomial test statistic in (1) is 3.43, which is significant at approximately the 0.0006 level.

For reasons connected to the spatial distribution of prey and whale foraging behavior, we expect that the Poisson model underlying the binomial test is unlikely to apply to this time-series of sperm whale foraging events. This expectation was confirmed by an analysis of the intervals between events, which revealed positive autocorrelation at short lags. As the intervals in a Poisson process are independent, this is evidence of non-Poisson behaviour in this point process. We therefore applied the rotation test to these data. The histogram of values of N_C based on 10,000 rotations is shown in Figure 2. Of these, 647 exceeded the observed value of 139 for an estimated two-sided significance level of approximately 0.13. In contrast to the binomial test, by conventional standards, the null hypothesis cannot be rejected by the rotation test. It is not possible to calculate a priori power estimates for the sperm whale data set, since

we do not know the true process generating the buzz time series data, and thus we can not produce the simulated data needed for power estimation.

Discussion

The rotation test is a general nonparametric approach that can be used when data exhibit serial dependence. The purpose of this paper has been to describe, evaluate, and illustrate this test in the specific context of testing for a treatment effect on the rate of a behavioural point process. We have shown that, in this context, the rotation test works well, maintaining the nominal significance level while providing high power when the data do not follow a Poisson process. In contrast, the binomial test is invalid in this case.

A common approach to analyzing behavioural point processes is to reduce the data to empirical rates within time bins (e.g, Cherry 1989; Mooring 1995; Paredes et al. 2005; Fernández-Juricic & Tran 2007). As a general proposition, binning point process data entails a loss of power (Dean & Balshaw 1997) and is not recommended. Moreover, the analysis of binned data is also affected by non-Poisson behaviour in the underlying point process. Briefly, if the underlying point process is Poisson, then the counts within bins will have Poisson distributions. Statistical methods for analyzing Poisson count data are reviewed in McCullagh & Nelder (1989). However, if the underlying point process is not Poisson, then the distribution of bin counts is also not Poisson and the results of these methods can be misleading (Paul & Banerjee 1998). A common alternative to the Poisson distribution for count data is the negative binomial distribution. Parametric methods for analyzing negative binomial data are

available (e.g., Barnwal & Paul 1988; Paul & Banerjee 1998). The rotation test provides a nonparametric alternative.

Turning to the results of the previous section, it is clear that no general conclusion about the effect of airgun noise on sperm whales can be drawn from the results of a single test. It is also worth pointing out that the hypothesized effect of airgun nose is a *reduction* in foraging. Had a one-sided test for such a reduction been performed, the significance level would have been around 0.065 which, in light of power considerations, is certainly suggestive of an effect.

Finally, although this paper has focused on the rotation test in the context of analyzing behavioural point process data, the same general method could be used in other situations. For example, Shapiro (2008) used a rotation test to determine whether the frequencies of different types of vocalizations in killer whales differed between behavioural states. In this case, the approach was used to account for serial dependence in vocalization type.

Acknowledgements

We are grateful to Peter Tyack for advice and helpful comments. We thank the crews and science parties of the research cruises on which sperm whale airgun exposure data were collected, especially Peter Tyack and Patrick Miller. Funding for the sperm whale experiments was provided by the Office of Naval Research, the U.S. Department of the Interior Minerals Management Service Cooperative Agreements Nos. 1435-01-02-CA-85186 and NA87RJ0445, and the Industry Research Funding Coalition. All approaches to animals for tagging were made

following the conditions of NMFS research permits 981-1578 and 981-1707. The Woods Hole Oceanographic Institution Animal Care and Use Committee approved this research.

References

Barnwal, R.K. & Paul, S.R. 1988. Analysis of one-way layout of count data with negative binomial variation. *Biometrika*, 75, 215-222.

Caldwell, J. & Dragoset, W. 2000. A brief overview of seismic air-gun arrays. *The Leading Edge*, 19, 898-902.

Cherry, J. A. 1989. Ultrasonic Vocalizations by Male Hamsters - Parameters of Calling and Effects of Playbacks on Female Behavior. *Animal Behaviour*, 38, 138-153.

Cox, D. R. & Lewis, P. A. W. 1978. *The statistical analysis of series of events*, 2nd edn. London: Chapman & Hall.

Dean, C.B . & Balshaw, R. 1997. Efficiency lost in analyzing counts rather than event times in Poisson and over-dispersed Poisson regression models. *Journal of the American Statistical Association,* 92, 1387-1398.

Fernández-Juricic, E. & Tran, E. 2007. Changes in vigilance and foraging behaviour with light intensity and their effects on food intake and predator detection in house finches. *Animal Behaviour,* 74, 1381-1390.

Gordon, J., Gillespie, D., Potter, J., Frantzis, A., Simmonds, M. P., Swift, R. & Thompson, D. 2003. A review of the effects of seismic surveys on marine mammals. *Marine Technology Society Journal*, 37**,** 16-34.

Haccou, P. & Meelis, E. 1992. *Statistical Analysis of Behavioural Data.* New York: Oxford University Press.

Harkness, R. D. & Isham, V. 1983. A bivariate spatial point pattern of ants' nests. *Applied Statistics*, 32, 293-303.

Jochens, A. E. & Biggs, D. C. 2003. Sperm whale seismic study in the Gulf of

Mexico: Annual report, year 1. New Orleans, LA: U.S. Department of the Interior Minerals management service, Gulf of Mexico OCS Region.

Jochens, A. E. & Biggs, D. C. 2004. Sperm whale seismic study in the Gulf of Mexico: Annual report, year 2. New Orleans, LA: U.S. Department of the Interior Minerals management service, Gulf of Mexico OCS Region.

Johnson, M. P. & Tyack, P. L. 2003. A digital acoustic recording tag for measuring the response of wild marine animals to sound. *IEEE Journal of Oceanic Engineering*, 28, 3-12.

Lawrance, A. J. & Lewis, P. A. W. 1979. Simulation of some autoregressive Markovian sequences of positive random variables. In: *Proceedings of the IEEE 11th Conference on Winter Simulation*, pp. 301-307. San Diego, CA, USA: IEEE.

Madsen, P. T., Johnson, M., Miller, P. J. O., Soto, N. A., Lynch, J. & Tyack, P. 2006. Quantitative measures of air-gun pulses recorded on sperm whales (*Physeter macrocephalus*) using acoustic tags during controlled exposure experiments. *Journal of the Acoustical Society of America*, 120, 2366-2379.

McCullagh, P. and J. A. Nelder. 1989. *Generalized Linear Models.* New York: Chapman & Hall.

Miller, P. J. O., Johnson, M. P. & Tyack, P. L. 2004a. Sperm whale behaviour indicates the use of echolocation click buzzes 'creaks' in prey capture. *Proceedings of the Royal Society of London Series B-Biological Sciences*, 271**,** 2239-2247.

Miller, P.J.O., Shapiro, A.D., Tyack, P.L. & Solow, A.R. 2004b. Call-type matching in vocal exchanges of free-ranging resident killer whales, *Orcinus orca. Animal Behaviour*, 67, 1099-1107.

Mooring, M. S. 1995. The effect of tick challenge on grooming rate by impala.

Animal Behaviour, 50**,** 377-392.

Paredes, R., Jones, I. L. & Boness, D. J. 2005. Reduced parental care, compensatory behaviour and reproductive costs of thick-billed murres equipped with data loggers. *Animal Behaviour*, 69, 197-208.

Paul, S.R. and Banerjee, T. 1998. Analysis of two-way layout of count data involving multiple counts in each cell. *Journal of the American Statistical Association*, 93, 1419-1429.

Richardson, W. J., Greene, C. R., Jr., Malme, C. I. & Thompson, D. H. 1995. *Marine Mammals and Noise*. San Diego, CA: Academic Press.

Shapiro, A.D. 2008. Orchestration: The movement and vocal behavior of free-ranging Norwegian killer whales (*Orcinus orca*). PhD thesis, MIT/WHOI.

Sibly, R.M., Nott, H.M.R. & Fletcher, D.J. 1990. Splitting behaviour into bouts. *Animal Behaviour*, 39**,** 63-69.

Slater, P.J. & Lester, N.P. 1982. Minimising errors in splitting behavior into bouts. *Behaviour*, 79, 153-161.

Stephens, M. A. 1986. Tests for the uniform distribution. In: *Goodness-of-fit techniques* (Ed. by D'Agostino, R. & Stephens, M. A.), pp. 331-365. Boca Raton, FL: CRC Press.

Thomas, M. 1949. A generalization of Poisson's binomial limit for use in ecology. *Biometrika*, 36**,** 18-25.

Watwood, S. L., Miller, P.J.O., Johnson, M., Madsen, P.T. & Tyack, P.L. 2006. Deep-diving foraging behaviour of sperm whales (*Physeter macrocephalus*). *Journal of Animal Ecology*, 75, 814–825.

Whitehead, H. 2003. *Sperm Whales: Social Evolution in the Ocean.* Chicago, IL: The University of Chicago Press.

Tables

Table 1. Validity of the binomial and rotation tests

	overall mean rate	
	500	1000
Poisson		
binomial	0.05	0.05
rotation	0.042	0.054
Thomas		
binomial	0.221	0.233
rotation	0.045	0.049
EAR		
binomial	0.247	0.251
rotation	0.052	0.052

The rate at which the null hypothesis of no treatment effect was falsely rejected in testing at the 0.05 significance level using the binomial test and the rotation test for data simulated from the Poisson, Thomas, and EAR models with overall mean rates of 500 and 1000. For the Thomas model, $\theta = 1$ and for the EAR model $\rho = 0.5$. Results are based on 1000 simulations except for the binomial test under the Poisson model where the theoretical result is given.

Table 2. Power of the rotation test

	overall mean rate					
	500			1000		
	f			f		
	1.5	2	3	1.5	2	3
Poisson						
binomial	1	1	1	1	1	1
rotation	0.61	0.90	0.99	0.82	0.98	1
Thomas						
rotation	0.34	0.63	0.88	0.56	0.86	0.97
EAR						
rotation	0.37	0.64	0.86	0.54	0.83	0.98

The power of the rotation test at the 0.05 significance level for data simulated under the Poisson, Thomas, and EAR models when the mean rate under treatment is a factor *f* greater than that under control and when the overall mean rate is fixed at 500 and 1000. For the Thomas model, we always used $\theta = 1$; for the EAR model we always used $\rho = 0.5$. For the Poisson model, results are also given for the binomial test. Results are based on 1000 simulations.

Table 3. Minimum detectable effect levels.

	overall mean rate	
	500	1000
Poisson		
binomial	1.3	1.2
rotation	1.7	1.5
Thomas		
rotation	2.5	1.8
EAR		
rotation	2.7	2.0

The minimum detectable effect size $f_{\min}$ – defined as the value of *f* for which the test at 0.05 significance level achieves a power of 0.8 – for the cases considered in Table 2. Results are based on 1000 simulations.

Figure Legends

Figure 1. Top panel: Dive profile of the tagged sperm whale. The grey line indicates whale depth, and black circles indicate the times of echolocation buzzes. Airgun exposure periods are shaded gray. Black lines connecting the top and bottom panels illustrate how dive ascents, descents and surface periods were cut from the dataset to produce the buzz time-series we analyzed. Only foraging periods (indicated by yellow shading) were included in the buzz time-series. Bottom Panel: Time-series of echolocation buzzes produced by the sperm whale during foraging periods. Black dots indicate the times of buzzes, and gray shaded areas indicate airgun exposure periods.

Figure 2. Histogram of values for N_C, the number of creaks during the control period, obtained in 10,000 rotations of the sperm whale dataset. (The value of N_C was 139 for the original, non-rotated dataset.)

Figures

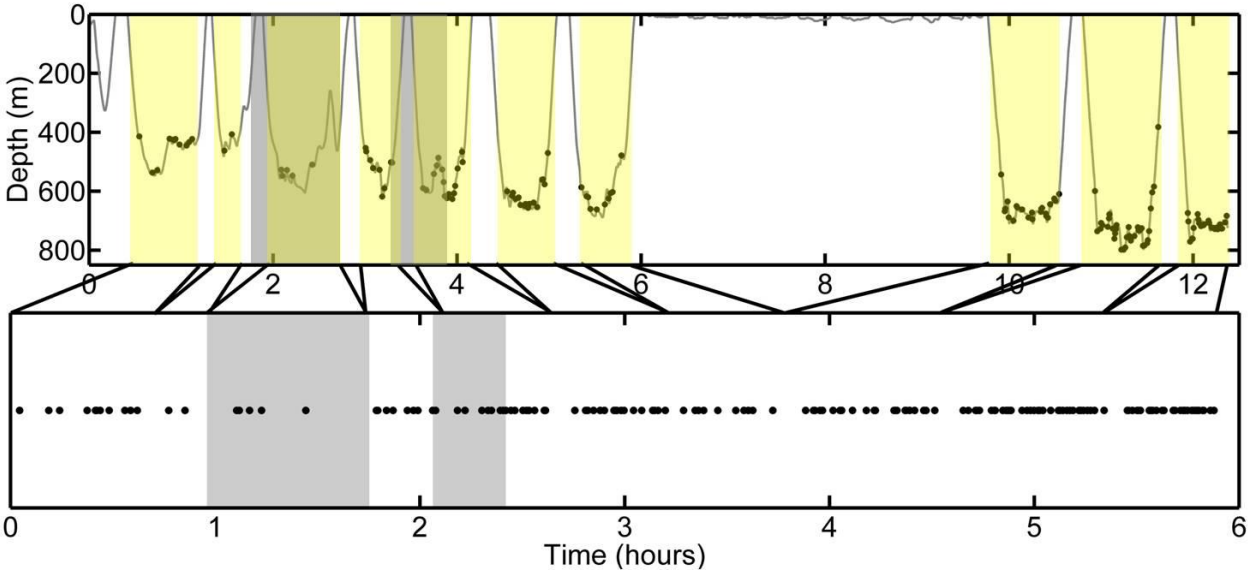
Depth (m)
0
200
400
600
800
0
2
4
6
8
10
12
0
1
2
3
4
5
6
Time (hours)

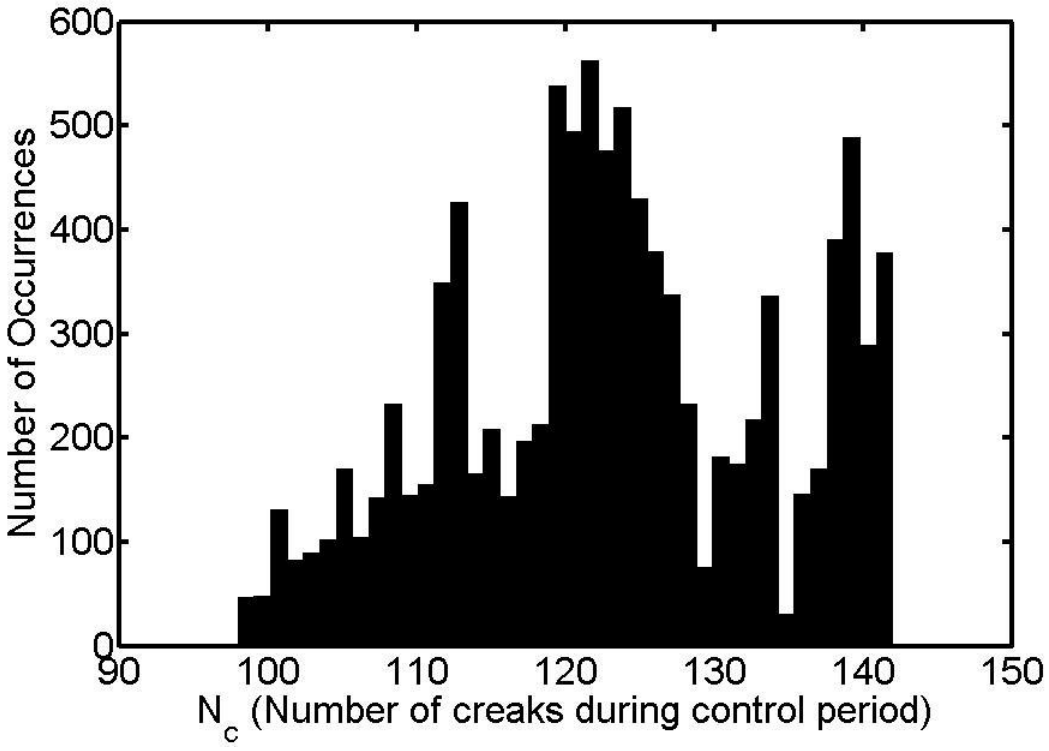
Number of Occurrences
600
500
400
300
200
100
0
90
100
110
120
130
140
150
N_c (Number of creaks during control period)

Appendix B: Matlab Code

Matlab Code Used in Chapter 2 (Porpoise Prey Capture Analysis)

Click Extraction and Measurement of Click Properties

```
%clickanal_june10b.m
%Data analysis script for analyzing the time surrounding prey capture
%events from F&B Jan 2008 dataset.  Extracts clicks, measures click
%parameters (level, frequency characteristics, duration, etc.), and %saves data
as matlab data matrices.
%
%Stacy DeRuiter, June 2008

%************************************************************************
%PRELIMINARIES
%************************************************************************

%set the paths for tag tools (tag data and audio data file locations)
settagpath('audio','E:\TagData', 'prh', 'C:\dtag\metadata\prh',… 'audit',
'C:\dtag\metadata\audit', 'raw' , 'C:\dtag\metadata\raw',…
'cal', 'C:\dtag\metadata\cals' ) ;

%if CHECKING = 0 then the program just runs for all trials. if CHECKING
%is not zero then you will have to inspect all click detection output
%in figures, then close the figures to approve them and continue analysis.
CHECKING = 0;

%load timing data
%load data matrix - includes times of prey capture events
load capturetimedata
```

```
%load data vector - indicates which of the 71 trials had successful
%prey captures
load capture_indices
dur = 30; %duration in seconds of clip to extract (half before and half
%after the capture event)
thr = 3e-04; %click detection threshold (wavfile level of the envelope
%of the signal)
blank = 0.0013; %blanking time between clicks (time after a click
%during which no subsequent clicks can be detected)
%(peak-peak sensitivity of the tag is 197dB re 1uPa)
cal = 191; %PEAK (not PP) sensitivity of tag in dB re 1 wavfile-unit per uPa

%**********************************************************************
%TAG DATA ANALYSIS, CLICK DETECTION
%**********************************************************************

%Repeat the following procedure each prey capture trial.
for k = 1:length(capture_indices)
   %analyze only the 67 successful captures
   n = capture_indices(k); %n is the trial # out of 71 for the kth
   %successful capture
   clear x3 afs rcue b a x2 x S w m toad near T TT Tcl TTcl
   %1.  Extract audio data from dur/2 sec before and dur/2 sec after
   %prey capture event
   [x3,afs,rcue] = tagwavread(tagids(n,:),Tcapture_cst(n) - …
   dur/2 , dur);
   %2a. high pass filter for DC, etc.
   [b,a] = butter(6,500/(0.5*afs),'high'); %6-pole Butterworth high
   %pass filter at 500Hz
```

```
x2 = filtfilt(b,a,x3); %apply the filter to the signal
%2b. band pass filter signal for plotting clicks and measuring
%click properties
[b,a] = butter(4,[100000/(0.5*afs) 200000/(0.5*afs)]); %4 pole
%bandpass Butterworth filter at 100 and 200 kHz
x = filtfilt(b,a,x2); %apply the filter to the signal
for ch = 1:2 %repeat analysis for each channel
   clear x3 gsig y envy emax d z r p p2 p1 q tsig clickwf…
   clickwf_filt toad near ee R ICIs
   disp(['prey capture trial number ' num2str(n) ' of '…
   num2str(length(Tcapture_cst)) ', channel ' num2str(ch)]);
   %display on screen the trial number and channel number of the
   %data to be analyzed
%3.  Run a click detector on the data.
%run modified peter madsen envelope click detector
[tsig, clickwf, clickwf_filt] = clickxtract_sdr10b( x2(:,ch),…
x(:,ch), thr, blank, afs);
tsig = tsig(:); %reshape tsig so it's the right shape for input to
%clickxtract_sdr
%If CHECKING ~=0, plot the resulting detected clicks on the data
%waveform to check click detector accuracy
if CHECKING ~=0
   for i = 1:dur %plot detected clicks on filtered waveform.  One
      %second at a time or memory will run out.
      %plot wavfile data (bandpass filtered tag data)
      V = figure(3); clf; plot((((i-1)*afs)+1:i*afs)./afs,…
            x(((i-1)*afs)+1:i*afs,ch) ,'k' , 'LineWidth', 1);
      hold on;
      %plot detected clicks on same figure
```

```
        plot(tsig, x(round(tsig*afs),ch), 'r*','MarkerSize', 10 );
        xlim([((i-1)*afs)+1,i*afs]./afs); %plot time series of data
         %with detected clicks as asterisks
        hold off;
        waitfor(V); % user must close figure to finish inspection
         %and move on to next time period
      end
   end
   %4. Measure click properties:
   %A. Level, Frequency and Duration measurements
   R = clickparams_sdr(clickwf_filt,afs, [],NaN, cal); %Mark Johnson
   %click measurement file (modified).  use on filtered data set!
   %B. Inter-click interval measurements
   ICIs(:,1) = [tsig - dur/2]; %col 1 of ICIs contains the time cues
   %of clicks (in seconds from capture -- negative is before and
   %positive is after))
   ee = diff(tsig); %calculate the ICI before each click
   ICIs(:,2) = [ee(1); ee]; %col 2 of ICIs contains the inter-click
   %interval from the preceding click to the one at t = ICIs(col 1)
   R.clickt = ICIs(:,1); %add the time cue data...
   R.ici = ICIs(:,2); %and the ICI data to the R data matrix.

%************************************************************************
%SAVE DATA
%************************************************************************

   %save data
   %save click parameter data
   save(['captureB' num2str(n) 'ch' num2str(ch)], 'R');
```

```
    %save waveform data
    save(['waves_captureB' num2str(n) 'ch' num2str(ch)],…
    'clickwf_filt', 'clickwf');
    end
end
```

Envelope-based Click Detector

```
function [tsig, clickwf, clickwf_filt] = clickxtract_sdr10b( x, x_filt, thr, blank, afs)
%extract porpoise clicks from pdtag recordings.
%from Michael Hansen (who got it from Peter Madsen), summer 2007.
%Modified by Stacy DeRuiter.
%
%INPUT VARIABLES: x is the input signal (wavfile data from tagwavread)
%x_filt is x, filtered between 100-200 kHz with a 4-pole Butterworth
%bandpass filter
%thr is the threshold for extracting clicks (signal level in envelope
%of signal) afs is the audio sampling frequency for the x and x_filt files.
%blank is the blanking time between clicks (after a detected click, the
%program will skip ahead "blank" seconds before searching for more
%clicks)
%
%OUTPUT VARIABLES: tsig is a vector of the times of detected clicks (in
%seconds since start of x)
%clickwf, clickwf_filt -- each column of clickwf or clickwf_filt is a
%clip of wavfile data containing a detected click (it is dt seconds
%long – dt is a variable defined in the function, below)

%**************************************************************************
%INITIALIZE AND DEFINE VARIABLES
```

```
%************************************************************************

clear sig dt int jump N2 esig clickwf tsig
siz=size(x_filt);            % size of input file in [samples, channels]
dt=0.001; %[seconds]   % Length of interval which is read from
                              % input file each time
int=round(dt*afs);          % Length of interval in samples
jump=round(blank*afs);% Start length of jump once a peak is
                              %detected
N1=1;                         % Starting extracting from sample 1
N2=N1+int;                  % N2 is the end sample interval in the
                              %desired segment.
p=0;                          % the variable p keeps track of number of
                              %detected clicks
q = 1;
lastici = 0.1;               % the previous inter-click interval (this
                              %is just a starting value to initialize)
lastp = 2*thr;              % the previous click's peak-of-envelope
                             %value (this is just a starting value to
                             %initialize)
ptrack = [ lastp lastp lastp];
icitrack = [ lastici lastici lastici];
click = 0;                  % index variable for keeping track of lastp

%************************************************************************
%DETECT CLICKS
%************************************************************************

while N2 < siz(1)                % Go on until end of file is reached
```

```
clear sig esig stime
sig=x_filt(N1:N2);      % Read a sound file segment
esig=sqrt(sig.^2+imag(hilbert(sig)).^2);  % Generate envelope
ip=find(esig==max(esig));% Find sample value for peak of envelope
thisici = ((N1+ip)/afs)-(click(q)/afs); %calculate the inter-click
                                        %interval before this click
if esig(ip)>thr && (esig(ip)>=lastp/2 && thisici >= lastici/5)
   %if click is above thresh, and at least 20% as loud as the last
   %one, and the new ici is not less than 1/5 of the previous
   %one...
   p=p+1;          % Click is detected
   q = p;          % index variable for keeping track of lastp
   stime = max([1,round((N1+ip)/afs*afs)-round((dt/2)*afs)]);
   %start time of click is dt/2 seconds before the time at which
   %max envelope level is attained, or the first sample in the
   %clip if max-dt/2 is before the start of the clip
      clickwf(1:length(x(stime:min(length(x),…
      stime+round(dt*afs)))),p)=x(stime:min(length(x),…
      stime+round(dt*afs)));
   %extract a clip from x and place it in column p of clickwf
   clickwf_filt(1:length(x_filt(stime:min(length(x),…
      stime+round(dt*afs)))),p) = x_filt(stime:min(length(x),…
      stime+round(dt*afs)));
   %extract a clip from x and place it in column p of clickwf_filt
   click(p)=N1+ip; %keep track of the time (in samples) of the
                   %detected click in the variable "click"
   tsig(:,p)=(click(p)/afs); %keep track of the time (in seconds)
                             %of the detected click in the
                             %variable "tsig"
```

```
    N1=N1+ip+jump; %increment N1 to give the start time to begin
                          %looking for the next click
    if esig(ip) < 3*mean(ptrack)%change lastp to the current click
       %value, unless this is a suddely really loud click >3x
       %louder than the last
      ptrack = [ptrack(2:3),esig(ip)]; %redefine ptrack so it
                                          %contains the last 3 click levels
      lastp = mean(ptrack); %calculate lastp (mean of level of
                                  %last 3 clicks).
    end
    if p > 1 && thisici < 0.1 %as long as the current click's ici
                                 %is lesss than 100msec,
       icitrack = [icitrack(2:3), thisici];%add it to icitrack.
       lastici = mean(icitrack); %calculate lastici (mean of ici
                                    %of last 3 clicks).
    end
elseif esig(ip)>thr && thisici > 2*lastici %also keep quiet clicks
    %after pauses/that are not echoes/reflections
    p=p+1;          % Click is detected
    q = p;          % index variable for keeping track of lastp
    stime = max([1,round((N1+ip)/afs*afs)-round((dt/2)*afs)]);
    %start time of click is dt/2 seconds before the time at which
    %max envelope level is attained, or the first sample in the
    %clip if max-dt/2 is before the start of the clip
    clickwf(1:length(x(stime:min(length(x),…
        stime+round(dt*afs)))),p)=x(stime:min(length(x),…
        stime+round(dt*afs)));
    %extract a clip from x and place it in column p of clickwf
    clickwf_filt(1:length(x_filt(stime:min(length(x),…
```

```
        stime+round(dt*afs)))),p) = x_filt(stime:min(length(x),…
        stime+round(dt*afs)));
    %extract a clip from x and place it in column p of clickwf_filt
    click(p)=N1+ip; %keep track of the time (in samples) of the
    %detected click in the variable "click"
    tsig(:,p)=(click(p)/afs); %keep track of the time (in seconds)
    %of the detected click in the variable "tsig"
    N1=N1+ip+jump; %increment N1 to give the start time to begin
    %looking for the next click
    ptrack = [esig(ip),esig(ip),esig(ip)];   %change lastp and
    %ptrack to the current click value,
    %so that subsequent quiet clicks will be detected
    lastp = mean(ptrack);
    icitrack = [0.1 0.1 0.1]; %reset icitrack and lastici to
    %default values, since a long pause has occurred
    lastici = 0.1;
elseif esig(ip)>thr && (esig(ip)>=2*lastp && thisici < lastici/5)
    %also keep clicks that are more than 2 times louder
    %than the previous click, even if the ICI is short.
    %this helps correct the program if it begins to detect surface
    %reflections rather than "main" outgoing clicks.
    p=p+1;          % Click is detected
    q = p;          % index variable for keeping track of lastp
    stime = max([1,round((N1+ip)/afs*afs)-round((dt/2)*afs)]);
    %start time of click is dt/2 seconds before the time at which
    %max envelope level is attained, or the first sample in the
    %clip if max-dt/2 is before the start of the clip
    clickwf(1:length(x(stime:min(length(x),…
        stime+round(dt*afs)))),p)=x(stime:min(length(x),…
```

```
        stime+round(dt*afs)));
    %extract a clip from x and place it in column p of clickwf
    clickwf_filt(1:length(x_filt(stime:min(length(x),…
        stime+round(dt*afs)))),p) = x_filt(stime:min(length(x),…
        stime+round(dt*afs)));
    %extract a clip from x and place it in column p of clickwf_filt
    %click(p)=N1+ip; keep track of the time (in samples) of the
    %detected click in the variable "click"
    tsig(:,p)=(click(p)/afs); %keep track of the time (in seconds)
    %of the detected click in the variable "tsig"
    N1=N1+ip+jump; %increment N1 to give the start time to begin
    %looking for the next click
    if esig(ip) < 3*mean(ptrack)%change lastp to the current click
    %value, unless this is a suddely really loud click >3x
    %louder than the last
       ptrack = [ptrack(2:3),esig(ip)];
       lastp = mean(ptrack);
    end
    %do not change lastici or icitrack in this case.
  else
    N1=N1+int; %if no click was detected, increment N1 to set the
    %start time of the next segment of the wavfile to search.
  end
  N2=N1+int; %set the end time of the next segment of the wavfile to
  %search.
end
```

Matlab Code Used in Chapter 3 (Transmission Loss in Porpoise Habitats)

Click Extraction from Data Wavefiles

```
function clickxtract_sdr(thr)
%Script to extract click times and click waveform wavefile data from
%porpoise transmission loss recordings (in Denmark or Grand Manan).
%from Michael Hansen (who got it from Peter Madsen), summer 2007.
%Modified by Stacy DeRuiter, 2007-2008
%Input variable thr is the threshold (envelope level in wavfile) for click detection

%**********************************************************************
%INITIALIZE AND DEFINE VARIABLES
%**********************************************************************

clear file sig1 fs nbits dt int jump N2 sig esig gsig
%before running this script, open data wav file in Adobe audition.
%Filter it with a 4-pole bandpass Butterworth filter between 100-166 kHz.
%In Audition, select and copy a segment of the file in which to detect clicks.
file = 'c:\Temp\CoolClipboard.wav'; % Path to input file from Adobe Audition
fid1=fopen(file);
[sig1 fs nbits]=wavread(file); % read input file
%  (optional) save the data file as a wavfile, so you know what you
% analyzed
% wavwrite(sig1,fs,16,'c:/porpoisetldata/test.wav')
siz=wavread(file,'size')   % Read size of input file
dt=0.001; %[seconds]       % Length of interval which is read from
                           % input file each time
int=dt*fs;                 % Length of interval in samples
jump=round(0.009*fs);      % length of jump once a peak is detected
N1=1;                  % Start sample number of the wavfile segment
                       % to be analyzed
```

```
N2=N1+int;              % N2 is the end sample number of the wavfile
                        % segment to be analyzed.
p=0;                    % Keeps tracks of number of detected clicks

%************************************************************************
%DETECT CLICKS
%************************************************************************

while N2 < siz(1),          % Go on until end of file is reached
   % Read a sound file segment
   [sig,fs,nbits]=wavread('c:/porpoisetldata/test.wav',[N1 N2]);
   % Generate signal envelope
   esig=sqrt(sig.^2+imag(hilbert(sig)).^2);
   % Find sample value for peak of envelope
   ip=find(esig==max(esig));
   if esig(ip)>thr,% If envelope level in the segment being
                   %analyzed is > thr,
      p=p+1                % Click is detected
      stime = max([1,N1+ip-round(0.0005*fs)]);
      %stime is the start time for extracting click data, in samples.
      %stime is 0.5 msec before the time at which envelope level
      %peaks
      gsig(:,p)=wavread(file,[ stime stime+round(0.0015*fs)]); %each
      %column of gsig is a 1.5-msec-long segment of wavfile data for
      %the detected click
      click(p)=N1+ip; %click is the time, in samples, at which
      %envelope level peaks (the click time)
      tsig(:,p)=(click(p)/fs); %sig is the click time in seconds
      %since start of file
```

```
        N1=N1+ip+jump; %increment N1 (file segment start time) to
        %examine the next wavfile segment
    else %if no click was detected
        N1=N1+int; %increment N1 (file segment start time) to examine
        %the next wavfile segment
    end
    N2=N1+int;%increment N2 (file segment end time) to examine the next
    %wavfile segment
end
plot(gsig) %plot detected click waveforms to check accuracy of click
%detection

%**********************************************************************
%SAVE DATA
%**********************************************************************

% save the detected click waveform data for level analysis by
% TLauto_sdr script
save 'c:\porpoisetldata\click1', gsig;
st = fclose('all') %close all files used
```

Click Level Determination (Grand Manan Datasets)

```
function TLauto_sdr(location, rr, zr)
%Analysis tool to determine peak-peak, RMS, and energy levels of clicks
%detected by clickxtract_sdr script.  For Grand Manan porpoise
%transmission loss datasets.
%Written by Peter Madsen, 27 Dec. 2006
%Modified by Stacy DeRuiter, July 2007, Jan 2008
%
```

```
%Input Variables:
% rr is source-receiver range
% zr is receiver depth
% CHOOSE ONE LOCATION: You can enter the number or the string.
% 1 = location1 = ['RL080806IronLady'];
% 2 = location2 = ['RL081006Roma'];
% 3 = location3 = ['RL081106PetitsCove'];
% 4 = location4 = ['RL081106Roma'];
% 5 = location5 = ['RL081206WhaleCove'];
% 6 = location6 = ['RL081206WhaleCoveB'];
% 7 = location7 = ['RL081306LongIsland'];

%**********************************************************************
%INITIALIZE AND DEFINE VARIABLES
%**********************************************************************

clear gain hp ppclip d z r x y p1 p2 envy emax RLpp RLE RLrms…
clicks_analyzed data data_upa mean_levels mean_upa cal gsig fs
names = {'RL080806IronLady','RL081006Roma', 'RL081106PetitsCove',…
'RL081106Roma', 'RL081206WhaleCove','RL081206WhaleCoveB',…
'RL081306LongIsland'};
if ~isstr(location)
   location = names{location};
end

%Information for click extraction and TL calculations
if strcmp(location, names{1})
   %Iron Lady, 8/8/06  records used:  1,3,5,11,12,16
   if zr == 5
```

```
    if rr == 5
        gain = 32; %gain of recording system
        hp = 4014; %hydrophone used (4014 or 4034)
        ppclip = 10; % pp clip level of recording
    elseif rr ==10
        gain = 32; %gain of recording system
        hp = 4014; %hydrophone used (4014 or 4034)
        ppclip = 4; % pp clip level of recording
    elseif rr == 25
        gain = 32; %gain of recording system
        hp = 4014; %hydrophone used (4014 or 4034)
        ppclip = 2; % pp clip level of recording
    elseif rr == 50
        gain = 32; %gain of recording system
        hp = 4014; %hydrophone used (4014 or 4034)
        ppclip = 2; % pp clip level of recording
    elseif rr == 100
        gain = 32; %gain of recording system
        hp = 4014; %hydrophone used (4014 or 4034)
        ppclip = 1; % pp clip level of recording
    elseif rr == 200
        gain = 32; %gain of recording system
        hp = 4014; %hydrophone used (4014 or 4034)
        ppclip = 0.2; % pp clip level of recording
    end
elseif zr ==3
    if rr == 5
        gain = 40; %gain of recording system
        hp = 4034; %hydrophone used (4014 or 4034)
```

```
            ppclip = 1; % pp clip level of recording
        elseif rr == 10
            gain = 60; %gain of recording system
            hp = 4034; %hydrophone used (4014 or 4034)
            ppclip = 4; % pp clip level of recording
        elseif rr == 25
            gain = 60; %gain of recording system
            hp = 4034; %hydrophone used (4014 or 4034)
            ppclip = 4; % pp clip level of recording
        elseif rr == 50
            gain = 60; %gain of recording system
            hp = 4034; %hydrophone used (4014 or 4034)
            ppclip = 1; % pp clip level of recording
        elseif rr == 100
            gain = 60; %gain of recording system
            hp = 4034; %hydrophone used (4014 or 4034)
            ppclip = 1; % pp clip level of recording
        elseif rr == 200
            gain = 60; %gain of recording system
            hp = 4034; %hydrophone used (4014 or 4034)
            ppclip = 1; % pp clip level of recording
        end
    end
elseif strcmp(location, names{2})
%Roma, 8/10/06  records used:  24, 25, 27, 28 (ch2), 29, 31, 33
    if zr ==5
        if rr ==5
            gain = 32; %gain of recording system
            hp = 4014; %hydrophone used (4014 or 4034)
```

```
        ppclip = 10; % pp clip level of recording
    elseif rr == 10
        gain = 32; %gain of recording system
        hp = 4014; %hydrophone used (4014 or 4034)
        ppclip = 4; % pp clip level of recording
    elseif rr == 25
        gain = 32; %gain of recording system
        hp = 4014; %hydrophone used (4014 or 4034)
        ppclip = 2; % pp clip level of recording
    elseif rr == 50
        gain = 32; %gain of recording system
        hp = 4014; %hydrophone used (4014 or 4034)
        ppclip = 2; % pp clip level of recording
    elseif rr == 100
        gain = 32; %gain of recording system
        hp = 4014; %hydrophone used (4014 or 4034)
        ppclip = 0.2; % pp clip level of recording
    elseif rr == 200
        gain = 32; %gain of recording system
        hp = 4014; %hydrophone used (4014 or 4034)
        ppclip = 0.2; % pp clip level of recording
    end
elseif zr ==3
    if rr == 5
        gain = 40; %gain of recording system
        hp = 4034; %hydrophone used (4014 or 4034)
        ppclip = 1; % pp clip level of recording
    elseif rr == 10
        gain = 60; %gain of recording system
```

```
            hp = 4034; %hydrophone used (4014 or 4034)
            ppclip = 4; % pp clip level of recording
        elseif rr == 25
            gain = 60; %gain of recording system
            hp = 4034; %hydrophone used (4014 or 4034)
            ppclip = 2; % pp clip level of recording
        elseif rr == 50
            gain = 60; %gain of recording system
            hp = 4034; %hydrophone used (4014 or 4034)
            ppclip = 1; % pp clip level of recording
        elseif rr == 100
            gain = 60; %gain of recording system
            hp = 4034; %hydrophone used (4014 or 4034)
            ppclip = 1; % pp clip level of recording
        elseif rr == 200
            gain = 60; %gain of recording system
            hp = 4034; %hydrophone used (4014 or 4034)
            ppclip = 1; % pp clip level of recording
        end
    end
elseif strcmp(location, names{3})
    %Petit's Cove, 8/11/06 records used: 18,20,21,22,23,24
    if zr ==5
        if rr == 5
            gain = 32; %gain of recording system
            hp = 4014; %hydrophone used (4014 or 4034)
            ppclip = 10; % pp clip level of recording
        elseif rr == 10
            gain = 32; %gain of recording system
```

```
        hp = 4014; %hydrophone used (4014 or 4034)
        ppclip = 4; % pp clip level of recording
    elseif rr == 25
        gain = 32; %gain of recording system
        hp = 4014; %hydrophone used (4014 or 4034)
        ppclip = 2; % pp clip level of recording
    elseif rr == 50
        gain = 32; %gain of recording system
        hp = 4014; %hydrophone used (4014 or 4034)
        ppclip = 1; % pp clip level of recording
    elseif rr == 100
        gain = 32; %gain of recording system
        hp = 4014; %hydrophone used (4014 or 4034)
        ppclip = 0.4; % pp clip level of recording
    elseif rr == 200
        gain = 32; %gain of recording system
        hp = 4014; %hydrophone used (4014 or 4034)
        ppclip = 0.2; % pp clip level of recording
    end
elseif zr ==3
    if rr == 5
        gain = 40; %gain of recording system
        hp = 4034; %hydrophone used (4014 or 4034)
        ppclip = 1; % pp clip level of recording
    elseif rr == 10
        gain = 60; %gain of recording system
        hp = 4034; %hydrophone used (4014 or 4034)
        ppclip = 4; % pp clip level of recording
    elseif rr == 25
```

```
            gain = 60; %gain of recording system
            hp = 4034; %hydrophone used (4014 or 4034)
            ppclip = 2; % pp clip level of recording
        elseif rr == 50
            gain = 60; %gain of recording system
            hp = 4034; %hydrophone used (4014 or 4034)
            ppclip = 1; % pp clip level of recording
        elseif rr == 100
            gain = 60; %gain of recording system
            hp = 4034; %hydrophone used (4014 or 4034)
            ppclip = 1; % pp clip level of recording
        elseif rr == 200
            gain = 60; %gain of recording system
            hp = 4034; %hydrophone used (4014 or 4034)
            ppclip = 1; % pp clip level of recording
        end
    end
elseif strcmp(location,names{4})
    %Roma, 8/11/06 records used: 0,3,6,7,9,12
    if zr ==5
        if rr == 5
            gain = 32; %gain of recording system
            hp = 4014; %hydrophone used (4014 or 4034)
            ppclip = 10; % pp clip level of recording
        elseif rr == 10
            gain = 32; %gain of recording system
            hp = 4014; %hydrophone used (4014 or 4034)
            ppclip = 4; % pp clip level of recording
        elseif rr == 25
```

```
        gain = 32; %gain of recording system
        hp = 4014; %hydrophone used (4014 or 4034)
        ppclip = 2; % pp clip level of recording
    elseif rr == 50
        gain = 32; %gain of recording system
        hp = 4014; %hydrophone used (4014 or 4034)
        ppclip = 1; % pp clip level of recording
    elseif rr == 100
        gain = 32; %gain of recording system
        hp = 4014; %hydrophone used (4014 or 4034)
        ppclip = 1; % pp clip level of recording
    elseif rr == 200
        gain = 32; %gain of recording system
        hp = 4014; %hydrophone used (4014 or 4034)
        ppclip = 0.2; % pp clip level of recording
    end
elseif zr ==3
    if rr == 5
        gain = 40; %gain of recording system
        hp = 4034; %hydrophone used (4014 or 4034)
        ppclip = 1; % pp clip level of recording
    elseif rr == 10
        gain = 60; %gain of recording system
        hp = 4034; %hydrophone used (4014 or 4034)
        ppclip = 4; % pp clip level of recording
    elseif rr == 25
        gain = 60; %gain of recording system
        hp = 4034; %hydrophone used (4014 or 4034)
        ppclip = 2; % pp clip level of recording
```

```
        elseif rr == 50
            gain = 60; %gain of recording system
            hp = 4034; %hydrophone used (4014 or 4034)
            ppclip = 2; % pp clip level of recording
        elseif rr == 100
            gain = 60; %gain of recording system
            hp = 4034; %hydrophone used (4014 or 4034)
            ppclip = 1; % pp clip level of recording
        elseif rr == 200
            gain = 60; %gain of recording system
            hp = 4034; %hydrophone used (4014 or 4034)
            ppclip = 1; % pp clip level of recording
        end
    end
elseif strcmp(location, names{5})
    %Whale Cove, 8/12/06 records used: 0 1 2 3 4 5 6
    if zr ==5
        if rr == 5
            gain = 32; %gain of recording system
            hp = 4014; %hydrophone used (4014 or 4034)
            ppclip = 10; % pp clip level of recording
        elseif rr == 10
            gain = 32; %gain of recording system
            hp = 4014; %hydrophone used (4014 or 4034)
            ppclip = 4; % pp clip level of recording
        elseif rr == 25
            gain = 32; %gain of recording system
            hp = 4014; %hydrophone used (4014 or 4034)
            ppclip = 2; % pp clip level of recording
```

```
    elseif rr == 50
        gain = 32; %gain of recording system
        hp = 4014; %hydrophone used (4014 or 4034)
        ppclip = 1; % pp clip level of recording
    elseif rr == 100
        gain = 32; %gain of recording system
        hp = 4014; %hydrophone used (4014 or 4034)
        ppclip = 0.4; % pp clip level of recording
    elseif rr == 200
        gain = 32; %gain of recording system
        hp = 4014; %hydrophone used (4014 or 4034)
        ppclip = 0.2; % pp clip level of recording
    elseif rr == 350
        gain = 32; %gain of recording system
        hp = 4014; %hydrophone used (4014 or 4034)
        ppclip = 0.2; % pp clip level of recording
    end
elseif zr ==3
    if rr == 5
        gain = 40; %gain of recording system
        hp = 4034; %hydrophone used (4014 or 4034)
        ppclip = 1; % pp clip level of recording
    elseif rr == 10
        gain = 60; %gain of recording system
        hp = 4034; %hydrophone used (4014 or 4034)
        ppclip = 4; % pp clip level of recording
    elseif rr == 25
        gain = 60; %gain of recording system
        hp = 4034; %hydrophone used (4014 or 4034)
```

```
        ppclip = 2; % pp clip level of recording
    elseif rr == 50
        gain = 60; %gain of recording system
        hp = 4034; %hydrophone used (4014 or 4034)
        ppclip = 1; % pp clip level of recording
    elseif rr == 100
        gain = 60; %gain of recording system
        hp = 4034; %hydrophone used (4014 or 4034)
        ppclip = 1; % pp clip level of recording
    elseif rr == 200
        gain = 60; %gain of recording system
        hp = 4034; %hydrophone used (4014 or 4034)
        ppclip = 1; % pp clip level of recording
    end
  end
elseif strcmp(location,names{6})
  %Whale Cove PART B, 8/12/06 records used: 25 23 22 19 17 15 6
  if zr ==5
    if rr == 5
        gain = 32; %gain of recording system
        hp = 4014; %hydrophone used (4014 or 4034)
        ppclip = 10; % pp clip level of recording
    elseif rr == 10
        gain = 32; %gain of recording system
        hp = 4014; %hydrophone used (4014 or 4034)
        ppclip = 4; % pp clip level of recording
    elseif rr == 25
        gain = 32; %gain of recording system
        hp = 4014; %hydrophone used (4014 or 4034)
```

```
        ppclip = 2; % pp clip level of recording
    elseif rr == 50
        gain = 32; %gain of recording system
        hp = 4014; %hydrophone used (4014 or 4034)
        ppclip = 1; % pp clip level of recording
    elseif rr == 100
        gain = 32; %gain of recording system
        hp = 4014; %hydrophone used (4014 or 4034)
        ppclip = 0.4; % pp clip level of recording
    elseif rr == 200
        gain = 32; %gain of recording system
        hp = 4014; %hydrophone used (4014 or 4034)
        ppclip = 0.2; % pp clip level of recording
    elseif rr == 350
        gain = 32; %gain of recording system
        hp = 4014; %hydrophone used (4014 or 4034)
        ppclip = 0.2; % pp clip level of recording
    end
elseif zr ==3
    if rr == 5
        gain = 40; %gain of recording system
        hp = 4034; %hydrophone used (4014 or 4034)
        ppclip = 2; % pp clip level of recording
    elseif rr == 10
        gain = 60; %gain of recording system
        hp = 4034; %hydrophone used (4014 or 4034)
        ppclip = 4; % pp clip level of recording
    elseif rr == 25
        gain = 60; %gain of recording system
```

```
        hp = 4034; %hydrophone used (4014 or 4034)
        ppclip = 2; % pp clip level of recording
    elseif rr == 50
        gain = 60; %gain of recording system
        hp = 4034; %hydrophone used (4014 or 4034)
        ppclip = 2; % pp clip level of recording
    elseif rr == 100
        gain = 60; %gain of recording system
        hp = 4034; %hydrophone used (4014 or 4034)
        ppclip = 1; % pp clip level of recording
    elseif rr == 200
        gain = 60; %gain of recording system
        hp = 4034; %hydrophone used (4014 or 4034)
        ppclip = 1; % pp clip level of recording
    end
  end
elseif strcmp(location, names{7})
  %Long Island, 8/13/06 records used:1 2 3 4 6 7
  if zr ==5
    if rr == 5
        gain = 32; %gain of recording system
        hp = 4014; %hydrophone used (4014 or 4034)
        ppclip = 10; % pp clip level of recording
    elseif rr == 10
        gain = 32; %gain of recording system
        hp = 4014; %hydrophone used (4014 or 4034)
        ppclip = 4; % pp clip level of recording
    elseif rr == 25
        gain = 32; %gain of recording system
```

```
        hp = 4014; %hydrophone used (4014 or 4034)
        ppclip = 2; % pp clip level of recording
    elseif rr == 50
        gain = 32; %gain of recording system
        hp = 4014; %hydrophone used (4014 or 4034)
        ppclip = 1; % pp clip level of recording
    elseif rr == 100
        gain = 32; %gain of recording system
        hp = 4014; %hydrophone used (4014 or 4034)
        ppclip = 0.4; % pp clip level of recording
    elseif rr == 200
        gain = 32; %gain of recording system
        hp = 4014; %hydrophone used (4014 or 4034)
        ppclip = 0.2; % pp clip level of recording
    end
elseif zr ==3
    if rr == 5
        gain = 40; %gain of recording system
        hp = 4034; %hydrophone used (4014 or 4034)
        ppclip = 1; % pp clip level of recording
    elseif rr == 10
        gain = 60; %gain of recording system
        hp = 4034; %hydrophone used (4014 or 4034)
        ppclip = 4; % pp clip level of recording
    elseif rr == 25
        gain = 60; %gain of recording system
        hp = 4034; %hydrophone used (4014 or 4034)
        ppclip = 2; % pp clip level of recording
    elseif rr == 50
```

```
        gain = 60; %gain of recording system
        hp = 4034; %hydrophone used (4014 or 4034)
        ppclip = 1; % pp clip level of recording
    elseif rr == 100
        gain = 60; %gain of recording system
        hp = 4034; %hydrophone used (4014 or 4034)
        ppclip = 1; % pp clip level of recording
    elseif rr == 200
        gain = 60; %gain of recording system
        hp = 4034; %hydrophone used (4014 or 4034)
        ppclip = 1; % pp clip level of recording
    end
  end
else error ('unrecognized experiment location')
end
%recording chain sensitivity PEAK (not pp)
if hp == 4014
  cal = 187 - gain + 20*log10(ppclip) -6;
elseif hp == 4034
  cal = 220 - gain + 20*log10(ppclip) -6;
end

%************************************************************************
%MEASURE CLICK CHARACTERISTICS
%************************************************************************

load c:\porpoisetldata\click1; %Loads extracted click data saved by
%clickxtract_sdr
szf=size(gsig); %store the size of the click matrix as a variable.
```

```
 %matrix has one click per column.
for i=1:(szf(2)) %for each click,
   y=gsig(:,i); %y is the ith click waveform
   envy = abs(hilbert(y(1:320))) ; %calculate the envelope of the
   %first 320 samples of y
   emax=find(envy>0.5*max(envy)); %find the times (in samples) at
   %which the envelope is at least half its maximum level
   d=y(max([1,(min(emax)-5)]):
   min([length(y),(min(emax)+70)]));%define the
   %analysis window  - it will be 75 samples long maximum, starting 5
   %samples before the time of the minimum envelop level and ending 70
   %samples after.
   z=(d(1:length(d)))'; %reshape d and rename it z
   r=round(80-length(d)); % r is the number of samples one would have
   %to add to z to make it 80 samples long
   x(:,i)=[z zeros(1,r)]'; %x is a matrix of click waveforms, one
   %click per column.  Each click is 75 or less samples, zero-padded
   %with r zeros so it is 80 samples long.
   p1=min(x(:,i)); %p1 is the min envelope level of the detected click
   p2=max(x(:,i)); %p2 is the max envelope level of the detected click
   % 1. Received level peak-peak (dB re 1uPa p-p)
   RLpp(:,i)= round(20*log10(p2-(p1))) + cal; % peak-to-peak level
   % 2. Received rms level, dB re. 1uPa (rms)
   RLrms(:,i)= round(10*log10(mean(x(:,i).^2))) + cal; %RMS level in
   %the emax window
   % 3. Received E level, dB re. 1uPa2s
   RLE(:,i) = round(RLrms(:,i)+10*log10((length(x(:,i)))/fs)); %energy
   %level in the emax window
end
```

```
%**********************************************************************
%ORGANIZE, CONVERT UNITS, AND SAVE DATA
%**********************************************************************

data=([RLpp' RLrms' RLE']); %place level data into the matrix "data"
clicks_analyzed = length(data(:,1)); %count the number of clicks analyzed
data_upa = 10.^(data./20); %convert level data in dB into uPascals
%calculate mean level (pp, rms, and E) of each click
mean_upa = [mean(data_upa(1:100,1)),mean(data_upa(1:100,2)),…
mean(data_upa(1:100,3))];
%convert the mean levels back to dB
mean_levels = 20.*log10(mean_upa)
%calculate standard deviation of level measurements (this is not kosher
%since really, since the measurements are in dB, and these values are
%not used in later analysis)
stdv = std(data(1:100,:));
%save data matrix
save([location '_r' num2str(rr) '_Zr' num2str(zr)], 'clicks_analyzed',…
'data', 'data_upa', 'mean_levels', 'mean_upa',  'cal', 'gsig' ,'fs')
```

Click Level Determination (Danish Datasets)

```
function TLauto_sdr_dk(location, rr, zr)
%Analysis tool to determine peak-peak, RMS, and energy levels of clicks
%detected by clickxtract_sdr script.  For Grand Manan porpoise
%transmission loss datasets.
%Written by Peter Madsen, 27 Dec. 2006
%Modified by Stacy DeRuiter, July 2007, Jan 2008
%
%Input Variables:
```

```
% rr is source-receiver range
% zr is receiver depth
% CHOOSE ONE LOCATION: You can enter the number or the string.
% 1-3

%************************************************************************
%INITIALIZE AND DEFINE VARIABLES
%************************************************************************

clear gain hp ppclip d z r x y p1 p2 envy emax RLpp RLE RLrms …
clicks_analyzed data data_upa mean_levels mean_upa cal gsig fs
names = {'RL090506','RL112906', 'RL041607', 'RL070606'};
if ~isstr(location)
   location = names{location};
end
hp = 4034; %(all measurements made with 4034 hydrophone)
%Information for click extraction and TL calculations
if strcmp(location, names{1})
   %location1 = 9/5/06;
   if zr == 5
      if rr == 5
         gain = 60; %gain of recording system
         ppclip = 10; % pp clip level of recording
      elseif rr ==10
         gain = 60; %gain of recording system
         ppclip = 10; % pp clip level of recording
      elseif rr == 25
         gain = 60; %gain of recording system
         ppclip = 10; % pp clip level of recording
```

```
    elseif rr == 50
        gain = 60; %gain of recording system
        ppclip = 10; % pp clip level of recording
    elseif rr == 100
        gain = 60; %gain of recording system
        ppclip = 10; % pp clip level of recording
    else
        gain = 60;
        ppclip = 10;
    end
elseif zr ==3
    if rr == 5
        gain = 60; %gain of recording system
        ppclip = 10; % pp clip level of recording
    elseif rr == 10
        gain = 60; %gain of recording system
        ppclip = 10; % pp clip level of recording
    elseif rr == 25
        gain = 60; %gain of recording system
        ppclip = 10; % pp clip level of recording
    elseif rr == 50
        gain = 60; %gain of recording system
        ppclip = 10; % pp clip level of recording
    elseif rr == 100
        gain = 60; %gain of recording system
        ppclip = 10; % pp clip level of recording
    else
        gain = 60;
        ppclip = 10;
```

```
        end
    end
elseif strcmp(location, names{2})
% 2 = location2 = 11/29/06;
    if zr == 5
        if rr == 5
            gain = 60; %gain of recording system
            ppclip = 4; % pp clip level of recording
        elseif rr ==10
            gain = 60; %gain of recording system
            ppclip = 4; % pp clip level of recording
        elseif rr == 25
            gain = 60; %gain of recording system
            ppclip = 4; % pp clip level of recording
        elseif rr == 50
            gain = 60; %gain of recording system
            ppclip = 4; % pp clip level of recording
        elseif rr == 100
            gain = 60; %gain of recording system
            ppclip = 4; % pp clip level of recording
        else
            gain = 60;
            ppclip = 4;
        end
    elseif zr ==3
        if rr == 5
            gain = 60; %gain of recording system
            ppclip = 4; % pp clip level of recording
        elseif rr == 10
```

```
            gain = 60; %gain of recording system
            ppclip = 4; % pp clip level of recording
        elseif rr == 25
            gain = 60; %gain of recording system
            ppclip = 4; % pp clip level of recording
        elseif rr == 50
            gain = 60; %gain of recording system
            ppclip = 4; % pp clip level of recording
        elseif rr == 100
            gain = 60; %gain of recording system
            ppclip = 4; % pp clip level of recording
        else
            gain = 60;
            ppclip = 4;

        end
    end
elseif strcmp(location, names{3})
    % 3 = location3 = 4/16/07;
    if zr == 5
        if rr == 5
            gain = 40; %gain of recording system
            ppclip = 4; % pp clip level of recording
        elseif rr ==10
            gain = 60; %gain of recording system
            ppclip = 4; % pp clip level of recording
        elseif rr == 25
            gain = 60; %gain of recording system
            ppclip = 4; % pp clip level of recording
```

```
    elseif rr == 50
        gain = 60; %gain of recording system
        ppclip = 4; % pp clip level of recording
    elseif rr == 100
        gain = 60; %gain of recording system
        ppclip = 4; % pp clip level of recording
    else
        gain = 60;
        ppclip = 4;
    end
elseif zr ==3
    if rr == 5
        gain = 40; %gain of recording system
        ppclip = 4; % pp clip level of recording
    elseif rr == 10
        gain = 60; %gain of recording system
        ppclip = 4; % pp clip level of recording
    elseif rr == 25
        gain = 60; %gain of recording system
        ppclip = 4; % pp clip level of recording
    elseif rr == 50
        gain = 60; %gain of recording system
        ppclip = 4; % pp clip level of recording
    elseif rr == 100
        gain = 60; %gain of recording system
        ppclip = 4; % pp clip level of recording
    else
        gain = 60;
        ppclip = 4;
```

```
      end
   end
elseif strcmp(location, names{4})
   gain = 60;
   ppclip = 10;
else error ('unrecognized experiment location')
end
%recording chain sensitivity PEAK (not pp)
if hp == 4014
   cal = 187 - gain + 20*log10(ppclip) -6;
elseif hp == 4034
   cal = 220 - gain + 20*log10(ppclip) -6;
end

%**************************************************************************
%MEASURE CLICK CHARACTERISTICS
%**************************************************************************

load c:\porpoisetldata\click1; %Loads extracted click data saved by
%clickxtract_sdr
szf=size(gsig); %store the size of the click matrix as a variable.
%Matrix has one click per column.
for i=1:(szf(2)) %for each click,
   y=gsig(:,i); %y is the ith click waveform
   envy = abs(hilbert(y(1:320))) ; %calculate the envelope of the
   %first 320 samples of y
   emax=find(envy>0.5*max(envy)); %find the times (in samples) at
   %which the envelope is at least half its maximum level
   d=y(max([1,(min(emax)-5)]):
```

```
    min([length(y),(min(emax)+70)]));%define the
    %analysis window  - it will be 75 samples long maximum, starting 5
    %samples before the time of the minimum envelop level and ending 70
    %samples after.
    z=(d(1:length(d)))'; %reshape d and rename it z
    r=round(80-length(d)); % r is the number of samples one would have
    %to add to z to make it 80 samples long
    x(:,i)=[z zeros(1,r)]'; %x is a matrix of click waveforms, one
    %click per column.  Each click is 75 or less samples, zero-padded
    %with r zeros so it is 80 samples long.
    p1=min(x(:,i)); %p1 is the min envelope level of the detected click
    p2=max(x(:,i)); %p2 is the max envelope level of the detected click
    % 1. Received level peak-peak (dB re 1uPa p-p)
    RLpp(:,i)= round(20*log10(p2-(p1))) + cal; % peak-to-peak level
    % 2. Received rms level, dB re. 1uPa (rms)
    RLrms(:,i)= round(10*log10(mean(x(:,i).^2))) + cal; %RMS level in
    %the emax window
    % 3. Received E level, dB re. 1uPa2s
    RLE(:,i) = round(RLrms(:,i)+10*log10((length(x(:,i)))/fs)); %energy
    %level in the emax window
end

%************************************************************************
%ORGANIZE, CONVERT UNITS, AND SAVE DATA
%************************************************************************

data=([RLpp' RLrms' RLE']); %place level data into the matrix "data"
clicks_analyzed = length(data(:,1)); %count the number of clicks analyzed
data_upa = 10.^(data./20); %convert level data in dB into uPascals
```

```
%calculate mean level (pp, rms, and E) of each click
mean_upa = [mean(data_upa(1:100,1)),mean(data_upa(1:100,2)),…
mean(data_upa(1:100,3))];
%convert the mean levels back to dB
mean_levels = 20.*log10(mean_upa);
%calculate standard deviation of level measurements (this is not OK
%really, since the measurements are in dB, and so these values are not
%used in later analysis)
stdv = std(data(1:100,:));
%save data matrix
save([location '_r' num2str(rr) '_Zr' num2str(zr)], 'clicks_analyzed',… 'data',
'data_upa', 'mean_levels', 'mean_upa',  'cal', 'gsig' ,'fs')
```

Matlab Code Used in Chapter 5 (Rotation Test & Semi-Markov Chain)

Example Sperm Whale Audit Data File

```
% swaudit.m
% example sperm whale audit file example
% Stacy DeRuiter, June 2008
% Data included:
% 1. variable, CST
% columns of CST are:
%       1:  seconds-from-tagon to the start of the buzz
%       2:  duration of the buzz in seconds
%       3:  1 if there is a blow sound following the
%           fast run, 0 otherwise
%       4:  length of the pause following the fast run in seconds.
%           NaN if the fast run is at the end of a dive and
%           coincides with the end of clicking.
% 2. variable, PAUSE
```

```
% columns of PAUSE are:
%       1: time in seconds-from-tagon of the start of the pause
%       2: duration of the pause in seconds
%       3: 1 if there is a blow sound after the pause, 0 if not
% 3. variable, CLICKING
% columns of CLICKING are:
%       1: time in seconds-from-tagon of start of regular clicking
%       2: time in seconds-from-tagon of end of regular clicking

CST = [
4040.9  11.7    0   2.5
4225.6  5.1 1   4.9
...
44526.7 1.0 1 5.3
] ;
PAUSE = [
163.0   21.0    1
264.9   5.7 1
...
23938.6 5.7 1
] ;
CLICKING = [
155.0   2195.9
...
3575    5842.3
] ;
```

Rotation Test for Changes in Buzz Rate (single whale)

```
function [Nc_rot] = ICI_agunonoff_rate(auditfile,n)
%ICI_agunonoff_rate - for one whale
```

```
%test the hypotheses that...
%null: the creak rate is the same during both control and airgun conditions
%alternate: the creak rate is lower during airgun conditions.
%n is the number of iterations for the rotation test/randomization.
%auditfile is a string containing the name of the m-file in which sperm
%whale behavior data is stored.
%Written by Stacy DeRuiter, 2007-2008

%************************************************************************
%INITIALIZE
%************************************************************************

% enter the data for each whale (audit data on creak times, and
% time of airgun start/stop); organize the data for analysis.

if strcmp(auditfile,'sw02_253aaud')
   Tss = 2639.9;
   Tse = 5651.1;
   Tss2 = []; Tse2=[];
   id = '253a';
elseif strcmp(auditfile,'sw02_254aaud')
   Tss = 5531.6;
   Tse = 8198.8;
   Tss2 = 9012.2;
   Tse2 = 10190.8;
   id = '254a';
elseif strcmp(auditfile,'sw02_254baud')
   Tss = 3455.6;
   Tse = 6309.5;
```

```
    Tss2 = 7428.5;
    Tse2 = 8708.8;
    id = '254b';
elseif strcmp(auditfile,'sw02_254caud')
    Tss = 4308.2;
    Tse = 7156.3;
    Tss2 = 8275.3;
    Tse2 = 9549.5;
    id = '254c';
elseif strcmp(auditfile,'sw03_164aaud')
    Tss = 22021;
    Tse = 24843;
    Tss2 = []; Tse2=[];
    id = '164a';
elseif strcmp(auditfile,'sw03_165aaud')
    Tss = 1777.9;
    Tse = 6554.3;
    Tss2 = []; Tse2=[];
    id = '165a';
elseif strcmp(auditfile,'sw03_165baud')
    Tss = 8233.1;
    Tse = 13107.9;
    Tss2 = []; Tse2=[];
    id = '165b';
else
    error('Unrecognized audit file name')
end
eval(auditfile); %this puts all the audit (whale behavior) data into
%the Matlab workspace
```

```
ct0 = CST(:,1);%col 1 of ct0 is time cues of creaks in seconds since tagon
CLICKING(:,3) = cumsum(CLICKING(:,2) - CLICKING(:,1)); %each row of
%CLICKING is a dive; 1st col. is start of reg clicking = foraging;
%2nd is end of reg clicking; 3rd column is total time regular clicking
%(cumulative) after that dive
%We want col 1 of ct to be time cues of creaks in seconds of foraging
%time (disinclude surface/silent time), so...
%calculate total time spent clicking
totalclickingdur = CLICKING(end,3);
%convert data on buzz times from seconds-since-tagon to
%seconds-since-start-of-foraging
for i = 1:length(ct0)
   d = find(CLICKING(:,2) > ct0(i), 1 , 'first');
   if d == 1 %if it's the first dive,
      %time since start of clicking is seconds-since-tagon minus
      %start of first-dive regular clicking
      ct(i,1) = ct0(i,1) - CLICKING(d,1);
   else %for other dives,
      %time since start of clicking is seconds-since-tagon minus
      %start of current dive plus total clicking time on previous
      %dives
      ct(i,1) = ct0(i,1) - CLICKING(d,1) + CLICKING(d-1,3);
   end
end
%make sure all the buzz events are in chronological order (if they are
%not, there is an error in the audit file.)
if ~isempty(find(diff(ct) < 0))
   find(diff(ct) < 0)
   error('There is an error in the audit file; not all creaks are in…
```

```
   sequential order.')
end

%FIND Nc, number of buzzes during control conditions:
agun_ind = zeros(length(ct),1); %preallocate space
if isempty(Tss2)
   agun_ind(find(ct >= Tss & ct <  Tse)) = 1; %if agun_ind is 1, then
   %it's airgun conditions
   %if agun_ind is 0, it's control conditions
%case 2: when there are 2 airgun exposure periods
else
   agun_ind(find(ct >= Tss & ct <  Tse)) = 1;
   agun_ind(find(ct >= Tss2 & ct <  Tse2)) = 1;
   %if agun_ind is 1, then it's airgun conditions
   %else, it's control conditions (INCLUDING times when airgun
   %exposure was halted temporarily for mitigation).
end
Ntot = length(agun_ind); %total number of buzzes
Na = sum(agun_ind);%number of creaks during airgun conditions
Nc = Ntot - Na %number of creaks during control conditions
Ttot = CLICKING(end,3); %total duration of foraging observed
%Calculate airgun exposure duration in seconds:
if isempty(Tss2)
   Ta = Tse - Tss;
else
   Ta = (Tse - Tss) + (Tse2 - Tss2)
end
Tc = Ttot - Ta; %calculate control conditions duration
%under the assumption that the creak rates are Poisson, and under the
```

```
%null, the number of creaks during control conditions
%should be binomially distributed with (n = total number of creaks)
%tries and p = Tc/Ttot (Tc is total control time, and Ttot is total
%time). So we can calculate a p-value:
p_poisson = 1 - binocdf(Nc , Ntot , Tc/Ttot);%one sided test for alt.
%hyp. = Nc larger than observed
disp(['P-value (assuming rates are Poisson) < ' num2str(p_poisson)]);
%try to estimate Beta (the factor by which creak rate is multiplied
%during airgun conditions)
%calculate binomial distribution fit and alpha = 0.05 confidence
%intervals
[phat, pci] = binofit(Nc,Ntot, 0.05);
beta = Tc*(1-phat)/(phat*Ta);
beta_CI95 = Tc.*(1-pci)./(pci.*Ta);
disp(['During airgun conditions, the creak rate was beta = ' num2str(beta) ' times
the rate during control conditions.'])
disp(['The 95 percent confidence interval for beta is ' num2str(beta_CI95) '.'])

%************************************************************************
%Relax the Poisson assumption
%and do a rotation test instead of the parametric test.  Nc is the test
%statistic.
 %************************************************************************

for k = 1:n
   ca = rand(1,1).*Ttot; %generate a random number between 0 and Ttot
   ct_rand = ct + ca; %rotate the ct event vector by ca seconds
   v = find(ct_rand > Ttot); %for events that now occur at times after
   %Ttot,
```

```
    ct_rand(v) = ct_rand(v) - Ttot; %subtract Ttot so they occur at the
    %start of the record
    ct_rand = sort(ct_rand); %sort the rotated ct data
    ai_rand = zeros(length(ct_rand),1); %allocate space
    %if there is only one airgun exposure:
    if isempty(Tss2)
        ai_rand(find(ct_rand >= Tss & ct_rand <  Tse)) = 1; %if ai_rand
        %is 1, then it's airgun conditions
        %if ai_rand is 0, it's control conditions
        %case 2: when there are 2 airgun exposure periods
    else
        ai_rand(find(ct_rand >= Tss & ct_rand <  Tse)) = 1;
        ai_rand(find(ct_rand >= Tss2 & ct_rand <  Tse2)) = 1;
        %if ai_rand is 1, then it's airgun conditions
        %else, it's control conditions (INCLUDING times when airgun
        %exposure was halted temporarily for mitigation).
    end
    Na_rot(k) = sum(ai_rand);%number of creaks during airgun conditions
    Nc_rot(k) = Ntot - Na_rot(k); %number of creaks during control
    %conditions
end
%plot a histogram of Nc_rot
figure(1); clf;
hist(Nc_rot,40);
set(gca,'FontName','Palatino', 'LineWidth',3,'FontSize',12);%set font
%type and size for the figure
title('Histogram of Nc (test statistic; from rotation test)')
xlabel(['Number of creaks during control period; Nc is ' num2str(Nc)]);
%find the p-value of the test
```

```
%p_rot = length(find(Nc_rot > Nc))/n; %one sided
p_rot = 2*length(find(Nc_rot > Nc))/n; %2 sided
disp(['p-value (rotation test) is ' num2str(p_rot)]);
%Save data, if desired
%save(['onoffdata2_' eval('id')], 'ct', 'Nc', 'Nc_rot', 'beta',… 'beta_CI95',
'p_poisson', 'p_rot', 'Ntot','Ttot','Tc');
```

Semi-Markov Chain Analysis

```
%GSCP_MCsim.m
%script to fit a semi-Markov chain to whale foraging behavior data and
%test the null hypothesis that the same sMC foraging behavior model
%fits the data during airgun exposure and control time periods.
%Stacy DeRuiter, 2007-2008

%**************************************************************************
%INITIALIZE AND DEFINE VARIABLES
%**************************************************************************

load WHALE
%the WHALE .mat-file must contain the following:
%   1. WHALE (a matrix).  WHALE summarizes the timing of whale foraging
%      events.
%      Column 1 of whale contains the time, in seconds since start of
%      foraging (not inlcuding other time periods), of each event.
%      Column 2 of whale is 1 if the event is search, 2 if buzz, 3 if
%      pause.
%      Column 3 of whale is the duration of the event in seconds.
%   2. Tss and Tse (scalar variables).  Tss is the time in seconds of
%     the start of airgun exposure.  Tse is the time in seconds of the
```

```
%      end of
%      airgun exposure.
%   3. Tss2 and Tse2 (scalar variables).  Start and end times of the
%      seconds airgun exposure.  Tss2 and tse2 should be [] if there
%      was only 1 exposure period.
%   4. agun_ind (vector variable).  agun_ind is the same length of
%      WHALE(:,1).  It is 1 if the event start time is during airgun
%      exposure, and zero otherwise.

WHALE_ctl = WHALE(find(agun_ind == 0),:);%store the subset of WHALE
%that occurred during control conditions in WHALE_ctl.
WHALE_agun = WHALE(find(agun_ind == 1),:);%store the subset of WHALE
%that occurred during airgun exposure in WHALE_agun.
logl_null_rand_all = zeros(10000,1);%pre-allocate space
logl_alt_rand_all = zeros(10000,1);%pre-allocate space

%**************************************************************************
%PARAMETER CALCULATIONS
%Calculate needed parameters:
   %1.  fit a gamma distribution to the observed dist of all waiting
   %times for each state
   %2.  fit a gamma dist to the control/airgun waiting times
   %separately
   %3.  matrices of transitions for all times, and for ctl and airgun
   %times separately
%**************************************************************************

%1.  fit a gamma distribution to the observed dist of all waiting times
%    for each state
```

```
%a.  search state
sdur = WHALE(find(WHALE(:,2)==1),3); %a set of all search waiting
%times
d = gamfit(sdur); %parameters of a gamma dist fit to the sdur data
a_null(1) = d(1); b_null(1) = d(2); %store parameters in variables
%a_null and b_null
%b.  creak state
cdur = WHALE(find(WHALE(:,2)==2),3); %a set of all buzz waiting times
d = gamfit(cdur); %parameters of a gamma dist fit to the cdur data
a_null(2) = d(1); b_null(2) = d(2);%store parameters in variables
%a_null and b_null
%c.  pause state
pdur = WHALE(find(WHALE(:,2)==3),3); %a set of all pause waiting
%times
d = gamfit(pdur);%parameters of a gamma dist fit to the pdur data
a_null(3) = d(1); b_null(3) = d(2);%store parameters in variables
%a_null and b_null
%2.  fit gamma dists to ctl and airgun times separately
%CONTROL
%a.  search state
sdur = WHALE(find(WHALE(:,2)==1 & agun_ind == 0),3);
%a set of all search waiting times
d = gamfit(sdur); %parameters of a gamma dist fit to the sdur data
a_ctl(1) = d(1); b_ctl(1) = d(2);%store parameters in variables a_ctl and b_ctl
%b.  creak state
cdur = WHALE(find(WHALE(:,2)==2 & agun_ind ==0),3); %a set of all buzz
%waiting times
d = gamfit(cdur);%parameters of a gamma dist fit to the cdur data
a_ctl(2) = d(1); b_ctl(2) = d(2);%store parameters in variables a_ctl %and b_ctl
```

```
%c.  pause state
pdur = WHALE(find(WHALE(:,2)==3 & agun_ind ==0),3); %a set of all pause
%waiting times
d = gamfit(pdur);%parameters of a gamma dist fit to the pdur data
a_ctl(3) = d(1); b_ctl(3) = d(2);%store parameters in variables a_ctl %and %b_ctl
%AIRGUN EXPOSURE
%a.  search state
sdur = WHALE(find(WHALE(:,2)==1 & agun_ind ==1),3); %a set of all search
%waiting times
d = gamfit(sdur); %parameters of a gamma dist fit to the sdur data
a_agun(1) = d(1); b_agun(1) = d(2);%store parameters in variables
%a_agun and b_agun
%b.  creak state
cdur = WHALE(find(WHALE(:,2)==2 & agun_ind ==1),3); %a set of all buzz
%waiting times
d = gamfit(cdur); %parameters of a gamma dist fit to the cdur data
a_agun(2) = d(1); b_agun(2) = d(2);%store parameters in variables
%a_agun and b_agun
%c.  pause state
pdur = WHALE(find(WHALE(:,2)==3 & agun_ind ==1),3); %a set of all pause
%waiting times
d = gamfit(pdur);%parameters of a gamma dist fit to the pdur data
a_agun(3) = d(1); b_agun(3) = d(2);%store parameters in variables
%a_agun and b_agun
%3. Find transition matrices (A) between states for a.) all data, b). control
%data, and c). airgun data.  Each matrix is 3 by 3; row/col 1 %is search, 2
%is creak, 3 is pause.  entry 1,2 is FROM search TO creak.
ntrans_null = length(WHALE) -1; %the total number of transitions
%preallocate space
```

```
T_null = zeros(3,3); T_ctl = zeros(3,3); T_agun = zeros(3,3);
for i = 1:3
   for j = 1:3
      for k = 1:ntrans_null %repeat for all observed transitions
         if WHALE(k,2) == i && WHALE(k+1,2) == j %if transition from
                  %state i to state j occurs,
            T_null(i,j) = T_null(i,j) + 1;%add 1 to the i,j entry
            %in matrix T-null, which records the number of each
               %type of transition that has occurred
            if agun_ind(k) == 0; %if the transition was in control
                     %conditions,
               T_ctl(i,j) = T_ctl(i,j) + 1; %log it in T_ctl as
               %well as in T_null;
            elseif agun_ind(k) == 1; %if the transition was in
               %airgun exposure conditions,
               T_agun(i,j) = T_agun(i,j) + 1; %log it in T_agun as
               %well as in T_null.
            else %if agun_ind and WHALE do not align, ERROR.
               error('mismatch between agun indicator vector and…
               WHALE matrix')
            end
         end
      end
   end
end
A_null = T_null./[sum(T_null,2),sum(T_null,2),sum(T_null,2)]; %transition
%matrix as proportions
A_ctl = T_ctl./[sum(T_ctl,2),sum(T_ctl,2),sum(T_ctl,2)]; %transition
%matrix as proportions
```

```
A_agun = T_agun./[sum(T_agun,2),sum(T_agun,2),sum(T_agun,2)]; %transition
%matrix as proportions


%************************************************************************
%LIKELIHOOD RATIO CALCULATION
%************************************************************************

%Calculate the log likelihood...
%...for all conditions together (null)
logl_null = 0; %initialize
for i = 1:length(WHALE)-1 %calculate likelihood of all events in WHALE
    j = WHALE(i,2); %j is the event type for event i, the "current"
    %event (1=search, 2=buzz, 3=pause)
    k = WHALE(i+1,2);%k is the "next" event (event i+1) type
    %(1=search, 2=buzz, 3=pause)
    p = A_null(j,k); %p is the probability (from transition matrix) of
    %j to k transition
    Pp = gampdf(WHALE(i,3),a_null(j),b_null(j)); %Pp is the
    %probability that a j event will last as long as event i did
    logl_null = logl_null + log(p) + log(Pp);%log likelihood of the
    %time-series up to event i = sum of likelihoods of previous events
    %+ log(p) + log(Pp)
end
%...under the alternate hyp
logl_alt = 0; %initialize
for i = 1:length(WHALE)-1%calculate likelihood of all events in WHALE
   if agun_ind(i) == 0%for events that began during control periods,
      j = WHALE(i,2);%j is the event type for event i, the "current"
```

```
        %event (1=search, 2=buzz, 3=pause)
        k = WHALE(i+1,2);%k is the "next" event (event i+1) type
        %(1=search, 2=buzz, 3=pause)
        p = A_ctl(j,k);%p is the probability (from transition matrix)
        %of j to k transition during control conditions
        Pp = gampdf(WHALE(i,3),a_ctl(j),b_ctl(j)); %Pp is the
        %probability that a j event, during control conditions, will
        %last as long as event i did
        logl_alt = logl_alt + log(p) + log(Pp);%log likelihood of the
        %time series up to event i = sum of likelihoods of previous
        %events + log(p) + log(Pp)
    elseif agun_ind(i) == 1
        j = WHALE(i,2);%j is the event type for event i, the "current"
        %event (1=search, 2=buzz, 3=pause)
        k = WHALE(i+1,2);%k is the "next" event (event i+1) type
        %(1=search, 2=buzz, 3=pause)
        p = A_agun(j,k);%p is the probability (from transition matrix)
        %of j to k transition during airgun exposure
        Pp = gampdf(WHALE(i,3),a_agun(j),b_agun(j)); %Pp is the
        %probability that a j event, during airgun exposure, will last
        %as long as event i did
        logl_alt = logl_alt + log(p) + log(Pp);%log likelihood of the
        %time series up to event i = sum of likelihoods of previous
        %events + log(p) + log(Pp)
    else
        error('problem with agun_ind vector') %note error if agun_ind
        %and whale don't match up in length
    end
end
```

```
%calculate the likelihood ratio test statistic for the data
TS_data = 2*(logl_alt - logl_null);

%**************************************************************************
%Markov Chain Monte Carlo test to determine test stat significance
%**************************************************************************

Ttot = WHALE(end,1) + WHALE(end,3); %calculate the total duration of
%the dataset
TS_rand = zeros(10000,1); %preallocate space
for nn = 1:10000 %do 10000 rotations
   %Output rotation number so user can track progress of analysis
   disp(['MC randomization number ' num2str(nn) ' of 10000 for '…
   name])
   %Make a synthetic data set the same duration as the real one under
   %the null hypothesis
   s1 = WHALE(1,2); %initial state is same as real whale
   clear WHALE_rot
   WHALE_rot(1,:) = [0, s1, gamrnd(a_null(s1),b_null(s1))];%first
   %event a time 0, with duration = a random sample from a gamma
   %distro with parameters a_null, b_null
   while WHALE_rot(end,1) < Ttot %continue until the synthetic dataset
      %is Ttot seconds long
      x = rand(1); %generate a random number
      statenow = WHALE_rot(end,2); %store the number of the current
      %state in the variable "statenow"
      nextevent = WHALE_rot(end,1) + WHALE_rot(end,3); % calculate
      %the time at which the next event will begin
```

```
    if x <= A_null(statenow,1)
        nextstate = 1; %next state is search with probability
        %A_null(statenow,1)
    elseif x <= (A_null(statenow,1) + A_null(statenow,2))
        nextstate = 2;%next state is buzz with probability
        %A_null(statenow,2)
    else
        nextstate = 3;%next state is pause with probability
        %A_null(statenow,3)
    end
    nextdur = gamrnd(a_null(nextstate),b_null(nextstate));
    %duration of next state is a random sample from a gamma distro
    %with parameters a_null, b_null
    WHALE_rot = [WHALE_rot; nextevent nextstate nextdur]; %add the
    %time, ID, and duration of the "next state" to the WHALE_rot
    %synthetic data matrix
end
    %make airgun index vector for this rotation
    ai_rand = zeros(length(WHALE_rot),1); %preallocate space
    if isempty(Tss2) %if there is only 1 airgun exposure period in
        %the real data
        ai_rand(find(WHALE_rot(:,1) >= Tss & WHALE_rot(:,1) …
                <  Tse)) = 1;
        %if agun_ind is 1, then it's airgun conditions
    else %if there are 2 airgun exposure periods in the real data
        ai_rand(find(WHALE_rot(:,1) >= Tss & WHALE_rot(:,1) < …
        Tse)) = 1;%if agun_ind is 1, then it's airgun conditions
        ai_rand(find(WHALE_rot(:,1) >= Tss2 & WHALE_rot(:,1) < …
        Tse2)) = 1;%if agun_ind is 1, then it's airgun conditions
```

```
   end
%fit the gamma distros
%1.  fit a gamma distribution to the observed dist of all
%waiting times for each state
%a.  search state
sdur_rand = WHALE_rot(find(WHALE_rot(:,2)==1),3); %a set of all
%search waiting times
d = gamfit(sdur_rand); %parameters of a gamma dist fit to the
%sdur data
ar_null(1) = d(1); br_null(1) = d(2);%store parameters in
%variables ar_null and br_null
%b.  creak state
cdur_rand = WHALE_rot(find(WHALE_rot(:,2)==2),3); %a set of all
%buzz waiting times
d = gamfit(cdur_rand); %parameters of a gamma dist fit to the
%cdur data
ar_null(2) = d(1); br_null(2) = d(2);%store parameters in
%variables ar_null and br_null
%c.  pause state
pdur_rand = WHALE_rot(find(WHALE_rot(:,2)==3),3); %a set of all
%pause waiting times
d = gamfit(pdur_rand);%parameters of a gamma dist fit to the
%pdur data
ar_null(3) = d(1); br_null(3) = d(2);%store parameters in
%variables ar_null and br_null
%2.  fit gamma dists to ctl and airgun times separately
%CONTROL
%a.  search state
sdur = WHALE_rot(find(WHALE_rot(:,2)==1 & ai_rand == 0),3); %a set
```

```
%of all search waiting times
d = gamfit(sdur); %parameters of a gamma dist fit to the sdur data
ar_ctl(1) = d(1); br_ctl(1) = d(2);%store parameters in variables
%ar_ctl and br_ctl
%b.  creak state
cdur = WHALE_rot(find(WHALE_rot(:,2)==2 & ai_rand ==0),3); %a set
%of all buzz waiting times
d = gamfit(cdur);%parameters of a gamma dist fit to the cdur data
ar_ctl(2) = d(1); br_ctl(2) = d(2);%store parameters in variables
%ar_ctl and br_ctl
%c.  pause state
pdur = WHALE_rot(find(WHALE_rot(:,2)==3 & ai_rand ==0),3); %a set
%of all pause waiting times
d = gamfit(pdur);%parameters of a gamma dist fit to the pdur data
ar_ctl(3) = d(1); br_ctl(3) = d(2);%store parameters in variables
%ar_ctl and br_ctl
%AIRGUN
%a.  search state
sdur = WHALE_rot(find(WHALE_rot(:,2)==1 & ai_rand ==1),3); %a set
%of all search waiting times
d = gamfit(sdur); %parameters of a gamma dist fit to the sdur data
ar_agun(1) = d(1); br_agun(1) = d(2);%store parameters in variables
%ar_agun and br_agun
%b.  creak state
cdur = WHALE_rot(find(WHALE_rot(:,2)==2 & ai_rand ==1),3); %a set
%of all buzz waiting times
d = gamfit(cdur); %parameters of a gamma dist fit to the cdur data
ar_agun(2) = d(1); br_agun(2) = d(2);%store parameters in variables
%ar_agun and br_agun
```

```
%c.  pause state
pdur = WHALE_rot(find(WHALE_rot(:,2)==3 & ai_rand ==1),3); %a set
%of all pause waiting times
d = gamfit(pdur);%parameters of a gamma dist fit to the pdur data
ar_agun(3) = d(1); br_agun(3) = d(2);%store parameters in variables
%ar_agun and br_agun
%3. Find transition matrices (A) between states for a.) all data,
%b). control data, and c). airgun data.  Each matrix is 3 by 3;
%row/col 1 is search, 2 is creak, 3 is pause.  entry 1,2 is FROM
%search TO creak.
ntrans_null = length(WHALE_rot) -1; %the total number of
%transitions
T_null_rand = zeros(3,3); T_ctl_rand = zeros(3,3);
T_agun_rand = zeros(3,3); %preallocate space
for i = 1:3
   for j = 1:3
      for k = 1:ntrans_null%repeat for all observed transitions
         if WHALE_rot(k,2) == i && WHALE_rot(k+1,2) == j %if
            %transition from state i to state j occurs,
            T_null_rand(i,j) = T_null_rand(i,j) + 1; %add 1 to
            %the i,j entry in matrix T_null_rand, which records
            %the number of each type of transition that has
            %occurred
            if ai_rand(k) == 0; %if the transition was in
               %control conditions,
               T_ctl_rand(i,j) = T_ctl_rand(i,j) + 1; %log it
               %in T_ctl_rand as well as in T_null_rand;
            elseif ai_rand(k) == 1;%if the transition was in
               %airgun conditions,
```

```
                T_agun_rand(i,j) = T_agun_rand(i,j) + 1;%log it
                %in T_agun_rand as well as in T_null_rand.
            else
                error('mismatch between agun indicator vector…
                and WHALE_rot matrix')
            end
        end
    end
end
A_null_rand = T_null_rand./[sum(T_null_rand,2), …
sum(T_null_rand,2),sum(T_null_rand,2)]; %transition matrix as
%proportions
A_ctl_rand = T_ctl_rand./[sum(T_ctl_rand,2),sum(T_ctl_rand,2),…
sum(T_ctl_rand,2)]; %transition matrix as proportions
A_agun_rand = T_agun_rand./[sum(T_agun_rand,2), …
sum(T_agun_rand,2), sum(T_agun_rand,2)]; %transition matrix as
%proportions
%**************************************************************************
%LIKELIHOOD RATIO CALCULATION FOR ROTATED DATA
%**************************************************************************
%Calculate the log likelihood...
%...for all conditions together (null)
logl_null_rand = 0; %initialize
for i = 1:length(WHALE_rot)-1 %repeat for all events
    j = WHALE_rot(i,2); %j is the event type for event i, the
    %"current" event (1=search, 2=buzz, 3=pause)
    k = WHALE_rot(i+1,2); %k is the "next" event (event i+1) type
    %(1=search, 2=buzz, 3=pause)
```

```
    p = A_null_rand(j,k); %p is the probability (from transition
    %matrix) of j to k transition
    Pp = gampdf(WHALE_rot(i,3),ar_null(j),br_null(j)); %Pp is the
    %probability that a j event will last as long as event i did
    logl_null_rand = logl_null_rand + log(p) + log(Pp);%log
    %likelihood of the time-series up to event i = sum of
    %likelihoods of previous events + log(p) + log(Pp)
end
%...under the alternate hyp
logl_alt_rand = 0;
for i = 1:length(WHALE_rot)-1
   if ai_rand(i) == 0 %if the event occurred during control
       %conditions,
       j = WHALE_rot(i,2);%j is the event type for event i, the
       %"current" event (1=search, 2=buzz, 3=pause)
       k = WHALE_rot(i+1,2);%k is the "next" event (event i+1)
       %type (1=search, 2=buzz, 3=pause)
       p = A_ctl_rand(j,k);%p is the probability (from transition
       %matrix) of j to k transition during control conditions
       Pp = gampdf(WHALE_rot(i,3),ar_ctl(j),br_ctl(j)); %Pp is
       %the probability that a j event, during control
       %conditions, will last as long as event i did
       logl_alt_rand = logl_alt_rand + log(p) + log(Pp);%log
       %likelihood of the time-series up to event i = sum of
       %likelihoods of previous events + log(p) + log(Pp)
   elseif ai_rand(i) == 1%otherwise, if the event occurred during
       %airgun exposure,
       j = WHALE_rot(i,2);%j is the event type for event i, the
       %"current" event (1=search, 2=buzz, 3=pause)
```

```
        k = WHALE_rot(i+1,2);%k is the "next" event (event i+1)
        %type (1=search, 2=buzz, 3=pause)
        p = A_agun_rand(j,k);%p is the probability (from
        %transition matrix) of j to k transition during airgun
        %exposure
        Pp = gampdf(WHALE_rot(i,3),ar_agun(j),br_agun(j)); %Pp is
        %the probability that a j event, during airgun exposure,
        %will last as long as event i did
        logl_alt_rand = logl_alt_rand + log(p) + log(Pp);%log
        %likelihood of the time-series up to event i = sum of
        %likelihoods of previous events + log(p) + log(Pp)
    else
       error('problem with ai_rand vector')
    end
end
%calculate the TS for this rotation
TS_rand(nn) = 2*(logl_alt_rand - logl_null_rand);
logl_alt_rand_all(nn) = logl_alt_rand;
logl_null_rand_all(nn) = logl_null_rand;
%save parameters from the rotations
A_null_rand_all(:,:,nn) = A_null_rand;
A_agun_rand_all(:,:,nn) = A_agun_rand;
A_ctl_rand_all(:,:,nn) = A_ctl_rand;
ar_null_all(nn,:) = ar_null;
br_null_all(nn,:) = br_null;
ar_ctl_all(nn,:) = ar_ctl;
br_ctl_all(nn,:) = br_ctl;
ar_agun_all(nn,:) = ar_agun;
br_agun_all(nn,:) = br_agun
```

```
end
%**********************************************************************
%CALCULATE P-VALUE OF PARAMETRIC TEST AND SAVE DATA/OUTPUT
%**********************************************************************

%Calculate the p-value of the test
pvalue = length(find(TS_rand > TS_data))/10000;
%save output
save(['gscpsim_' name],'pvalue', 'TS_data', 'TS_rand', 'A_null', …
'A_ctl', 'A_agun', 'a_null', 'b_null', 'a_ctl', 'b_ctl', 'a_agun',…
 'b_agun', 'logl_null', 'logl_alt', 'logl_null_rand_all',…
'logl_alt_rand_all', 'A_null_rand_all', 'A_agun_rand_all', …
'A_ctl_rand_all', 'ar_null_all', 'br_null_all', 'ar_ctl_all',…
 'br_ctl_all', 'ar_agun_all', 'br_agun_all');

%######################################################################
%Rotation test to determine significance of the test statistic
%######################################################################

Ttot = WHALE(end,1) + WHALE(end,3); %total time in this whale record %(sum
is total time for all whales)
%preallocate space;
TS_rand = ones(10000,1);
logl_alt_rand_all = ones(10000,1);
logl_null_rand_all = ones(10000,1);
if isempty(Tss2)
    Tss_rand = zeros(10000,1);
    Tse_rand = zeros(10000,1);
    Tss2 = [];
```

```
    Tse2 = [];
    adur = Tse - Tss;
else
    Tss_rand = zeros(10000,1);
    Tse_rand = zeros(10000,1);
    Tss2_rand = zeros(10000,1);
    Tse2_rand = zeros(10000,1);
    adur = Tse2 - Tss;
end

for nn = 1:10000 %do 10000 rotations
    disp(['rotation ' num2str(nn) ' of 10000 for whale ' name]);
    clear ai_rand
    %calculate random airgun start (Tss) and end (Tse) times:
    if isempty(Tss2) %for experiments with one airgun exposure period
        Tss_rand(nn) = trand(nn)*(Ttot - adur);
        Tse_rand(nn) = Tss_rand(nn) + adur;
    else %for experiments with two airgun periods
        Tss_rand(nn) = trand(nn)*(Ttot - adur);
        Tse_rand(nn) = Tss_rand(nn) + (Tss-Tse);
        Tss2_rand(nn) = Tss_rand(nn) + adur - (Tse2-Tss2);
        Tse2_rand(nn) = Tss_rand(nn) + adur;
    end
    %make airgun index vector for this rotation
    ai_rand = zeros(length(WHALE),1); %preallocate space
    if isempty(Tss2)
        ai_rand(find(WHALE(:,1) >= Tss_rand(nn) & WHALE(:,1) < …
        Tse_rand(nn))) = 1; %if agun_ind is 1, then it's airgun
        %conditions
```

```
else
   ai_rand(find(WHALE(:,1) >= Tss_rand(nn) & WHALE(:,1) <…
   Tse_rand(nn))) = 1;
   ai_rand(find(WHALE(:,1) >= Tss2_rand(nn) & WHALE(:,1) < …
   Tse2_rand(nn))) = 1;
end
%fit the gamma distros
%1.  fit a gamma distribution to the observed dist of all waiting
%times for each state
%a.  search state
sdur_rand = WHALE(find(WHALE(:,2)==1),3); %a set of all search
%waiting times
d = gamfit(sdur_rand); %parameters of a gamma dist fit to the sdur
%data
ar_null(1) = d(1); br_null(1) = d(2);
%b.  creak state
cdur_rand = WHALE(find(WHALE(:,2)==2),3); %a set of all buzz
%waiting times
d = gamfit(cdur_rand); %parameters of a gamma dist fit to the cdur
%data
ar_null(2) = d(1); br_null(2) = d(2);
%c.  pause state
pdur_rand = WHALE(find(WHALE(:,2)==3),3); %a set of all pause
%waiting times
d = gamfit(pdur_rand);%parameters of a gamma dist fit to the pdur
%data
ar_null(3) = d(1); br_null(3) = d(2);
%2.  fit gamma dists to ctl and airgun times separately
%CONTROL
```

```
 %a.  search state
 sdur = WHALE(find(WHALE(:,2)==1 & ai_rand == 0),3); %a set of all
 %search waiting times
 d = gamfit(sdur); %parameters of a gamma dist fit to the sdur data
ar_ctl(1) = d(1); br_ctl(1) = d(2);
 %b.  creak state
 cdur = WHALE(find(WHALE(:,2)==2 & ai_rand ==0),3); %a set of all
 %buzz waiting times
 d = gamfit(cdur);%parameters of a gamma dist fit to the cdur data
 ar_ctl(2) = d(1); br_ctl(2) = d(2);
 %c.  pause state
 pdur = WHALE(find(WHALE(:,2)==3 & ai_rand ==0),3); %a set of all
 %pause waiting times
 d = gamfit(pdur);%parameters of a gamma dist fit to the pdur data
 ar_ctl(3) = d(1); br_ctl(3) = d(2);
 %AIRGUN
 %a.  search state
 sdur = WHALE(find(WHALE(:,2)==1 & ai_rand ==1),3); %a set of all
 %search waiting times
 d = gamfit(sdur); %parameters of a gamma dist fit to the sdur data
 ar_agun(1) = d(1); br_agun(1) = d(2);
 %b.  creak state
 cdur = WHALE(find(WHALE(:,2)==2 & ai_rand ==1),3); %a set of all
 %buzz waiting times
 d = gamfit(cdur); %parameters of a gamma dist fit to the cdur data
 ar_agun(2) = d(1); br_agun(2) = d(2);
 %c.  pause state
 pdur = WHALE(find(WHALE(:,2)==3 & ai_rand ==1),3); %a set of all
 %pause waiting times
```

```
    d = gamfit(pdur);%parameters of a gamma dist fit to the pdur data
    ar_agun(3) = d(1); br_agun(3) = d(2);
    %3. Find transition matrices (A) between states for a.) all data,
    %b). control
    %data, and c). airgun data.  Each matrix is 3 by 3; row/col 1 is
    %search, 2 is creak, 3 is pause.  entry 1,2 is FROM search TO
    %creak.
    ntrans_null = length(WHALE) -1; %the total number of transitions
    T_null_rand = zeros(3,3); T_ctl_rand = zeros(3,3);
    T_agun_rand = zeros(3,3);
for i = 1:3
    for j = 1:3
        for k = 1:ntrans_null %repeat for all observed transitions
            if WHALE(k,2) == i && WHALE(k+1,2) == j %if a state i to
                %state j transition occurrs,
                T_null_rand(i,j) = T_null_rand(i,j) + 1;%increment the
                %i,j entry of T_null_rand
                if ai_rand(k) == 0; %if  the behavior began during
                    %control period,
                    T_ctl_rand(i,j) = T_ctl_rand(i,j) + 1; %also
                    %increment the i,j entry of T_ctl_rand
                elseif ai_rand(k) == 1; %if it began during airgun
                    % period,
                    T_agun_rand(i,j) = T_agun_rand(i,j) + 1;%then
                    %increment i,j entry of T_agun_rand
                else
                    error('mismatch between agun indicator vector and…
                    WHALE matrix')
                end
```

```
        end
      end
   end
end
A_null_rand = T_null_rand./[sum(T_null_rand,2),sum(T_null_rand,2)…
,sum(T_null_rand,2)]; %transition matrix as proportions
A_ctl_rand = T_ctl_rand./[sum(T_ctl_rand,2),sum(T_ctl_rand,2),…
sum(T_ctl_rand,2)]; %transition matrix as proportions
A_agun_rand = T_agun_rand./[sum(T_agun_rand,2),sum(T_agun_rand,2),…
sum(T_agun_rand,2)]; %transition matrix as proportions

%#####################################################################
%LIKELIHOOD RATIO CALCULATION
%#####################################################################

%Calculate the log likelihood...
%...for all conditions together (null)
%see previous likelihood ratio calcs for detailed annotation of the
%following calculations
logl_null_rand = 0;
for i = 1:length(WHALE)-1
    j = WHALE(i,2);
    k = WHALE(i+1,2);
    p = A_null_rand(j,k);
    Pp = gampdf(WHALE(i,3),ar_null(j),br_null(j));
    logl_null_rand = logl_null_rand + log(p) + log(Pp);
end
%...under the alternate hyp
logl_alt_rand = 0;
```

```
for i = 1:length(WHALE)-1
    if ai_rand(i) == 0
        j = WHALE(i,2);
        k = WHALE(i+1,2);
        p = A_ctl_rand(j,k);
        Pp = gampdf(WHALE(i,3),ar_ctl(j),br_ctl(j));
        logl_alt_rand = logl_alt_rand + log(p) + log(Pp);
    elseif ai_rand(i) == 1
        j = WHALE(i,2);
        k = WHALE(i+1,2);
        p = A_agun_rand(j,k);
        Pp = gampdf(WHALE(i,3),ar_agun(j),br_agun(j));
        logl_alt_rand = logl_alt_rand + log(p) + log(Pp);
    else
       error('problem with ai_rand vector')
    end
end
%calculate the TS for this rotation
TS_rand(nn) = 2*(logl_alt_rand - logl_null_rand);
logl_alt_rand_all(nn) = logl_alt_rand;
logl_null_rand_all(nn) = logl_null_rand;
%save parameters from the rotations
A_null_rand_all(:,:,nn) = A_null_rand;
A_agun_rand_all(:,:,nn) = A_agun_rand;
A_ctl_rand_all(:,:,nn) = A_ctl_rand;
ar_null_all(nn,:) = ar_null;
br_null_all(nn,:) = br_null;
ar_ctl_all(nn,:) = ar_ctl;
br_ctl_all(nn,:) = br_ctl;
```

```
ar_agun_all(nn,:) = ar_agun;
br_agun_all(nn,:) = br_agun;
end

%************************************************************************
%Calculate the p-value of the test
%************************************************************************

pvalue = length(find(TS_rand > TS_data))/10000;
save(['gscprotTss14_' name],'pvalue', 'TS_data', 'TS_rand', 'A_null',…
'A_ctl', 'A_agun', 'a_null', 'b_null', 'a_ctl', 'b_ctl', 'a_agun', …
'b_agun', 'logl_null', 'logl_alt', …
'logl_null_rand_all','logl_alt_rand_all', 'A_null_rand_all', ...
    'A_agun_rand_all', 'A_ctl_rand_all', 'ar_null_all', …
'br_null_all', 'ar_ctl_all', 'br_ctl_all', 'ar_agun_all', …
'br_agun_all');
```

Appendix C: Calculations Related to Doppler Shift Compensation by Porpoises

One study measured the maximum swimming speed of harbor porpoises to be 4.3 m/sec, and their average speed to be 1 m/sec (0.1 - 0.2%, Otani *et al.*, 2000). Herring can attain swimming speeds of 16-24 cm/sec (Onsrud *et al.*, 2005) or 10-12 body lengths per second (for 50 mm fish, Turnpenny, 1983) with reported bursts of swimming at up to 1.74 m/s (http://www.fishbase.org) or 2-4.5 m/sec (Boyar, 1961). Say that the velocity of a prey item (herring) relative to an echolocating porpoise is 4 m/sec. The Doppler shift (Δf) of an echo returning from the herring will be 695 Hz (0.53% of 130 kHz). Alternately, say that the velocity of the prey item relative to the porpoise is about 1 m/sec (this relative velocity is probably a more realistic estimate of the maximum relative velocity that one might expect to observe in the wild). Then the Doppler shift will be 173 Hz (0.13% of 130 kHz).

Calculations:

$$\Delta f = f_e \left(\frac{2v}{c - v} \right) = 130,000Hz \left(\frac{2(4\frac{m}{sec})}{(1500\frac{m}{sec} - 4\frac{m}{sec})} \right) = 695Hz$$

$$\Delta f = f_e \left(\frac{2v}{c - v} \right) = 130,000Hz \left(\frac{2(1\frac{m}{sec})}{(1500\frac{m}{sec} - 4\frac{m}{sec})} \right) = 173Hz$$

Harbor porpoises are capable of discriminating frequency differences as small as 0.1-0.2% (Ketten, 2000) in long-duration signals, although their discrimination capability remains untested (and is likely less acute) for shorter signals like clicks. Bats (*Rhinolophus ferrumequinium*) lower the frequency of their outgoing cries to stabilize the frequency of echoes from an approaching target at frequency differences at least as small as 0.5% (Thomas *et al.*, 2004). It should be noted, however, that their signals are at least 500 times longer than those of porpoises.

For Doppler-compensating bats (*Rhinolophus ferrumequinium*), the smallest resolvable change in target velocity is 0.1 m/sec (Simmons, 1974). That velocity corresponds to a frequency difference of 40Hz or 0.05% of 83 kHz. Harbor porpoise frequency discrimination is comparable to that of bats of suborder Microchiroptera (Ketten, 2000), at least for long-duration signals. If porpoises were to attain the same minimum resolvable frequency shift as the bats mentioned above for short signals like their echolocation clicks, they would be able to detect velocity changes with resolution of 0.36 m/sec. (This comparison is highly speculative.)

Calculations:

$$\Delta f = 130,000Hz\left(\frac{40Hz}{83,000Hz}\right) = 62.7Hz$$

$$DopplerShift = f_e\left(\frac{2v}{c-v}\right),$$

where f_e is the porpoise click center frequency, here 130 kHz, v is the velocity of the target relative to echolocating animal, and c is sound speed, here 1500 m/sec. So, solving for v,

$$v = \frac{1500\frac{m}{sec}}{2(\frac{130,000Hz}{62.7Hz}+\frac{1}{2})} = \frac{1500}{4147.7} = 0.36\frac{m}{sec}$$

References

Boyar, H. C. (**1961**). "Swimming speed of immature Atlantic herring with reference to the Passamaquoddy Tidal Project," Transactions of the American Fisheries Society **90**, 21-26.

Ketten, D. R. (**2000**). "Cetacean Ears," in *Hearing by Whales and Dolphins*, edited by W. W. L. Au, A. N. Popper, and R. R. Fay (Springer, New York, NY), pp. 43-108.

Onsrud, M. S. R., Kaartvedt, S., and Breien, M. T. (**2005**). "In situ swimming speed and swimming behaviour of fish feeding on the krill *Meganyctiphanes norvegica*," Canadian Journal of Fisheries and Aquatic Sciences **62**, 1822-1832.

Otani, S., Naito, Y., and Kato, A. (**2000**). "Diving behavior and swimming speed of a free-ranging harbor porpoise, *Phocoena phocoena*," Marine Mammal Science **16**, 811-814.

Simmons, J. A. (**1974**). "Response of the Doppler echolocation system in the bat, *Rhinolophus ferrumequinum*," Journal of the Acoustical Society of America **56**, 672-682.

Thomas, J. A., Moss, C. F., and Vater, M. (eds). (**2004**). *Echolocation in bats and dolphins* (University of Chicago Press, Chicago, IL).

Turnpenny, A. W. H. (**1983**). "Swimming performance of juvenile sprat, *Sprattus sprattus* L., and herring, *Clupea harengus* L., at different salinities," Journal of Fish Biology **23**, 321-325.